



**Międzyuczelniany Wydział
Biotechnologii**

Uniwersytetu Gdańskiego
i Gdańskiego Uniwersytetu Medycznego

ROZPRAWA DOKTORSKA

Mgr Klaudia Szymczak

**Fotodynamiczna inaktywacja wielolekoopornego
Staphylococcus aureus i redukcja jego wirulencji
z wykorzystaniem nowych porfiryn
koordynowanych jonami galu (III)**

Photodynamic inactivation of multidrug-resistant
Staphylococcus aureus and reduction of its virulence
using novel gallium(III)-coordinated porphyrins

Praca przedstawiona
Radzie Dyscypliny Biotechnologia Uniwersytetu Gdańskiego
celem uzyskania stopnia doktora
w dziedzinie nauk ścisłych i przyrodniczych
w dyscyplinie naukowej biotechnologia

Promotor: dr hab. Joanna Nakonieczna, prof. UG
Zakład Fotobiologii i Diagnostyki Molekularnej

GDAŃSK 2023

Podziękowania

Zanim wprowadzę Państwa w świat aktywowanych światłem porfiryń galowych oraz wewnątrzkomórkowych infekcji, chciałabym gorąco podziękować osobom, które towarzyszyły mi podczas mojej doktoranckiej drogi. Jestem niesamowicie wdzięczna za to, jak ta droga się potoczyła oraz ile nauczyłam się podczas jej realizacji. Swoje największe podziękowania pragnę skierować do:

Dr hab. Joanny Nakoniecznej, prof. UG za mentorstwo, zaufanie, każdą poprawkę, czy uwagę, ogromną cierpliwość, wsparcie, rozwijanie mojej pasji do nauki i za możliwość realizacji każdego, nawet najbardziej szalonego eksperymentu naukowego. Za zaszczerpienie we mnie ciekawości i dociekliwości oraz za owocną publikacyjną współpracę.

Dr hab. Mariusza Grinholc, prof. UG za wspólną pracę, stworzenie niesamowitej atmosfery w laboratorium, każdą pomoc merytoryczną i duchową,

Dr Michała Rychłowskiego, dziękuję za współpracę przy manuskryptach, za każdą radę, za przepiękne zobrazowanie ko-kultur i przybliżenie mojej pracy do poziomu ludzkiego oka,

Dr Agnieszki Bernat-Wójtowskiej i Dr Magdy Rybickiej-Misiejko za wprowadzenie mnie do świata komórek eukariotycznych i wsparcie (nie tylko w trudach dydaktycznych),

Mojej Grupy Wsparcia z p.116 – dr Agacie, Natalii, dr Oli, dr Michałowi, dr Patrycji, Beatce i Izie za niesamowitą atmosferę w laboratorium, wspólne wieczory (nie)naukowe przy winie, wspólne podróże, za wszelką pomoc merytoryczną, za wspólną doktorancką drogę w radościach i smutkach,

Mojej kochanej Rodziny – dziękuję moim kochanym Rodzicom, Dziadkom i Siostram za niesamowite wsparcie, wiarę, motywację i możliwość kroczenia swoją pasją przez życie. Za to, że mogłam zawsze znaleźć w Was azyl, za Waszą dumę ze mnie i za otrzymaną bezgraniczną miłość.

Mojej Rodziny - tej z wyboru, kieruję do Emilii, Marcina, Pauliny, Tomka, Agaty, Czarka, Beaty, Dawida, Oli, Kuby, Kamili, Pawłowi, Krzyśka i Dominiki - za wprowadzenie pierwiastka normalności, za każdą próbę zrozumienia mojego naukowego świata, za próbę nauczania work-life balance i każde trzymanie kciuków, szczególnie na etapie pisania!

Na koniec chciałabym podziękować mojej życiowej skale, bez której ta praca nigdy nie ujrzałaby światła dziennego – **mojemu mężowi Bartkowi**. Za niesamowite wsparcie, za bezgraniczną miłość, za każdy kopniak motywacji, za wyrozumiałość (szczególnie na etapie pisania). Za przekucie moich porażek labowych w dalszą siłę do działania. Za przeżycie ze mną tych trudnych, lecz pięknych 4 lat.

*„Niczego w życiu nie należy się bać,
należy to tylko zrozumieć.”*

*‘Nothing in life is to be feared,
it is only to be understood.’*

~ Maria Skłodowska-Curie

Moim Rodzicom

TABLE OF CONTENT

| | |
|---|-----|
| RESEARCH FUNDING..... | 6 |
| INCLUDED PUBLICATIONS..... | 7 |
| ABBREVIATIONS | 8 |
| STRESZCZENIE PRACY | 9 |
| ABSTRACT..... | 10 |
| 1. INTRODUCTION | 11 |
| 1.1. ANTIMICROBIAL RESISTANCE AND VIRULENCE OF <i>STAPHYLOCOCCUS AUREUS</i> | 11 |
| 1.2. INTRACELLULAR INVASION OF <i>S. AUREUS</i> AS A FEATURE OF VIRULENCE..... | 12 |
| 1.3. INFECTION CYCLE OF INTRACELLULAR <i>S. AUREUS</i> | 13 |
| 1.4. ANTIMICROBIAL PHOTODYNAMIC INACTIVATION (APDI) AS AN ALTERNATIVE TO ANTIBIOTIC THERAPY | 15 |
| 1.5. DUAL-FUNCTION GALLIUM(III)-COORDINATED PORPHYRINS: TROJAN HORSE STRATEGY | 18 |
| 1.6. HEME-ACQUISITION MACHINERY OF <i>S. AUREUS</i> FOR TARGETED DELIVERY OF GALLIUM PORPHYRINS | 20 |
| 1.7. APPLICATION OF LIGHT-ACTIVATED GALLIUM METALLOPORPHYRINS ON VARIOUS <i>S. AUREUS</i> MODELS ²² | |
| 2. OBJECTIVES | 25 |
| 3. PUBLICATION NO. 1..... | 26 |
| GALLIUM MESOPORPHYRIN IX-MEDIATED PHOTODESTRUCTION: A PHARMACOLOGICAL TROJAN HORSE STRATEGY TO ELIMINATE MULTIDRUG-RESISTANT <i>STAPHYLOCOCCUS AUREUS</i> | 26 |
| 3.1 Summary of the publication..... | 26 |
| 3.2 Publication | 28 |
| 4. PUBLICATION NO. 2..... | 44 |
| PHOTOACTIVATED GALLIUM PORPHYRIN REDUCES <i>STAPHYLOCOCCUS AUREUS</i> COLONIZATION ON THE SKIN AND SUPPRESSES ITS ABILITY TO PRODUCE ENTEROTOXIN C AND TSST-1 | 44 |
| 4.1 Summary of the publication | 44 |
| 4.2 Publication..... | 46 |
| 5. MANUSCRIPT NO. 3..... | 64 |
| HARNESSING LIGHT-ACTIVATED GALLIUM PORPHYRINS TO COMBAT INTRACELLULAR <i>STAPHYLOCOCCUS AUREUS</i> IN DERMATITIS: INSIGHTS FROM A SIMPLIFIED MODEL | 64 |
| 5.1 Summary of the Manuscript..... | 64 |
| 5.2 Manuscript | 66 |
| 6. SUMMARY..... | 99 |
| 7. OTHER PHD ACCOMPLISHMENT | 101 |
| 7.1 Publications not included in the thesis..... | 101 |
| 7.2 Conferences | 101 |

| | | |
|-----------|---|------------|
| 7.3 | <i>Grants</i> | 102 |
| 7.4 | <i>Trainings</i> | 102 |
| 7.5 | <i>Awards</i> | 102 |
| 8. | LITERATURE | 103 |
| 9. | ATTACHMENTS | 110 |
| 9.1 | <i>Supplementary Materials from Publication no. 1</i> | 110 |
| 9.2 | <i>Supplementary Materials from Publication no. 2</i> | 123 |
| 9.3 | <i>Supplementary Materials from Manuscript no. 3</i> | 132 |
| 9.4. | <i>P1- Statements of contributions</i> | 137 |
| 9.5. | <i>P2- Statements of contributions</i> | 143 |
| 9.6 | <i>P3- Statements of contributions</i> | 150 |

Research Funding

The research presented in this doctoral dissertation was financed by:



University of Gdańsk as part of the Small Grants Program of UGrants-start 1 (no. 533-0C30-GS31-21) and 3 programs (no. 533-0C30-GS28-23).



funds for Statutory Activities
for the Laboratory of Photobiology and Molecular Diagnostics,
Intercollegiate Faculty of Biotechnology of the University of Gdańsk and
MUG



National Science Center a part of
OPUS Grant no. 2017/27/B/NZ7/02323

INCLUDED PUBLICATIONS

The research presented in this doctoral dissertation was prepared based on:

P1 - Publication no. 1

Klaudia Michalska, Michał Rychłowski, Martyna Krupińska, Grzegorz Szewczyk, Tadeusz Sarna, and Joanna Nakonieczna

„Gallium Mesoporphyrin IX-Mediated Photodestruction: A Pharmacological Trojan Horse Strategy To Eliminate Multidrug-Resistant *Staphylococcus aureus*”, *Molecular Pharmaceutics* 2022, 19, 5, 1434–1448, <https://doi.org/10.1021/acs.molpharmaceut.1c00993>

IF= 4.9, Q1, MNiSW = 140

P2 - Publication no. 2

Klaudia Szymczak, Grzegorz Szewczyk, Michał Rychłowski, Tadeusz Sarna, Lei Zhang, Mariusz Grinholc, and Joanna Nakonieczna

„Photoactivated Gallium Porphyrin Reduces *Staphylococcus aureus* Colonization on the Skin and Suppresses Its Ability to Produce Enterotoxin C and TSST-1”, *Molecular Pharmaceutics* 2023, 20,10,5108–5124, <https://doi.org/10.1021/acs.molpharmaceut.3c00399>

IF= 4.9, Q1, MNiSW = 140

P3 - Manuscript no. 3 (prepared for submission)

Klaudia Szymczak, Michał Rychłowski, Lei Zhang, and Joanna Nakonieczna

„Harnessing light-activated gallium porphyrins to combat intracellular *Staphylococcus aureus* in dermatitis: insights from a simplified model”

ABBREVIATIONS

Agr – accessory gene regulator
aPDI – antimicrobial photodynamic inactivation
AD – atopic dermatitis
AMR – antibiotic multidrug resistance
CFU – colony-forming unit
ClfA – clumping factor A
Eap – extracellular adherence protein
EMA – European Medicines Agency
ESKAPE – acronym of six members of multi-drug resistant pathogens (*Enterococcus* spp., *Staphylococcus aureus*, *Klebsiella pneumoniae*, *Acinetobacter baumannii*, *Pseudomonas aeruginosa* and *Enterobacter cloacae*)
FDA – U.S. Food and Drug Administration
FnBPs – fibronectin-binding proteins
Ga³⁺MPs – gallium metalloporphyrins, gallium(III)-coordinated porphyrins
HaCaT – immortalized human keratinocytes cell line
Hts – heme transport system
HrtAB – heme efflux pump, heme-regulated transporter
HssRS – heme sensor system
ILK – integrin-linked kinase
Isd – iron-regulated surface determinant system
IsdB – surface determinant B
LED – light emitting diode
MDR – multidrug-resistant
MHC – major histocompatibility complex
MRSA – methicillin-resistant *S. aureus*
NB UV – narrow-band ultraviolet B
NEAT – Near Transporter
aPDI – antimicrobial photodynamic inactivation
PDT – photodynamic therapy
PS – photosensitizer
ROS – reactive oxygen species
SCVs – small colonies variants
SEC – staphylococcal enterotoxin C
SEs – staphylococcal enterotoxins
SSTIs – skin and soft tissue infections
TCR – T-cell receptor
TSS – toxic shock syndrome
TSST-1 – toxic shock syndrome toxin
UV-A – ultraviolet A

STRESZCZENIE PRACY

Gronkowiec złocisty (*Staphylococcus aureus*) jest Gram-dodatnim patogenem z grupy ESKAPE, odpowiedzialnym za około 80% wszystkich skórnych infekcji. Na jego wirulencję składają się czynniki, takie jak produkcja toksyn, tworzenie biofilmu, czy zdolność do internalizacji do komórek gospodarza. Przetrwanie wewnątrzkomórkowe *S. aureus* w komórkach gospodarza jest powiązane z nawracającymi infekcjami, które przyczyniają się do niepowodzeń terapeutycznych. Ze względu na niską penetrację, terapie antybiotykowe nie są wysoko skuteczne wobec wewnątrzkomórkowego *S. aureus*. Obecnie poszukuje się alternatywnych metod przeciwdrobnoustrojowych, które mogą efektywnie obniżyć wewnątrzkomórkowy rezerwuar bakteryjny. Jedną z opcji terapeutycznych może być przeciwdrobnoustrojowa metoda fotodynamiczna (ang. *antimicrobial photodynamic inactivation*, aPDI), opierająca się na związku chemicznym - fotosensybilizatorze, który ulega wzbudzeniu pod wpływem światła o danej długości fali w środowisku tlenowym. W wyniku działania trzech komponentów, generowane są reaktywne formy tlenu, które przyczyniają się do śmierci bakterii poprzez uszkodzenia biomolekuł komórkowych takich jak: białka, DNA, lipidy. Porfiryny koordynowane jonami galu (III) (Ga^{3+}MPs) są związkami o podwójnej funkcjonalności, czyli wykazują właściwości związków fotosensybilizujących w ścieżce zależnej od światła, natomiast w ścieżce niezależnej od światła blokują metabolizm zależny od jonów żelaza, naśladując strukturę naturalnego liganda – hemu. Ga^{3+}MPs są analogami hemu, przez co mogą być rozpoznawane przez specyficzne receptory dla hemu z systemu Isd (ang. *Iron surface determinant*). Po zakumulowaniu we wnętrzu bakterii, jony galu zostają uwolnione z pierścienia porfiryнового, interferując w szlaki metaboliczne zależne od jonów żelaza.

Niniejsza rozprawa doktorska skupia się na zbadaniu efektywności aPDI wobec *S. aureus* w oparciu o zastosowanie nowych związków fotosensybilizujących - porfiryn koordynowanych jonami galu (III). Celem badań jest ocena, czy wzbudzenie Ga^{3+}MPs światłem zielonym może prowadzić do istotnego zmniejszenia aktywności czynników wirulencji, takich jak: toksyny, biofilm, czy wewnątrzkomórkowe przetrwanie *S. aureus*. Efektywność aPDI przebadano na kilku modelach: hodowli zawiesinowej, biofilmie *in vitro* i *ex vivo* (kolonizacja świńskiej skóry) oraz na modelu infekcyjnym ludzkich keratynocytów. W badaniach na modelu infekcyjnym, przetestowano trzy strategie implementacji metody fotodynamicznej celem zbadania: I) możliwości eliminacji bakterii uwolnionych z komórek gospodarza; II) wpływu aPDI na adherencję i internalizację; III) efektywności aPDI w eliminacji wewnątrzkomórkowego *S. aureus*.

Przedstawione wyniki niniejszej rozprawy wskazują, że aPDI ma wysoką efektywność przeciwdrobnoustrojową wobec *S. aureus* w hodowli zawiesinowej, jak i na modelach biofilmu. Wykazano, że aPDI skutecznie inaktywuje biologiczną funkcjonalność istotnych czynników wirulencji, takich jak enterotoksyna gronkowcowa C i toksyna wstrząsu toksycznego TSST-1. Metoda fotodynamiczna może stanowić skuteczną metodę prowadzącą do eliminacji bakterii uwolnionych z gospodarza. Również przedstawiono, że aPDI obniża adherencję *S. aureus* do komórek gospodarza, lecz nie ma znaczącego wpływu na wydajność procesu internalizacji. Wyniki badań wykazały również, że aPDI efektywnie obniża sygnał GFP pochodzący od wewnątrzkomórkowego *S. aureus*. Po raz pierwszy zaprezentowano efektywność nowych porfiryn koordynowanych jonami galu (III) i światła zielonego w zmniejszeniu wewnątrzkomórkowego rezerwuaru *S. aureus*. Znacząco poszerza to możliwości terapeutyczne metody fotodynamicznej w oparciu o Ga^{3+}MPs o przeciwdziałanie nawracającym infekcjom gronkowcowym.

ABSTRACT

Staphylococcus aureus is a Gram-positive pathogen of the ESKAPE group, responsible for about 80% of all skin infections. Its virulence consists of factors such as toxin production, biofilm formation and the ability to internalize into host cells. The intracellular survival of *S. aureus* in host cells is associated with recurrent infections, which contribute to therapeutic failures. Due to low penetration, antibiotics are not highly effective against intracellular *S. aureus*. Alternative antimicrobial therapies are currently being sought that can effectively reduce the intracellular bacterial reservoir. One therapeutic option may be antimicrobial photodynamic inactivation (aPDI), based on a chemical compound, known as a photosensitizer, which is excited when exposed to light of a given wavelength in an aerobic environment. As a result of the three components action, reactive oxygen species are generated, which contribute to bacterial death by damaging cellular biomolecules such as proteins, DNA and lipids. Gallium(III)-coordinated porphyrins (Ga³⁺MPs) are dual-functional compounds, i.e. they exhibit the photodynamic properties of a photosensitizer in the light-dependent pathway, while in the light-independent pathway they block iron-dependent metabolism by mimicking the structure of the natural ligand – heme. Ga³⁺MPs are heme analogues and can thus be recognized by specific receptors for heme from the iron surface determinant (Isd) system. Once accumulated in the bacterial interior, gallium ions are released from the porphyrin ring, interfering with iron ion-dependent metabolic pathways.

This dissertation focuses on investigating the effectiveness of aPDI against *S. aureus* based on the use of novel photosensitizing compounds - gallium (III)-coordinated porphyrins. The aim of the study is to assess whether excitation of Ga³⁺MPs with green light leads to a significant reduction in the activity of virulence factors such as toxins, biofilm and intracellular survival of *S. aureus*. The effectiveness of aPDI was tested on the following models: planktonic cultures; *in vitro* and *ex vivo* biofilm (porcine skin model), and an infection model of human keratinocytes. On the infection model, three strategies for implementing the photodynamic method were proposed to study: I) the ability to eliminate bacteria released from the host, II) the effect on adherence and internalization III) the effectiveness of aPDI in reducing intracellular *S. aureus* load.

The results presented in this dissertation indicate that aPDI has high antimicrobial efficacy against *S. aureus* in suspension cultures, as well as on biofilm models. It was shown that aPDI effectively inactivates the biological functionality of important virulence factors, such as staphylococcal enterotoxin C and toxic shock toxin TSST-1. The photodynamic inactivation can be an effective method for eliminating bacteria released from the host. Pretreatment with aPDI contributes to a significant reduction in bacterial adherence to the host, but without a significant effect on internalization. The results also showed that aPDI effectively decreases GFP signal derived from intracellular *S. aureus*. This is the first study that presents the efficacy of novel Ga³⁺MPs combined with green light in reducing the intracellular *S. aureus*. This significantly extends the therapeutic potential of the Ga³⁺MPs-mediated photodynamic method against recurrent staphylococcal infections.

1. INTRODUCTION

1.1. Antimicrobial resistance and virulence of *Staphylococcus aureus*

According to O'Neill's report, by 2050, the era of functional antibiotics will end. Infectious diseases will cause the highest mortality rates, and the number of deaths will reach up to 10 million per year, which will be even higher than the number of deaths caused by cancer ¹. Despite the cooperation between science and the pharmaceutical industry in the synthesis of new antibiotics, we are unable to cope with the growing **antibiotic resistance (AMR)**. Emerging AMR pathogens are mainly classified as the ESKAPE group, whose name indicates their ability to escape the antibiotic action ^{2,3}. The ESKAPE group includes six multidrug-resistant (MDR) pathogens such as *Enterococcus* spp., *Staphylococcus aureus*, *Klebsiella pneumoniae*, *Acinetobacter baumannii*, *Pseudomonas aeruginosa* and *Enterobacter cloacae* ³. The urgent emergence of these pathogens necessitates the development of innovative treatment technologies for their effective elimination ⁴.

This work focuses mainly on *Staphylococcus aureus*, a methicillin-resistant Gram-positive human pathogen. Methicillin resistance in *S. aureus* clinical isolates (MRSA) was first identified in the early 1960s due to the widespread and global overuse of penicillin ³. Both hospital- and community-acquired MRSA now account for 60% of all isolates in patients ^{5,6}. The emergence of MRSA strains has a major impact on the economic costs of healthcare and the course of infection through increased morbidity, prolonged hospitalization, and high mortality ⁷.

S. aureus colonization predominantly causes skin and soft tissue infections (SSTIs) ⁸. *S. aureus* is responsible for over 80% of all skin infections worldwide ⁹. In the pathogenesis of atopic dermatitis (AD), *S. aureus* is a predominant pathogen in the whole skin microbiota, infecting/colonizing ~80% of all AD patients ¹⁰. Moreover, this bacterium has been implicated in toxic shock syndrome (TSS) or systemic infections such as osteomyelitis, endocarditis, or wound infections, that are extremely severe, chronic, and unresponsive to conventional antibiotic treatment ¹¹.

In addition to its drug-resistance profile, *S. aureus* is highly virulent due to the production of multiple virulence factors that alter the host immune response and promote more severe infection outcomes. Various factors contribute to its virulence, including toxins production, biofilm formation, and intracellular persistence inside the host cells ¹².

During infection, *S. aureus* secretes various exotoxins that modulate the host's immune responses to promote higher bacterial persistence ^{13,14}. Superantigens such as staphylococcal enterotoxins (SEs) are strong immune inducers of pro-inflammatory cytokines that enhance inflammation and disturb the functioning of the immune system ¹⁵. SEs, such as staphylococcal enterotoxin C (SEC) or toxic shock syndrome toxin (TSST-1) exhaust the activity of more than 50% of T cells by strongly binding with either T cell receptor TCR-V β region or major histocompatibility complex (MHC) class II molecules ^{14,16,17}. Moreover, despite superantigenicity, SEs are highly resistant to physical factors such as proteolysis, heat, acidic environment

or drought ¹⁴. Production of SEC is strongly linked to sepsis, pneumonia, endocarditis, and osteomyelitis ¹⁶. Within the SEC structure, a disulfide loop is responsible for the emetic activity of the toxin that contributes to food poisoning ¹⁵. Whereas, TSST-1 is associated with TSS that cause acute systematic illness ¹⁷. Overall, virulence-reducing approaches, which include suppressing the production or reducing the functionality of virulence factors, may be a valuable tool in attenuating and controlling ESKAPE infections.

S. aureus skin colonization depends mainly on the ability to form biofilm as a feature of its virulence. Biofilm provides adequate adherence to host cells and long-term persistence ¹⁷. In osteomyelitis *in vivo* models, the ability of *S. aureus* to form biofilm corresponds with more chronic infection ¹⁸. Biofilm is a heterogeneous reservoir of multiple subpopulations with a divergent antibiotic resistance profile ¹⁷. Bacteria within biofilm community are much more resistant to antibiotic or host immune action than free-floating bacteria ¹⁹. About 100–1000 times higher concentrations of antibiotics are required to eradicate biofilm ^{20,21}. As a cause of environmental adaptation, *S. aureus* biofilm is attached to various surfaces, including the skin. In the pathogenesis of atopic dermatitis, the colonization of *S. aureus* in the form of a cutaneous biofilm is associated with a more severe disease progression ²². It is also reported that biofilm produces various exotoxins that modulate immune responses and impair skin barrier function by directly affecting keratinocytes ²³. For instance, the secretion of α -toxin by biofilm leads to the cell death of keratinocytes with strong induction of the T-cells response ^{24,25}. Moreover, *S. aureus* biofilm inhibited keratinocyte terminal differentiation ²⁶. This indicates the vital role that biofilm-forming ability plays in *Staphylococcus aureus* virulence.

1.2. Intracellular invasion of *S. aureus* as a feature of virulence

A significant problem associated with staphylococcal infections is the frequency of their recurrence. Literature data shows that 39% of patients with SSTIs experience a recurrence of infection within three months and more than 50% at six months after initial antibiotic treatment ²⁷. The cause of recurrent infections is *S. aureus* invasion and intracellular survival in the host cells as one of its virulence features ²⁸. Over some decades, scientists revealed that antibiotic-persisted SCVs (small colony variants) are responsible for the clinical recurrence of infection ^{29,30}. SCVs are primarily associated with the recurrence of cystic fibrosis, osteomyelitis, device-related infections, or SSTIs ^{31,32}. Infection caused by SCVs is found to be more aggressive and virulent in multiple animal and human models ^{28,33}. This phenotype undergoes many changes in gene expression – for example, reduced pattern of virulence factor production ^{32,34}.

So far, *S. aureus* has been considered as an extracellular pathogen, but many scientific reports highlight its intracellular phenotype as a feature of its virulence ^{35,36}. This phenotype occurs *in vivo* in infected cell cultures or animal models ^{37–39}. *S. aureus* can invade and persist for several days within professional or non-professional phagocytes such as keratinocytes ⁴⁰, thus avoiding the action of the complement system, antibodies, and external antibiotics, which penetrate poorly

through eukaryotic membranes^{41,42}. Once internalized, bacterial cells are subject to two types of selective pressure: the external antibiotic action and the intracellular environment of the host cells. Those selective pressures generate the intracellular niche that could serve as a reservoir for relapsing infection or chronic carriage³⁵. For years, the scientists had linked the SCVs phenotype to intracellular survival^{31,33,43}. However, a recent study has shown that non-growing, non-responsive normal-size colonies are also capable of surviving inside host cells but for a much shorter time of persistence³³. This phenotype still exhibits metabolic activity despite adaptive changes in the transcriptome induced by the intracellular environment. Also, it has been shown that intracellular phenotype could exhibit greater tolerance to antibiotics⁴⁴. This phenotype is stable but fully reversible under favorable conditions (i.e. the absence of antibiotic pressure)⁴⁴. Once the pressure of the external antibiotic is lifted, the phenotype can be switched back to the parental phenotype and start intracellular replication, contributing to the initiation of secondary infection⁴⁵.

1.3. Infection cycle of intracellular *S. aureus*

Bacterial adherence to the host cell is necessary to initiate the invasion (**Fig 1**). In the non-professional phagocytes, the internalization occurs through a zipper-type mechanism utilizing bacterial surface fibronectin-binding proteins (FnBPs), fibronectin, and $\alpha_5\beta_1$ integrins on the host cells^{33,35,46}. Also, FnBPs play a crucial role in the rearrangements of host cell cytoskeleton⁴⁷. In the FnBP-independent pathway, the internalization could be mediated by extracellular adherence protein (Eap) or other surface bacterial proteins such as clumping factor A (ClfA) or iron-regulated surface determinant B (IsdB)⁴⁸. Cytoskeleton remodeling immediately activates integrin-linked kinase (ILK) signal transduction, which is needed for further cellular uptake of pathogen⁴⁹.

Once internalized, *S. aureus* undergoes many adjustments in the gene expression pattern to promote intracellular survival within host cells⁵⁰. At first hours post-infection, there is a massive downregulation in the genes involved in the replication and metabolism with up-regulation of virulence, iron acquisition, or ROS neutralization genes⁵⁰. Those global changes allow *S. aureus* to persist for up to weeks within host⁵¹.

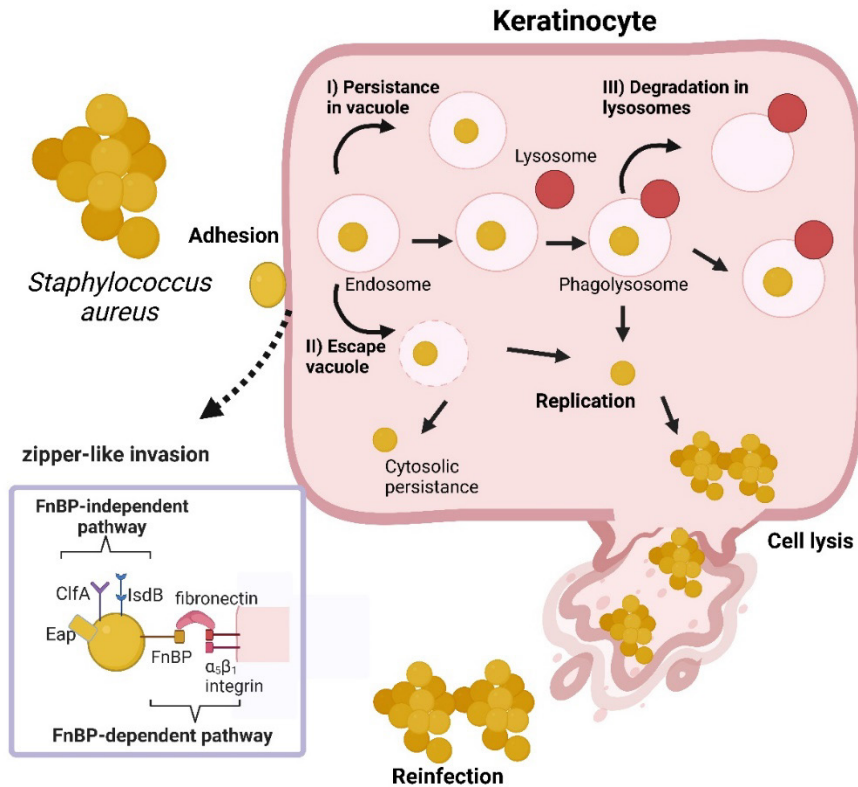


Fig 1. The cycle of infection of human keratinocytes by *S. aureus*. At first, *S. aureus* attaches to the host membrane and invades it via a zipper-like mechanism, either with FnBP-independent (mediated by Eap, ClfA or IsdB proteins) or FnBP-dependent pathway (complex of FnBPs, fibronectin and $\alpha_5\beta_1$ integrins) pathway. *S. aureus* enters the endosome inside the host cell. It has been documented that intracellular *S. aureus* can undergo the following processes: I) persistence in vacuoles; II) escape from the endosome to survive in the cytosol with minimal cytotoxicity or initiate replication; III) transfer to the phagolysosome for bacterial degradation, persist in lysosomal structures, or escape from them for reinfection. During reinfection, the bacteria begin to replicate inside the host in cytoplasm, and once they reach a certain intracellular load, *S. aureus* lyses the host cell to release bacteria and reinfect more host cells. Adapted from: Garzoni C, Kelley WL. (2009). Created with Biorender (K. Szymczak, 2023).

Intracellular load of bacteria might be gradually titrated over time or persist with minimal cytotoxicity to the host (**Fig 1**). Bacterial clearance may be due to the degradation in lysosomes. Persistence may occur within organelle structures such as vacuoles or within the cytosol³⁵. This process depends on several factors related to the pathogen or host, such as the multiplicity of infection, the genotype of the *S. aureus* strain, the host cell type, or a change in the gene expression pattern^{45,46}. For example, an *agr*-deficient strain of *S. aureus* persisted inside longer than the strain with a functional gene^{52,53}. An accessory gene regulator (*agr*) is a regulator of virulence factors that functions in a quorum-sensing mechanism-dependent manner⁵⁴.

When the external selective pressure of antibiotic is diminished, it might promote either phagosomal or endosomal escape of *S. aureus* to the cytoplasm to initiate the replication within the host cells^{40,46}. This translocation is a strain-dependent process, particularly on the functionality of the *agr* regulon. Thus, the lack of it reduces the ability to escape phagosome⁵³. Virulence exotoxins production

such as pore-forming α -toxin and α -type phenol-soluble modulins (PSM α), regulated by Agr, are crucial for cytoplasmic bacterial replication within non-professional phagocytes^{55,56}. Moreover, it was shown only for keratinocytes that production of Pantan-Valentine leucocidin (PVL) might be needed for the *S. aureus* escaping process⁵⁷.

After the cytoplasmic bacterial burden is reached, the host cell is lysed, and the released bacteria restart the secondary infection (**Fig 1**). It is worth mentioning that this secondary infection is driven by intracellular inoculum, which can exhibit a multidrug tolerance phenotype^{44,58}. Intracellular environment is a niche for recurrent infections associated with therapeutic failures⁵⁹.

The ability to persist intracellularly within the host is one of the virulence features of *S. aureus*¹². Intracellular *S. aureus* phenotype is primarily caused by antibiotic action and this phenotype may lead to relapsing infections⁵⁹. Therefore, it is essential to expand knowledge about the pathogenesis of intracellular *S. aureus* from a more clinical point of view. It is important for scientists to explore novel antimicrobial therapies with the assessment of their efficacy in combating intracellular infections.

1.4. Antimicrobial photodynamic inactivation (aPDI) as an alternative to antibiotic therapy

There is global interest in alternative antibiotic therapies to combat multidrug-resistant pathogens. One proposed method is antimicrobial photodynamic inactivation (aPDI), derived from photodynamic therapy (PDT) used in anticancer approaches. The action of aPDI is based on three components: light, oxygen, and a small molecular weight compound – a photosensitizer (PS). A photon of light is absorbed to excite the PS to the short-lived excited singlet state ($^1PS^*$) (**Fig 2**). This state goes through an intersystem crossing to the longer-lived triplet state ($^3PS^*$). Next, a Type I or II reaction occurs in the oxygen environment. In Type I reaction, electron transfer from PS to oxygen promotes superoxide ($\bullet O_2^-$), hydroxyl radicals (HO \bullet), and hydrogen peroxide (H₂O₂) production. Meanwhile, in Type II reaction, the energy transfer from $^3PS^*$ to molecular oxygen generates the highly cytotoxic singlet oxygen (1O_2). Both Type I and Type II products are highly reactive, affect all types of biomolecules in the cell and cause microbial cell death in the multi-target action^{60,61}.

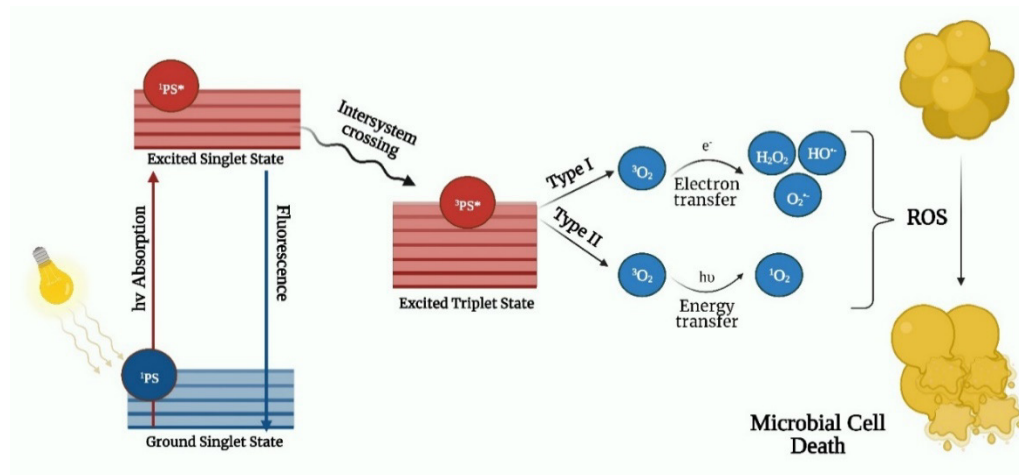


Fig 2. Mechanism of antimicrobial photodynamic inactivation (aPDI) action.

PS – photosensitizer, $^3\text{O}_2$ – molecular oxygen, $\text{O}_2^{\cdot-}$ – superoxide anion, OH^{\cdot} – hydroxyl radical, H_2O_2 – hydrogen peroxide, $^1\text{O}_2$ – singlet oxygen, ROS – reactive oxygen species Adapted from: Hamblin, 2016, Rapacka-Zdończyk 2021. Created with Biorender (K. Szymczak, 2023).

aPDI is highly effective against ESKAPE group bacteria *in vitro* in planktonic and biofilm cultures. Moreover, it exhibits high antimicrobial efficacy in multiple *in vivo* models ^{4,62}. The aPDI efficacy is independent of the antibiotic resistance profile of microorganisms, which makes this method extremely attractive in the context of the growing problem of drug resistance ⁶³. This method is not able to completely replace antibiotics, but in situations where there is a local infection, it can be a much better option than classic antibiotics. aPDI can reduce bacterial virulence by decreasing the production of multiple virulence factors or reducing their biological activity ^{64–66}. aPDI efficiently kills ESKAPE pathogens in synergy with traditionally used antibiotics, allowing for a significant reduction in antibiotic use while, in the long run, reducing the spread of AMR ^{67,68}. Due to the multitarget effect of aPDI, the microbial resistance to the aPDI has not yet been reported. However, there are findings of bacterial tolerance following repeated exposure to aPDI treatments ^{69–71}. aPDI therapy has also been used against viral infections, including the CoV19-SARS2 virus, fungi, or parasites ⁷². aPDI has been successfully used to treat acne vulgaris, diabetic foot ulcers, keratitis, chronic wounds, and oral infections ^{72,73}. Recently, Canadian company – Ondine adapted aPDI for nasal photodisinfection for commercial use.

An integral element of aPDI is light, which excites a photosensitizing compound. Light-based treatments consist primarily of the wavelengths of ultraviolet A (UV-A), narrow-band ultraviolet B (NB UV-B), or visible light. However, there is some controversy regarding the safety of using UV-band lights for clinical treatment. This is mainly a concern based on the poor light penetration through the epithelial tissue with a high impact on the promotion of carcinogenesis ⁷⁴. Application of light at the visible range (approx. 400 nm to 700 nm) seems to be a safer clinical option compared to UV light. So far, only two light sources in visible range - blue (405 nm) and red light (650 nm) has been approved by the FDA (U.S. Food and Drug Administration) and the EMA (European Medicines Agency) for clinical practice. Visible blue light (approx. 400 nm) in aPDI penetrates the epithelial

barrier to a depth of approx. 1 mm ⁷⁵. However, it has been reported that visible blue light induces significant biological photodamage of the skin by exciting chromophores within the skin such as porphyrins, and melanin, overlapping with their absorption spectrum ⁷⁶. Red light (>600 nm) works in the so-called 'therapeutic window' with deeper penetration into the dermis layer (~5 mm) and lower phototoxicity to human cells ⁷⁵. However, the pain effect of red light might be an obstacle to wide clinical application ⁷⁷. In the experiments presented in the thesis, I used one source of 522 nm (green light). Green light can compensate the disadvantages of red or blue light. Exposure to green light is less painful than red light in the treatment of facial solar keratoses ⁷⁸. Many studies also emphasized green light's role in reducing acute and chronic pain ^{79,80}. To date, aPDI applications have not significantly focused on using green light. The main reason is the narrow number of available and safe photosensitizers that can be effectively excited within those wavelengths. Without proper excitation of a photosensitizer, specifically in the absorption spectrum of the compound, the antimicrobial effect of aPDI may not be as effective as expected ⁸¹.

The ideal candidate for PS should exhibit photodynamic properties such as a high quantum yield of ROS production and a high molar absorption coefficient. Even more, the compound should have a lower toxic effect in the dark with a high phototoxic effect after illumination against microbial cells ^{61,72,82}. Even better, the PS structure's design is modified by adding cationic charges to promote greater efficacy towards Gram-negative representatives that are generally hard to eliminate ^{83,84}. The negatively charged outer membrane of bacteria might efficiently bind cationic PS. For Gram-positive bacteria, a positively charged compound might react with teichoic acids on the peptidoglycan ⁸⁵. Moreover, adding cationic charges into a neutral PS might influence its water solubility ⁸⁶. Another feature of an ideal antimicrobial PS is its selectivity for prokaryotic cells ⁶¹. Most porphyrins are good PS candidates, but their main disadvantage is poor water solubility, which may affect their effectiveness in the aPDI treatment due to the unstable concentration of the compound ⁸⁷.

A review by Akilov et al. highlighted the limitations of photosensitizers used in aPDI for anti-intracellular applications. One problem was the proper reaching of PS to the intracellular pathogen ⁸⁸. Crucial for effective elimination of the intracellular *S. aureus* is the simultaneous colocalization of a photosensitizer and the bacteria in the same intracellular cluster inside the host. Antibiotics do not achieve such colocalization through low penetration into the interior of eukaryotic cells ⁵⁹. Some photosensitizers i.e., porphyrins can penetrate inside eukaryotic cells mainly based on slow passive diffusion ⁸⁹. The accumulation time of photosensitizing compounds in eukaryotic cells is much longer (hours) than accumulation in bacteria (minutes) ⁶¹. After accumulation, the photosensitizer can be excreted externally by efflux pumps, metabolized, or accumulate in the cytoplasm or other intracellular clusters ⁸⁸. For instance, porphyrins are predominantly accumulated in the mitochondria ⁹⁰. In general, photosensitizers' intracellular fate depends mainly on its properties: its structure, the charge carried, hydrophilic and lipophilic properties ^{88,90}. To date, efficacy of aPDI against intracellular *S. aureus* has not been broadly studied. Metalloporphyrins such as gallium(III)-coordinated porphyrins (gallium

metalloporphyrins, Ga³⁺MPs) has not been explored in anti-intracellular approach so far. The metalloporphyrins may be an interesting photosensitizing agents to this approach due to their high similarity to heme. Heme (iron(III) protoporphyrin IX, Fe³⁺PPIX) is a natural source of essential iron for both eukaryotic and bacterial cells^{91,92}.

1.5. Dual-function gallium(III)-coordinated porphyrins: Trojan Horse strategy

In this subsection, I would like to characterize gallium(III)-coordinated porphyrins, which have a dual mechanism of action. In the light-independent action, gallium compounds might block the iron-dependent metabolism by mimicking the structure of the natural ligand – heme and in the light-dependent pathway, those compounds might work as photosensitizers in aPDI process (**Fig 3**). Ga³⁺MPs might be a good candidates for targeted PSs delivery due to their high similarity to heme.

Even though the mechanism of action of aPDI, which is based on the generation of ROS, does not focus on a specific molecular target in the cell, a new concept based on the directional delivery of PS to the bacterial cell has recently emerged¹⁰⁷. The action of targeted PSs is based on ligand-receptor interaction, whereas the designed compound mimics the natural ligand and might be recognized by the receptor on the bacterial surface^{93,94}. This targeted PS also improves the selectivity of compounds in *in vivo* approaches, assuring a safer therapeutic option in clinical practice⁹⁵. In a light-independent manner, Ga³⁺MPs can be recognized and acquired by specific receptors for heme and thus penetrate the cell as the Trojan Horse. Ga³⁺MPs uptake relies on the membrane heme-acquisition receptors, which recognize the compounds as a natural ligand – heme⁹⁶. Toxic gallium ions could be released inside the cells, just as iron ions are released from heme molecules. As a consequence of this process, iron-dependent cellular metabolism is blocked.

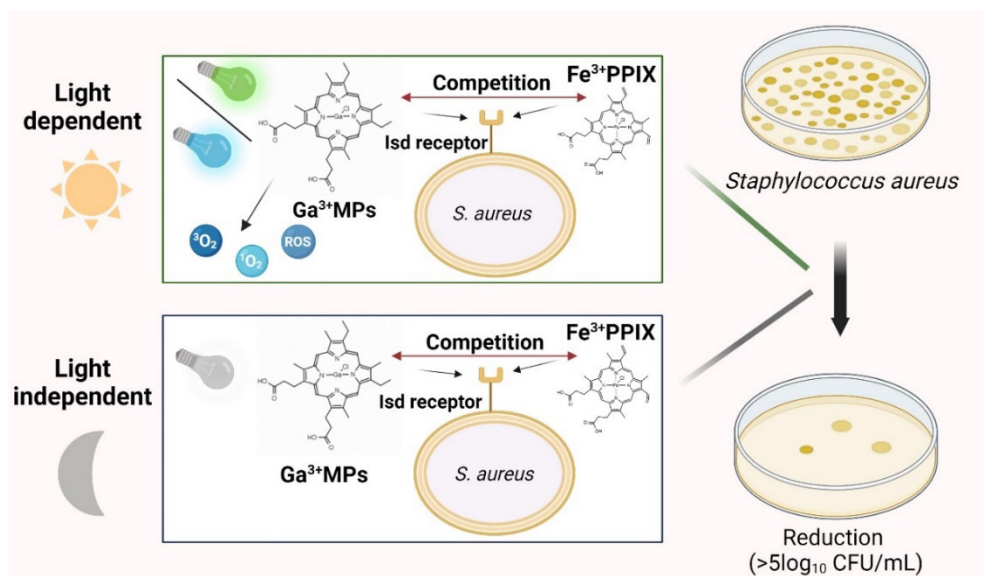


Fig 3. Dual-function of Ga³⁺MPs in light-dependent and light-independent action that reduce the *S. aureus* viability. Illustration created in software Biorender by K. Szymczak (2022).

After accumulation, gallium(III)-coordinated porphyrins might also work in a light-dependent action as photosensitizers due to the photodynamic properties of the porphyrin ring, i.e. absorption of light and subsequent generation of ROS. Gallium(III)-coordinated porphyrins could absorb the light in two characteristic regions of the absorption spectrum: Soret and Q-bands. The Soret region is the strong band at ~400 nm, standard to all porphyrins. At the same time, weaker-absorbing Q-bands are localized between 500-700 nm. The main difference between non-metal porphyrins and metalloporphyrins is that non-metal porphyrins possess four bands in the Q-region. In contrast, Ga³⁺MPs have only two bands in that area (**Fig 4**). In general, porphyrins are efficient photosensitizers with high photoproduction of singlet oxygen, acting mainly according to the Type II photodynamic reaction⁸⁷. Previous study has shown that gallium protoporphyrin IX (Ga³⁺PPIX) showed a high, >6 log₁₀ reduction in the number of *S. aureus* CFUs after blue light (405 nm) irradiation⁹⁷. However, there are no published reports on the antimicrobial efficacy after excitation of gallium(III)-coordinated porphyrins at the region of their Q-bands. For this purpose, we chose commercially available gallium mesoporphyrin IX (Ga³⁺MPIX) and cationic gallium porphyrin (Ga³⁺CHP), synthesized in collaboration with prof. Lei Zhang (Tianjin University, China)⁹⁸ (**Fig 4**). Excitation of these compounds in Q-bands with a lower absorption potential than the Soret region, using green light, may be a much safer therapeutic option for human cells and constitutes one of the novelties of the presented work.

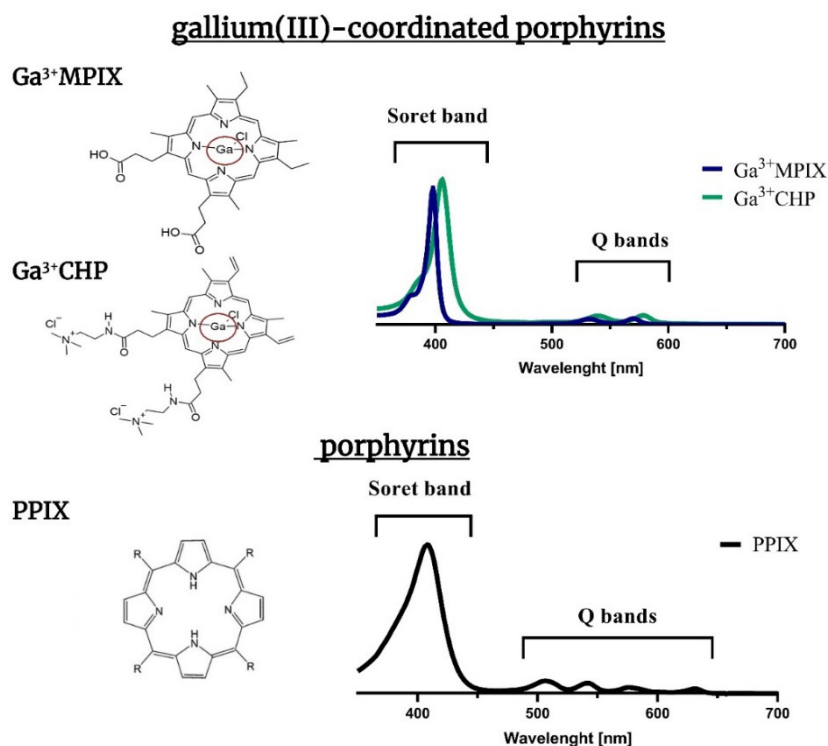


Fig 4. Structure and spectroscopic properties of gallium(III)-coordinated porphyrins (gallium mesoporphyrin IX ($\text{Ga}^{3+}\text{MPIX}$), the cationic gallium porphyrin (Ga^{3+}CHP)) and free non-metal porphyrins. Illustration created in software Biorender by K. Szymczak (2023).

1.6. Heme-acquisition machinery of *S. aureus* for targeted delivery of gallium porphyrins

In this subsection, I will briefly consider the role of the mechanism of heme acquisition by *S. aureus* for a deeper understanding of the Trojan Horse strategy of gallium metalloporphyrins uptake.

S. aureus has highly specialized receptors that allow it to uptake heme from the environment. Iron is essential in the pathogenesis and proper metabolism of bacteria; however, 99.9% of the iron in the host environment is structured in heme or bound in complexes with hemoglobin or haptoglobin^{99,100}. As a part of its survival in the host, *S. aureus* adapts to the increased need for iron uptake by efficiently producing heme uptake receptors⁹¹. Two systems to acquire exogenous heme are described – the heme transport system (Hts) and the iron-regulated surface determinant (Isd) system¹⁰¹.

So far, the Isd system is the best studied system of heme acquisition based on binding of free heme or heme complexes with proteins (**Fig 5**). Firstly, complexed heme is recognized by surface receptors IsdB and IsdH, while a free heme is bound mainly by IsdA¹⁰². All the proteins, IsdB, IsdH, and IsdA contain the highly conserved amino acid domains of Near Transporter (NEAT)⁹¹. The NEAT domains recognize heme by tyrosine residues. It was shown that porphyrins containing either Ga^{3+} or Mn^{3+} have high affinity to the NEAT domains of IsdH¹⁰³. Ga^{3+} protoporphyrin IX ($\text{Ga}^{3+}\text{PPIX}$) has a porphyrin ring with the central gallium ion at the oxidation state (III) that mimics the heme structure. The difference in the size

of metal ions between Fe^{3+} and Ga^{3+} is less than 5%, indicating their high similarity. Bacterial heme receptors cannot distinguish such minor differences between Ga^{3+} MPs and the natural ligand.

After recognition, heme is transferred to the cell wall localized IsdC receptor. Then, it is transmitted directly to IsdE lipoprotein, the component of the IsdDEF membrane transporter. IsdE passes heme to the IsdF, the ABC permease, that moves ligand through the membrane with energy derived from the ATP hydrolysis process of IsdD activity⁹¹. Heme is transferred to the cytoplasm, where the porphyrin ring of heme might be cleaved by two heme oxygenases – IsdG and IsdI to release free iron ions¹⁰⁴. After intracellular cleavage of accumulated Ga^{3+} MPs, gallium ions might be released, which could disturb the iron-dependent metabolism. Ga^{3+} ions could replace the Fe^{3+} ions in many enzymes where iron is a cofactor. Moreover, gallium can affect metabolic pathways and increase oxidative stress due to the overproduction of ROS¹⁰⁵. Literature data confirmed the antimicrobial action of gallium porphyrin (Ga^{3+} PPIX) in the light-independent pathway towards members of the ESKAPE group in both suspension and biofilm cultures^{106–112} and eliminated *Neisseria gonorrhoeae* in the murine model of vaginal infection¹¹³. This indicates that gallium porphyrins work as an antimicrobial agent with dual-functionality – not only as a photosensitizer in light-dependent action, but also it exhibited the dark toxicity in light-independent action. The combination of two pathways might be highly efficient against *S. aureus*.

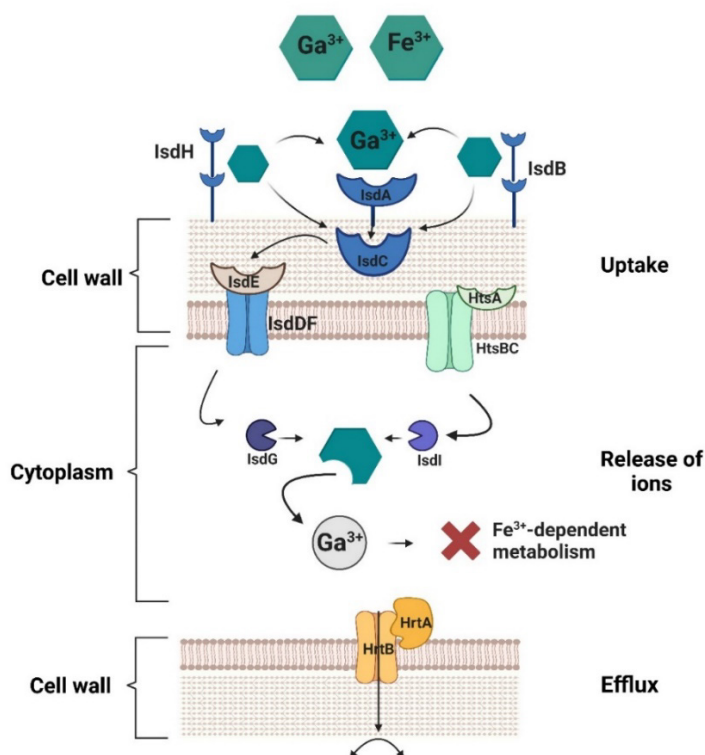


Fig 5. The Trojan Horse strategy of gallium porphyrins. Gallium(III)-coordinated porphyrins mimic the structure of heme (Fe^{3+} PPIX) that could be recognized by Isd or Hts heme-acquisition protein systems on the cell wall. In the cytoplasm, the porphyrin ring might be cleaved, and gallium ions could be released, disrupting the iron-dependent metabolism of *S. aureus*. Heme efflux pump (HrtAB) could

also play a role in the increased toxicity of gallium porphyrins. However, this is still poorly understood. Source: Illustration created in software Biorender by K. Szymczak (2023).

Although heme is a primary iron source for bacteria, its high intracellular accumulation can induce a cytotoxic effect ^{101,114}. A heme-regulated transporter (HrtAB) is an ABC-like transporter that works as an efflux pump for heme and/or heme degradation metabolites ⁹¹. The HrtA is an ATPase, while HrtB is a membrane transport channel ¹¹⁵. The heme sensor system (HssRS) controls the level of intracellular heme and regulates the activity of the HrtAB efflux pump as part of the adaptive response ¹¹⁶. However, there are findings that HrtAB is not a specialized efflux pump to metalloporphyrins despite their similarity to heme ¹¹⁷. Targeting HrtAB efflux pump might be a potential factor in increasing the toxicity of accumulated gallium metalloporphyrins.

1.7. Application of light-activated gallium metalloporphyrins on various *S. aureus* models

In this work, the antimicrobial efficacy of two modified gallium metalloporphyrins: Ga³⁺MPIX and Ga³⁺CHP in the light-independent and light-dependent action (aPDI) was investigated against *S. aureus* suspension cultures and staphylococcal biofilms grown *in vitro* or *ex vivo* on the porcine skin model. Moreover, during my experimental work, I established and characterized a cellular model of recurrent skin infections by infecting a cell line of immortalized human keratinocytes (HaCaT) with *S. aureus*. This developed infection model provides insights about the level of cellular adherence, internalization, and intracellular persistence of *S. aureus* within keratinocytes. I used this model to evaluate the potential of the aPDI method to eradicate intracellular *S. aureus*, which could contribute to the reduction of chronic infections.

In the recurrent skin infection model, the application of aPDI can be evaluated within three strategies, depending on the cycle of infection (**Fig 6**):

- I) aPDI affects *S. aureus* released from the originally infected cell, thereby lowering transmission to downstream host cells (**Fig. 6 Strategy 1**)
- II) aPDI affects the adhesion and internalization of *S. aureus* in keratinocytes (**Fig. 6 Strategy 2**)
- III) aPDI can eradicate intracellular bacteria (**Fig. 6 Strategy 3**)

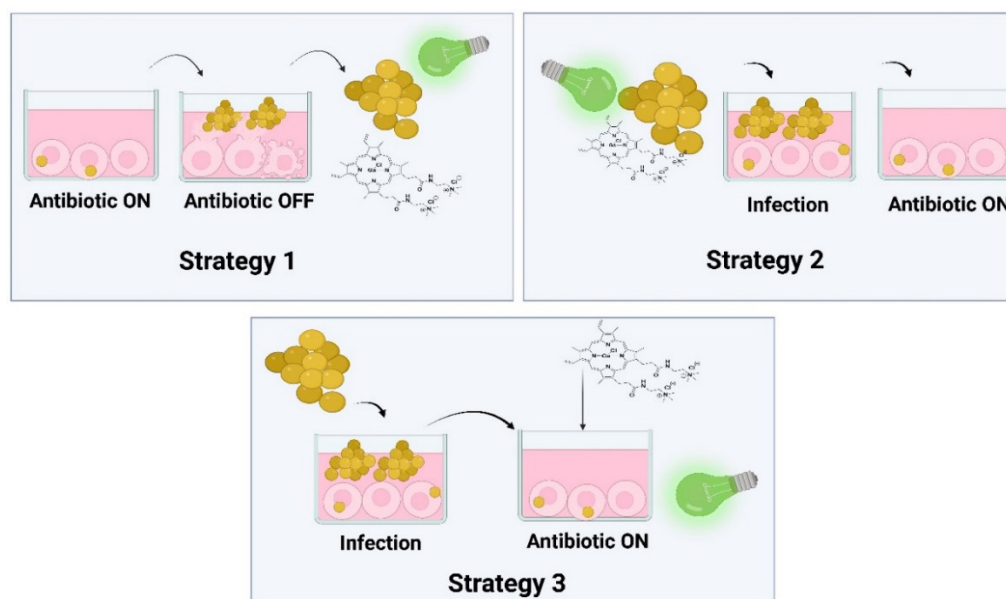


Fig 6. Strategies to implement light-activated gallium(III)-coordinated porphyrins to overcome *S. aureus* in the infection model. Strategy 1 involved applying aPDI to eliminate reinfections. Strategy 2 involved applying aPDI to *S. aureus* prior to cell infection to test its effect on bacterial adhesion and internalization in the host cells. In Strategy 3, photosensitizers were incubated in the dark to penetrate and localize inside host cells and then reach intracellular *S. aureus*. After incubation, cells were treated with light for elimination of intracellular *S. aureus*. Source: P3 Manuscript, K. Szymczak *et. al.* (2023).

Anti-intracellular therapeutic options could be used to overcome persistent or recurrent infections ¹¹⁸. So far, those approaches have been mainly based on modifying traditional antibiotics to improve their delivery to host cells using nanoparticles or liposomes ^{119,120}. Furthermore, researchers explored the conjugation of antibiotics with an antibody or active antimicrobial agent such as lysostaphin to target intracellular *S. aureus* ^{121,122}. Another method of approaching intracellular pathogens is indirect killing strategies based on boosting the host cells to more pronounced ROS production or activation of immune responses by silver nanoparticles, muramyl peptides exposure, or cold atmospheric plasma treatment ^{123,124}. Previous studies showed that the combination of a red light-activated silicon phthalocyanine conjugate with the cell-binding domain of phage endolysin (CBD3-700DX) was efficient against intracellular *S. aureus* in HeLa cells ¹²⁵. Another approach used gallium-substituted hemoglobin on silver nanoparticles to eliminate intracellular *S. aureus* within macrophages ¹²⁶. To date, aPDI has not been considered in anti-intracellular approaches in keratinocytes, the main cells that build the epidermis. In both studies, bioconjugated photosensitizer with other molecule – antibody or nanoparticles, were used as photosensitizing agent. In my dissertation, I focused on structural modifications of gallium(III)-coordinated porphyrins that might improve their photophysical properties, which could affect their accumulation into host intracellular clusters. So far, gallium(III)-coordinated porphyrins alone has not been considered as a photosensitizing agent for an anti-intracellular approach. I analyzed the accumulation of both modified Ga³⁺MPs derivatives to select a compound that strongly accumulates in intracellular clusters

and could potentially reach the intracellular *S. aureus*. In previous anti-intracellular approaches, aPDI toxicity studies of anti-intracellular approach were limited only to uninfected cells viability studies in a narrow time frame^{125,126}. In my thesis, I focused on comparing the phototoxicity of aPDI (Ga³⁺CHP and green light) on both infected and uninfected cultures with real-time growth analysis at each point: cells seeding, infection with *S. aureus*, post-infection, Ga³⁺CHP dark incubation, before and after aPDI treatment. I considered that infection itself can affect the rate of proliferation, the rate of photodamage repair and overall survival after aPDI treatment.

Viewing all results from this dissertation, we can effectively evaluate the broad antimicrobial potential of light-activated gallium(III)-coordinated porphyrins in multiple strategies of application towards *Staphylococcus aureus*, which is also an anti-intracellular approach.

2. Objectives

The presented dissertation focuses on investigating whether antimicrobial photodynamic inactivation (aPDI), defined as the combination of porphyrins coordinated with gallium ions as photosensitizers and green light, can contribute to reducing the virulence and survival of multidrug-resistant *Staphylococcus aureus*. The experiments investigated two modified gallium metalloporphyrins: gallium mesoporphyrin IX ($\text{Ga}^{3+}\text{MPIX}$) and cationic gallium porphyrin (Ga^{3+}CHP).

The first part of this thesis compares the light-dependent antimicrobial efficacy of these two compounds against several *S. aureus* strains in suspension cultures and in biofilm. Furthermore, using *S. aureus* mutants for heme acquisition and detoxification, the level of compounds accumulation in bacterial cells and aPDI efficacy were analyzed.

In the second part of the thesis, the combination of each compound and light was made to reduce virulence factors produced such as staphylococcal enterotoxins.

The third part of my thesis presents three aPDI strategies and evaluates their effectiveness on a model of intracellular *S. aureus* infection in human keratinocytes (HaCaT) cells. These strategies analyze the effect of aPDI on adherence, internalization and efficacy in eliminating intracellular *S. aureus* infections.

This work focuses on achieving the following specific objectives:

1. Investigation of the efficacy of aPDI with $\text{Ga}^{3+}\text{MPIX}$ and Ga^{3+}CHP against *S. aureus* in suspension cultures and biofilm model,
2. Analysis of the impact of the heme acquisition (Isd, Hts) and detoxification (HrtAB) systems on the aPDI with gallium metalloporphyrins: $\text{Ga}^{3+}\text{MPIX}$ and Ga^{3+}CHP ,
3. Determination of the effect of aPDI with gallium metalloporphyrins on selected virulence factors produced by *S. aureus*,
4. Evaluation of the impact of aPDI with gallium metalloporphyrins on the adherence, internalization, and intracellular persistence of *S. aureus* in the recurrent infection model.

The results of my research presented in this doctoral dissertation are contained in three manuscripts (P1-P3). Manuscripts: P1 and P2 have been published in Molecular Pharmaceutics (Ed. American Chemical Society). Manuscript P3 was prepared for submission in the high impact journal. All three were included in the thesis and constitute a thematically coherent set of articles.

3. Publication no. 1

Gallium Mesoporphyrin IX-Mediated Photodestruction: A Pharmacological Trojan Horse Strategy To Eliminate Multidrug-Resistant *Staphylococcus aureus*

3.1 Summary of the publication

Gallium(III)-coordinated porphyrins are dual-functional compounds working in the light-dependent action as a photosensitizer, and with light-independent in the Trojan Horse strategy⁹⁶. Previous studies showed that gallium(III) protoporphyrin IX (Ga³⁺PPIX) was highly accumulated by heme Isd receptors and was effective against several *S. aureus* strains after excitation with blue (405 nm) light at the Soret peak⁹⁷. Studies have emerged that indicate that the visible blue light generates significant biological photodamage of skin by inducing the DNA damage⁷⁶. So far, the antimicrobial efficacy of aPDI treatment during the excitation of gallium(III)-coordinated porphyrins in the lower absorption Q-bands has not been studied. The green light, overlapping this region, represents a much safer light to human cells.

The aim of the study was to investigate the antimicrobial efficacy against *S. aureus* in the light-dependent pathway of two gallium metalloporphyrin derivatives upon excitation with Q-band at 522 nm. Two derivatives used for the study were: Ga³⁺PPIX and modified gallium mesoporphyrin IX (Ga³⁺MPIX) with minor rearrangements in groups at the periphery of the porphyrin macrocyclic structure. The study also evaluated how changes within the compound's structure would affect the solubility, absorption spectrum and compounds' recognition by Isd heme receptors in the light-independent action.

Within publication no. 1, the light-dependent (aPDI process) and light-independent (iron blocking mechanism) action against several *S. aureus* strains was compared between Ga³⁺PPIX and Ga³⁺MPIX. The vinyl group in the Ga³⁺PPIX structure was changed to ethyl in Ga³⁺MPIX, resulting in noticeable differences in absorption spectra. The Ga³⁺MPIX absorption peaks at the Q-band were shifted toward shorter wavelengths (λ_{\max} Ga³⁺MPIX = 532 nm and 570 nm vs. λ_{\max} Ga³⁺PPIX = 541 and 580 nm). As a result, the Ga³⁺MPs absorption better matched to the emission spectrum of the green light emitting diode (LED) used. Additionally, the change improved the solubility in aqueous solutions and efficacy in light-dependent action against *S. aureus*. Both compounds were efficient photogenerators of the singlet oxygen under green light excitation. The light-dependent action of Ga³⁺MPIX resulted in the eradication of bacteria (reduction >5 log₁₀ CFU/mL), while the efficacy of Ga³⁺PPIX was reflected only in sublethal reduction (0.3 – 1.8 log₁₀ CFU/mL). Both actions of Ga³⁺MPIX exhibited relative safety for human keratinocytes with no extensive or prolonged cyto- and photo-toxicity. **This indicates that the green light excitation in the Q-band region of Ga³⁺MPIX was effective as an antibacterial method and a safer therapeutic option for eukaryotic cells.** So far, both blue and red lights had been used to excite porphyrins in a light-dependent photodynamic process¹²⁷. However, blue light exhibited significant toxicity and low

penetration, while the red light causes pain¹²⁸. Using the wavelengths corresponding to visible green light is a novel approach that balances those disadvantages. This study was the first to demonstrate the possibility of excitation of gallium metalloporphyrins in the lower absorption region that still showed high antimicrobial efficacy.

The efficacy of Ga³⁺MPIX-mediated aPDI and intracellular accumulation of the compound was strongly dependent on iron or heme availability. **Despite the change within the porphyrin structure, Ga³⁺MPIX could be recognized as a natural ligand by heme uptake system, preferably by Isd.** This study used *S. aureus* mutants in the heme-acquisition machinery (Δ IsdD, Δ HtsA) or heme efflux pump (Δ HrtA) to evaluate their role in the accumulation and photodynamic process. The impairment in the heme efflux pump revealed as the most sensitive phenotype to Ga³⁺MPIX in both light-dependent and light-independent action.

In conclusion, the change in porphyrin ring structure (ethyl groups replaced by vinyl groups), continues to mimic the ability of the compound to be recognized by the heme uptake systems making the Trojan Horse strategy a viable option to target *S. aureus*. Ga³⁺MPIX maintained dual functionality in light-dependent and light-independent mechanisms of action. The introduced modifications significantly influenced the compound's solubility and increased the antimicrobial effectiveness in the photodynamic process against *S. aureus*. It has been shown for the first time that gallium(III)-coordinated porphyrins exhibited antimicrobial efficacy when excited in lower absorption bands, with the green light that has lower eukaryotic toxicity.

3.2 Publication

For online version, please scan QR code of Publication no. 1:



Note: Supplementary material from Publication no. 1 can be found in section 9.1 (Attachments).

Gallium Mesoporphyrin IX-Mediated Photodestruction: A Pharmacological Trojan Horse Strategy To Eliminate Multidrug-Resistant *Staphylococcus aureus*

Klaudia Michalska, Michał Rychłowski, Martyna Krupińska, Grzegorz Szewczyk, Tadeusz Sarna, and Joanna Nakonieczna*



Cite This: *Mol. Pharmaceutics* 2022, 19, 1434–1448



Read Online

ACCESS |

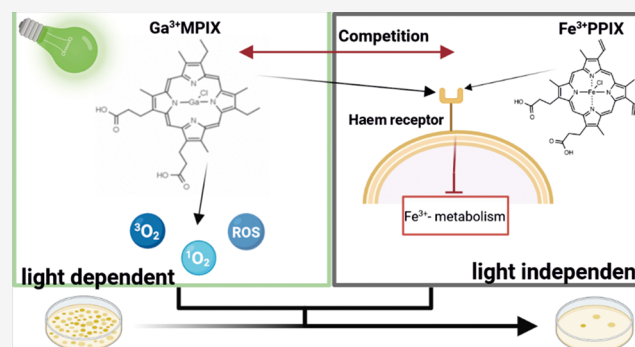
Metrics & More

Article Recommendations

Supporting Information

ABSTRACT: One of the factors determining efficient antimicrobial photodynamic inactivation (aPDI) is the accumulation of a light-activated compound, namely, a photosensitizer (PS). Targeted PS recognition is the approach based on the interaction between the membrane receptor on the bacterial surface and the PS, whereas the compound is efficiently accumulated by the same mechanism as the natural ligand. In this study, we showed that gallium mesoporphyrin IX (Ga^{3+} MPIX) provided dual functionality—iron metabolism disruption and PS properties in aPDI. Ga^{3+} MPIX induced efficient ($>5\log_{10}$ reduction in CFU/mL) bacterial photodestruction with excitation in the area of Q band absorption with relatively low eukaryotic cytotoxicity and phototoxicity. The Ga^{3+} MPIX is recognized by the same systems as haem by the iron-regulated surface determinant (Isd). However, the impairment in the ATPase of the haem detoxification efflux pump was the most sensitive to the Ga^{3+} MPIX-mediated aPDI phenotype. This indicates that changes within the metalloporphyrin structure (vinyl vs ethyl groups) did not significantly alter the properties of recognition of the compound but influenced its biophysical properties.

KEYWORDS: *isd system, photodynamic therapy, porphyrins, targeted delivery, MRSA*



INTRODUCTION

In 1928, Alexander Fleming discovered penicillin, which revolutionized medicine and improved the quality of human life. Currently, after almost 100 years, one of the main challenges for both the academic and pharmaceutical industries is antibiotic multidrug resistance (AMR). According to the report of O'Neil, 10 million deaths per year would be caused by AMR infections by 2050.¹ Antimicrobial photodynamic inactivation (aPDI), primarily used to photokill cancer cells,^{2–4} is now considered an alternative method for eradication of both Gram-positive and Gram-negative bacteria with different drug response profiles.^{5–7} The aPDI approach is based on three components: oxygen, light, which activates a dye known as a photosensitizer (PS). In an oxygen-rich environment, reactive oxygen species (ROS) might be generated through either energy (type II mechanism) or electron (type I mechanism) transfer from an irradiated PS. ROS generated in aPDI are cytotoxic because of their multitarget action on proteins, lipids, or nucleic acids. The ideal PS should exhibit low dark toxicity and high phototoxicity, which usually correlates with a high quantum yield of ROS photogeneration and application safety toward eukaryotic cells. Photodynamic

inactivation eradicates microbial species efficiently despite their drug resistance profile.^{8–10} Moreover, recent studies by Woźniak et al. revealed a synergy between photodynamic therapy and clinically used antimicrobials.^{11,12} aPDI has an impact on the production of virulence factors, which cause pathogens to be less virulent.^{13,14} Despite our recent studies of aPDI tolerance and an increased stress response upon consecutive cycles of sublethal treatments,^{15,16} resistance to photodestruction has not yet been observed. aPDI is efficient in both in vitro¹⁷ and in vivo studies.^{18,19}

The efficiency of aPDI might be dependent on PS uptake.^{20,21} PSs can accumulate in a different manner, depending on the wall structure of bacterial cells, environmental factors, and the type of the involved mechanism, for instance, active transport.²² The concept of targeted PS

Received: December 22, 2021

Revised: April 1, 2022

Accepted: April 1, 2022

Published: April 13, 2022



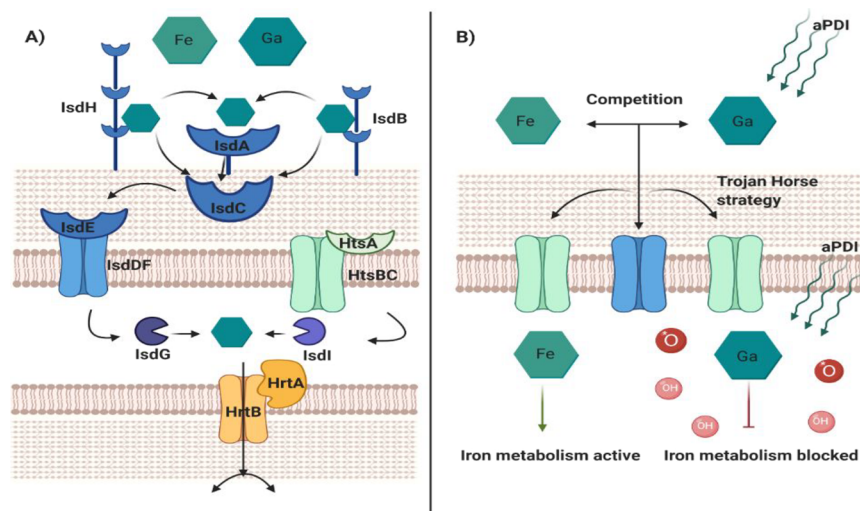


Figure 1. Haem acquisition machinery in *S. aureus* and proposed uptake of gallium³⁺ porphyrin conjugates via the Trojan Horse strategy. (A) In *S. aureus*, Fe³⁺protoporphyrin IX (known as haem) is recognized by Isd and Hts protein machineries. Haem complexed with hemoglobin or haptoglobin–hemoglobin is recognized and released by IsdB and IsdH cell wall-anchored receptors. Also, free haem in the environment is bound to IsdA and then transferred through the cell wall to membranes by IsdCDEF. Another uptake mechanism is known as HtsABC, which directly transfers haem from the cell wall to the cytoplasm. Haem oxygenases (IsdG and IsdI) recognize and cleave the porphyrin structure. In the higher level of haem, the HrtAB detoxification machinery is upregulated and acts as an efflux pump. (B) Because of the structural similarity between Fe³⁺protoporphyrin IX and gallium MPs, bacteria do not distinguish compounds and could take up gallium conjugates. Gallium MPs might work as “Trojan Horse” and disrupt bacterial cells by blocking iron metabolism. In addition, because of the porphyrin ring structure, those compounds generate ROS including singlet oxygen upon light exposure. (Created with BioRender)

recognition is based on PS uptake using membrane receptors, which recognize PSs as a similarly structured natural ligand. Proposed compounds for targeted PSs are metals conjugated with a protoporphyrin (metalloporphyrins, MPs).²³ The gallium protoporphyrin IX and gallium mesoporphyrin IX conjugates, formed with the metal oxidation state III, mimic the haem structure (Fe³⁺ protoporphyrin IX) and thus possibly bind to elements of haem acquisition machinery.^{24,25} Gallium compounds are active in disturbing iron metabolism by intracellularly accumulating via the Trojan Horse strategy (Figure 1B).^{23,26} Previous studies showed that Ga³⁺PPIX displayed light-independent antimicrobial activity against both Gram-positive and Gram-negative bacteria by blocking iron metabolism.^{26–31} Gallium MPs also demonstrated antibiofilm activity.^{32,33} Moreover, Ga³⁺PPIX exhibited antimicrobial photodynamic action against *Staphylococcus aureus*.^{34,35}

S. aureus is a Gram-positive member of ESKAPE pathogens that can effectively “escape” antibacterial drug action.³⁶ During infection, the pool of available iron is limited to pathogens such as *S. aureus*. To overcome the low iron availability, bacteria assimilate haem in either free form or bound in complexes with hemoglobin or haptoglobin in vivo (Figure 1A).³⁷ The classified mechanism of the *iron-regulated surface determinants* (Isd) or *haem transport system* (Hts) for acquiring iron ions from haem has been reviewed in detail previously.^{37,38} Briefly, IsdH and IsdB are primary receptors for haptoglobin–hemoglobin complexes or hemoglobin alone, respectively.³⁹ Both contain conserved *near transporter* domains that recognize and extract haem from the complex.⁴⁰ IsdA protein binds haem from the environment or receives the compound from IsdH or IsdB membrane receptors. Then, haem is transferred through the cell wall to the IsdC component and to IsdE, a membrane lipoprotein. IsdE acquires the haem and delivers it to IsdF, an ATP-binding cassette (ABC) permease. By ATP-hydrolyzing energy

produced by IsdD, haem is passed through the membrane to the cytoplasm, where IsdG and IsdI, haem oxygenases, release iron from the structure of haem.^{37,39,41,42} The second well-known iron assimilation machinery is the membrane-localized ABC transporter HtsABC. Hts works in a similar manner to the complex of IsdDEF. HtsA is a membrane-associated lipoprotein, while HtsBC are two ABC transporters. However, their role is described mostly in the transport of staphyloferrin A.^{38,41}

Paradoxically, haem itself may induce toxicity at higher concentrations.⁴³ The two-component *haem-regulated transporter* (HrtAB) detects and pumps an overdose of the compound out of the cell. HrtAB is an ABC-type transporter, where HrtA acts as an ATPase and HrtB is a permease with the role of a membrane transport channel.^{37,39,41} Deletion of genes encoding the HrtAB transporter revealed an impairment of bacterial growth under high concentrations of haem.⁴⁴ Efflux pump gene expression is regulated by the *haem sensor system* (HssRS), which is required for the adaptive response to haem.⁴⁵

Based on the existing knowledge concerning haem transport in *S. aureus*, we investigated whether Ga³⁺ mesoporphyrin IX (Ga³⁺MPIX) could accumulate and act as a PS against methicillin-resistant *Staphylococcus aureus*. To answer these questions, we evaluated the antimicrobial effect using Ga³⁺MPIX against several staphylococcal strains, including clinical isolates with the multidrug resistance (MDR) phenotype and haem acquisition mutants. Our hypothesis assumed that Ga³⁺MPIX can be efficiently accumulated or retained in *S. aureus* because of the presence or absence of specific haem transporters. In addition, the intracellular activity of Ga³⁺MPIX can act in two ways: independent of light (blocking haem metabolism) or dependent on light (photodynamic action).

EXPERIMENTAL SECTION

Bacterial Strains and Culture Media. This study was conducted with several *S. aureus* strains listed in Table 1.

Table 1. Staphylococcal Strains Used in This Study

| <i>S. aureus</i> strain | relevant characteristic(s) | source/reference |
|-------------------------|---|---|
| ATCC 25923 | reference strain | ATCC |
| 4046/13 | MDR strain (Table S1) | clinical blood isolate |
| 1814/06 | MDR strain (Table S1) | clinical blood isolate |
| Newman NCTC 8178 | wild-type (WT) strain | |
| Δ HtsA | Δ htsA via allelic replacement | 38 |
| Δ HrtA | Δ hrtA via allelic replacement | 44 |
| Δ IsdD | <i>isd::erm</i> | 37 |
| 5 N | <i>sec^c</i> , <i>tsst-1⁺</i> , spa type: t2223, MSSA strain | clinical nasal isolate from adult patients with atopic dermatitis |

Bacterial cultures were grown for 16–20 h with shaking (150 rpm) in either the iron-rich medium tryptic soy broth

(TSB) (Biomerieux, France) or iron-deficient TSB treated with Chelex-100 (Sigma–Aldrich, USA) and supplemented with 400 μ M MgSO₄. The *S. aureus* Δ IsdD strain was cultured in the presence of erythromycin 10 μ g mL⁻¹ (Fluka, Buchs, Switzerland).

Chemicals. Ga³⁺ mesoporphyrin IX chloride (Ga³⁺MPIX) (Figure 2B) and Ga³⁺ protoporphyrin IX chloride (Ga³⁺PPIX) (Figure 2B) were purchased from Frontier Scientific, USA; stock solutions were prepared according to manufacturer recommendations and kept in the dark at 4 °C. Ga³⁺MPIX was dissolved in 0.1 M NaOH to 1 mM concentration, whereas 1 mM stock of Ga³⁺PPIX was diluted in the mixture 50:50 (v:v) 0.1 M NaOH:DMSO Protoporphyrin IX (PPIX) was purchased from Sigma–Aldrich, USA (Figure S2A); a 1 mM solution was prepared in dimethyl sulfoxide (DMSO) and stored in the dark at room temperature. Protoporphyrin diarginate (PPIXArg₂, Figure S2B), delivered by the Institute of Optoelectronics, Military University of Technology, Poland, was dissolved in Milli-Q water and stored at -20 °C in darkness until use.¹⁰ Haem (Sigma–Aldrich, USA) was dissolved in 0.1 M NaOH solution and kept in the dark at 4 °C.

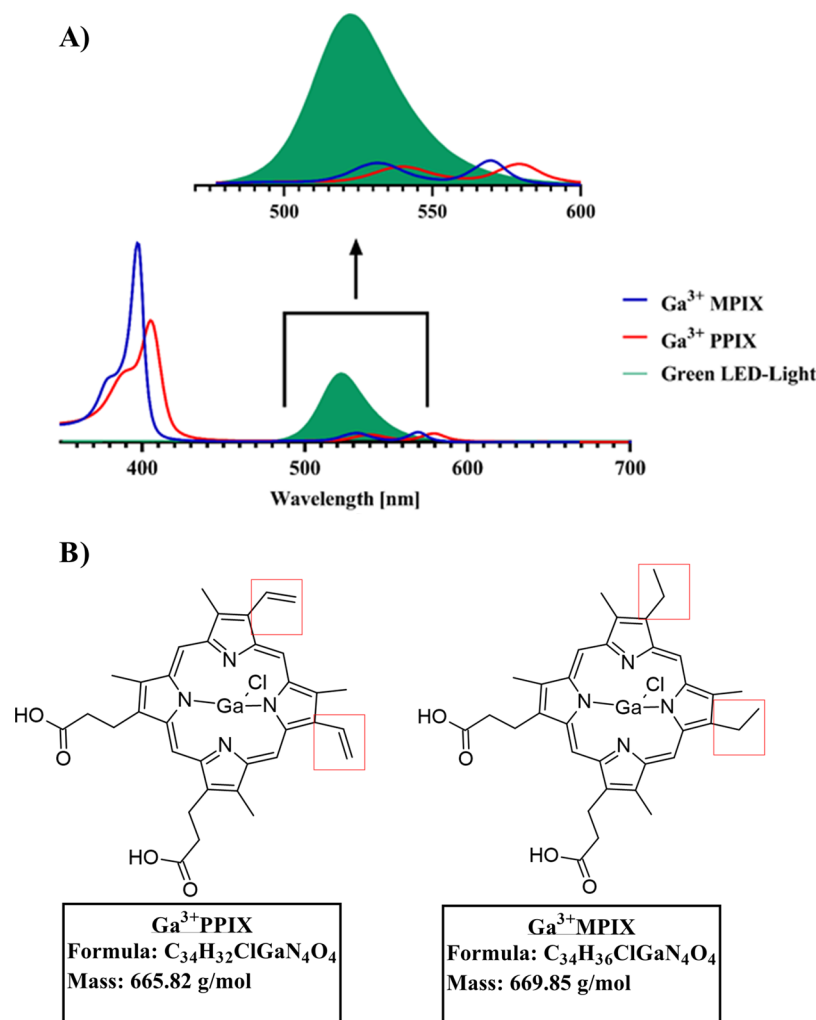


Figure 2. Characteristic of Ga³⁺PPIX and Ga³⁺MPIX. (A) Absorbance spectra of Ga³⁺PPIX and Ga³⁺MPIX titrated to PBS buffer with the imposed scheme of the emission spectrum of a green LED light source used in this study (λ_{\max} = 522 nm, FWHM = 34 nm). (B) Ga³⁺PPIX and Ga³⁺MPIX chemical structure, created in ChemSketch. Graphics created in GraphPad Prism 9.

Light Source. Illumination was performed with a light-emitting diode (LED) light source, emitting green light ($\lambda_{\text{max}} = 522$ nm, irradiance = 10.6 mW/cm², FWHM = 34 nm, Figure 2A) (Cezos, Poland).

Photoinactivation Experiments. Microbial cultures were grown overnight in medium in the absence or presence of iron ion concentrations. Then, cultures were adjusted to an optical density of 0.5 McFarland units (McF) (approx 10⁷ CFU/mL) and transferred to a 96-well plate alone or with PS combined. The aPDI samples treated with Ga³⁺MPIX were incubated at 37 °C with shaking in the dark for 10 min and illuminated with different green light doses up to 31.8 J/cm². The number of colony-forming units (CFU/mL) was determined by serial dilutions of 10 μ L aliquots and plating bacterial cells on TSA plates. The control consisted of untreated bacteria. TSA plates were incubated at 37 °C for 16–20 h, and then CFU/mL were counted. Lethal and sublethal aPDI conditions were defined similarly to our previous studies.^{15,18} For competition testing, Ga³⁺MPIX was mixed with different concentrations of haem in a mixture with a volume ratio of 1:1 (v/v) and then incubated and irradiated as in photoinactivation experiments. Molar ratios of the studied molecules were as follows: (Ga³⁺MPIX:haem— μ M: μ M) 1:0, 1:1, 1:10, and 0:10. Each experiment was performed in three independent biological replicates.

Growth Curve Analysis. Overnight culture was diluted 1:20 (v/v) in TSB or TSB-Chelex medium. A chosen PS (Ga³⁺MPIX, Ga³⁺PPIX, PPIX, or PPIXArg₂) was added to 450 μ L aliquots of bacterial strain to a final concentration of 10 μ M. The control group of bacterial cells was not treated with any PS. Prepared samples were loaded into 48-well plates and then placed in an EnVision Multilabel Plate Reader (PerkinElmer, USA), where the optical density ($\lambda = 600$ nm) was measured every 30 min for 16 h with incubation at 37 °C with shaking (150 rpm).

Time-Resolved Detection of Singlet Oxygen Phosphorescence. A solution of the PSs in D₂O-based phosphate buffer containing a small amount of DMSO (pD adjusted to 7.8) in a 1 cm fluorescence cuvette (QA-1000; Hellma, Mullheim, Germany) was excited for 15 s with laser pulses at 532 nm, generated by an integrated nanosecond DSS Nd:YAG laser system equipped with a narrow-bandwidth optical parameter oscillator (NT242-1k-SH/SFG; Ekspla, Vilnius, Lithuania), operating at 1 kHz repetition rate. The near-infrared luminescence was measured perpendicularly to the excitation beam using a system described elsewhere.⁴⁶ At the excitation wavelength, the absorption of Ga³⁺MPIX was 0.196, while that of Ga³⁺PPIX was 0.235. The measurements were typically carried out in air-saturated solutions. To confirm the singlet oxygen nature of the detected phosphorescence, measurements were compared at 1215, 1270, and 1355 nm by employing additional dichroic narrow-band filters NBP, (NDC Infrared Engineering Ltd., Bates Road, Maldon, Essex, UK) and in the presence and absence of 5 mM sodium azide, a known quencher of singlet oxygen. Quantum yields of singlet oxygen photogeneration by the PSs were determined by comparative measurements of the initial intensities of 1270 nm phosphorescence induced by photoexcitation of rose bengal and the PSs with 532 nm laser pulses of increasing energies, using neutral density filters. The absorption of rose bengal solution, used as a standard of singlet oxygen photogeneration, was adjusted to match that of the examined PSs.

Electron Paramagnetic Resonance (EPR) Spin Trapping Measurements. EPR spin trapping was carried out using 100 mM 5,5-dimethyl-1-pyrroline N-oxide (DMPO) (Dojindo Kumamoto, Japan DMPO) as a spin trap. Samples containing DMPO and about 0.1 mM of the PSs in 70% DMSO/water with pH adjusted to neutral pH were placed in 0.3 mm-thick quartz EPR flat cells and irradiated in situ in a resonant cavity with green light (516–586 nm, 45 mW cm⁻²) derived from a 300 W high-pressure compact arc xenon illuminator (Cermanx, PE300CE-13FM/Module300W; PerkinElmer Opto-electronics, GmbH, Wiesbaden, Germany) equipped with a water filter, a heat reflecting mirror, a cut-off filter blocking light below 390 nm, and a green additive dichroic filter 585FD62-25 (Andover Corporation, Salem, NC, USA). The EPR measurements were carried out employing a Bruker-EMX AA spectrometer (Bruker BioSpin, Germany), using the following apparatus settings: 10.6 mW microwave power, 0.05 mT modulation amplitude, 332.4 mT center field, 8 mT scan field, and 84 s scan time. Simulations of EPR spectra were performed with EasySpin toolbox for Matlab.⁴⁷

MTT Survival Assay. HaCaT cells (CLS 300493) were seeded at a density of 1 \times 10⁴ cells per well in 96-well plates 24 h before the experiment. Cells were divided into two plates for light and dark treatment. Cells were grown in a standard humidified incubator at 37 °C in a 5% CO₂ atmosphere in Dulbecco's modified Eagle's medium (DMEM). Ga³⁺MPIX was added to a final concentration of 0–100 μ M and then incubated for 10 min at 37 °C in the dark. HaCaT cells were washed twice with PBS and covered with fresh PS-free DMEM. Next, the cells were illuminated with 522 nm light (dose: 31.8 J/cm²). Twenty-four hours post-treatment, MTT reagent [3-(4,5-dimethylthiazol-2-yl)-2,5-diphenyltetrazolium bromide] was added to the cells, and the assay was conducted.¹⁷ The results are presented as a fraction of untreated cells and calculated as the mean of three independent biological experiments with the standard deviation of the mean. The data were analyzed using two-way analysis of variance (ANOVA) and Tukey's multiple comparisons test in Graph-Pad software. A *p* value <0.05 indicated a significant difference.

Analysis of Real-Time Cell Growth Dynamics. HaCaT cells (CLS 300493) were seeded the day before treatment in seven technical replicates for each condition at a density of 1 \times 10⁴ per well on E-plate PET plates (ACEA Biosciences Inc., USA). Cells were grown in a standard humidified incubator at 37 °C and in a 5% CO₂ atmosphere in DMEM in the xCELLigence real-time cell analysis (RTCA) device (ACEA Biosciences Inc., USA).¹⁷ When cells were estimated to be in the exponential phase of growth (cell index (CI) = ~2), the experiment was conducted. The PS was added to the cells at a concentration of 0, 1, or 10 μ M and left for 10 min in the dark incubation at 37 °C. Then, the cells were washed twice with PBS, and the medium was changed to PS-free. Afterward, light-treated cells were exposed to 522 nm light (dose of light: 31.8 J/cm²). In the case of dark-treated cells, plates were incubated for the corresponding time of irradiation in the dark at room temperature. Then, the plates were returned to the xCELLigence device, and the cell index was measured every 10 min and recorded automatically until the cells reached the plateau phase under each condition.

PS Accumulation. Microbial overnight *S. aureus* cultures were adjusted to an optical density of 0.5 McF. Ga³⁺MPIX was added to 800 μ L bacterial aliquots to final concentrations in the range of 1–10 μ M. In a competition assay, bacterial

cultures were cultivated in TSB-Chelex medium and incubated with a mixture of PS and haem to obtain an appropriate ratio of concentrations. Samples were incubated for 10 min or 2 h at 37 °C in darkness with shaking. After incubation, the bacterial cells were washed twice with PBS, and lysates were prepared by incubating in a solution containing 0.1 M NaOH/1% sodium dodecyl sulfate (SDS) (w/v) for 24 h at room temperature to lyse cells. The fluorescence intensity of 100 μ L of each sample was measured in the dark in 96-well plates spectrophotometrically with the use of an EnVision Multilabel Plate Reader (PerkinElmer, USA). Intracellular accumulation of the PS was calculated based on its calibration curve prepared in lysis solution. Uptake values are presented as PS molecules accumulated per cell based on the accumulation protocol and the following formula.⁴⁸

$$\text{GaMPIX molecules per cell} = \frac{[\text{GaMPIX}]}{M_w \text{ GaMPIX}} \times \frac{\text{NA}}{\text{CFU}}$$

where [GaMPIX] is the concentration [g/mL] of molecules obtained from a calibration curve based on known concentrations of the compound, M_w is the molecular weight of GaMPIX (669.85 g/mol), NA is the Avogadro's number (6.023×10^{23}), and CFU is the colony-forming unit obtained using serial dilutions counted for 1 mL of the analyzed samples.

Confocal Microscopy Imaging. *S. aureus* Newman and its isogenic Δ HrtA, Δ HtsA, and Δ IsdD mutants were grown in either iron-rich or iron-poor medium overnight for 16–20 h. Then, microbial cultures were diluted to an optical density of 0.5 MacF units. Cells were incubated with 10 μ M Ga^{3+} MPIX for 2 h at 37 °C with shaking. In control cells, tested compounds were not added. Bacterial samples were washed once in PBS buffer. Afterward, cells were imaged using a Leica SP8X confocal laser scanning microscope with a 100 \times oil immersion lens with excitation at 405 nm and fluorescence emission at 551–701 nm (Leica, Germany).

Statistical Analysis. Statistical analysis was performed using GraphPad Prism 9 (GraphPad Software, Inc., CA, USA). Quantitative variables were characterized by the arithmetic mean and the standard deviation of the mean. Data were analyzed using two-way ANOVA and Tukey's multiple comparison test. A p value of <0.05 indicated a significant difference.

RESULTS

Gallium MPs Delayed Staphylococcal Growth Light-Independently. Previous studies on several MPs have revealed the broad spectrum of gallium ion toxicity by blocking iron metabolism.²³ We assumed that the presence of ethyl groups in the macrocycle structure of Ga^{3+} MPIX (instead of vinyl groups in Ga^{3+} PPIX) would not affect its toxicity. The growth of the *S. aureus* 25923 reference strain was compared after exposing cells to gallium MP (Ga^{3+} PPIX, Ga^{3+} MPIX) and non-MP (PPIX and PPIXArg₂) in incubation during constant cultivation in iron-rich medium (Figure 3, Table S2). A slower specific growth rate (μ_{max}) at the exponential phase was observed after exposure of the *S. aureus* 25923 strain to Ga^{3+} MPIX ($\mu_{\text{max}} = 0.15$) or Ga^{3+} PPIX ($\mu_{\text{max}} = 0.126$) compared to untreated cells ($\mu_{\text{max}} = 0.354$). Exposure to non-MPs such as PPIX ($\mu_{\text{max}} = 0.282$) or water-soluble PPIXArg₂ ($\mu_{\text{max}} = 0.282$) did not influence *S. aureus* 25923 growth. These observations confirm that despite the difference

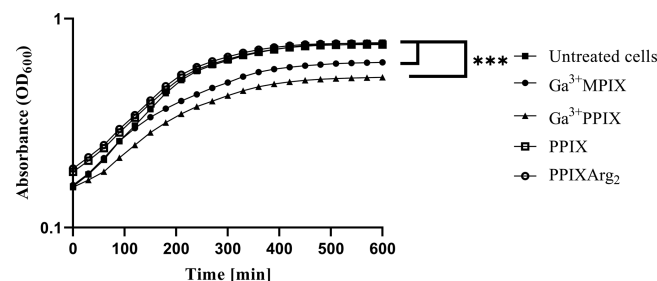


Figure 3. Staphylococcal growth under exposure to porphyrin compounds. Overnight cultures of the *S. aureus* 25923 reference strain in TSB medium were diluted 1:20 (v:v) and exposed to 10 μ M Ga^{3+} MPIX, Ga^{3+} PPIX, PPIX, or PPIXArg₂. The growth of each condition was monitored by measuring the optical density at 600 nm (OD_{600}) on an Envision plate reader. The experiment was conducted in three independent biological repetitions. Significance at the respective p -values is marked with asterisks (***) with respect to untreated *S. aureus* 25923 cells.

in the structure (ethyl groups vs vinyl groups), Ga^{3+} MPIX still induces dark toxicity against *S. aureus*, which is related to the presence of gallium ions in the compound.

Green-Light Irradiation of Ga^{3+} MPIX Generates ROS.

To check the mechanism underlying the photodynamic potential of Ga^{3+} MPIX, direct measurements of the PS ability to photogenerate ROS were performed.

Excitation of the PSs by 532 nm laser pulses induced phosphorescence that was strongly dependent on the observable wavelength (Figure 4A). Thus, intense phosphorescence was only observed at 1270 nm, which coincides with maximum emission of singlet oxygen in water. Although D₂O phosphate buffer was used, the apparent lifetime of the observed phosphorescence was about 40 μ s, which is shorter than that reported in pure D₂O. This shortening could be attributed to a small amount of DMSO and H₂O, which were used to prepare stock solutions of the PSs. Consistent with the singlet oxygen nature, the observed phosphorescence was significantly quenched by the addition of 5 mM azide (Figure 4B). The quencher reduced both the intensity and lifetime of the phosphorescence, which is most likely due to the quencher interaction with the triplet excited state of the PS and quenching of singlet oxygen. The final test of singlet oxygen nature of the 1270 nm phosphorescence is the effect of exchanging air for argon in the examined samples (Figure 4C). It is evident that saturating the PS solutions with argon completely abolished the singlet oxygen phosphorescence. A weak long-lasting phosphorescence detected in argon-saturated samples could be attributed to emissive relaxation of the porphyrin triplet excited states.

Quantum yields of singlet oxygen photogeneration of the examined PSs, employing rose bengal as a standard for singlet oxygen photogeneration with a yield of 0.75,⁴⁹ were determined to be very similar for both dyes—0.69 for Ga^{3+} MPIX and 0.67 for Ga^{3+} PPIX, indicating that in aqueous media these porphyrin derivatives are efficient photogenerators of singlet oxygen (Figure 4D,E).

Using EPR spin trapping, we were able to detect, after irradiation with green light (516–586 nm) of the PSs in a mixture of DMSO/H₂O, the spin adduct with spectral parameters consistent with that of DMPO-OOH, (AN = 1.327 ± 0.008 mT; AH α = 1.058 ± 0.006 mT; AH β = 0.131 ± 0.004 mT⁵⁰) indicating the photogeneration of super-

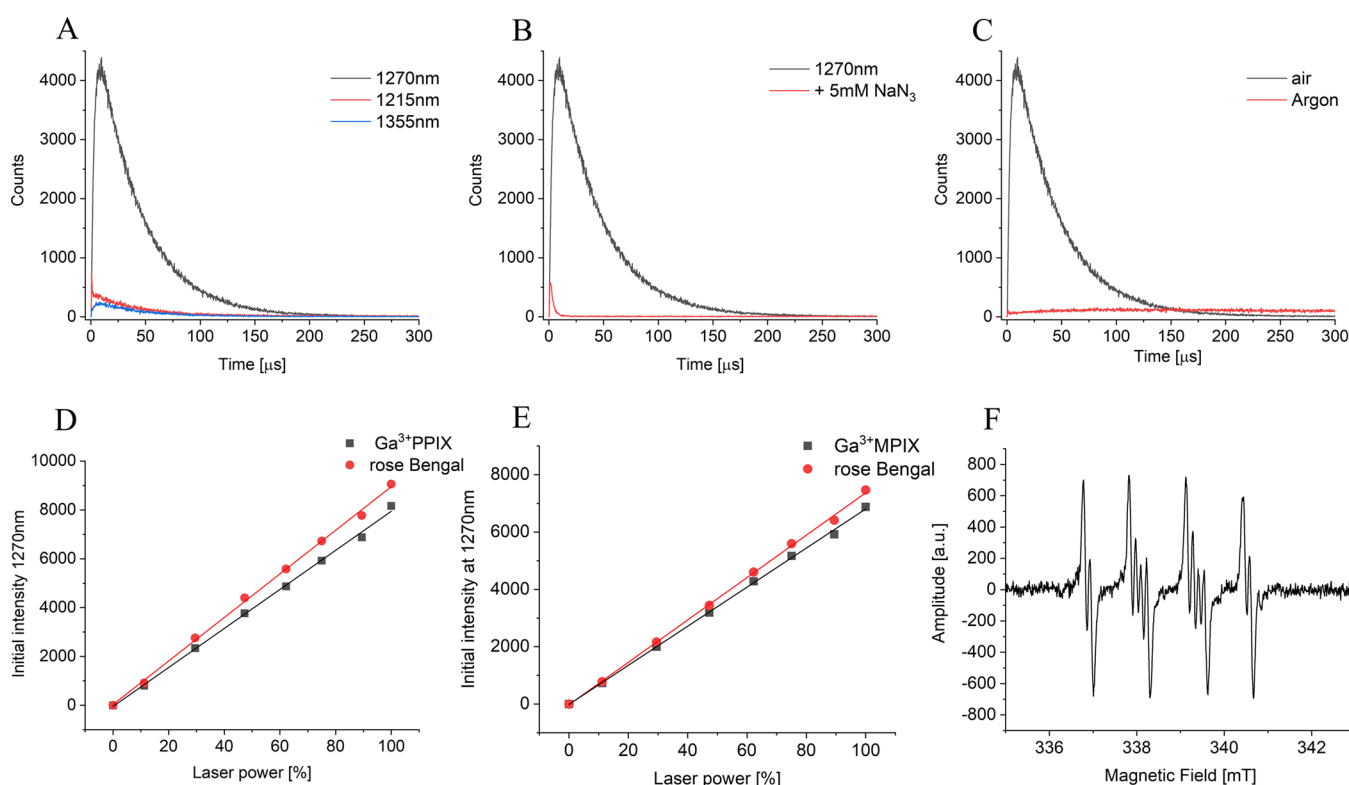


Figure 4. Direct detection of Ga³⁺MPIX- and Ga³⁺PPIX-generated ROS. Photoreactivity of Ga³⁺MPIX and Ga³⁺PPIX showing signals with 1270 nm wavelength, characteristic of singlet oxygen phosphorescence (A), with sodium azide, singlet oxygen quencher (B), and argon-saturated sample (C). Quantum yields of singlet oxygen photogeneration compared to rose bengal (D, E). Samples were irradiated with 532 nm laser light. Characteristic superoxide/DMPO adduct can also be observed with EPR spin trapping (F), although the signal was of low intensity.

Table 2. Phototreatment of *S. aureus* Strains with Ga³⁺PPIX or Ga³⁺MPIX with Green LED Light

| strain | mean reduction of survival (log ₁₀ CFU/mL) ^a ± SD | | | | |
|---------|---|--------------|-----------------------|--------------|--------------|
| | Ga ³⁺ MPIX | | Ga ³⁺ PPIX | | |
| | light (+) | light (-) | light (+) | light (-) | light-only |
| 25923 | 5.33 ± 0.065**** | 0.022 ± 0.03 | 1.11 ± 0.65* | -0.03 ± 0.08 | 0.21 ± 0.28 |
| 4046/13 | 4.1 ± 0.5*** | 0.05 ± 0.07 | 1.01 ± 0.15** | 0.04 ± 0.05 | 0.00 ± 0.03 |
| 1814/06 | 2.9 ± 0.24*** | 0.07 ± 0.11 | 1.83 ± 0.03*** | 0.22 ± 0.08 | 0.15 ± 0.16 |
| 5 N | 6.08 ± 0.1**** | -0.03 ± 0.16 | 0.34 ± 0.082 | -0.07 ± 0.1 | 0.077 ± 0.09 |

^aPhototreatment conditions: 10 min preincubation with 10 μM Ga³⁺PPIX or Ga³⁺MPIX at 37 °C with shaking without washing; green LED light 31.8 J/cm²; log₁₀ CFU/mL reduction was assessed with respect to nontreated cells, initial number of cells ~10⁷ CFU/mL. Light (+)—light-dependent; Light (-)—light-independent; light-only—bacterial cells irradiated without any PS applied. Significance at the respective *p*-values marked with asterisks: * = *p* < 0.05, ** = *p* < 0.01, *** = *p* < 0.001, and **** = *p* < 0.0001 with respect to “Light-only” treatment.

oxide anions (Figure 4F). While both PSs photogenerated, under the conditions used, a superoxide anion, Ga³⁺PPIX was a slightly more efficient generator of the oxygen radical. However, it must be stressed that the yield of generation of superoxide anions by the examined PSs is rather low and cannot be compared with their ability to photogenerate singlet oxygen.

The production of ROS in vitro has also been confirmed by the use of ROS detection probes (HPF and SOSG) after irradiation with two light doses, 12.72 and 31.8 J/cm², in the presence of Ga³⁺MPIX at two concentrations (Supplementary Figure S3A,B). We could observe quite a good correlation with the lower concentration of the compound used (1 μM). In both tested ROS types (HPF for radical detection and SOSG for singlet oxygen detection), we could observe that at a higher light dose (31.8 J/cm²) the signals for both probes were higher compared to the lower dose (12.72 J/cm²). However, at a

higher (10 μM) Ga³⁺MPIX concentration, this relationship is completely lost, which indicates that this is the maximum signal that can be obtained under our experimental conditions. Both ROS are generated during aPDI with Ga³⁺MPIX, which confirms the photodynamic properties of this compound.

In addition, using ROS quenchers, we examined the predominant types of ROS produced during aPDI in vivo, which are likely responsible for the observed death of bacterial cells. We used quenchers of free radicals predominantly formed by type I photochemistry (mannitol, superoxide dismutase), singlet oxygen generated by type II photochemistry (NaN₃), and ROS formed by mixed type I/II photochemistry (tryptophan, Trp). We observed cell protection after the use of the type II quencher NaN₃ and Trp, indicating that singlet oxygen was mainly responsible for cell death (Figure S3C). Interestingly, the enzyme catalase (CAT) also caused a statistically significant protection of bacterial cells against

Ga³⁺MPIX, which indicates the potential role of H₂O₂ in the Ga³⁺MPIX-mediated cell death process. On the contrary, mannitol, superoxide dismutase (SOD) did not provide significant protection. This is in agreement with the small amounts of photogenerated superoxide anions detected by EPR trapping. In summary, singlet oxygen appears to be the major ROS produced during Ga³⁺MPIX-mediated aPDI in vitro and in vivo, and the amount of singlet oxygen produced is comparable to Ga³⁺PPIX.

Phototreatment of *S. aureus* with Ga³⁺MPIX Reduced Bacterial Viability despite Divergent MDR Profiles.

Based on its absorbance spectrum, Ga³⁺MPIX might be excited by green LED light because of peaks called Q-bands, which are near the emission spectrum of the light source used (Figure 2A). However, the aPDI efficiency might differ among strains of *S. aureus*.⁹ Several staphylococcal strains with divergent MDR profiles and different origins were taken for further investigations with 10 μM Ga³⁺MPIX or Ga³⁺PPIX illuminated with green light. The results are presented in Table 2 as the means of viability reduction for a discriminating light dose of 31.8 J/cm². A reduction of more than 3 log₁₀ units in the number of CFUs (99.9%) was considered a bacterial eradication/lethal dose. However, sublethal doses were defined as a 0.5–2 log₁₀ reduction in CFU/mL.¹⁴ Light-only treatment and light-independent, 50 min exposure to 10 μM of each compound did not influence the bacterial viability. Ga³⁺MPIX revealed a higher efficiency in bacterial reduction upon green illumination than Ga³⁺PPIX. For Ga³⁺PPIX-mediated aPDI, only sublethal conditions were obtained, despite the 5 N strain, where sublethal reduction was not even reached. Ga³⁺MPIX-mediated aPDI resulted in bacterial eradication for strains: ATCC 25923, clinical isolate 5 N, and 4046/13. In the case of MDR strain 1814/06, aPDI with the Ga³⁺MPIX compound reduced bacterial viability, achieving lethal doses. The response to Ga³⁺MPIX-mediated aPDI is strain-dependent, however, independent of the MDR profile. Interestingly, the addition of a single wash step to the aPDI protocol influenced the effectiveness of aPDI, albeit in different ways (Supplementary Table S3). We observed that the inclusion of a single wash step in the photoinactivation protocol resulted in a better performance of Ga³⁺PPIX-mediated aPDI against bacteria. With Ga³⁺MPIX, the results were more diffuse, some strains were less efficiently photoinactivated, and others remained unchanged or increased. Nevertheless, the efficacy of Ga³⁺MPIX was still better than that of Ga³⁺PPIX. Because of the higher efficiency of Ga³⁺MPIX-mediated phototreatment under green light illumination, we chose this compound for further analysis.

Phototreatment of *S. aureus* with Ga³⁺MPIX Effectively Reduced Bacterial Viability in an Fe-Dependent Manner.

Limited availability of iron in the culture medium impacts the higher expression of certain iron-haem receptors.³⁷ To check the hypothesis that the observed efficiency of Ga³⁺MPIX-mediated aPDI might be due to similar recognition of Ga³⁺MPIX molecules by haem receptors, the survival of the *S. aureus* 25923 reference strain was examined upon green LED light irradiation with Ga³⁺MPIX upon cultivation in the absence (–Fe) or presence (+Fe) of iron in the medium (Figure 5). In iron-rich medium, we observed a maximum reduction in the number of bacteria of 4.6 log₁₀ units in CFU/mL for 1 μM at 31.8 J/cm². Compared to these data, in an iron-depleted medium, the maximum viability of bacteria was noticeable at the limit of detection, which was a 5.3 log₁₀ unit

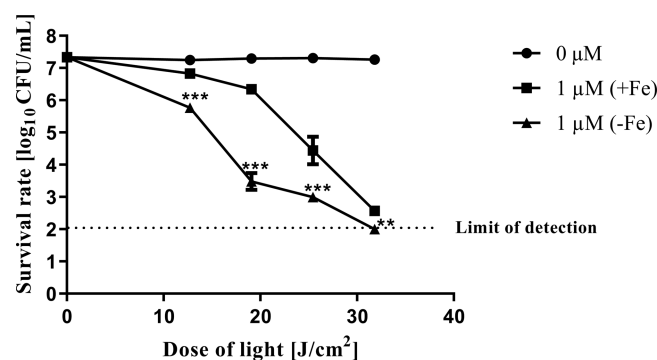


Figure 5. Photoinactivation of *S. aureus* 25923 with Ga³⁺MPIX in the presence and absence of iron. Overnight cultures of *S. aureus* 25923 strain were diluted to 0.5 MacF in medium with either the presence (+Fe) or absence (–Fe) of iron, then exposed to 0 or 1 μM Ga³⁺MPIX for 10 min at 37 °C, and then irradiated with different green LED light doses ranging from 0 to 31.8 J/cm². Colony-forming units (CFU/mL) were estimated with serial dilutions of 10 μL aliquots of irradiated samples and plated on TSA agar. Plots present the reduction of log₁₀ units of CFU/mL. The detection limit was 100 CFU/mL. Each experiment was performed in three biological experiments. The value is a mean of three separate experiments with bars as ± SD of the mean. Significance at the respective *p*-values is marked with asterisks [**p* < 0.05; ***p* < 0.01; ****p* < 0.001] with respect to 1 μM (+Fe) cells.

reduction in bacterial viability. Iron deficiency resulted in a higher efficiency of aPDI, with a 2.86 log₁₀ difference in bacterial viability at a sublethal dose of 12.72 J/cm² between two cultivation conditions. The efficiency of Ga³⁺MPIX-mediated aPDI is dependent on iron availability in the culture medium.

After phototreatment of *S. aureus* 25923 strain with Ga³⁺MPIX (1 μM, 25.4 J/cm²), surviving bacteria formed a small-colony variant (SCV) phenotype, which significantly differed from the original morphology. SCVs are classified as an atypical morphology with a lack of pigmentation, a smaller size, and a slower growth rate than the original cells. In iron-rich medium, only ~10% of the total pool of surviving bacteria formed SCVs with the same pigmentation as original cells before treatment (Figure S4AB). However, under iron-poor conditions, SCV cells constituted nearly 60% of the total number of surviving bacteria. Moreover, constant, 20-h exposure to Ga³⁺MPIX during culturing (without light) had induced the SCV morphology in 100% of survived bacteria (Figure S4C). Continuous iron starvation and exposure to Ga³⁺MPIX promoted the SCV phenotype, which indicated the effect on iron metabolism. Interestingly, the long exposure to Ga³⁺MPIX cells was efficiently eradicated after green light irradiation (Figure S4D–F), indicating that SCVs are sensitive to Ga³⁺MPIX-mediated aPDI.

Haem Has a Protective Effect on aPDI and the Accumulation of Ga³⁺MPIX. Porphyrins with central metals in the oxidation state (III) might mimic structural haem and have an affinity to haem receptors.²⁴ Ga³⁺MPIX might also be recognized by haem transporters and accumulate in a similar manner to haem. To determine whether the presence of haem influences the effectiveness of aPDI against *S. aureus*, we incubated bacterial cells with a mixture of haem and Ga³⁺MPIX and then irradiated them with lower (19.08 J/cm²) and higher (31.8 J/cm²) doses of light (Figure 6). By incubating cells with equal concentration or excess haem (1×

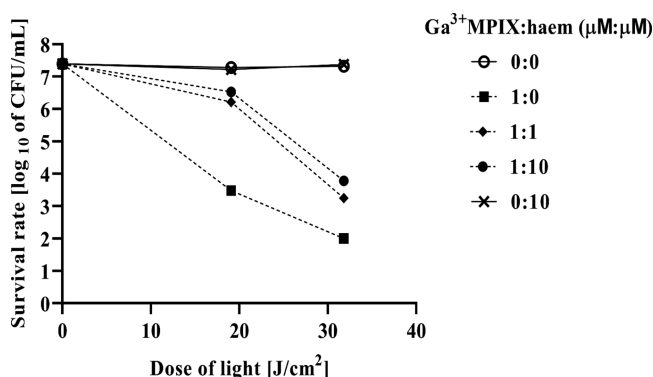


Figure 6. Protective effect of haem on Ga³⁺MPIX-mediated photodynamic treatment of the *S. aureus* ATCC 25923 strain. Iron-starved staphylococcal bacteria were incubated for 10 min with a mixture of Ga³⁺MPIX and haem at different ratios as indicated in the legend and then illuminated with a lower (19.08 J/cm²) or higher (31.8 J/cm²) dose of green light. Survival of bacteria was measured by serially diluting cells and counting the colony plated on agar plates after treatment (CFU/mL). The survival fraction is expressed as the number of CFU obtained after PDI treatment with respect to the number of CFU of nonlight-treated cells. The values are the means of three separate experiments. The value is a mean of three separate experiments with bars as \pm SD of the mean.

or 10 \times), we observed a protective effect, that is, much fewer bacterial cells were photoinactivated compared to the situation when there was no haem in the reaction mixture, exhibiting a decrease of 1.25 log₁₀ units in the reduction of CFU/mL for 1 and 1.7 log₁₀ for a 10 \times higher haem concentration. This effect was especially observed with a lower light dose (decrease in CFU reduction of 2.73 log₁₀ and 3 log₁₀ for 1- or 10-fold haem concentration). We did not observe a difference between the 1-fold and 10-fold excess haem used. The observed protective effect of haem may be related to more efficient accumulation of haem in bacterial cells and competition of haem molecules with Ga³⁺MPIX for binding sites in/on cells.

Next, we examined whether Ga³⁺MPIX accumulation in *S. aureus* is dependent on iron availability in the culture medium (Figure 7). In the absence of iron in the medium (−Fe), the

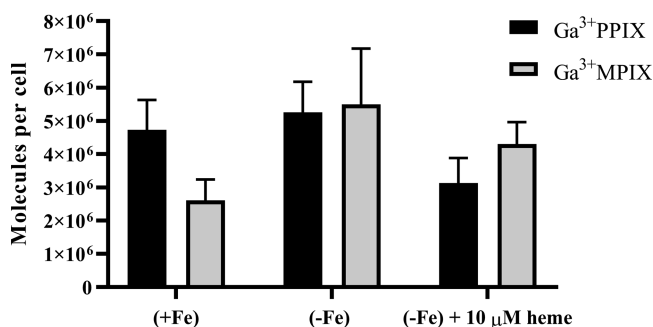


Figure 7. Uptake of Ga³⁺MPIX and Ga³⁺PPIX by the *S. aureus* ATCC 25923 strain in the presence (+Fe), absence (−Fe) of iron, or addition of haem. PS uptake was carried out in the presence of 10 μM of Ga³⁺MPIX or Ga³⁺PPIX. Bacterial cultures were incubated with the compound for 10 min at 37 °C with shaking followed by 24 h lysis as described in the Experimental Section, and then the fluorescence was measured. The value of the accumulated PS is represented as the number of molecules per cell, based on the standard curve of the compound in 0.1 M NaOH/1% SDS lysing buffer. The experiment was conducted in three independent biological repetitions.

intracellular accumulation of Ga³⁺MPIX at 10 μM was 2.1 times higher than the accumulation at the same compound concentration in the presence of iron (+Fe). The accumulation of Ga³⁺MPIX was dose-dependent (data not shown). Iron starvation of *S. aureus* promotes higher accumulation of the compound. Based on our results, we checked whether the protective effect of haem in aPDI treatment would be reflected as lower intracellular accumulation of PS. *S. aureus* was incubated with a mixture of Ga³⁺MPIX and haem at a protective concentration of 10 μM in the absence of iron. The addition of haem resulted in a decrease in Ga³⁺MPIX uptake by 22% (1.2 × 10⁶ molecules per cell) with respect to PS accumulation alone in the absence of iron. The accumulation of Ga³⁺MPIX is also dependent on the presence of haem in the culture medium. The addition of the ligand for haem recognition receptors decreased the uptake of Ga³⁺MPIX by *S. aureus* cells, although statistical significance was not achieved in this situation. These results together with haem protection from Ga³⁺MPIX-mediated phototoxicity confirm that Ga³⁺MPIX is recognized in the same manner as haem.

Under the tested conditions, Ga³⁺PPIX also accumulated in *S. aureus* cells in an iron-dependent manner. In the absence of iron in the medium (−Fe), the intracellular accumulation of Ga³⁺PPIX at 10 μM was 1.11 times higher than the accumulation at the same compound concentration in the presence of iron (+Fe). The addition of haem reduced the Ga³⁺PPIX uptake by 40% (2.3 × 10⁶ molecules per cell) with respect to the accumulation of PS in the absence of iron. It is worth noting that under standard conditions, that is, in the presence of iron, bacterial cells accumulated more Ga³⁺PPIX compared to Ga³⁺MPIX, which may explain the greater toxicity of Ga³⁺PPIX in light-independent survival tests (Figure 3).

Impairment in the HrtA Detoxification Efflux Pump Promotes Dark Toxicity of Ga³⁺MPIX. As the presence of haem influenced the level of Ga³⁺MPIX accumulation and aPDI efficiency, we hypothesized that haem acquisition machinery might also be involved in PS recognition. To understand the molecular mechanism responsible for the uptake and detoxification of gallium conjugates, we analyzed the growth of *S. aureus* Newman (WT) and its isogenic mutants deprived of genes engaged in haem uptake (Δ IsdD and Δ HtsA) and detoxification (Δ HrtA). The growth curves of *S. aureus* of each phenotype were analyzed after constant exposure to gallium MPs such as Ga³⁺MPIX or Ga³⁺PPIX (Figure 8) in an iron-rich environment. We compared several growth parameters such as maximum specific growth rate (μ_{\max}), duplication time (T_d) of the exponential phase and for the stationary phase: time to reach the stationary phase, and maximum density (A_{\max}) in each mutant after treatment with gallium compounds (Supplementary Table S4). Both compounds Ga³⁺PPIX and Ga³⁺MPIX reduced the μ_{\max} of each strain studied in a similar manner, that is, the highest inhibition was observed for Δ HrtA and Δ IsdD. Each treatment was compared to the control—untreated cells of each mutant (calculated as 100%). Despite gene deletion, untreated mutants achieved a similar growth rate to untreated WT. Under exposure to Ga³⁺PPIX, the growth of each strain at the end of the exponential phase (after 270 min of analysis, taken as the point of inhibition of the exponential growth—cutoff point) was estimated to be 72–77% of the growth of respective untreated controls, which indicated the higher toxicity of the compound. However, the main difference between mutants' growth was observed under Ga³⁺MPIX exposure. The WT,

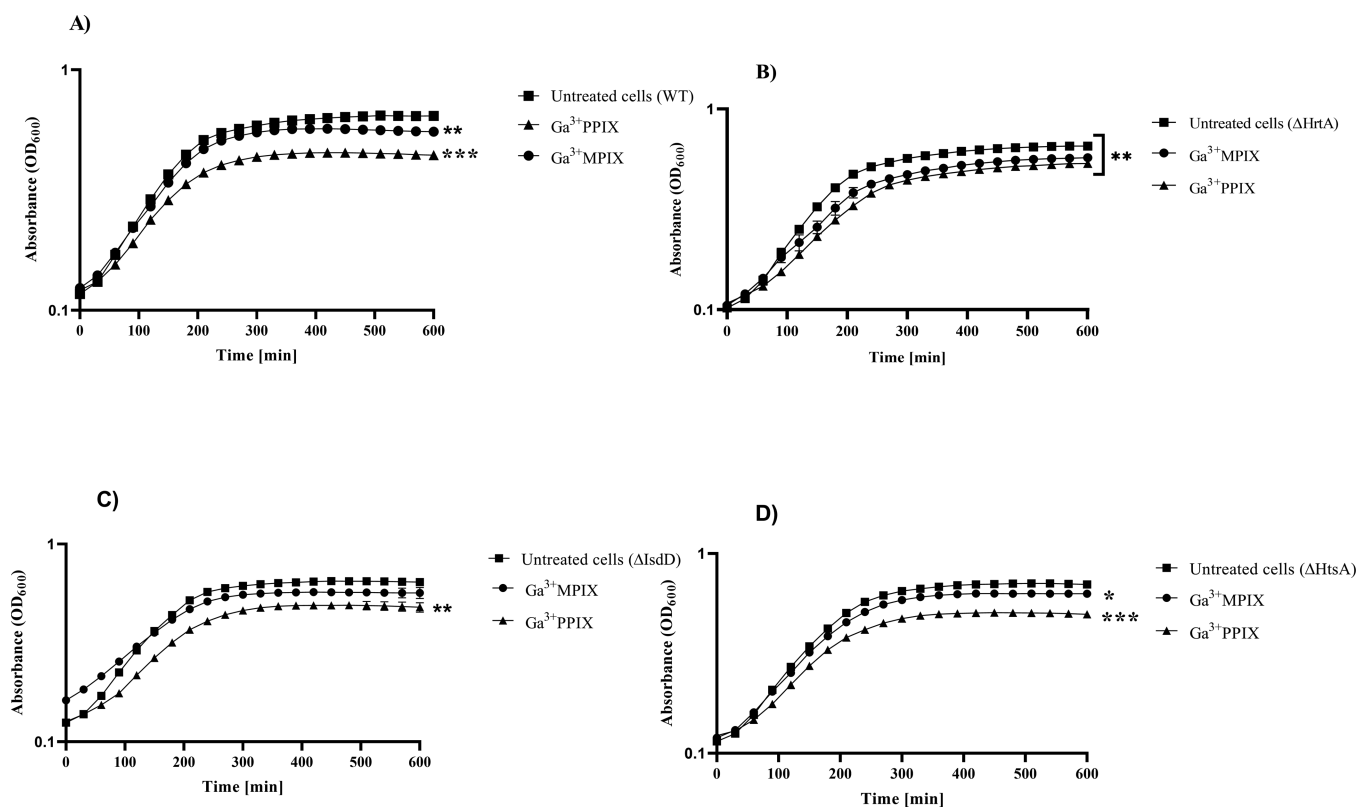


Figure 8. *S. aureus* Newman and its isogenic mutants (Δ HrtA, Δ IsdD, and Δ HtsA) grown under exposure to MP and non-MP compounds in the presence of iron in medium. Overnight cultures of *S. aureus* Newman WT (A), Δ HrtA (B), Δ IsdD (C), and Δ HtsA (D) in the iron-rich medium were diluted 1:20 and exposed for 10 μ M of Ga^{3+} MPIX, Ga^{3+} PPIX, or left untreated (untreated cells). Growth of each condition was monitored by measurement of optical density at 600 nm (OD_{600}) on an Envision plate reader. Experiment was conducted on three independent biological repetitions. Error bars represent the SD values. Significance at the respective p -values is marked with asterisks [$*p < 0.05$; $**p < 0.01$; $***p < 0.001$] with respect to untreated cells of each phenotype.

Δ IsdD, and Δ HtsA strain grew up to 90–93% in a medium containing Ga^{3+} MPIX, whereas in Δ HrtA it was only 82%, thus indicating that Ga^{3+} MPIX was the most toxic for this mutant. Impairment in the HrtAB efflux pump resulted in the more pronounced toxicity of Ga^{3+} MPIX toward *S. aureus* in comparison to other phenotypes. Interestingly, a clear effect in the form of a significant extension of the doubling time (T_d) was also observed in relation to Δ IsdD, where Ga^{3+} MPIX toxicity resulted in an increased T_d parameter from 1.46 to 2.06 OD_{600}/h .

HrtA-Lacking Mutant Is the Most Sensitive Phenotype to Ga^{3+} MPIX-Mediated aPDI. In our previous studies on aPDI on the Newman WT strain and its isogenic mutants, Δ HrtA was the most susceptible to PPIX-mediated aPDI.⁴⁸ Here, we were interested in whether differences among haem transport mutants could also be observed in the sensitivity to Ga^{3+} MPIX-based aPDI. Therefore, we performed aPDI against *S. aureus* Newman and its isogenic mutants (10 μ M Ga^{3+} MPIX, 19.8–38.16 J/cm^2) in the presence (Figure 9A) and absence of iron (Figure 9B). We increased the dose of green light to 38.16 J/cm^2 to observe more pronounced differences between phenotypes. In the presence of iron, the maximal bacterial reduction in CFU/mL was observed as follows: 3.78 – Δ HrtA, 3.15 – Δ IsdD, 2.5 – Δ htsA, and 3.15 \log_{10} units for WT. In the absence of iron, the maximal reduction in CFU/mL was estimated to be 3.5 – Δ HrtA, 2.75 – Δ IsdD, 1.44 – Δ HtsA, and 1.5 \log_{10} units for WT. Interestingly, the absence of Fe^{3+} in the medium did not

significantly increase the efficiency of aPDI. Under both cultivation conditions, the Δ HrtA mutant presented the most PDI-sensitive phenotype. Moreover, the Δ HtsA mutant was the most resistant to aPDI treatment among all phenotypes. Taking these results together, impairment in HrtA ATPase in the HrtAB detoxification system provides higher sensitivity to Ga^{3+} MPIX-based aPDI.

To understand the mechanism of the superior efficiency of aPDI in the Δ HrtA mutant, the accumulation of Ga^{3+} MPIX was investigated in each phenotype. Briefly, bacterial cells were cultivated in different iron contents at the stationary phase of growth, diluted, and then incubated in the dark with PS for 2 h at 37 °C with shaking. Then, bacterial lysates were prepared and measured as described in the Experimental Section. In the presence of iron (+Fe), we did not observe significant differences in accumulation between the studied phenotypes (Figure 10). Iron starvation (–Fe) increased PS uptake in comparison to iron presence in the media for each phenotype, except for Δ IsdD, in which the accumulation remained at the same level. Ga^{3+} MPIX accumulation in Δ HrtA was 2-fold higher than that in the WT strain in the absence of iron. Additionally, the uptake of the PS was decreased by approximately 50% for Δ HtsA and 90% by Δ IsdD compared to the WT strain.

The use of fluorescence microscopy did not give unequivocal results; that is, a stronger fluorescence signal was observed for Δ HrtA and WT under both (+Fe) and (–Fe) conditions (Figures S5 and S6). In contrast, Δ IsdD and

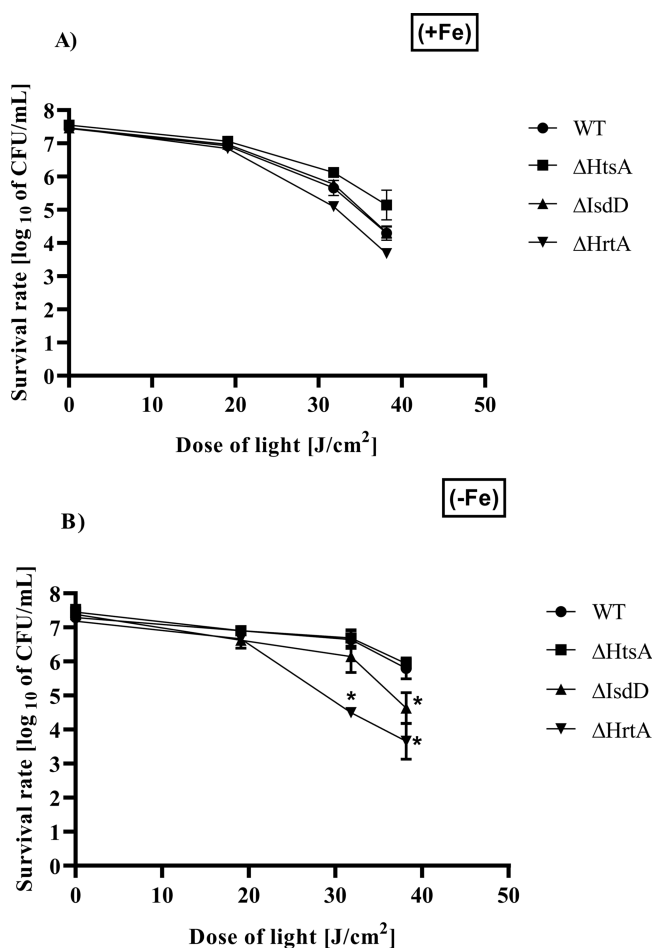


Figure 9. Phototreatment of *S. aureus* Newman and its isogenic mutants (Δ HrtA, Δ IsdD, and Δ HtsA) with $10 \mu\text{M}$ Ga^{3+} MPIX under green light irradiation in the presence (A) and absence (B) of Fe^{3+} in the medium. After incubation with $10 \mu\text{M}$ Ga^{3+} MPIX, the analyzed strains were subjected to green light (19.8 – 38.16 J/cm^2). Bacterial survivals were measured by serially diluting cells and counting the CFUs plated on agar plates after treatment. Each experiment was conducted in three independent biological experiments for every condition. The values represent the means of survived bacteria with bars as \pm SD of the mean. Significance at the respective p -values is marked with asterisks [$*p < 0.001$] with respect to WT cells.

Δ HtsA showed a stronger fluorescence signal under ($-\text{Fe}$) compared to ($+\text{Fe}$) (Figure S7). This indicates that the presence of Fe^{3+} influences Ga^{3+} MPIX uptake rather than removal from the cell.

Ga^{3+} MPIX Does Not Promote Extensive and Prolonged Cytotoxicity or Phototoxicity against Human Keratinocytes. PS safety toward eukaryotic cells is a crucial factor for optimization and further applications of photoinactivation protocols. We examined the phototoxicity and cytotoxicity of Ga^{3+} MPIX against human keratinocytes. Variations in concentrations of Ga^{3+} MPIX were used for treatment under both light and dark conditions with twice wash step (Figure 11) and once wash step (Figure S8). The highest dose of green light (31.8 J/cm^2) was selected, which corresponds to the bactericidal effect toward several *S. aureus* strains. Additionally, we increased the concentration of the PS up to $100 \mu\text{M}$ to ensure its high excess. Based on the MTT assay results in Figure 11A, the viability of cells was affected by neither the presence of Ga^{3+} MPIX alone (94.73 and 93.7%

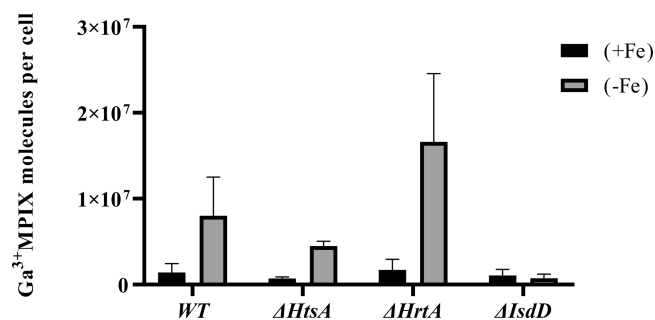


Figure 10. Ga^{3+} MPIX uptake in *S. aureus* Newman and its isogenic mutants (Δ HrtA, Δ IsdD, and Δ HtsA) in the presence ($+\text{Fe}$) or absence ($-\text{Fe}$) of Fe^{3+} in the medium. Overnight bacterial cultures of each phenotype were diluted and incubated with a PS for 2 h at 37°C with shaking and then, washed twice with PBS buffer and suspended in 0.1 M NaOH/ 1% SDS solution. After 24 h of incubation, the fluorescence of the lysate was measured (ex/em $398/573 \text{ nm}$). The values represented in the graph are the mean with SD of triple biological repetition for every strain in each condition.

survival upon 1 and $10 \mu\text{M}$) nor under green light irradiation (92.87 and 86.9% survival upon 1 or $10 \mu\text{M}$). Cell survival estimated at $\sim 80\%$ is considered acceptable, modest toxicity to eukaryotic cells.¹⁷ Increasing the compound concentration to $100 \mu\text{M}$ under green light showed significantly increased phototoxicity toward HaCaT cells (36.57% cell survival) in comparison to cells exposed only to light without the PS. In the dark, $100 \mu\text{M}$ Ga^{3+} MPIX had no significant impact on cell viability (estimated 92.55% survival). Ga^{3+} MPIX exhibited relative safety on HaCaT cell survival at 31.8 J/cm^2 green light irradiation up to $10 \mu\text{M}$ concentration.

However, cytotoxicity and phototoxicity were more pronounced when the cells were washed once compared to two times (Supplementary Figure S8A). After washing the cells once, a concentration of $100 \mu\text{M}$ Ga^{3+} MPIX (31.8 J/cm^2) almost completely reduced the number of the viable HaCaT cells, while approximately 50% of the cells survived the treatment with $10 \mu\text{M}$ Ga^{3+} MPIX (31.8 J/cm^2). The light-independent cytotoxicity decreased to approx 80% ($100 \mu\text{M}$) compared to the twice-washing procedure when this value was negligible.

However, the MTT assay has some methodological limitations, such as measuring only at a specific time point. Additionally, the cell proliferation rate and morphology were not taken into consideration. RTCA on E-plates is a method consisting of electrographic detection of the cell number, morphology, adhesion, and rate of proliferation under experimental conditions. Based on real-time cell growth dynamic curves (Figure 11B), we observed a slower proliferation rate of HaCaT cells after treatment with 1 or $10 \mu\text{M}$ Ga^{3+} MPIX under either dark or illumination conditions. Untreated cells resumed growth and reached the plateau phase at approximately the 60th h. Ga^{3+} MPIX dark-treated cells reached the plateau phase at approximately 85 h at $1 \mu\text{M}$ and 100 h at $10 \mu\text{M}$. After photodynamic treatment ($1 \mu\text{M}$ Ga^{3+} MPIX, 31.8 J/cm^2), HaCaT cells reached a plateau phase at the same hour as dark-treated cells at the same concentration of Ga^{3+} MPIX. A higher difference between light-exposed and dark-kept cells was observed in $10 \mu\text{M}$ Ga^{3+} MPIX, where the cell recovery phase was reduced, and the plateau phase was detected after 120 h . The cell proliferation rate and recovery were lowered in a concen-

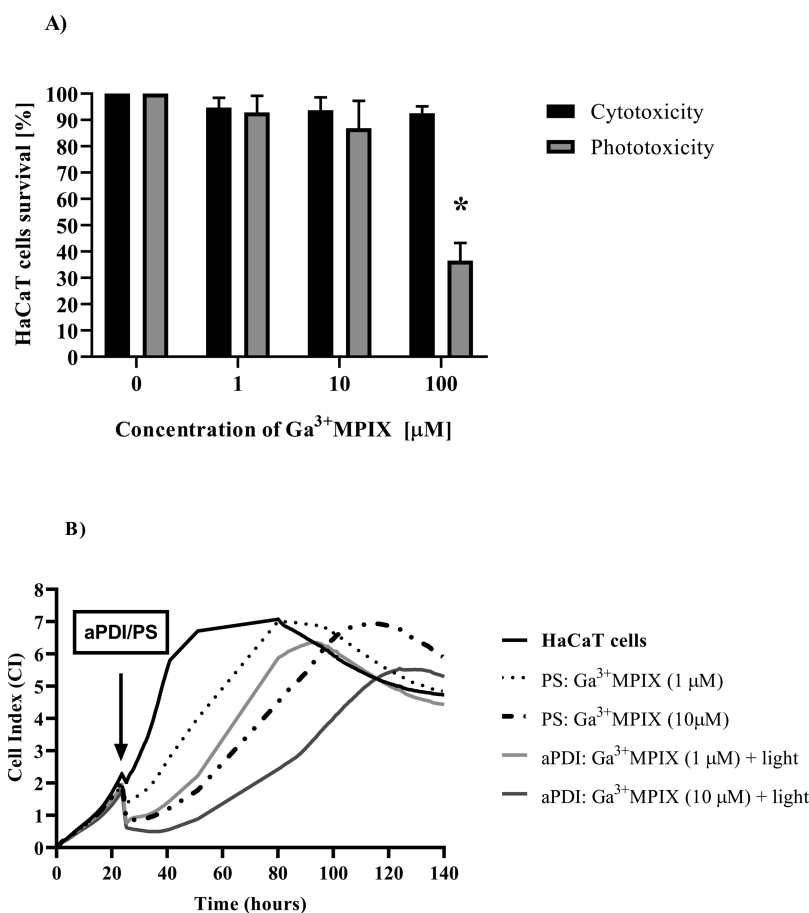


Figure 11. Effect of aPDI with Ga³⁺MPIX on the HaCaT cell line model. (A) MTT cell viability assay. HaCaT cells were exposed to various concentrations of Ga³⁺MPIX. Control cells (0 μM) to which no test compound was added. After incubation with Ga³⁺MPIX, cells were either irradiated with green light (31.8 J/cm²) represented by gray bars (Phototoxicity) or kept simultaneously in the dark (black bars for cytotoxicity). Each result is the mean ± SD of the mean. Significance at the respective *p*-values is marked with asterisks (* *p* < 0.05) for untreated cells in each condition. (B) Cell growth dynamics. Cells were seeded at 10⁴ cells/well and after obtaining a CI of 2, cells were treated with Ga³⁺MPIX in the dark and incubated at 37 °C for 10 min. The samples were then illuminated with a green light dose of 31.8 J/cm², while the HaCaT cells or PS only treatment was allowed to incubate in the dark at room temperature. The CI (represented as the Y axis) was measured for each condition every 10 min. The x-axis shows the experimental duration in hours. The values presented are the average of the 7 technical repetitions.

tration-dependent manner. The illuminated PS provided higher inhibition of HaCaT growth dynamics than the PS in the dark. During aPDI treatment, a fraction of the cells was damaged, but in most aPDI-treated cells, the damage was repaired, and the cells continued to grow and divide. Growth dynamics of HaCaT cells after aPDI with one wash step instead of the two washes (Figure S8B) was similar, showing the highest phototoxicity for 10 μM Ga³⁺MPIX. Thus, we claim that Ga³⁺MPIX alone or under photodynamic treatment does not promote extensive and prolonged cytotoxicity or phototoxicity against human keratinocytes.

DISCUSSION

Targeted PS recognition in aPDI is a novel trend of action against microorganisms, which developed from the origin of cancer cell phototreatments.⁵¹ Based on the Trojan Horse strategy of action, gallium MPs could be potent antimicrobial agents. Recognized by bacterial cells in the same manner as the natural ligand haem, gallium compounds might interrupt haem/iron metabolism.²³ Many studies have only confirmed the activity of gallium MPs toward several ESKAPE pathogens, including antimicrobial and antibiofilm action.^{25,26,28,29} Ga³⁺MPIX resulted in the same MIC value for *S. aureus* (1.6

μg/mL) as Ga³⁺PPIX.²³ Interestingly, porphyrins without metal ions (i.e., PPIX and MPPIX) were not efficient inhibitors of bacterial growth.²³ The rationale for choosing Ga³⁺MPIX for our research stems from studies on metalloporphyrins which showed effective induction of HrtAB, a molecular haem transport system. Previous studies on metalloporphyrin toxicity and the molecular mechanism underlying this process have shown that the HssRS—haem detoxification system is quite widely activated by metalloporphyrins, while the HrtAB efflux pump will only be sensitive to certain metalloporphyrins, in particular Ga³⁺PPIX or Mn³⁺PPIX.⁵² These observations prompted us to investigate the accumulation in cells and efficacy of the Ga³⁺MPIX compound in aPDI, excitation in a spectrum which is not commonly used in research, that is, green light. In particular, we were interested in studying the functionality of the vinyl group (protoporphyrin IX) to ethyl group (mesoporphyrin IX) change in the porphyrin macrocycle, as from the literature to date, the modification of the side compound chains was presented with minor interest, such as changes inside the porphyrin ring (i.e., central metal^{34,53}). We hypothesized that despite this difference, Ga³⁺MPIX might be recognized by haem receptors, and consequently, released gallium ions induce dark toxicity similar to Ga³⁺PPIX. The

dependence of the accumulation of Ga³⁺MPIX in bacterial cells on iron and the protective role of haem in aPDI indicates competition for binding with haem receptors and shows that specific haem transport systems into or out of the cell may play a role in the photoinactivation process. This is because bacteria do not distinguish some MPs from their natural ligand, the haem, and use them in their natural metabolic processes leading to inhibition of cell growth and death. Previously published data showed that only some MPs can do this, for example, Ga³⁺PPIX³⁴ and Mn³⁺PPIX.⁵² Here, we showed that Ga³⁺MPIX can also behave in a similar manner. Furthermore, the molecular structure of the MPs to be used as a substrate for the targeted delivery to bacterial cells is of primary importance. Previously published data indicated that porphyrin ring ion groups (carboxyl) have been shown to be important for interactions with haem uptake systems. Replacing them with esters that cannot be ionized has resulted in the loss of selective uptake by haem extraction systems to the advantage of nonspecific uptake.³⁴ In our experiments, the transition from more hydrophobic vinyl (in Ga³⁺PPIX) to less hydrophobic ethyl (in Ga³⁺MPIX) groups in the porphyrin macrocycle resulted in several different behaviors, including solubility, absorption, but also accumulation and photoinactivation.

The two molecules Ga³⁺MPIX and Ga³⁺PPIX are similar in terms of their general structure (the only difference being vinyl vs ethyl groups) and production of singlet oxygen (in aqueous solution), yet they differ in light-dependent (significantly) and light-independent (slightly) activity. The observed difference between the activity of both compounds without light is most likely due to the more effective accumulation of Ga³⁺PPIX than Ga³⁺MPIX (Figure 7) which results in a greater reduction in the growth rate of bacterial cells (Figures 3 and 8). The chemical modification of the porphyrin macrocycle seems to alter the potency of these compounds to regulate haem metabolism in vivo. Those molecules may differently react with their molecular targets in the bacterial cells, which results in the observed differences in the light-independent process. However, the issue of light-dependent action of the two compounds is more related to the biophysical properties of the compounds themselves. First, the differences in absorption spectra, although slight, are nevertheless noticeable. For Ga³⁺PPIX, the absorption maxima in the Q band region are $\lambda_{\max} = 541$ nm and $\lambda_{\max} = 580$ nm, while the analogous Ga³⁺MPIX maxima are $\lambda_{\max} = 532$ and $\lambda_{\max} = 570$ nm and are shifted toward shorter wavelengths. As a result, they better match the emission spectrum of the LED lights we used. The second and more important element explaining the different effectiveness of both compounds is the solubility in aqueous solutions. As is well known, porphyrin compounds do not readily dissolve in aqueous solvents. In our experiments, Ga³⁺MPIX dissolved much better in the aqueous solution (0.1 M NaOH titrated to PBS) than Ga³⁺PPIX. Ga³⁺PPIX in 0.1 M NaOH titrated to PBS generated a double peak, which is most likely responsible for the appearance of oligomeric forms in the solution (Figure S1). The addition of 50% DMSO shifted the equilibrium of monomeric and oligomeric forms toward the one resulting in a higher absorption signal (Figure S1) and most likely corresponding to a monomer.⁵⁴ Thus, the difference in the structure of both compounds (ethyl vs. vinyl groups) has a significant impact on their solubility in an aqueous solution. This feature is extremely important from a clinical point of view. From the available literature data, it appears that the difference between the activities of porphyrin

and mesoporphyrin was not that significant (estimated as at most 1 log₁₀)^{53,55} as observed in our experimental setup. It is worth noticing, however, that the elsewhere tested compounds were dissolved in solutions with the addition of DMSO, which strongly affects the solubility of protoporphyrin derivatives. Because of the potential clinical use of aPDI, photosensitizing compounds should be dissolved in aqueous solutions, avoiding the use of organic solvents. In this case, Ga³⁺MPIX meets this requirement and Ga³⁺PPIX does not.

The recent study of Morales-de-Echegaray et al. revealed the dual functionality of Ga³⁺PPIX. Despite gallium toxicity, these compounds might also act as PSs in aPDI upon blue light irradiation (405 nm, 140 mW/cm²) with maximal staphylococcal reduction >6 log₁₀ of bacterial viability.³⁴ The photodestruction was characterized as rapid (after 10 s of irradiation), and authors suggested that high-affinity surface hemin receptors such as the Isd system might have a role in the process.³⁴ Moreover, the Skaar group recently showed that anti-Isd monoclonal antibody together with aPDI proved to be effective against drug-resistant *S. aureus* in a murine model of soft tissue infections.⁵⁶ Based on the literature, the lack of iron upregulates the gene expression of haem receptors of the Isd system on the bacterial surface.²³ This might be the possible explanation for the higher aPDI efficiency, where Ga³⁺MPIX is recognized by Isd or Hts similarly to haem. We confirmed this by studying aPDI in an Fe-dependent manner (Figure 5), and we observed the protective effect of haem in the process of aPDI (Figure 6) or accumulation of Ga³⁺MPIX (Figure 7). In our study, the impairment of haem surface receptors, such as IsdD or HtsA, was manifested by a reduction in Ga³⁺MPIX accumulation as measured by two fluorescence methods. Based on these results, we hypothesized that despite the ethyl instead of vinyl groups in the side chains of the porphyrin structure, Ga³⁺MPIX is recognized by haem uptake receptors (mainly Isd) and is a competitor of haem. Impairment in the HrtA component of the efflux pump potentiated the effect of aPDI, and this effect was the most visible of all mutants tested, although many factors could influence its efficacy.⁵⁷ We previously reported that increased aPDI efficacy in Δ HrtA mutant can also be observed because of physical changes in the membrane composition and not the lack of functional protein.⁴⁸ The lipid content of the bacterial membrane might also contribute to the observed result in Ga³⁺MPIX-mediated aPDI.⁵⁷ However, the substrate of the HrtAB efflux pump or the molecular mechanism of detoxification of gallium MPs is currently unknown, and further studies in this area should be encouraged.

Most studies on the antimicrobial activity of Ga³⁺PPIX were conducted in a light-independent manner.^{23,27–29} Light-dependent action was demonstrated only for blue light with excitation in the Soret band (~405 nm).^{34,35} In this study, we propose the excitation of Ga³⁺MPIX within one of the Q-bands using green light. Green light ensures deeper tissue penetration than blue light while preserving sufficient energy to activate the compound. Moreover, the green LED lamp ($\lambda_{\max} = 522$ nm) exhibits a low light toxicity level toward bacterial cells themselves, as demonstrated in our current study. In light-only treatments, there was no pronounced excitation of endogenous porphyrins, so the aPDI effect was related to only exogenously applied PSs. In the case of Ga³⁺MPIX-mediated aPDI, we observed a maximal reduction in bacterial viability in the range of 3–6 log₁₀ (2–5 log₁₀ after a wash). This indicates that Ga³⁺MPIX has good efficiency against *S.*

aureus compared to other Ga³⁺PPIX excited with a shallow penetrating blue light.^{53,55} Because of the use of green light, it is potentially possible to photoinactivate bacteria that penetrate deeper layers of the skin than blue light. Verifying such an approach, however, would require additional research on more complex in vivo models.

Iron starvation alters bacterial metabolism by changes in the expression of several staphylococcal genes involved in iron acquisition, glycolysis, and virulence via a Fur-mediated mechanism. These changes are related to different colony phenotypes known as SCVs.⁵⁸ Based on previous research, MPs such as Ga³⁺PPIX induced this phenotype by inhibiting respiration or inducing oxidative stress, which was indistinguishable from genetic SCVs.⁵² The SCV phenotype appears to be responsible for chronic and recurrent infections and is also highly resistant to antibiotics.⁵⁹ We observed the presence of the SCV phenotype during 16–20 h of light-independent, constant cultivation of bacteria with Ga³⁺MPIX (Figure S4A–C). At the same time, it is worth noting that the exposure to Ga³⁺MPIX caused sensitization of SCVs to light and, as a result, the eradication of microbial cells upon green light (Figure S4D–F).

Red light is usually employed in photodynamic applications of porphyrins because of the depth of tissue penetration (dermis layers). The use of green light to treat superficial skin lesions seems particularly attractive. Because green light does not penetrate as deeply into the skin as red light causes much less pain during the irradiation in patients.⁶⁰ It penetrates only the epidermis without irritating the nerve fibers. Ga³⁺MPIX can be efficiently activated by green light without causing extensive and prolonged phototoxicity against HaCaT cells. Although, under our experimental conditions the observed phototoxicity seems to be higher compared to Ga³⁺PPIX published by others, where only minor phototoxicity was observed after blue light activation.³⁴ Ga³⁺MPIX under photodynamic treatment does not promote extensive phototoxicity against human keratinocytes; however, cells exhibit a slower proliferation rate than untreated cells. The cells with moderate or none photodamage resume growth and divide thus indicating that there is a place here for “therapeutic window.” The observed growth delay was not prolonged. These in vitro experiments confirmed the safety of Ga³⁺MPIX-mediated aPDI application to further studies on ex vivo models (e.g., porcine skin) or in vivo models (e.g., mouse models).

Research on photosensitizing compounds using natural bacterial cell transport systems is an extremely interesting path in the development of targeted PDI. The Trojan Horse strategy based on haem analogues, proposed years ago,²³ shows that discrete changes in the structure of PS molecules can significantly affect its properties and enable further development of this strategy against *S. aureus* infections.

CONCLUSIONS

In conclusion, Ga³⁺MPIX acts in two ways: independent of light (by blocking iron metabolism) or dependent on light (photodynamic action). This type of two-way mechanism of action provides very good protection against the selection of *S. aureus* mutants resistant to photodestruction. This study demonstrated that green light excitation of Ga³⁺MPIX in the Q band absorption area resulted in eradication of bacteria (reduction >Slog₁₀ CFU/mL) while maintaining relative safety for the eukaryotic cells tested. We have demonstrated that Ga³⁺MPIX-mediated aPDI exhibits Fe-dependent efficiency,

and haem has a protective effect, indicating the importance of specific haem transport systems in the aPDI system under study. We have shown that Ga³⁺MPIX, with ethyl groups in the porphyrin macrocycle instead of vinyl groups present in Ga³⁺PPIX, can be recognized by haem uptake machinery, preferably by Isd. Impairment in the HrtA efflux pump turned out to be the most sensitive to aPDI with Ga³⁺MPIX. This study showed that despite the structural changes around the porphyrin ring, Ga³⁺MPIX was able to sustain its dual functionality. In addition, these changes can improve other properties of the compound, such as a higher efficiency in the photodynamic action.

ASSOCIATED CONTENT

Supporting Information

The Supporting Information is available free of charge at <https://pubs.acs.org/doi/10.1021/acs.molpharmaceut.1c00993>.

Antibiotic resistance profiles and parameters describing the growth rate of the tested *S. aureus* strains, information on Ga³⁺MPIX and Ga³⁺PPIX absorbance spectra, ROS detection results with fluorescent probes in vitro and in vivo using ROS quenchers, photoinactivation of SCVs, accumulation of Ga³⁺MPIX under a confocal microscope, and cyto- and phototoxicity tests against *S. aureus* and HaCaT cells (single wash condition) (PDF)

AUTHOR INFORMATION

Corresponding Author

Joanna Nakonieczna – Laboratory of Photobiology and Molecular Diagnostics, Intercollegiate Faculty of Biotechnology, University of Gdansk and Medical University of Gdansk, Gdansk 80-307, Poland; orcid.org/0000-0002-2420-664X; Email: joanna.nakonieczna@biotech.ug.edu.pl

Authors

Klaudia Michalska – Laboratory of Photobiology and Molecular Diagnostics, Intercollegiate Faculty of Biotechnology, University of Gdansk and Medical University of Gdansk, Gdansk 80-307, Poland

Michał Rychłowski – Laboratory of Virus Molecular Biology, Intercollegiate Faculty of Biotechnology, University of Gdansk and Medical University of Gdansk, Gdansk 80-307, Poland

Martyna Krupińska – Laboratory of Photobiology and Molecular Diagnostics, Intercollegiate Faculty of Biotechnology, University of Gdansk and Medical University of Gdansk, Gdansk 80-307, Poland; orcid.org/0000-0002-4447-9143

Grzegorz Szewczyk – Department of Biophysics, Faculty of Biochemistry, Biophysics and Biotechnology, Jagiellonian University, Krakow 30-387, Poland

Tadeusz Sarna – Department of Biophysics, Faculty of Biochemistry, Biophysics and Biotechnology, Jagiellonian University, Krakow 30-387, Poland

Complete contact information is available at:

<https://pubs.acs.org/doi/10.1021/acs.molpharmaceut.1c00993>

Author Contributions

K.M. performed experiments, created the figures, performed statistical analysis, and wrote the manuscript, M.R. performed

the confocal microscopy images, M.K. performed screening of light-dependent and independent action on several *S. aureus* strains, G.S. and T.S. performed, wrote the section of direct detection of ROS generation and critically reviewed the manuscript, and J.N. was involved in the coordination, conception, and design of the study and wrote the manuscript. All authors have read and agreed to the published version of the manuscript.

Funding

This work was supported, in part, by UGrants—start (No.533-0C30-GS31-21 (KM)) funded by the University of Gdansk, and by SHENG (No. 2018/30/Q/NZ7/00181) funded by National Science Centre, Poland.

Notes

The authors declare no competing financial interest.

ACKNOWLEDGMENTS

The authors wish to thank Dr. Eric P. Skaar from the Department of Microbiology and Immunology at Vanderbilt University Medical Center for source of *S. aureus* Newman and its isogenic mutants.

REFERENCES

- (1) O'Neill, J. *Antimicrobial Resistance: Tackling a Crisis for the Health and Wealth of Nations The Review on Antimicrobial Resistance Chaired*. Rev. Antimicrob. Resist. 2014.
- (2) Macdonald, I. J.; Dougherty, T. J. Basic Principles of Photodynamic Therapy. *J. Porphyr. Phthalocyanines* **2001**, *05*, 105–129.
- (3) Juarranz, Á.; Jaén, P.; Sanz-Rodríguez, F.; Cuevas, J.; González, S. Photodynamic Therapy of Cancer. Basic Principles and Applications. *Clin. Transl. Oncol.* **2008**, *10*, 148–154.
- (4) Sharma, S. K.; Mroz, P.; Dai, T.; Huang, Y. Y.; Denis, T. G. S.; Hamblin, M. R. Photodynamic Therapy for Cancer and for Infections: What Is the Difference? *Isr. J. Chem.* **2012**, *52*, 691–705.
- (5) Maisch, T. A New Strategy to Destroy Antibiotic Resistant Microorganisms: Antimicrobial Photodynamic Treatment. *Mini. Rev. Med. Chem.* **2009**, *9*, 974–983.
- (6) Hamblin, M. R.; Hasan, T. Photodynamic Therapy: A New Antimicrobial Approach to Infectious Disease? *Photochem. Photobiol. Sci.* **2004**, *3*, 436–450.
- (7) Hamblin, M. R. Antimicrobial Photodynamic Inactivation: A Bright New Technique to Kill Resistant Microbes. *Curr. Opin. Microbiol.* **2016**, *33*, 67–73.
- (8) Grinholc, M.; Rapacka-Zdonczyk, A.; Rybak, B.; Szabados, F.; Bielawski, K. P. Multiresistant Strains Are as Susceptible to Photodynamic Inactivation as Their Naïve Counterparts: Protoporphyrin IX-Mediated Photoinactivation Reveals Differences between Methicillin-Resistant and Methicillin-Sensitive Staphylococcus Aureus Strains. *Photomed. Laser Surg.* **2014**, *32*, 121–129.
- (9) Kossakowska, M.; Nakonieczna, J.; Kawiak, A.; Kurlenda, J.; Bielawski, K. P.; Grinholc, M. Discovering the Mechanisms of Strain-Dependent Response of Staphylococcus Aureus to Photoinactivation: Oxidative Stress Tolerance, Endogenous Porphyrin Level and Strain's Virulence. *Photodiagn. Photodyn. Ther.* **2013**, *10*, 348–355.
- (10) Grinholc, M.; Szramka, B.; Olender, K.; Graczyk, A. Bactericidal Effect of Photodynamic Therapy against Methicillin-Resistant Staphylococcus Aureus Strain with the Use of Various Porphyrin Photosensitizers. *Acta Biochim. Pol.* **2007**, *54*, 665–670.
- (11) Wozniak, A.; Grinholc, M. Combined Antimicrobial Activity of Photodynamic Inactivation and Antimicrobials-State of the Art. *Front. Microbiol.* **2018**, *9*, 930.
- (12) Wozniak, A.; Rapacka-Zdonczyk, A.; Mutters, N. T.; Grinholc, M. Antimicrobials Are a Photodynamic Inactivation Adjuvant for the Eradication of Extensively Drug-Resistant Acinetobacter Baumannii. *Front. Microbiol.* **2019**, *10*, 229.
- (13) Bartolomeu, M.; Rocha, S.; Cunha, Â.; Neves, M. G. P. M. S.; Faustino, M. A. F.; Almeida, A. Effect of Photodynamic Therapy on the Virulence Factors of Staphylococcus Aureus. *Front. Microbiol.* **2016**, *7*, 267.
- (14) Ogonowska, P.; Nakonieczna, J. Validation of Stable Reference Genes in Staphylococcus Aureus to Study Gene Expression under Photodynamic Treatment: A Case Study of SEB Virulence Factor Analysis. *Sci. Rep.* **2020**, *10*, 16354.
- (15) Rapacka-Zdonczyk, A.; Wozniak, A.; Pieranski, M.; Wozniwodzka, A.; Bielawski, K. P.; Grinholc, M. Development of Staphylococcus Aureus Tolerance to Antimicrobial Photodynamic Inactivation and Antimicrobial Blue Light upon Sub-Lethal Treatment. *Sci. Rep.* **2019**, *9*, 9423.
- (16) Pieranski, M.; Sitkiewicz, I.; Grinholc, M. Increased Photoinactivation Stress Tolerance of Streptococcus Agalactiae upon Consecutive Sublethal Phototreatments. *J. Free Radic. Biol. Med.* **2020**, *160*, 657–669.
- (17) Nakonieczna, J.; Wolnikowska, K.; Ogonowska, P.; Neubauer, D.; Bernat, A.; Kamysz, W. Rose Bengal-Mediated Photoinactivation of Multidrug Resistant Pseudomonas Aeruginosa Is Enhanced in the Presence of Antimicrobial Peptides. *Front. Microbiol.* **2018**, *9*, 1949.
- (18) Fila, G.; Krychowiak, M.; Rychlowski, M.; Bielawski, K. P.; Grinholc, M. Antimicrobial Blue Light Photoinactivation of Pseudomonas Aeruginosa: Quorum Sensing Signaling Molecules, Biofilm Formation and Pathogenicity. *J. Biophotonics* **2018**, *11*, No. e201800079.
- (19) Hamblin, M. R.; Abrahamse, H. Can Light-Based Approaches Overcome Antimicrobial Resistance? *Drug Dev. Res.* **2019**, *80*, 48–67.
- (20) Minnock, A.; Vernon, D. I.; Schofield, J.; Griffiths, J.; Parish, J. H.; Brown, S. B. Mechanism of Uptake of a Cationic Water-Soluble Pyridinium Zinc Phthalocyanine across the Outer Membrane of Escherichia Coli. *Antimicrob. Agents Chemother.* **2000**, *44*, 522–527.
- (21) Demidova, T. N.; Hamblin, M. R. Effect of Cell-Photosensitizer Binding and Cell Density on Microbial Photoinactivation. *Antimicrob. Agents Chemother.* **2005**, *49*, 2329–2335.
- (22) Alves, E.; Faustino, M. A.; Neves, M. G.; Cunha, A.; Tome, J.; Almeida, A. An Insight on Bacterial Cellular Targets of Photodynamic Inactivation. *Future Med. Chem.* **2014**, *6*, 141–164.
- (23) Stojiljkovic, I.; Kumar, V.; Srinivasan, N. Non-Iron Metalloporphyrins: Potent Antibacterial Compounds That Exploit Haem/Hb Uptake Systems of Pathogenic Bacteria. *Mol. Microbiol.* **1999**, *31*, 429–442.
- (24) Moriwaki, Y.; Caaveiro, J. M. M.; Tanaka, Y.; Tsutsumi, H.; Hamachi, I.; Tsumoto, K. Molecular Basis of Recognition of Antibacterial Porphyrins by Heme-Transporter IsdH-NEAT3 of Staphylococcus Aureus. *Biochemistry* **2011**, *50*, 7311–7320.
- (25) Kelson, A. B.; Carnevali, M.; Truong-le, V. Gallium-Based Anti-Infectives: Targeting Microbial Iron-Uptake Mechanisms. *Curr. Opin. Pharmacol.* **2013**, *13*, 707–716.
- (26) Kaneko, Y.; Thoendel, M.; Olakanmi, O.; Britigan, B. E.; Singh, P. K. The Transition Metal Gallium Disrupts Pseudomonas Aeruginosa Iron Metabolism and Has Antimicrobial and Antibiofilm Activity. *J. Clin. Invest.* **2007**, *117*, 877–888.
- (27) Hijazi, S.; Visaggio, D.; Pirolo, M.; Frangipani, E.; Bernstein, L.; Visca, P. Antimicrobial Activity of Gallium Compounds on ESKAPE Pathogens. *Front. Cell. Infect. Microbiol.* **2018**, *8*, 316.
- (28) Arivett, B. A.; Fiester, S. E.; Ohneck, E. J.; Penwell, W. F.; Kaufman, C. M.; Relich, R. F.; Actis, L. A. Antimicrobial Activity of Gallium Protoporphyrin IX against Acinetobacter Baumannii Strains Displaying Different Antibiotic Resistance Phenotypes. *Antimicrob. Agents Chemother.* **2015**, *59*, 7657–7665.
- (29) Hijazi, S.; Visca, P.; Frangipani, E. Gallium-Protoporphyrin IX Inhibits Pseudomonas Aeruginosa Growth by Targeting Cytochromes. *Front. Cell. Infect. Microbiol.* **2017**, *7*, 12.
- (30) Goss, C. H.; Kaneko, Y.; Khuu, L.; Anderson, G. D.; Ravishankar, S.; Aitken, M. L.; Lechtzin, N.; Zhou, G.; Czyn, D. M.; McLean, K.; Olakanmi, O.; Shuman, H. A.; Teresi, M.; Wilhelm, E.; Caldwell, E.; Salipante, S. J.; Hornick, D. B.; Siehnel, R. J.; Becker, L.; Britigan, B. E.; Singh, P. K. Gallium Disrupts Bacterial Iron

Metabolism and Has Therapeutic Effects in Mice and Humans with Lung Infections. *Sci. Transl. Med.* **2018**, *10*, No. eaat7520.

(31) Choi, S.-R.; Britigan, B.; Narayanasamy, P. Iron/Heme Metabolism-Targeted Gallium (III) Nanoparticles Are Active against Extracellular and Intracellular *Pseudomonas Aeruginosa* and *Acinetobacter Baumannii*. *Antimicrob. Agents Chemother.* **2019**, *63*, e02643–e02618.

(32) Richter, K.; Thomas, N.; Claeys, J.; McGuane, J.; Prestidge, C. A.; Coenye, T.; Wormald, P.-J.; Vreugde, S. A Topical Hydrogel with Deferiprone and Gallium-Protoporphyrin Targets Bacterial Iron Metabolism and Has Antibiofilm Activity. *Antimicrob. Agents Chemother.* **2017**, *61*, e00481–e00417.

(33) Richter, K.; Ramezanzpour, M.; Thomas, N.; Prestidge, C. A.; Wormald, P.-J.; Vreugde, S. Mind “De GaPP”: In Vitro Efficacy of Deferiprone and Gallium-Protoporphyrin Against. *Int. Forum Allergy Rhinol.* **2016**, *6*, 737–743.

(34) Morales-de-Echegaray, A. V.; Maltais, T. R.; Lin, L.; Younis, W.; Kadasala, N. R.; Seleem, M. N.; Wei, A. Rapid Uptake and Photodynamic Inactivation of Staphylococci by Ga(III)-Protoporphyrin IX. *ACS Infect. Dis.* **2018**, *4*, 1564–1573.

(35) Morales-de-Echegaray, A. V.; Lin, L.; Sivasubramaniam, B.; Yermembetova, A.; Wang, Q.; Abutaleb, N. S.; Seleem, M. N.; Wei, A. Antimicrobial Photodynamic Activity of Gallium-Substituted Haemoglobin on Silver Nanoparticles. *Nanoscale* **2020**, *12*, 21734.

(36) Nakonieczna, J.; Wozniak, A.; Pieranski, M.; Rapacka-Zdonczyk, A.; Ogonowska, P.; Grinholc, M. Photoinactivation of ESKAPE Pathogens: Overview of Novel Therapeutic Strategy. *Future Med. Chem.* **2019**, *11*, 443–461.

(37) Mazmanian, S. K.; Skaar, E. P.; Gaspar, A. H.; Humayun, M.; Gornicki, P.; Jelenska, J.; Joachmiak, A.; Missiakas, D. M.; Schneewind, O. Passage of Heme-Iron across the Envelope of *Staphylococcus Aureus*. *Science* **2003**, *299*, 906–909.

(38) Mason, W. J.; Skaar, E. P. Assessing the Contribution of Heme-Iron Acquisition to *Staphylococcus Aureus* Pneumonia Using Computed Tomography. *PLoS One* **2009**, *4*, No. e6668.

(39) Choby, J. E.; Skaar, E. P. Heme Synthesis and Acquisition in Bacterial Pathogens. *J. Mol. Biol.* **2016**, *428*, 3408–3428.

(40) Grigg, J. C.; Vermeiren, C. L.; Heinrichs, D. E.; Murphy, M. E. P. Haem Recognition by a *Staphylococcus Aureus* NEAT Domain. *Mol. Microbiol.* **2007**, *63*, 139–149.

(41) Hammer, N. D.; Skaar, E. P. Molecular Mechanisms of *Staphylococcus Aureus* Iron Acquisition. *Annu. Rev. Microbiol.* **2011**, *65*, 129–147.

(42) Hammer, N. D.; Reniere, M. L.; Cassat, J. E.; Zhang, Y.; Hirsch, A. O.; Indriati Hood, M.; Skaar, E. P. Two Heme-Dependent Terminal Oxidases Power *Staphylococcus Aureus* Organ-Specific Colonization of the Vertebrate Host. *MBio* **2013**, *4*, e00241–e00213.

(43) Anzaldi, L. L.; Skaar, E. P. Overcoming the Heme Paradox: Heme Toxicity and Tolerance in Bacterial Pathogens. *Infect. Immun.* **2010**, *78*, 4977–4989.

(44) Torres, V. J.; Stauff, D. L.; Pishchany, G.; Bezbradica, J. S.; Gordy, L. E.; Iturregui, J.; Anderson, K. L. L.; Dunman, P. M.; Joyce, S.; Skaar, E. P. A *Staphylococcus Aureus* Regulatory System That Responds to Host Heme and Modulates Virulence. *Cell Host Microbe* **2007**, *1*, 109–119.

(45) Stauff, D. L.; Skaar, E. P. Bacillus Anthracis HssRS Signalling to HrtAB Regulates Haem Resistance during Infection. *Mol. Microbiol.* **2009**, *72*, 763–778.

(46) Szewczyk, G.; Zadlo, A.; Sarna, M.; Ito, S.; Wakamatsu, K.; Sarna, T. Aerobic Photoreactivity of Synthetic Eumelanins and Pheomelanins: Generation of Singlet Oxygen and Superoxide Anion. *Pigment Cell Melanoma Res.* **2016**, *29*, 669–678.

(47) Stoll, S.; Schweiger, A. EasySpin, a Comprehensive Software Package for Spectral Simulation and Analysis in EPR. *J. Magn. Reson.* **2006**, *178*, 42–55.

(48) Nakonieczna, J.; Kossakowska-Zwierucho, M.; Filipiak, M.; Hewelt-Belka, W.; Grinholc, M.; Bielawski, K. P. Photoinactivation of *Staphylococcus Aureus* Using Protoporphyrin IX: The Role of Haem-

Regulated Transporter HrtA. *Appl. Microbiol. Biotechnol.* **2016**, *100*, 1393–1405.

(49) Redmond, R. W.; Gamlin, J. N. A Compilation of Singlet Oxygen Yields from Biologically Relevant Molecules. *Photochem. Photobiol.* **1999**, *70*, 391–475.

(50) Buettner, G. R. Spin Trapping: ESR Parameters of Spin Adducts. *J. Free Radical. Biol. Med.* **1987**, *3*, 259–303.

(51) Shirasu, N.; Nam, S. O.; Kuroki, M. Tumor-Targeted Photodynamic Therapy. *Anticancer Res.* **2008**, *1*, 590.

(52) Wakeman, C. A.; Stauff, D. L.; Zhang, Y.; Skaar, E. P. Differential Activation of *Staphylococcus Aureus* Heme Detoxification Machinery by Heme Analogues. *J. Bacteriol.* **2014**, *196*, 1335–1342.

(53) Kato, H.; Komagoe, K.; Inoue, T.; Masuda, K.; Katsu, T. Structure-Activity Relationship of Porphyrin-Induced Photoinactivation with Membrane Function in Bacteria and Erythrocytes. *Photochem. Photobiol. Sci.* **2018**, *17*, 954–963.

(54) Maitra, D.; Pinsky, B. M.; Soherawardy, A.; Zheng, H.; Banerjee, R.; Omary, M. B. Protein-Aggregating Ability of Different Protoporphyrin-IX Nanostructures Is Dependent on Their Oxidation and Protein-Binding Capacity. *J. Biol. Chem.* **2021**, *297*, No. 100778.

(55) Cruz-Oliveira, C.; Almeida, A. F.; Freire, J. M.; Caruso, M. B.; Morando, M. A.; Ferreira, V. N. S.; Assunção-Miranda, I.; Gomes, A. M. O.; Castanho, M. A. R. B.; Da Poian, A. T. Mechanisms of Vesicular Stomatitis Virus Inactivation by Protoporphyrin IX, Zinc-Protoporphyrin IX, and Mesoporphyrin IX. *Antimicrob. Agents Chemother.* **2017**, *61*, e00053–e00017.

(56) Drury, S. L.; Miller, A. R.; Laut, C. L.; Walter, A. B.; Bennett, M. R.; Su, M.; Bai, M.; Jing, B.; Joseph, S. B.; Metzger, E. J.; Bane, C. E.; Black, C. C.; Macdonald, M. T.; Dutter, B. F.; Romaine, I. M.; Waterson, A. G.; Sulikowski, G. A.; Jansen, E. D.; Crowe, J. E.; Sciotti, R. J.; Skaar, E. P. Simultaneous Exposure to Intracellular and Extracellular Photosensitizers for the Treatment of *Staphylococcus Aureus* Infections. *Antimicrob. Agents Chemother.* **2021**, *65*, No. e0091921.

(57) Rapacka-Zdonczyk, A.; Wozniak, A.; Michalska, K.; Pieranski, M.; Ogonowska, P.; Grinholc, M.; Nakonieczna, J. Factors Determining the Susceptibility of Bacteria to Antibacterial Photodynamic Inactivation. *Front. Med.* **2021**, *8*, No. 642609.

(58) Haley, K. P.; Skaar, E. P. A Battle for Iron: Host Sequestration and *Staphylococcus Aureus* Acquisition. *Microbes Infect.* **2012**, *14*, 217–227.

(59) Proctor, R. A.; von Eiff, C.; Kahl, B. C.; Becker, K.; McNamara, P.; Herrmann, M.; Peters, G. Small Colony Variants: A Pathogenic Form of Bacteria That Facilitates Persistent and Recurrent Infections. *Nat. Rev. Microbiol.* **2006**, *4*, 295–305.

(60) Osiecka, B.; Nockowski, P.; Szepietowski, J. Treatment of Actinic Keratosis with Photodynamic Therapy Using Red or Green Light: A Comparative Study. *Acta Derm. Venereol.* **2018**, *98*, 689–693.

4. Publication no. 2

Photoactivated Gallium Porphyrin Reduces *Staphylococcus aureus* Colonization on the Skin and Suppresses Its Ability to Produce Enterotoxin C and TSST-1

4.1 Summary of the publication

Atopic dermatitis (AD) is a multifactorial, chronic inflammatory skin disease¹²⁹. Mutations resulting in the lack of functional filaggrin, a protein responsible for epidermal integrity, are a common risk factor for the development of atopic dermatitis¹³⁰. There is a strong correlation between *Staphylococcus aureus* colonization and the occurrence of mutations in filaggrin. More than half of AD patients carry *S. aureus*^{10,131,132}. This bacterium that resides on atopic skin often produces a variety of toxins, that cause excessive activation of the immune system and more severe inflammation¹³³. Staphylococcal enterotoxin C (SEC) and toxic shock syndrome toxin 1 (TSST-1) act as superantigens, excessively stimulating T-cells to produce proinflammatory cytokines, e.g. interleukin 2 (IL-2)¹³⁴.

The purpose of this study was to evaluate the antimicrobial efficacy of two modified gallium(III)-coordinated porphyrins, Ga³⁺MPIX and cationic Ga³⁺CHP, after excitation with green light, against several clinical isolates of *S. aureus* from patients with AD. In addition, the efficacy of the combination of gallium(III)-coordinated porphyrins and green light was evaluated for its ability to reduce *S. aureus* virulence based on the analysis of two relevant virulence factors: SEC and TSST-1. The last goal was to assess the phototoxicity of both compounds in the action of aPDI on human keratinocytes with silenced expression of the filaggrin gene as a simplified model of atopic skin.

Novel gallium(III)-coordinated porphyrin – cationic Ga³⁺CHP was synthesized by our collaborators as a part of the NCN Sheng project. This compound possesses two positively charged quaternary ammonium groups that increase its water solubility and improve the antimicrobial efficacy⁹⁸. Despite modifications, Ga³⁺CHP maintained dual-functionality at light-dependent and light-independent action. Ga³⁺CHP itself was a safe and biocompatible compound studied in the *in vivo* mouse model⁹⁸. When Ga³⁺CHP was excited in the Q-bands with green light, the PS effectively photogenerated singlet oxygen and also produced low but measurable levels of superoxide anion radicals. **Ga³⁺CHP-mediated aPDI exhibited significantly higher efficacy against both suspension and biofilm cultures of *S. aureus* compared to Ga³⁺MPIX-mediated aPDI.** Higher efficacy of Ga³⁺CHP-mediated aPDI was obtained with much lower concentrations and light doses (reduced irradiation time) than in Ga³⁺MPIX-mediated aPDI. Also, Ga³⁺CHP and green light decolonized *S. aureus* biofilm produced on an *ex vivo* porcine skin model. The proposed explanation of this predominant aPDI efficacy of cationic Ga³⁺CHP was its higher intracellular accumulation. The compound recognition depended on iron and heme availability, and the Isd system was involved in its recognition and acquisition. The impairment in HrtA ATPase of the heme efflux

pump was the most responsive phenotype in Ga³⁺CHP-mediated aPDI, indicating that toxicity of gallium metalloporphyrins might be elevated by blocking the heme detoxification system. **Addition of two quaternary ammonium moieties to the gallium(III)-coordinated porphyrins structure did not change the recognition of the compound as heme analog, however it improved antimicrobial action in light-dependent process.**

Green light excitation for the photodynamic process of Ga³⁺CHP also impacted the staphylococcal enterotoxin in the gene expression pattern, protein production, and activity. Sublethal doses of aPDI decreased *sec* gene expression and slightly upregulated the *tst* gene. However, pre-treatment of either SEC or TSST-1 toxin decreased its biological activity reflected as decreased IL-2 production by toxin-exposed PBMC fraction.

The eukaryotic safety of aPDI based on the combination of Ga³⁺CHP and green light for keratinocytes with filaggrin expression was also investigated. The study compared the effect of both compounds and light doses, which showed the highest effectiveness against *S. aureus*. Based on survival analyses and real-time cell growth, **it was found that Ga³⁺CHP-based aPDI was less toxic than Ga³⁺MPIX-based treatment.** Despite this, both cell lines eventually reached a plateau phase after exposure to aPDI. Green light with Ga³⁺MPs can be used despite variable filaggrin expression levels, but more complex models, e.g., *in vivo* skin infection mouse model, should be considered in further studies of atopic dermatitis. **In conclusion, excitation of cationic Ga³⁺CHP in the Q-bands region is effective in eliminating *S. aureus* – for example in the decolonization of the atopic skin.** This was the first published study to investigate phototoxicity and safety of aPDI treatment with the green light on the atopic dermatitis model. Reducing the activity of staphylococcal enterotoxins as superantigens might be beneficial in lowering inflammatory responses in patients with AD. The aPDI approach using green light is much safer and may provide a therapeutic alternative to blue light excitation. In addition, applying the green light may be a key to eliminating the pain factor of highly sensitive atopic skin; however, more advanced animal skin models should be used to evaluate its potential ⁷⁹.

4.2 Publication

For online version, please scan QR code of Publication no. 2:



Note: Supplementary material from Publication no. 2 can be found in section 9.2. (Attachments).

Photoactivated Gallium Porphyrin Reduces *Staphylococcus aureus* Colonization on the Skin and Suppresses Its Ability to Produce Enterotoxin C and TSST-1

Klaudia Szymczak, Grzegorz Szewczyk, Michał Rychłowski, Tadeusz Sarna, Lei Zhang, Mariusz Grinholc, and Joanna Nakonieczna*



Cite This: *Mol. Pharmaceutics* 2023, 20, 5108–5124



Read Online

ACCESS |

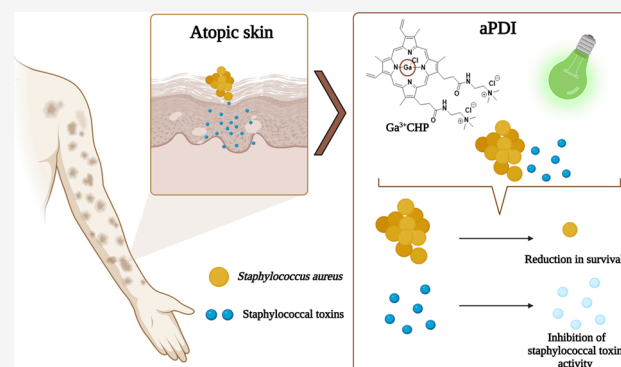
Metrics & More

Article Recommendations

Supporting Information

ABSTRACT: *Staphylococcus aureus* is a key pathogen in atopic dermatitis (AD) pathogenicity. Over half of AD patients are carriers of *S. aureus*. Clinical isolates derived from AD patients produce various staphylococcal enterotoxins, such as staphylococcal enterotoxin C or toxic shock syndrome toxin. The production of these virulence factors is correlated with more severe AD. In this study, we propose cationic heme-mimetic gallium porphyrin (Ga^{3+}CHP), a novel gallium metalloporphyrin, as an anti-staphylococcal agent that functions through dual mechanisms: a light-dependent mechanism (antimicrobial photodynamic inactivation, aPDI) and a light-independent mechanism (suppressing iron metabolism). Ga^{3+}CHP has two additive quaternary ammonium groups that increase its water solubility. Furthermore, Ga^{3+}CHP is an efficient generator of singlet oxygen and can be recognized by heme-target systems such as Isd, which improves the intracellular accumulation of this compound. Ga^{3+}CHP activated with green light effectively reduced the survival of clinical *S. aureus* isolates derived from AD patients ($>5 \log_{10}$ CFU/mL) and affected their enterotoxin gene expression. Additionally, there was a decrease in the biological functionality of studied toxins regarding their superantigenicity. In aPDI conditions, there was no pronounced toxicity in HaCaT keratinocytes with both normal and suppressed filaggrin gene expression, which occurs in $\sim 50\%$ of AD patients. Additionally, no mutagenic activity was observed. Green light-activated gallium metalloporphyrins may be a promising chemotherapeutic to reduce *S. aureus* colonization on the skin of AD patients.

KEYWORDS: antimicrobial treatment, atopic dermatitis, photodynamic inactivation, reactive oxygen species, superantigens



1. INTRODUCTION

The ESKAPE pathogens (*Enterococcus faecium*, *Staphylococcus aureus*, *Klebsiella pneumoniae*, *Acinetobacter baumannii*, *Pseudomonas aeruginosa*, and *Enterobacter species*) are the leading cause of infections throughout the world. *Staphylococcus aureus* is a Gram-positive bacterium and a key member of the ESKAPE superbugs, which are considered a dynamic group of emerging antimicrobial-resistant pathogens.¹ *S. aureus* produces a range of virulence factors, such as staphylococcal enterotoxins (SEs), that increase its virulence and pathogenicity.^{2,3} SEs such as staphylococcal enterotoxin C (SEC) or toxic shock syndrome toxin (TSST-1) are potent, nonspecific superantigens that stimulate over 50% of the T-cell pool.⁴ SEs aggravate and enhance inflammation in atopic dermatitis (AD) patients.⁵ Clinical isolates of *S. aureus* derived from AD patients are a genetically heterogeneous population in terms of the presence of superantigen genes. AD patients are a source of specific isolates that are more potent in colonizing AD skin and altering immunological responses.^{6,7}

AD is a multifactorial chronic inflammatory skin disorder that affects both adults and children, and its occurrence has increased over the last decade.^{3,8} Crucial factors involved in AD development are genetic background, immune system disorders, and defects in the epidermal barrier.⁹ These factors influence the skin microbiome.^{2,3} Compared with healthy individuals, AD patients show higher colonization levels of methicillin-resistant *S. aureus* (MRSA) strains. Approximately 55% of AD patients are persistent carriers of *S. aureus*.¹⁰ Staphylococcal colonization might be related to changes in skin pH and low levels of ceramides and antimicrobial peptides.⁵ There is also a correlation between a mutation in the filaggrin

Received: May 5, 2023
Revised: August 21, 2023
Accepted: August 22, 2023
Published: September 1, 2023



gene (*FLG*) and increased *S. aureus* colonization on the skin of AD patients.¹¹ Many cohort studies have demonstrated that 25–50% of AD patients possess a mutation in the *FLG* gene.¹² Filaggrin is a key protein that maintains proper hydration and epidermal integrity by cross-linking keratin filaments. Lack of this protein significantly enhances allergen and microbial penetration into the skin.^{13,14}

Antimicrobial AD treatment is not yet predominant due to the multifactorial nature of the disease. Antibiotic therapy remains the gold standard treatment for fighting staphylococcal infections in AD patients. However, the number of available and effective antimicrobials is shrinking due to increasing antimicrobial resistance. Antimicrobial photodynamic inactivation (aPDI) might be an alternative way to reduce *S. aureus* colonization on atopic skin. This approach is based on three components: oxygen, light at the proper wavelength, and a compound known as a photosensitizer (PS). Briefly, under light illumination, the PS is excited to its triplet state, and then two types of mechanisms can occur. In the type I mechanism, electrons are transferred between the excited PS and biomolecules to produce cytotoxic reactive oxygen species (ROS) such as the superoxide anion, hydrogen peroxide, and/or hydroxyl radicals.¹⁵ In the type II reaction, singlet oxygen is produced by transferring energy of the excited PS to molecular oxygen. To date, there has been no evidence of antimicrobial resistance to aPDI.¹⁶ Gallium metalloporphyrins (Ga^{3+}MPs) are effective PSs in aPDI against *S. aureus* despite divergent multidrug responses.¹⁷ Ga^{3+}MPs are dual-function compounds that act according to light-independent and light-dependent mechanisms, and they mimic their natural analogue—heme.¹⁸ On the staphylococcal membrane, there are two types of heme acquisition receptors, *isd* (iron-surface determinate) or *hts* (heme transport system), that can recognize Ga^{3+}MPs in the same manner as heme, allowing Ga^{3+}MPs to accumulate inside the cell.¹⁹ After cleavage of the porphyrin ring, gallium ions are released and inhibit iron-dependent metabolic pathways. Moreover, there are reports stating that Ga^{3+}MPs could be detoxified in a manner similar to heme by the heme-regulated transporter HrtAB efflux pump.²⁰ Ga^{3+}MPs have photodynamic potential after illumination at the proper wavelength in the Soret or Q band area, which are the high- and low-energy parts of the porphyrin absorption spectrum, respectively.^{17,20} In addition, they have additive quaternary ammonium groups that increase their water solubility. Moreover, a previous study showed that this compound was effective in iron-blocking antibacterial therapy against Gram-positive and Gram-negative bacteria with visible light irradiation in the area of the Soret band.²¹ Our previous study reported that structural changes such as vinyl to ethyl groups in the structure of the porphyrin ring of gallium mesoporphyrin IX ($\text{Ga}^{3+}\text{MPIX}$) did not change the recognition of the compound, although the aqueous solubility was increased and a shift in the absorbance spectrum was observed. Additionally, these changes improved the efficacy of aPDI against *S. aureus* under illumination with green light in the Q band region.²⁰ Using the wavelengths nearest to the visible green light might be a crucial therapeutic strategy for treating AD due to deeper light penetration through the epidermal barrier.²²

In this work, the photoexcitation of Ga^{3+}CHP (Figure 1) was studied under 522 nm illumination to characterize the photodynamic potential of this compound. Furthermore, we investigated whether the presence of two additive quaternary

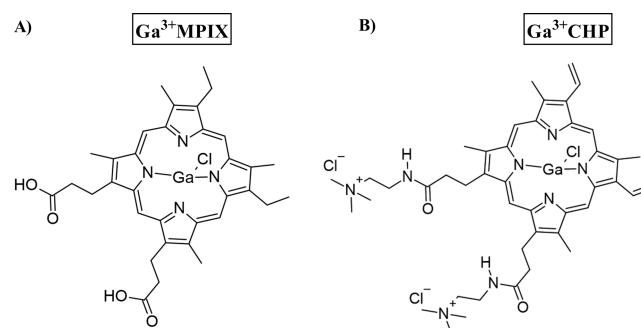


Figure 1. Chemical structures of $\text{Ga}^{3+}\text{MPIX}$ (A) and Ga^{3+}CHP (B) drawn in ChemSketch.

ammonium groups could affect the recognition of the compound by heme acquisition receptors and detoxification machinery. The efficacy of aPDI of both gallium compounds, Ga^{3+}CHP and $\text{Ga}^{3+}\text{MPIX}$ (Figure 1), was examined against *S. aureus* clinical isolates derived from AD patients in planktonic culture and ex vivo porcine skin models. The mutagenicity and safety of the compounds in keratinocytes with divergent filaggrin expression were also investigated. Finally, the effect of aPDI with both gallium compounds on the gene expression, protein production, and biological activity of two virulence factors, SEC and TSST-1, was investigated.

2. MATERIALS AND METHODS

2.1. Bacterial Strains and Growth Conditions. Bacterial strains are listed in Table 1. *S. aureus* cultures were grown in trypticase soy broth (TSB, bioMérieux, France) or TSB pretreated with Chelex-100 resin (Sigma-Aldrich, USA) in an iron-depleted medium at 37 °C on trypticase soy agar-coated plates (TSA, bioMérieux, France) with shaking (150 rpm). Erythromycin (10 $\mu\text{g}/\text{mL}$) was added to the cultivation medium of the *S. aureus* ΔIsdD mutant strain. Glycerol stocks of *E. coli* and *S. typhimurium* and the necessary growth media for mutagenicity testing were purchased from commercially available Ames Penta 2 (Xenometrix, Allschwil, Switzerland).

2.2. Cell Cultures and Growth Conditions. The human immortalized keratinocyte HaCaT cell line was used in this study. Cells were either treated with empty vector (sc-108080, *FLG* ctrl) or infected with lentiviral particles containing *FLG* shRNA (sc-43364-V) to construct *FLG* knockdown (*FLG* sh) cells.²⁵ Cells were grown in a standard humidified incubator at 37 °C in a 5% CO_2 atmosphere in Dulbecco's modified Eagle's medium (DMEM) with 10% fetal bovine serum (FBS), 4.5 g/L glucose, 1 mM sodium pyruvate, 100 U/mL penicillin, 100 $\mu\text{g}/\text{mL}$ streptomycin, 2 mM L-glutamine, and 1 mM nonessential amino acids (Gibco, Thermo Fisher Scientific, USA).

Human PBMCs were purified from the blood samples of healthy donors obtained from the Buffy Coat Blood Bank. Cells were harvested using Lymphoprep (Stemcell, Grenoble, France) and frozen at -80 °C until the experiment. PBMCs were cultivated in RPMI-1640 medium (Sigma-Aldrich, USA) with the addition of the supplementary cell growth additives mentioned above.

2.3. Chemicals. Ga^{3+} mesoporphyrin IX chloride ($\text{Ga}^{3+}\text{MPIX}$; Frontier Scientific, USA) was prepared as previously described (Figure 1A).²⁰ Ga^{3+}CHP was synthesized, and its structure is described by Zhang et al. (Figure 1B).²¹ Five millimolar stocks of Ga^{3+}CHP were prepared in Milli-Q

Table 1. Bacterial Strains Used in This Study^a

| species | strain | characteristic of strain | presence of SAg genes | reference |
|-----------------------|-------------|--|--|---|
| <i>S. aureus</i> | 3 N | AZS clinical isolate, MSSA; <i>spa</i> type: t091; MLST-CC type: CC7 | <i>sea</i> (+), <i>sec</i> (+), <i>sed</i> (+) | Department of Dermatology, Venerology, and Allergology, Medical University of Gdańsk |
| | 5 N | AZS clinical isolate, MSSA; <i>spa</i> type: t2223; MLST-CC type: CC45 | <i>sec</i> (+), <i>tst</i> (+) | |
| | 38 N | AZS clinical isolate, MSSA; <i>spa</i> type: t091; MLST-CC type: CC7 | (-) | |
| | XEN40 | clinical, bioluminescence isolate derived from the parental strain <i>S. aureus</i> UAMS-1 | <i>sea</i> (+), <i>tst</i> (+) | PerkinElmer, USA |
| | 25923 | reference strain | (-) | ATCC®, USA |
| | Newman | wild-type (WT) strain | (-) | 23 |
| | ΔHrtA | Δ <i>hrtA</i> via allelic replacement | (-) | 24 |
| | ΔHtsA | Δ <i>htsA</i> via allelic replacement | (-) | 23 |
| | ΔIsdD | <i>isd:erm</i> | (-) | 19 |
| <i>E. coli</i> | wp2 uvrA | deletion of <i>uvrA</i> | (-) | Xentometrix (Switzerland) |
| | TA1535 | deletion of <i>uvrA</i> and <i>rfa</i> | (-) | |
| <i>S. pyphimurium</i> | | | | |

^aLegend: MSSA—methicillin-sensitive *Staphylococcus aureus*, SAg—superantigens; *sea*, *sec*, *sed*, *tst*—staphylococcal enterotoxin A, C, D, and toxic shock syndrome toxin 1; (-)—absence of SAg genes.

water and kept in the dark at room temperature. Heme (Sigma-Aldrich, USA) was dissolved in a 0.1 M NaOH solution and kept in the dark at 4 °C.

2.4. Light Source. In this study, we used a light-emitting diode (LED) light source emitting green light ($\lambda_{\max} = 522$ nm, irradiance = 10.6 mW/cm², FWHM = 34 nm) (Cezos, Poland) (Figure 2). The irradiation time ranged from 2.5 to 50 min. During irradiation, no heat was generated (Figure S1).

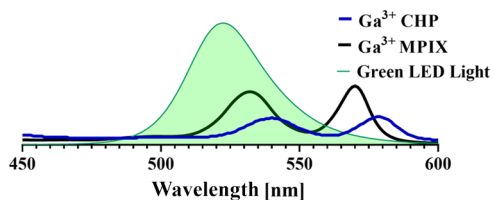


Figure 2. Absorbance spectra of Ga³⁺CHP and Ga³⁺MPIX [10 μM] with the emission spectrum of a green light source used in this study ($\lambda_{\max} = 522$ nm, FWHM = 34 nm).

2.5. Characterization of the Photodynamic Properties of Ga³⁺CHP. The quantum yield of Ga³⁺CHP-mediated singlet oxygen photogeneration in phosphate-buffered D₂O was determined by comparing the initial intensities of 1270 nm phosphorescence induced by photoexcitation of both the standard rose bengal (RB) (for which the established quantum yield of singlet oxygen generation is 0.75) and the experimental

photosensitizer Ga³⁺CHP with 540 nm laser pulses of increasing energies using neutral density filters. Time-resolved singlet oxygen phosphorescence induced by excitation of solutions of Ga³⁺CHP or RB, adjusted to the same absorbance at 540 nm, with nanosecond laser pulses generated by an integrated DSSNd:YAG laser system equipped with a narrow bandwidth optical parametric oscillator (NT242-1k-SH/SFG; Ekspla, Vilnius, Lithuania), was detected by a photomultiplier module H10330-45 working in the photon counting mode (Hamamatsu Photonics K. K., Hamamatsu City, Japan), equipped with a 1100 nm cut-off filter and additional dichroic narrow-band filters NBP, selectable from the spectral range 1150–1355 nm (NDC Infrared Engineering Ltd., Bates Road, Maldon, Essex, UK). Data were collected using a computer-mounted PCI-board multichannel scaler (NanoHarp 250; PicoQuant GmbH, Berlin, Germany). Data analysis, including first-order luminescence decay fitted by the Levenberg–Marquardt algorithm, was performed by custom-written software.

Electron paramagnetic resonance (EPR) spin trapping was carried out using 100 mM 5,5-dimethyl-1-pyrroline *N*-oxide (DMPO) (Dojindo Kumamoto, Japan) as a spin trap. Samples containing DMPO and approximately 0.1 mM PSs in 75% dimethylsulfoxide (DMSO) with an adjusted neutral pH were placed in 0.3 mm-thick quartz EPR flat cells and irradiated in situ in a resonant cavity with 540 nm green LED light. The EPR measurements were carried out using a Bruker-EMX AA

spectrometer (Bruker BioSpin, Germany) with the following apparatus settings: 10.6 mW microwave power, 0.05 mT modulation amplitude, 332.4 mT center field, 8 mT scan field, and 84 s scan time. Simulations of EPR spectra were performed with the EasySpin toolbox for MATLAB.

2.6. Antimicrobial aPDI. Photoinactivation experiments were performed as previously described.²⁰ Briefly, *S. aureus* was grown in either full TSB medium or TSB pretreated with Chelex-100 resin to chelate iron ions (Sigma-Aldrich, USA) for 16–20 h. Cultures were diluted to 10⁷ CFU/mL (0.5 MacFarland units), and then 90 μ L of bacterial aliquots was transferred to a 96-well plate with the addition of 10 μ L of either pure medium or PS (Ga³⁺MPIX or Ga³⁺CHP). For the heme competition assay, Ga³⁺CHP was mixed with heme at a ratio of 1:1 (v:v) at different concentration ratios, and then the aPDI protocol was followed. The aPDI samples were incubated at 37 °C with shaking in the dark for 10 min and illuminated with the light source (Table 2). Serial dilutions of aliquots were prepared and plated on TSA plates to calculate the colony-forming units (CFU/mL).

Table 2. Light Doses and Corresponding Irradiation Times Used in This Study

| light dose [J/cm ²] | irradiation time [min] |
|---------------------------------|------------------------|
| 1.59 | 2.5 |
| 3.18 | 5 |
| 6.4 | 10 |
| 12.72 | 20 |
| 19.08 | 30 |
| 31.8 | 50 |

2.7. Accumulation of PS. The intracellular accumulation of each photosensitizer was determined according to our previously published protocols.^{20,26} Both compounds (1–10 μ M) were added separately to bacterial aliquots to produce a final volume of 800 μ L. In the heme competition assay, Ga³⁺CHP was mixed with heme in a 1:1 volume ratio (v/v) at different concentration ratios [μ M: μ M]. Bacterial suspensions were incubated for 10 min at 37 °C in the dark with shaking. Ten microliters of bacterial suspensions was then collected for a serial dilution to count CFU/mL. The cells were then centrifuged and washed twice with PBS. Cells were resuspended in lysis buffer (0.1 M NaOH/1% SDS) and kept for 24 h at room temperature. The fluorescence intensity of each sample was measured with an EnVision Multilabel Plate Reader (PerkinElmer, USA) at the following emission/excitation wavelengths: Ga³⁺MPIX at 406/573 nm and Ga³⁺CHP at 406/582 nm. Accumulation calculations for each PS were made from a compound calibration curve prepared in the lysis solution. The uptake values are presented as PS molecules accumulated per cell based on the previously shown formula.²⁶ The molecular weight of Ga³⁺CHP was calculated to be 907.08 g/mol and that of Ga³⁺MPIX was calculated to be 669.85 g/mol.

2.8. aPDI in an Ex Vivo Porcine Skin Model. Ex vivo porcine skin was collected and cut into 2 \times 2 cm skin grafts. They were then treated twice with 70% ethanol for 15 min, followed by PBS washing. To enhance skin decontamination before the procedure, grafts were treated with UV radiation for 15 min on each side. The grafts were then plated on a HEPES agar solid medium (10 mM HEPES, 136 mM NaCl, 4 mM KCl, 10 mM glucose, 1% agar). Overnight cultures of the

bioluminescence strain of *S. aureus* Xen40 were diluted to a 0.5 MacFarland standard, and 100 μ L of the bacterial suspensions was inoculated on the grafts. Bacteria were incubated at 37 °C for 24 h. The bioluminescent signal of each graft was measured with ChemiDoc XRS+ (Bio-Rad, USA) and referred to as the “before” measurement. Then, 200 μ L of a 10 μ M Ga³⁺CHP solution or sterile Milli-Q water was placed on the infected skin and incubated in the dark for 10 min. The skin was then exposed to green light or left in the dark. The bioluminescence signal was measured immediately after each treatment, referred to as the “after” measurement. The bioluminescence signal for each treatment at the appropriate time point was calculated using ImageJ software. The change in bioluminescent signal was measured for each condition the experiment was independently repeated in triplicate.

2.9. Prokaryotic Mutagenicity. The mutagenicity analysis was performed using a commercially available Ames Penta 2 kit (Xenomatrix, Allschwil, Switzerland), and all steps followed the manufacturer’s protocol. The day before the experiment, three independent biological cultures of each indicator strain of *Escherichia coli* uvrA or *Salmonella typhimurium* TA1535 were prepared. After 14 h of incubation at 37 °C with shaking, the cultures were diluted in exposure medium and treated with Ga³⁺MPIX or Ga³⁺CHP. The cultures were allowed to incubate in the dark for 10 min and then irradiated with green light at the proper dose. For positive controls, cultures were treated with mutagenic chemicals such as N⁴-aminocytidine (N⁴-ACT) for *S. typhimurium* TA1535 and 4-nitroquinoline-N-oxide (4-NQO) for *E. coli* uvrA. Cells incubated without a compound and without light exposure were used as negative controls. All treatments were incubated for 90 min after mutagen or aPDI treatment. Exposure medium was then added to all samples, and 50 μ L of each sample was aliquoted into 384-well plates. All microplates were covered with sterile foil and incubated for 48 h at 37 °C. The number of revertants after each treatment was counted following the incubation period. This experiment was performed with three independent biological replicates that each had three technical replicates of each treatment group.

2.10. Photo- and Cytotoxicity Assays on Human Keratinocytes. HaCat cells with silenced expression of *FLG* (*FLG* sh) and normal *FLG* gene expression (*FLG* ctrl) were tested for photo- and cytotoxicity using the MTT assay and cell growth dynamics using the xCELLigence real-time cell analyzer (RTCA) device (ACEA Biosciences Inc., USA). In the MTT assay, cells were seeded the day before the experiment at a density of 1 \times 10⁴ cells per well in 96-well plates. Cells were divided into two plates for light treatment and dark control. Cells were grown in a standard humidified incubator at 37 °C in a 5% CO₂ atmosphere in DMEM. Ga³⁺MPIX or Ga³⁺CHP was added to the cells to a final concentration of 10 μ M and then incubated for 10 min at 37 °C in the dark. After incubation, the medium was changed to fresh PS-free DMEM. Next, cells were irradiated with light at 522 nm with established doses for each PS, 31.9 J/cm² for Ga³⁺MPIX, and 1.59 J/cm² for Ga³⁺CHP. MTT reagent was added to cells 24 h posttreatment, and after 4 h of incubation, the cells were lysed, and the absorbance of the released formazan was measured with a plate reader at 550 nm.

For real-time analysis of cell growth dynamics, each cell line was seeded the day before treatment in seven technical replicates for each condition at a density of 1 \times 10⁴ per well on an E-plate (ACEA Biosciences Inc., USA). Cells were grown in

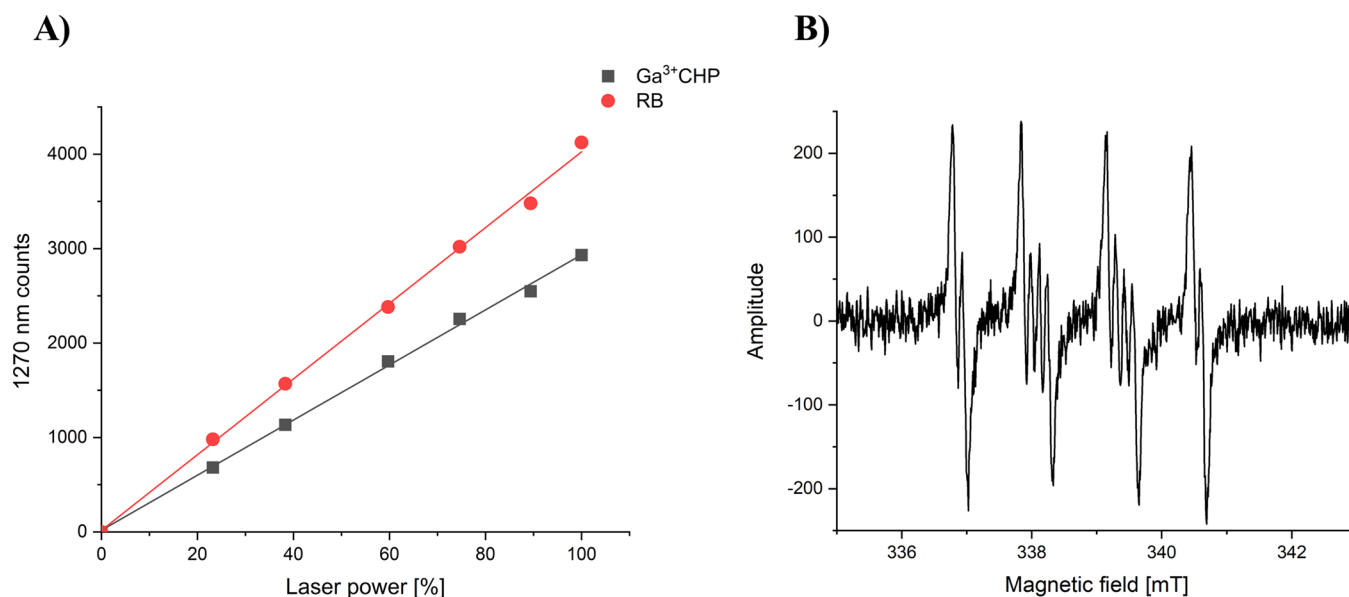


Figure 3. Photodynamic properties of Ga³⁺CHP under green light illumination. (A) Efficiency of singlet oxygen photogeneration by Ga³⁺CHP compared to that by the standard RB. Measurements of singlet oxygen photogeneration were performed in deuterium oxide (D₂O). Samples were excited at 540 nm laser light. Maximum power density was ca. 7 mW/cm²; the laser emits the beam at a frequency of 1 kHz, which gives about 7 μJ/cm² of each pulse (this is as 100% on the graph). (B) Detection of the superoxide anion generated by Ga³⁺CHP by EPR spin trapping using DMPO as a spin trap dissolved in 75% DMSO.

a standard humidified incubator at 37 °C and a 5% CO₂ atmosphere in DMEM on the xCELLigence device. When the cell index (CI) was in the range of 1.5–2.0, the cells were treated with aPDI. The appropriate photosensitizer was added to the cells at a concentration of 10 μM and incubated for 10 min in the dark at 37 °C. The medium was then changed to PS-free DMEM. Test cells were exposed to green light either at 31.9 J/cm² for Ga³⁺MPIX or at 1.59 J/cm² for Ga³⁺CHP, while control cells (treated with PS alone) were kept in the dark outside of the incubator for the same time as irradiation. After treatment, the plates were returned to the xCELLigence instrument, and the CI was measured every 10 min. Experiments were carried out until a plateau phase was reached.

2.11. qRT-PCR Gene Expression Analysis. RNA isolation and purification, reverse transcription, and qPCR were performed according to previously published data.²⁷ Briefly, RNA was isolated and purified from the *S. aureus* 5 N isolate (OD₆₀₀ = 0.5) after samples were treated with sublethal doses of aPDI (reduction in bacterial cell count ~0.5 log₁₀ units) using a Syngen Blood/Cell RNA Mini Kit (Syngen, Poland). The TranScriba kit (A&A Biotechnology, Poland) was used to transcribe the RNA to complementary DNA (cDNA). qPCR assays were performed using a LightCycler 480 II (Roche Life Science, Germany). The reaction mixture (10 μL total) consisted of 5 μL of Fast SG qPCR Master Mix (EURx, Poland), 200–400 nM of each primer (TIB MOLBIOL, Germany) (Table S1), nuclease-free water, and 1 μL of fivefold dilution of cDNA. The following steps were implemented (Table S2). Melting curve analysis was carried out to exclude primer-dimer formation or nonspecific amplification. Relative changes in the expression of the *sec*, *tst*, *srrA*, and *srrB* genes were normalized to the *gmk* reference gene.

2.12. Western Blot Immunodetection. *S. aureus* 5 N was grown in TSB until the logarithmic phase of growth was

reached (OD₆₀₀ = 1.5), diluted 10× in TSB, and then treated with sublethal conditions of aPDI using each of the test compounds to obtain a reduction in bacterial cell count of ~1 log₁₀ unit. After irradiation, bacterial supernatants were harvested 1 h after treatment. aPDI-treated and untreated supernatants were mixed 1:1 (v/v) with 2× Laemmli buffer (Bio-Rad, USA) supplemented with β-mercaptoethanol (Sigma-Aldrich, USA). Samples were heated to 95 °C for 5 min, centrifuged (13,200 rpm/min), and stored at –20 °C. The total protein concentration in the tested samples was determined with the RC DC Protein Assay kit I (Bio-Rad, USA) based on a standard curve prepared from the γ-globulin protein standard (Bio-Rad, USA). SEC or TSST-1 (Toxin Technology, Inc., USA) standard proteins and lysates were separated by SDS-PAGE at 180 V for 1 h and then wet transferred to PVDF membranes (Bio-Rad, USA) for 1 h at 100 V. The membrane was washed twice with TBS buffer (0.01 M Tris–HCl, pH 7.5, 0.05 M NaCl) and then incubated in TBS-T (TBS buffer with 0.5% (v/v) Tween 20, CHEMPUR, Poland) suspended in a 1% solution of skim milk powder for 30 min. After washing with TBS, the membrane was incubated with primary rabbit antibodies against the toxins (1:10,000) (Toxin Technology, Inc., USA) overnight at 4 °C with gentle shaking. The membrane was then washed three times with TBS and incubated with anti-rabbit alpaca secondary antibodies labeled with HRP (1:10,000 in TBS-T with 1% milk) (Jackson ImmunoResearch Laboratories Inc., USA) for 30 min with shaking at room temperature. Excess antibodies were removed by washing three times with TBS-T for 5 min, and residual detergent was removed by washing twice with TBS. Membranes were placed in the ChemiDoc XRS+ gel documentation system and visualized using the Clarity Max membrane reagent (Bio-Rad, USA).

2.13. IL-2 ELISA. Human PBMCs were counted, diluted in RPMI-1640 medium, and seeded at 1 × 10⁵ per well in a 96-well round-bottom plate (Corning, USA). aPDI-treated or

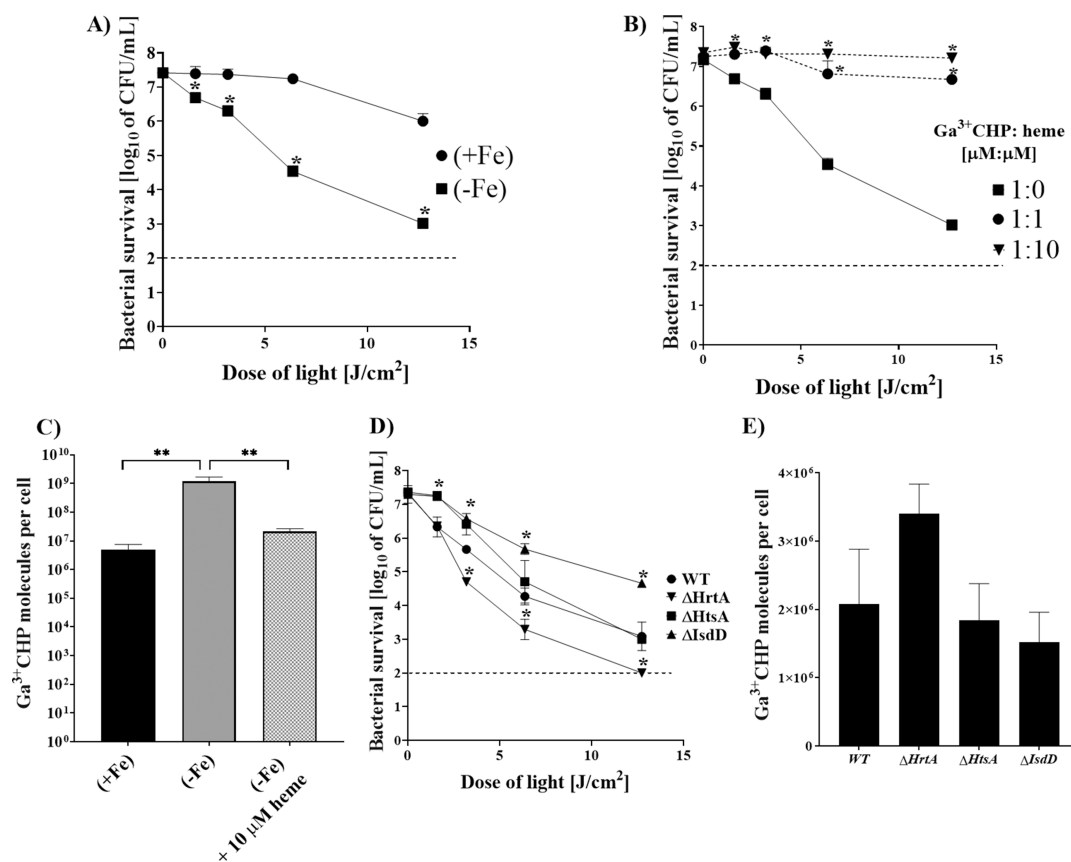


Figure 4. Dependence of the Ga^{3+} CHP-mediated aPDI effect and intracellular accumulation on heme and iron. Experiments were conducted using two *S. aureus* strains: 25923 (A–C) and Newman (WT) together with its isogenic mutants (ΔHrtA , ΔIsdD , and ΔHtsA) (D, E) in the presence (+Fe) or absence (–Fe) of iron. (A) Effect of aPDI on bacterial survival after treatment with $1\ \mu\text{M}$ Ga^{3+} CHP and green light in the presence or absence of iron. Significance at the respective p values is indicated with asterisks ($*p < 0.001$). *S. aureus* 25923 cells cultured in the presence of iron (+Fe) were used as a control. (B) Effect of aPDI on the different ratios of Ga^{3+} CHP to the natural ligand heme [$\mu\text{M}:\mu\text{M}$]. Prior to the experiment, bacterial cells were cultivated in medium without iron. (C) Intracellular accumulation of $10\ \mu\text{M}$ Ga^{3+} CHP in *S. aureus* cultured with varying iron levels in the medium and after the addition of $10\ \mu\text{M}$ heme (corresponding to a PS:heme concentration ratio of 1:1). Significance at the respective p values is indicated with asterisks ($**p < 0.005$). *S. aureus* 25923 cells cultured in the absence of iron (–Fe) were used as a control. (D) Phototreatment of the wild-type strain or deletion mutants (ΔHrtA , ΔIsdD , and ΔHtsA) with $1\ \mu\text{M}$ Ga^{3+} CHP under green light irradiation (522 nm) in the presence of iron in the medium. Significance at the respective p values is indicated with asterisks ($*p < 0.001$) for *S. aureus* Newman WT. (E) Ga^{3+} CHP uptake at $1\ \mu\text{M}$ by the Newman *S. aureus* strain and its isogenic mutants in the presence of iron in the medium. All experiments were conducted in three biological replicates, and the data are presented as the mean \pm SD. The dashed line (A, B, D) at $2\ \log_{10}$ CFU/mL is the detection limit of the test.

untreated SEC or TSST-1 toxin (80 ng/mL) was added to PBMCs and incubated for 24 h at $37\ ^\circ\text{C}$ in a 5% CO_2 atmosphere. Afterward, the plate was centrifuged ($300 \times g/5\ \text{min}/4\ ^\circ\text{C}$), and supernatants were collected and kept at $-80\ ^\circ\text{C}$ for further analysis. IL-2 production measurements in each condition were determined with an IL-2 Human Uncoated ELISA Kit (Invitrogen, USA) according to the manufacturer's protocol. Three independent biological replicates of PBMCs derived from three different donors with three technical repetitions of aPDI were used in this experiment. The absorbance at 450 nm was measured, and the signal was calculated as IL-2 production based on the standard curve of human IL-2. As a positive control, PBMCs were chemically treated with 150 ng/mL phorbol 12-myristate 13-acetate (PMA) (Sigma-Aldrich, USA) and 75 ng/mL ionomycin (Sigma-Aldrich, USA).

2.14. Statistical Analysis. Statistical analysis was performed using GraphPad Prism 9 (GraphPad Software, Inc., CA, USA). Quantitative variables were characterized by the arithmetic mean and the standard deviation of the mean.

Data were analyzed using either one-way or two-way ANOVA with Dunnett's multiple comparison test.

3. RESULTS

3.1. Ga^{3+} CHP Is an Efficient Photogenerator of ROS under Green Light Illumination. We recently synthesized Ga^{3+} CHP, a novel antimicrobial compound, which comprises a porphyrin ring moiety, a Ga^{3+} metal ion, and two quaternary ammonium groups at the ends, which significantly increased the solubility of the compound in water compared to that of protoporphyrin IX loaded with gallium ions (Ga^{3+} PP) ($40.3\ \text{mg}\ \text{mL}^{-1}$ for Ga^{3+} CHP vs $<0.1\ \text{mg}\ \text{mL}^{-1}$ for Ga^{3+} PP) (Figure 3).²¹ Here, we were interested in whether the newly synthesized Ga^{3+} CHP efficiently produces ROS upon visible light excitation (522 nm). The quantum yield of singlet oxygen photogeneration of Ga^{3+} CHP in comparison to the singlet oxygen photogeneration of standard RB is shown in Figure 3A. Ga^{3+} CHP exhibited singlet oxygen photogeneration at a yield of 0.55, indicating that during photodynamic action, this compound efficiently generates singlet oxygen. Furthermore,

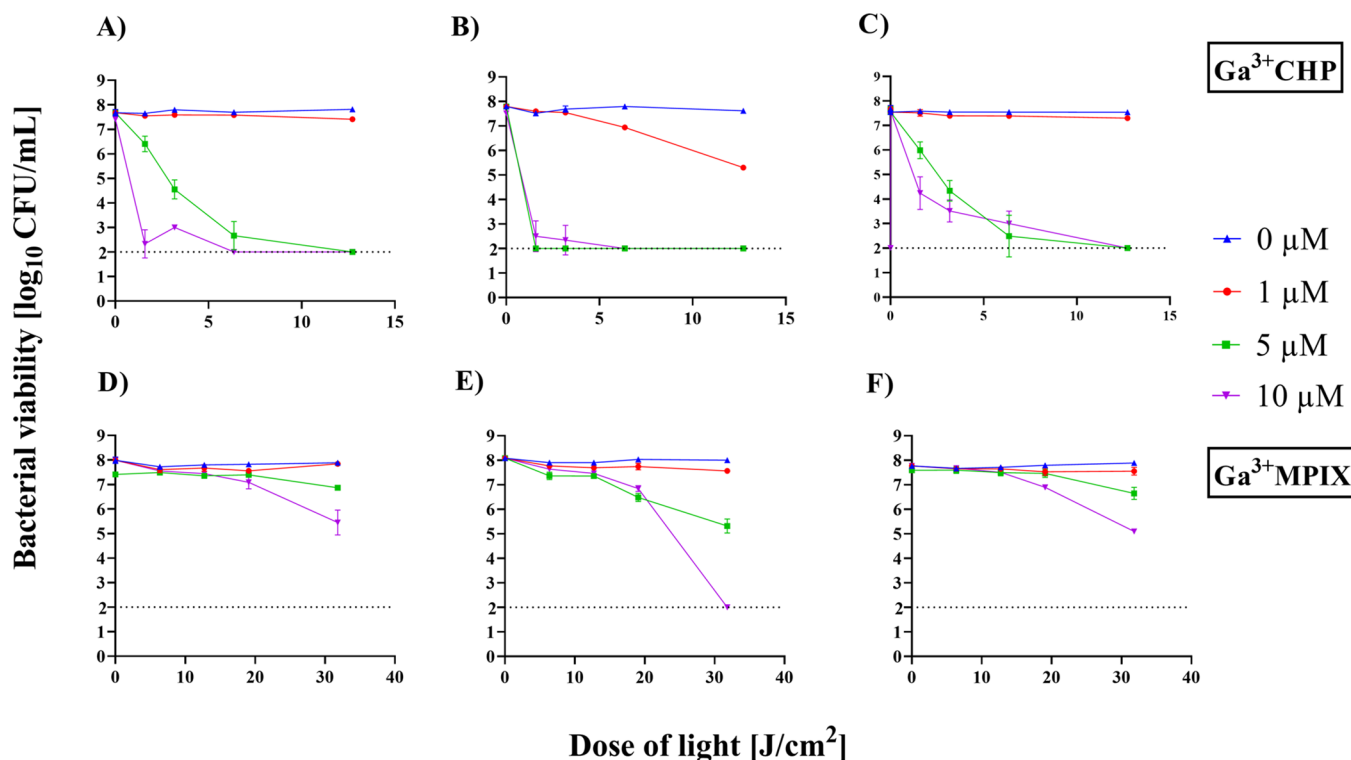


Figure 5. Photoinactivation of *S. aureus* isolates from patients with atopic dermatitis. Two photosensitizers, Ga^{3+}CHP (A–C) and $\text{Ga}^{3+}\text{MPIX}$ (D–F), activated with green (522 nm) light were used to evaluate the effectiveness of aPDI on the survival of 3 N (A, D), 5 N (B, E) and 38 N (C, F) isolates. The detection limit was 100 CFU/mL (dashed lines). Each experiment was performed in three independent biological replicates. The data are presented as the mean \pm SD of three separate experiments. The dashed line at 2 \log_{10} CFU/mL is the detection limit of the test.

by EPR spin trapping, we found a spin adduct with spectral parameters consistent with that of DMPO-OOH, indicating the photogeneration of superoxide anions, although at very low yield, after green light irradiation with Ga^{3+}CHP in a mixture of 75% DMSO (Figure 3B). The results suggested that Ga^{3+}CHP is mainly a type II photosensitizer that uses the energy transfer from the triplet state of the PS to produce highly toxic singlet oxygen ($^1\text{O}_2$). Ga^{3+}CHP also generated superoxide anions at a low but detectable level.

3.2. Ga^{3+}CHP Is Recognized and Accumulated by Heme-Specific Receptors and a Heme-Specific Efflux Pump. The modification of the core porphyrin ring with two positively charged quaternary ammonium groups equipped the molecule with the ability to efficiently bind negatively charged bacterial surface, allowing the cells to efficiently accumulate the PS via electrostatic interactions. We further wanted to investigate whether Ga^{3+}CHP could be actively accumulated by staphylococcal cells similar to its structural analogue—heme. We tested this in several experiments: (i) analysis of aPDI in conditions of iron availability or absence, (ii) intracellular accumulation of compounds, and (iii) use of mutants with disabled heme transport proteins. We examined the effect of aPDI with 1 μM Ga^{3+}CHP and green light illumination on bacterial survival using divergent iron availability in the environment (Figure 4A). Iron starvation potentiated the aPDI effect, showing a reduction in bacterial survival of 4.5 \log_{10} CFU/mL compared to bacteria cultured in the presence of iron, showing a reduction in survival of only 1.5 \log_{10} CFU/mL. Literature data indicated that in the absence of iron, elevated production of heme transport proteins by bacterial cells was observed; as a consequence, more of the compound accumulated in the cells,²⁸ which in our case

resulted in increased aPDI efficiency. Higher aPDI efficiency in iron-starved bacteria was reversed by the addition of iron-containing heme. The addition of the same concentration (1 μM) or a 10-fold excess of heme significantly reduced the effect of Ga^{3+}CHP -mediated aPDI, indicating that both compounds (heme and Ga^{3+}CHP) compete for the same heme transport proteins (Figure 4B).

This was confirmed by the results of Ga^{3+}CHP accumulation, which was significantly reduced in bacteria in the presence of iron compared to lack of iron. Addition of heme, competing with Ga^{3+}CHP for binding to heme transport proteins, resulted in a significant reduction of Ga^{3+}CHP accumulation in an iron-depleted medium, confirming that Ga^{3+}CHP is recognized by heme transport proteins (Figure 4C).

We further investigated the role of selected heme acquisition (Isd or Hts) and heme detoxification (HrtAB efflux pump) systems in aPDI (Figure 4D). Staphylococcal cells with an impaired heme efflux pump (ΔHrtA) showed the most sensitive phenotype to Ga^{3+}CHP -mediated aPDI, presenting a decrease in bacterial survival by 5.3 \log_{10} CFU/mL (Figure 4D). ΔIsdD cells lacking a functional heme acquisition mechanism were the most tolerant to aPDI treatment among the studied mutants, with only a 2.6 \log_{10} CFU/mL reduction in bacterial counts. This finding was also reflected in intracellular accumulation of Ga^{3+}CHP , where efflux pump impairment showed the greatest accumulation of the compound, while the cells without IsdD demonstrated the lowest accumulation (Figure 4E). In this case, we observed a difference in accumulation, but statistical significance was not reached. These results showed that heme-specific Isd receptors

and the HrtAB efflux pump may be important for Ga³⁺CHP accumulation and phototreatment.

3.3. Ga³⁺CHP Effectively Photosensitizes *S. aureus* Isolates during Phototreatment. To determine whether photoinactivation with Ga³⁺CHP is an effective treatment for reducing *S. aureus* colonization in patients with AD, we first investigated its efficacy against three clinical isolates of *S. aureus* (Figure 5). Photoinactivation of bacterial cells with 5 μM Ga³⁺CHP followed by irradiation (12.7 J/cm²) resulted in a reduction in the number of bacteria by ~5.5 log₁₀ CFU/mL for all tested strains. The concentration of the reference metalloporphyrin Ga³⁺MPIX had to be increased to 10 μM and the light dose to 31.8 J/cm² to observe a decrease in the number of bacterial cells of the 5 N isolate below the detection limit, while for the other two isolates tested, 3 and 38 N reached a lethal effect (for 3 N – 2.5 log₁₀ CFU/mL; for 38 N – 2.6 log₁₀ CFU/mL). The PS concentrations and doses of green light used to achieve effective aPDI significantly differed between the two compounds. A sufficient reduction in bacterial cell number was obtained by Ga³⁺CHP-mediated aPDI using suitable conditions, and the irradiation time was shorter for Ga³⁺CHP-mediated aPDI than for Ga³⁺MPIX-mediated aPDI. A strain-dependent response to aPDI was also observed, with the 5 N isolate being the most sensitive to aPDI regardless of the PS used. We also tested the effectiveness of both compounds against the biofilm formed by the clinical isolate of *S. aureus* 5 N. In this case, we observed a Ga³⁺CHP concentration- and light dose-dependent reduction in the number of biofilm-forming cells. In the case of biofilms, aPDI using Ga³⁺CHP proved significantly more effective than Ga³⁺MPIX (Figure S3).

To explain the superior efficacy of Ga³⁺CHP-mediated aPDI compared to that of Ga³⁺MPIX-mediated aPDI, we compared the intracellular accumulation of tested compounds across all studied strains (Figure 6). Incubation of the cells with 1 μM PSs resulted in the accumulation of 10⁴–10⁵ and 10⁵ molecules per cell for Ga³⁺MPIX and Ga³⁺CHP, respectively. After increasing the concentrations of the tested compounds to 10 μM, Ga³⁺CHP was strongly accumulated in each tested strain,

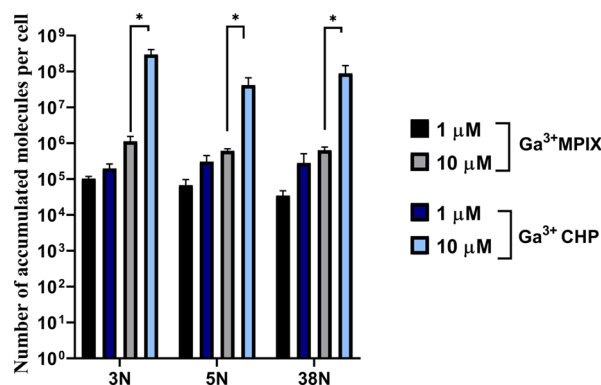


Figure 6. *S. aureus* accumulation of the photosensitizers. The *S. aureus* strains 3, 5, and 38 N were exposed to either Ga³⁺MPIX or Ga³⁺CHP for 10 min with shaking at 37 °C. Then, the cells were washed twice to eliminate extracellular PS and resuspended in lysis buffer. After 24 h of incubation in the dark, the fluorescence of the lysates was measured on a plate reader. The data are presented as the mean of accumulated PS molecules from three biological repetitions, calculated based on the standard curve of each compound in the lysis buffer.

reaching an order of magnitude of 10⁷–10⁸ molecules per cell. In comparison, the accumulation of Ga³⁺MPIX at the same 10 μM concentration remained in the range of 10⁵–10⁶ molecules per cell. We also evaluated the accumulation of both compounds in the *S. aureus* strain 25923 using fluorescence confocal microscopy (Figure S2). Compared to Ga³⁺MPIX, Ga³⁺CHP accumulated at significantly higher levels, which was reflected by its higher fluorescence intensity. Undoubtedly, the Ga³⁺CHP accumulation was higher than that of Ga³⁺MPIX in all tested strains, which explains its higher efficiency in aPDI.

3.4. Ga³⁺CHP-Based Photosensitization Reduced the Viability of *S. aureus* in an Ex Vivo Porcine Skin Model.

To evaluate whether the significant reduction in viability obtained in vitro could be translated into a more complex biological system, we applied an ex vivo porcine skin model. In this experiment, we used the bioluminescent *S. aureus* strain Xen40 for the colonization of porcine skin ex vivo. After establishing a biofilm on the surface of the skin (24 h post bacteria application), Ga³⁺CHP was added and aPDI was performed. The viability of bacteria was determined by measuring the bioluminescence signal of *S. aureus* before and after treatment with Ga³⁺CHP alone, light alone, or combined treatment (Figure 7A). The change in the bioluminescence signal was calculated and is presented in Figure 7B. Untreated cells and cells treated with Ga³⁺CHP showed only slightly altered bioluminescence signals, indicating that the bacteria were still present on the skin. In contrast, the bioluminescence

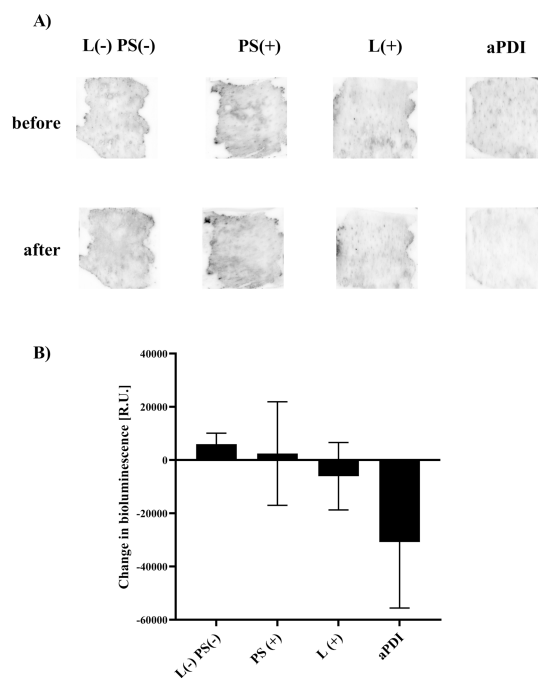


Figure 7. Evaluation of Ga³⁺CHP-mediated aPDI treatment against the *S. aureus* strain Xen40 in an ex vivo porcine skin model. (A) Bioluminescent *S. aureus* strain was applied to clean porcine skin grafts 24 h before treatment. Ga³⁺CHP was applied for 20 min and incubated at 37 °C before irradiation (12.72 J/cm²). The bioluminescence signal was measured before and immediately after aPDI treatment (10 μM Ga³⁺CHP, 12.72 J/cm²). (B) Bioluminescence was measured by ChemiDoc and Bio-Rad instruments and calculated by ImageJ software. The change in the bioluminescent signal was measured for each condition, and the average of three independent biological replicates is presented in the graph. The data are presented as the mean ± SD of before vs after treatment.

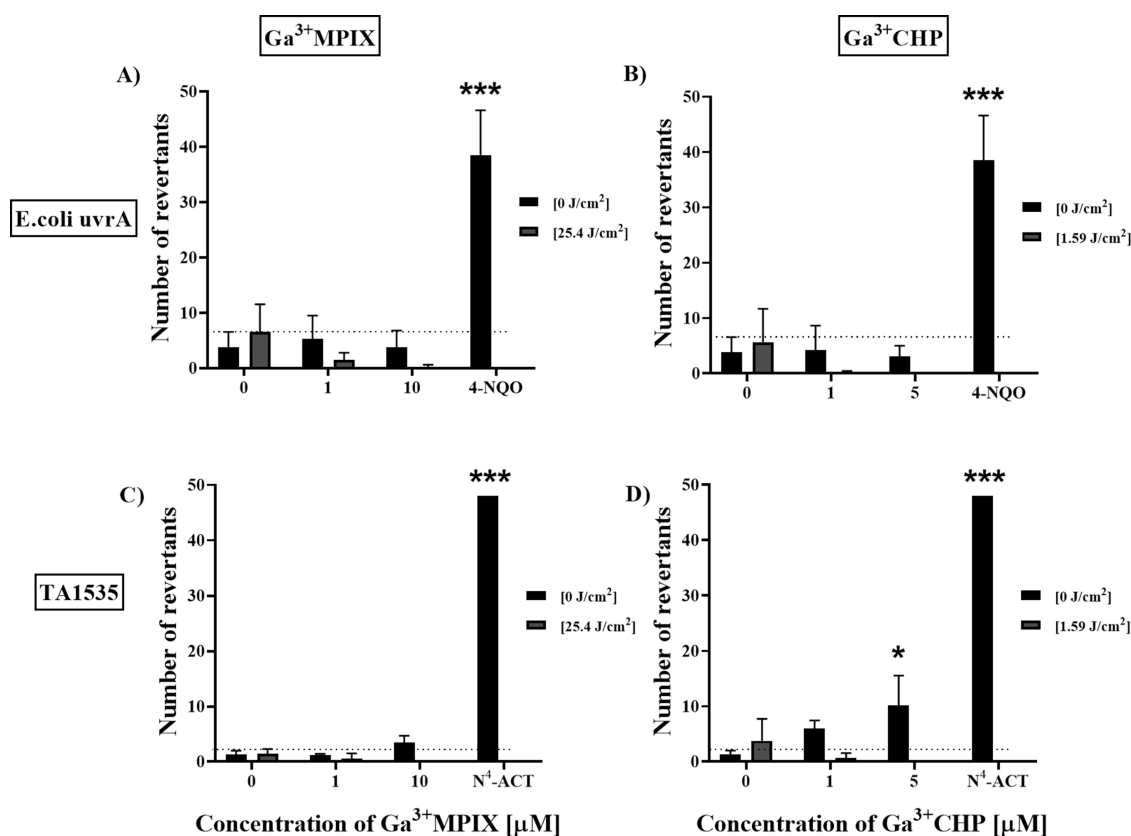


Figure 8. Examination of mutagenicity of photoinactivation with gallium metalloporphyrins. *E. coli uvrA* (A, B) and TA1535 (C, D) strains were exposed to both gallium compounds: Ga³⁺MPIX (A, C) or Ga³⁺CHP (B, D) either in the dark or under green light conditions. Additionally, two types of controls were included: untreated cells (0 μM, 0 J/cm²) as the negative control and chemically induced revertants with 90 min incubation with mutagens 4-NQO for *E. coli uvrA* or N⁴-ACT for TA1535 as positive controls. All treatment groups were incubated with mutagen or gallium compound for 90 min at 37 °C. For the light-activated treatment groups, after 10 min of incubation with compounds, cells were exposed to green light at the proper dosage and then incubated for 90 min. Then, exposure medium was added to the incubated cultures, and the samples were divided into 384-well plates with each sample being distributed to 48 wells with three technical repetitions. The microplates were incubated for 48 h at 37 °C. The assessment of revertants was conducted by determining the change in exposure medium color (from blue to yellow) in each well. Yellow color represented the occurrence of revertants. The experiment was performed in three biological replicates with three technical replicates of each treatment group in each experiment. Data are presented as the mean ± SD of the number of revertants. The dashed line indicates the level of spontaneously formed revertants (baseline). Cyto- and phototoxicity of aPDI against indicator strains are presented in the Supporting Information (Figure S5).

signal decreased after aPDI treatment, indicating a reduction in the viability of bacterial cells. Light-only treatment also exhibited a decrease in the bioluminescence signal, but the decrease was not as severe as that resulting from aPDI treatment. Ga³⁺CHP combined with green light irradiation might be a promising method for the reduction of *S. aureus* colonization on the skin. Although measurement of the bioluminescent signal indicated differences between aPDI treated and untreated samples, the values of the measured signal did not reach statistical significance. On the other hand, the direct method of counting bacterial cells before and after aPDI treatment indicated a statistically significant difference between the number of cells after aPDI treatment compared to cells treated only with Ga³⁺CHP or treated only with light (Figure S4).

3.5. Ga³⁺MPs Are Not Mutagenic under Light or Dark Conditions. To assess the safety of aPDI treatment with Ga³⁺MPs, we tested the mutagenic potential of both gallium compounds on two reference bacterial strains designed to quantify the mutagenic potential of various compounds, namely, *Escherichia coli uvrA* and *Salmonella typhimurium* TA1535. We tested both compounds, Ga³⁺MPIX and

Ga³⁺CHP, with or without exposure to green light to test the potential mutagenicity of the compounds independent of light and in a light-dependent manner (aPDI treatment). We applied two types of aPDI conditions: (i) mild, in which the reduction in *S. aureus* cell number did not exceed 1 log₁₀ CFU/mL, and (ii) strong, in which the reduction in *S. aureus* cell number was at least 2 log₁₀ CFU/mL. Thus, for each compound, the aPDI conditions were different. At the same time, the aPDI doses would have to be sublethal for the indicator strains (*E. coli* and *S. typhimurium*) in order for us to determine the number of revertants formed (Figure S5). Based on the *E. coli uvrA* strain analysis data, we did not observe an increased number of revertants when using either compound under light activation or dark conditions (Figure 8A,B). In the case of *S. typhimurium* indicator strain TA1535, we observed an increased number of revertants at 5 μM concentration: for Ga³⁺CHP in the dark conditions (Figure 8C,D). It is noteworthy that the number of revertants obtained after treatment slightly exceeded the baseline; however, these results are still significantly lower than for the chemically induced positive control (Figure 8C,D). After excitation of Ga³⁺CHP with light, the number of revertants never exceeded the

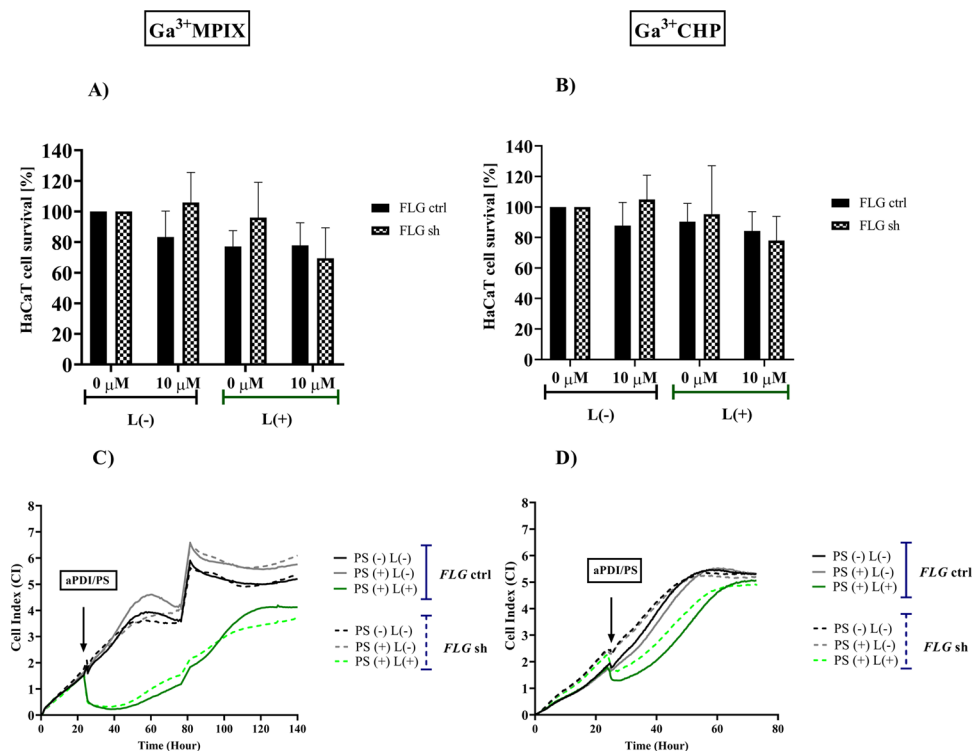


Figure 9. Effect of photoinactivation with Ga³⁺MPIX and Ga³⁺CHP on human keratinocytes with divergent filaggrin (FLG) expression. (A, B) Viability of HaCaT cells with normal filaggrin expression (*FLG ctrl*) and filaggrin knockdown (*FLG sh*) was measured with the MTT assay after dark or light exposure to Ga³⁺MPIX (31.9 J/cm²) (A) or Ga³⁺CHP (1.59 J/cm²) (B). (C, D) Cell growth dynamics of both lines: *FLG ctrl* or cells impaired in filaggrin expression—(*FLG sh*) after dark/light exposure to 10 μM Ga³⁺MPIX (31.9 J/cm²) (C) or Ga³⁺CHP (1.59 J/cm²) (D). The CI (represented as the Y-axis) was measured for each condition every 10 min. The x-axis shows the experimental duration in hours. The values presented are the average of the 7 technical repetitions. PS (+/−) refers to the presence/absence of a photosensitizer and L (+/−) to light.

baseline. The results obtained indicated that both compounds were not mutagenic after light activation, while the observed increased number of revertants after treatment in the dark would require more in-depth analyses to conclusively resolve the safety of Ga³⁺CHP.

3.6. Ga³⁺CHP Is less Phototoxic Than Ga³⁺MPIX to Human Keratinocytes and Is Not Dependent on Filaggrin Levels. To determine whether the aPDI conditions used for efficient photoinactivation of bacterial cells are toxic to eukaryotic cells, we tested them on HaCaT human keratinocytes (i) with normal filaggrin expression (*FLG ctrl*) and (ii) with filaggrin suppression (*FLG sh*). The HaCaT *FLG sh* cell line was used as a model of atopic skin as the expression level of filaggrin in AD patients is significantly reduced.¹¹ According to the MTT assay results, the cytotoxicity of HaCaT cells with both normal and aberrant *FLG* expression was negligible as the viability of both cell groups was in the range of 83–105% compared to that of untreated cells. Regarding phototoxicity, the viability of both cell lines was estimated to be ≥78% 24 h after aPDI treatment according to the MTT assay, which is considered an acceptable toxicity value (Figure 9A,B). Since the MTT assay only measures toxicity at a selected measurement point, we used the xCELLigence technique to investigate the cell growth and proliferation dynamics of both cell lines after aPDI treatment. Ga³⁺MPIX-mediated aPDI inhibited the proliferation and growth of both cell lines (*FLG ctrl* and *FLG sh*), and the number of surviving cells reached a plateau after approx. 140 h of the experiment, however, without reaching the cell index (CI) value of

untreated cells (Figure 9C). In comparison, the Ga³⁺CHP-mediated aPDI group showed significantly lower phototoxicity, with both cell groups reaching a plateau and a CI value equal to untreated cells after only 70 h, which was twice as fast as Ga³⁺MPIX-mediated aPDI (Figure 9D). Interestingly, compared to *FLG ctrl* HaCaT cells, *FLG sh* HaCaT cells showed slightly faster growth after aPDI treatment. Both gallium compounds excited with green light reduced the viability and proliferation rate of human keratinocytes; however, only cells treated with Ga³⁺CHP were viable enough to reach the plateau phase in a time period similar to that of untreated cells. It is worth mentioning that we did not observe cytotoxicity when the compounds were tested in dark conditions.

3.7. Effect of aPDI with Ga³⁺MPs on SEC Superantigen Expression, Production, and Biological Functionality. *S. aureus* has been shown to colonize the skin surface of AD patients, promoting its pathogenicity by producing a number of virulence factors, such as SEC or TSST-1 superantigens.^{29,30} We investigated whether Ga³⁺MPs in combination with light could affect the expression level, production, or biological functionality of these superantigens. A decrease in *sec* expression levels was observed not only after aPDI treatment (a decrease of 1.47 log₂ units) but also after treatment with light alone (a decrease of 0.89 log₂ units) and photosensitizer alone (1.35 log₂ units) compared to untreated cells (Figure 10A). In contrast, after Ga³⁺CHP-mediated aPDI, a significant downregulation of *sec* expression was observed (2.6 log₂ unit decrease), whereas light alone or compound alone did not alter *sec* expression (Figure 10B). At the protein

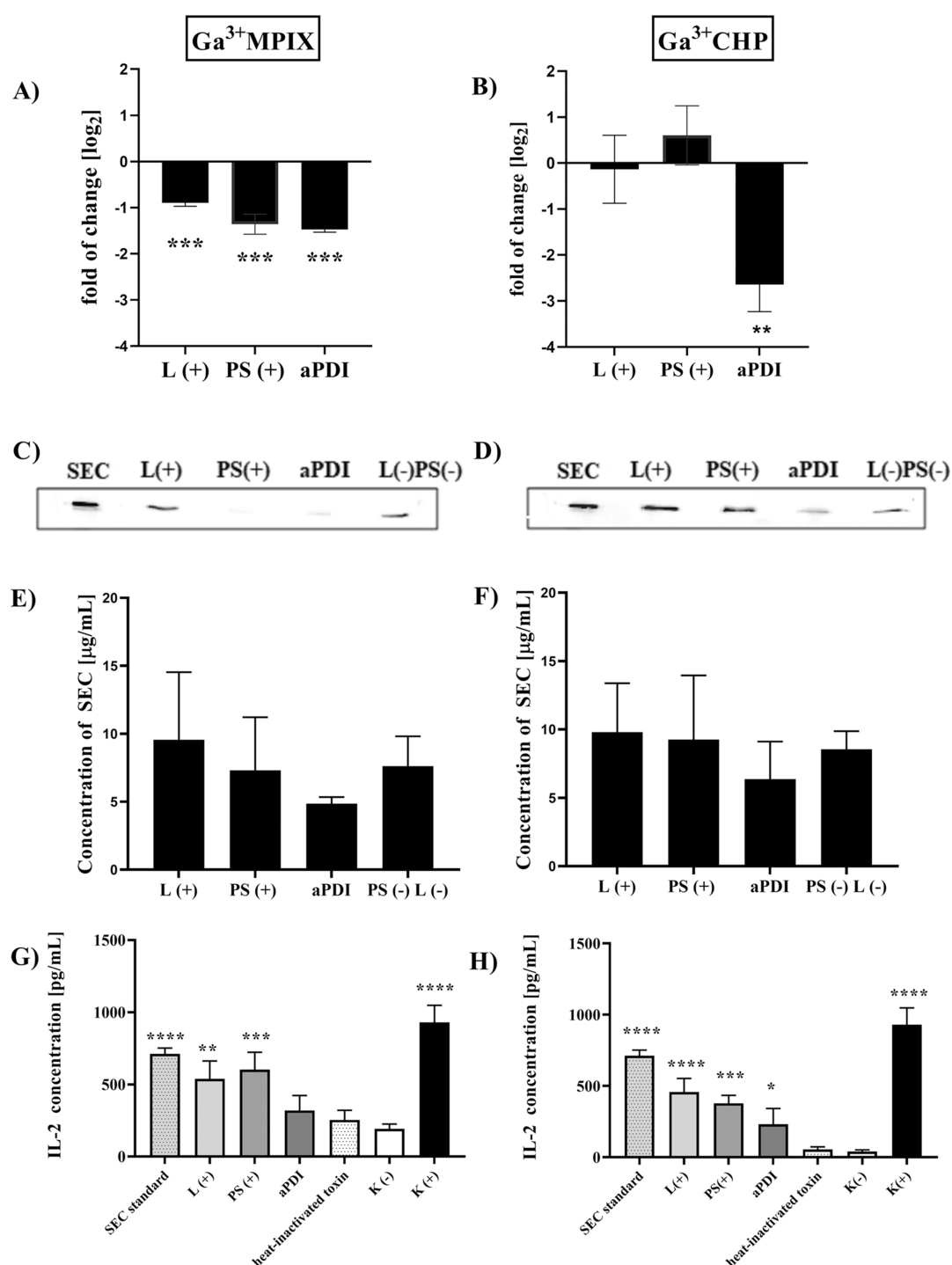


Figure 10. Effect of photoinactivation with gallium metalloporphyrins on gene expression, protein production, and biological activity of SEC. (A, B) Relative gene expression of *sec* normalized to the reference gene *gmk*. Cells were diluted 1:100 and grown until the OD₆₀₀ was 0.5, incubated with the proper photosensitizer—10 μ M Ga³⁺MPIX (A) or 1 μ M Ga³⁺CHP (B) for 10 min and illuminated with 522 nm light (12.7 J/cm² for Ga³⁺MPIX or 1.52 J/cm² for Ga³⁺CHP). The expression of *sec* was measured in three biological samples with three technical repetitions of each sample. Error bars represent the standard error of the mean (SEM) values. (C–F) Western blot analysis after each treatment in the presence or absence of 522 nm light and Ga³⁺MPIX (C) or Ga³⁺CHP (D). Supernatants were harvested 1 h after aPDI treatment, and 10 μ g of supernatant, calculated by the modified Lowry protocol, was added to the gel for each treatment. The intensity of the band was measured by ImageJ software and calculated according to the SEC protein standard curve. (G, H) IL-2 measurements from activated PBMCs exposed to SEC toxin untreated or pretreated with aPDI or 10 μ M Ga³⁺MPIX with 12.72 J/cm² (G) or 2 μ M Ga³⁺CHP with 6.36 J/cm² (H). The toxin was also exposed to light alone (L+) or photosensitizer alone (PS+), where the controls were heat-inactivated toxin (incubated for 1 h at 99 °C), K(–)—PBMC cells not exposed to toxin and K(+)—chemically activated PBMC cells. Significance at the respective p values is marked with asterisks [$*p < 0.05$; $**p < 0.01$; $***p < 0.001$, $****p < 0.0001$ with respect to untreated samples (cells maintained in dark conditions)].

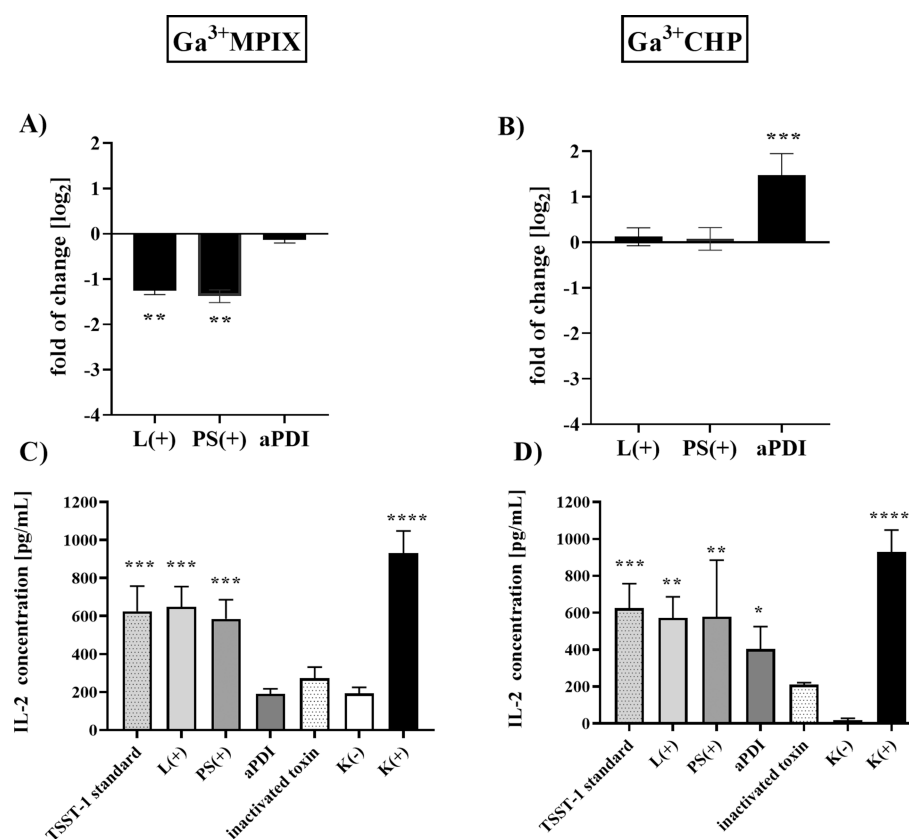


Figure 11. Effect of photoinactivation with gallium metalloporphyrins on gene expression, protein production, and biological activity of TSST-1. (A, B) Relative expression of the *tst* gene was normalized to the *gmk* reference gene and measured by quantitative PCR. Cells were diluted 1:100 and grown until the OD_{600} was 0.5, incubated with the proper photosensitizer—10 μ M Ga^{3+} MPIX (A) or 1 μ M Ga^{3+} CHP (B) for 10 min and illuminated with 522 nm light (12.7 J/cm² for Ga^{3+} MPIX or 1.59 J/cm² for Ga^{3+} CHP). The expression of *tst* was measured in three biological samples with three technical replicates each. Error bars represent SEM values. (C, D) IL-2 measurements from activated PBMCs exposed to TSST-1 toxin untreated or pretreated with aPDI: 10 μ M Ga^{3+} MPIX with 12.72 J/cm² (G) or 10 μ M Ga^{3+} CHP with 12.72 J/cm² (H). The toxin was also exposed to light alone (L+) or photosensitizer alone (PS+), where the controls were heat-inactivated toxin (incubated with 1 h 99 °C), K(−)—PBMC cells not exposed to toxin, and K(+)—chemically activated PBMC cells. Significance at the respective *p* values is marked with asterisks [**p* < 0.05; ***p* < 0.01; ****p* < 0.001 with respect to untreated samples (cells maintained in dark conditions)].

level, both light-activated Ga^{3+} MPs only slightly reduced SEC production (no statistical significance) (Figure 10C–F), probably due to the insufficient sensitivity of the Western blot technique used in these analyses. However, we did not observe any significant difference between treatment with Ga^{3+} MPIX (Figure 10C,E) or with Ga^{3+} CHP (Figure 10D,F). Next, we were interested to know whether light excitation of Ga^{3+} MPs affected the biological activity of SEC. In this experiment, SEC toxin was subjected to aPDI with Ga^{3+} MPIX (Figure 10G) or Ga^{3+} CHP (Figure 10H), and then SEC activity was evaluated in human peripheral mononuclear cells (PBMCs) after exposure to treated SEC. Bacterial superantigens, such as SEC and TSST-1, stimulate strong non-specific activation and proliferation of lymphocytes resulting in the production of a large amount of cytokines.³¹ We tested superantigen activity by measuring interleukin 2 (IL-2), which is produced as a proinflammatory factor in response to SEC and TSST-1.³² The biological activity of SEC, as measured by IL-2 levels, was significantly reduced after treatment with Ga^{3+} MPIX-mediated aPDI (319 pg/mL) compared to untreated toxin (712.5 pg/mL). The level of IL-2 after PBMC exposure to the aPDI-treated toxin decreased to the level of IL-2 produced by cells treated with heat-inactivated SEC or cells not exposed to the toxin. Moreover, treatment with light or a photosensitizer alone had no effect on the proinflammatory

activity of SEC. Similarly, IL-2 levels were also reduced by aPDI with Ga^{3+} CHP-treated toxin (Figure 10H) compared to the untreated enterotoxin-, L(+)-alone, or PS(+)-alone treated toxin. Photoinactivation with both Ga^{3+} MPs reduced the biological functionality of the SEC superantigen, although it did not significantly alter the total protein levels. Moreover, only Ga^{3+} CHP-mediated aPDI significantly affected *sec* gene expression levels.

3.8. Phototherapy with Both Ga^{3+} MPs Affects the Biological Function of TSST-1. The second important superantigen we selected for our analyses was TSST-1, a virulence factor strongly associated with the exacerbation of inflammation in atopic skin. We investigated the effects of both green light-activated gallium compounds on the gene expression, protein levels, and biological function of the TSST-1 toxin. Ga^{3+} MPIX-mediated aPDI did not alter the expression of the *tst* gene (Figure 11A), while treatment with light or photosensitizer alone decreased *tst* expression levels 1.259 log₂ units and 0.38 log₂ units, respectively. Interestingly, Ga^{3+} CHP-mediated aPDI significantly upregulated *tst* expression by 1.5 log₂ units (Figure 11B), while treatment with light alone or photosensitizing compound alone had no effect on *tst* expression levels. Next, we tested the biological functionality of TSST-1 after aPDI treatment using each of the tested compounds in vitro by measuring the level of IL-2

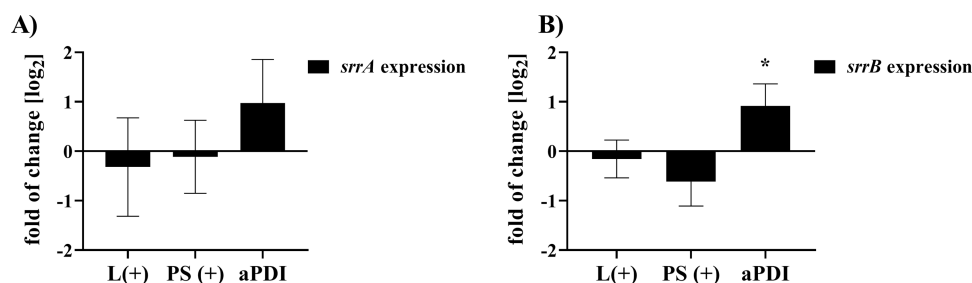


Figure 12. Effect of photoinactivation with gallium metalloporphyrin on the expression of the genes in the two-component SrrAB system. (A, B) Relative expression of the *srrA* (A) and *srrB* (B) genes normalized to the *gmk* reference gene. Cells were diluted 1:100, grown until the OD₆₀₀ was 0.5, incubated with a photosensitizer (1 μ M Ga³⁺CHP) for 10 min, and irradiated with light at 522 nm (1.59 J/cm²). The expression of both genes was measured in three biological repetitions with three technical replicates in each. The data are presented as the mean \pm SEM.

secreted by stimulated PBMCs, similar to the SEC study. TSST-1 treated with Ga³⁺MPIX-mediated aPDI reduced the level of IL-2 produced by activated PBMCs to levels estimated for nonactivated cells or after exposure to heat-inactivated TSST-1 toxin (Figure 11C). A reduction in IL-2 production in activated PBMCs was also observed after the TSST-1 toxin was treated with Ga³⁺CHP-mediated aPDI (Figure 11D). Pretreatment of TSST-1 with both compounds in the dark or light alone did not reduce IL-2 production, indicating that only aPDI has an effect on the superantigenic activity of TSST-1.

We did not quantify the level of the TSST-1 protein after aPDI treatment due to the low level of production of this protein. The *in vitro* biological functionality of the superantigen of TSST-1 was examined after both treatments.

3.9. Expression of the *tst* Gene Is Positively Correlated with the Expression of the *srrAB* Regulatory Genes after aPDI. The result of upregulated expression of the *tst* gene after Ga³⁺CHP aPDI was unexpected. To understand the mechanism of the observed upregulation, we investigated the genes of the SrrAB regulatory system, which modulates the production of the TSST-1 toxin in response to the presence of ROS in the environment.³³ The expression of the *srrA* and *srrB* genes was investigated after Ga³⁺CHP phototreatment (Figure 12). We observed that the expression levels of both the *srrA* and *srrB* genes increased after aPDI treatment, which is consistent with the observed upregulation of the *tst* gene after photoinactivation. The expression of the TSST-1 toxin gene is positively correlated with the expression of the SrrAB regulatory system genes after aPDI.

4. DISCUSSION

The skin microbiome differs between AD patients and healthy individuals. There is a significant increase in commensal bacterial load in the skin microbiome of AD patients, and *S. aureus* is a key pathogen in AD.³⁴ Methods for staphylococcal decolonization in AD patients are mainly based on antibiotic therapies; however, due to increasing global antimicrobial resistance, antibiotic therapy remains a temporary solution. Most types of light-based treatments consist of ultraviolet A (UV-A) or narrow-band ultraviolet B (NB UV-B) exposure.³⁵ UV-B treatment was shown to reduce the viability of colonized *S. aureus* on the skin of AD patients^{36,37} as 308 nm excimer light showed similar results.³⁸ However, UV-B light penetrates through the epidermis layer of the skin, which generates a huge number of side effects and may promote carcinogenesis.³⁹ Visible light-based therapies, such as antimicrobial photodynamic inactivation, are currently being considered to reduce *S. aureus* colonization on atopic skin.² Photodynamic therapy

(PDT) is currently approved in Europe and the USA for the treatment of actinic keratosis. The case study reported by Pozzi and Asero showed that PDT with a narrow-band red light (630 nm, 75 J/cm²) and 5-aminolevulinic acid (ALA) as a PS precursor can be successfully used in the treatment of AD patients. Three PDT sessions were used to treat skin lesions; however, the effect on *S. aureus* viability was not investigated.⁴⁰ Red light penetrates deeper than UV light into the dermis layer; unfortunately, the pain effect can be a substantial obstacle in the case of AD patients with hypersensitive skin. Green light, on the other hand, penetrates the epidermis without causing as much pain, so the use of wavelengths in this spectral range may be a promising approach for the treatment of atopic skin.⁴¹ In this study, we have shown that Ga³⁺CHP can be effectively excited with green light, resulting in the production of singlet oxygen and to a lesser extent superoxide anion, which significantly reduced the viability of clinical *S. aureus* isolates derived from atopic skin (5 log₁₀ CFU/mL for Ga³⁺CHP and 2.6 log₁₀ CFU/mL for Ga³⁺MPIX). Additionally, we observed that aPDI treatment with Ga³⁺CHP effectively decolonized *S. aureus* in the *ex vivo* porcine skin model. Porcine skin has been used as the skin model due to its great similarity to human skin. This model has been applied in biofilm formation studies, skin barrier research, and wound infection models.^{42,43} However, studies on more complex models, such as *ex vivo* human atopic skin grafts or *in vivo* animal models, are needed.

Ga³⁺MPs are dual-function compounds that act according to light-independent and light-dependent mechanisms.⁴⁴ In the light-independent mechanism, they are antimicrobial agents that slow bacterial growth by blocking iron metabolism based on their structural similarity to heme (Fe³⁺PPIX) in planktonic cultures and biofilms.^{18,20,45,46} These compounds can also act as photosensitizers in aPDI, as they are able to absorb visible light and, in the presence of molecular oxygen, photogenerate cytotoxic ROS.^{17,20} Porphyrins are a group of naturally occurring type II photosensitizers mainly producing singlet oxygen rather than radicals.⁴⁷ The main disadvantage of porphyrin compounds is the formation of aggregates, resulting in poor solubility in aqueous solutions.^{48,49} The water solubility of antimicrobials has a great influence on their *in vivo* antimicrobial activity and biocompatibility in various tissues. Gallium porphyrin (Ga³⁺PP) is dissolved only in toxic organic solvents such as DMSO, whereas Ga³⁺MPIX is dissolved in an aqueous solution such as 0.1 M NaOH.²⁰ The addition of two quaternary ammonium groups to the porphyrin core in the Ga³⁺CHP structure (Figure 1) significantly increased its solubility in water to 40.3 g mL⁻¹,

while the water solubility of Ga³⁺PP was <0.1 g mL⁻¹.²¹ Despite the modification of the structure by the addition of ammonium groups, the Ga³⁺CHP structure remained similar to the heme structure, and it was still effectively accumulated by bacterial cells (Figures 6 and S2). Accumulation in bacterial cells is essential for the effective light-dependent and light-independent action of the compound. Bacterial cells contain heme acquisition receptors, the Isd system, and the HrtAB heme detoxification machinery, which seem to play a role in the sequestration and utilization of Ga³⁺CHP (Figure 4). Ga³⁺CHP-mediated aPDI efficacy, as well as its accumulation, strongly depended on heme or iron availability, further indicating that natural bacterial systems are responsible for Ga³⁺CHP uptake. ΔIsdD, a mutant in the transmembrane transporter, was the most tolerant to Ga³⁺CHP-mediated aPDI with the lowest Ga³⁺CHP accumulation, which indicated the predominant role of the Isd system in compound recognition and transmembrane transport. In our previous study on the meso-derivative Ga³⁺MPIX, we reported that Isd was involved in intracellular accumulation of Ga³⁺MPIX.²⁰ It was also found that Isd receptors are involved in the uptake of Ga³⁺PPIX.¹⁷ Studies by Moriwaki et al. showed that there is stable binding between Ga³⁺MPs and IsdH receptors, which contain NEAT domains, supporting the hypothesis that the Isd system might play a role in intracellular accumulation.⁵⁰ However, a thorough study of the receptor–ligand interaction for either Ga³⁺MPIX or Ga³⁺CHP needs to be conducted to evaluate whether such structural changes are crucial for compound recognition by the Isd system. To date, there is limited knowledge concerning the role of heme detoxification in the process of non-iron metalloporphyrin utilization. The expression of heme detoxification machinery genes was upregulated after exposure to Ga³⁺MPs, and the activation of this system is needed to partly overcome the toxicity of those compounds.⁵¹ We have previously shown that the ΔHrtA *S. aureus* mutant was more sensitive than the WT to aPDI treatment with various porphyrin compounds, e.g., PPIX or Ga³⁺MPIX.^{20,26} The current study revealed the same pattern for Ga³⁺CHP (Figure 4D). Without light exposure, Ga³⁺MPIX was revealed to be the most toxic for the ΔHrtA mutant among other compounds, such as Ga³⁺PPIX or PPIX.²⁰ However, Wakeman et al. showed that there was no significant change in Ga³⁺PPIX accumulation between *S. aureus* WT and ΔHrtB despite higher cytotoxicity under dark conditions.⁵¹ In our case, ΔHrtA accumulated the highest level of Ga³⁺CHP molecules per cell among all tested phenotypes; however, there was no significant difference in comparison to the WT strain (Figure 4E). The same observation was made for Ga³⁺MPIX. All these findings support the hypothesis that HrtAB may not be a specific or the only export pump of Ga³⁺MP molecules; however, by blocking its activity, the toxicity of gallium compounds may increase in both light-activated and dark conditions. Since there are currently no HrtAB efflux pump blockers on the market, this field deserves to be explored due to its high application potential.

An ideal photosensitizer candidate should exhibit high phototoxicity with low toxicity in the dark, a high quantum yield of singlet oxygen production and/or other ROS photogeneration, and high safety in eukaryotic cells.⁵² In this study, we characterized the light-dependent mechanism of Ga³⁺CHP. In general, for porphyrins, the quantum yield of singlet oxygen generation is estimated to be between 0.5 and 0.8.⁵³ Ga³⁺CHP is a type II photosensitizer that generates

singlet oxygen with a quantum yield of 0.55 and produces a low level of the superoxide anion through electron transfer mechanisms (Figure 3). However, despite the lower quantum yield of singlet oxygen generation, Ga³⁺CHP was more efficient in aPDI than Ga³⁺MPIX (quantum yield of singlet oxygen generation—0.69) (Figure 5).²⁰ The higher efficacy of Ga³⁺CHP-mediated aPDI in the reduction of *S. aureus* might be explained by the ~10× higher intracellular accumulation of Ga³⁺CHP compared to that of Ga³⁺MPIX (Figure 6). PS localization near sensitive targets is a crucial factor for photodynamic efficacy due to the short diffusion length of photogenerated singlet oxygen or other ROS. Thus, Ga³⁺CHP appeared to localize more closely with aPDI-sensitive targets inside the bacterial cells, leading to higher photodynamic efficacy.

Host cell safety is critical when exploring new potential therapeutic agents. The phototherapies presented here had acceptable (Ga³⁺MPIX) or favorable (Ga³⁺CHP) safety in vitro when applied to human keratinocytes both with normal and silenced *FLG* expression. However, we observed that Ga³⁺CHP-mediated aPDI was less toxic to keratinocytes (Figure 9D) than Ga³⁺MPIX-mediated aPDI (Figure 9C), as measured by the delay in the proliferation of cells. There may be a difference in the accumulation rate inside eukaryotic cells between these two PSs, which might correspond to the greater toxicity. An important factor in aPDI and its potential use in skin decontamination is exposure time. In PDT, light delivery should last for a few seconds or minutes and ensure effective PS excitation. Green light doses were lower for Ga³⁺CHP than for Ga³⁺MPIX, which in practice corresponds to shorter irradiation times (~10–20 min for Ga³⁺CHP; 50 min for Ga³⁺MPIX, 10.6 mW/cm²). It was previously reported that only 10 s of blue light irradiation (405 nm, 140 mW/cm²) was sufficient to eliminate >6 log₁₀ viable numbers of *S. aureus* using Ga³⁺PPIX. However, this porphyrin excitation was performed in the Soret band, which is the spectrum with the highest absorption coefficient. As a result, a shorter time is sufficient for providing the optimal energy dose to excite the compound. However, blue light treatment might be mildly cytotoxic to eukaryotic cells.⁵⁴ Excitation with the green Q band presented in this paper was very effective in activating Ga³⁺MPIX or Ga³⁺CHP while being safe for eukaryotic cells. Moreover, we did not observe mutagenic effects (Figure 8).

The main cellular target of aPDI treatment is cellular proteins. Other biomolecules, such as lipids, sugars, or DNA, may also be targeted by aPDI depending on the type of PS and its location. Nevertheless, proteins are the main target of photogenerated ROS attacks, mainly because they are the most abundant biomolecules. Additionally, virulence factors such as the superantigens presented in this work, which are extremely resistant to physical factors (heat, proteolysis, acidic environment, and desiccation), can be effectively inactivated by photogenerated ROS in vitro (Figures 10G,H and 11C,D). aPDI might be a potential method for the inactivation of bacterial virulence factors. Our team reported that aPDI treatment reduced the activity of exogenous virulence factors in *S. aureus*.⁵⁵ Additionally, other groups showed the effect of aPDI (based on 665 nm laser light combined with methylene blue) on the biological activity of V8 protease, α-hemolysin, and sphingomyelinase produced by *S. aureus*.⁵⁶ White light-activated Tetra-Py⁺-Me decreased the activity level of staphylococcal enterotoxin A (SEA) and SEC toxins by approximately 68% according to a reverse passive latex agglutination

(RPLA) test.⁵⁷ These results demonstrated that aPDI can effectively inactivate virulence factors in vitro, but in vivo verification of this feature is required to demonstrate the biological relevance of the aPDI-based approach. In our analyses, we used a very sensitive assay that measures the superantigen activity of the tested toxins, namely, measurement of IL-2 produced by toxin-exposed T lymphocytes. SEC and TSST-1 are potent, nonspecific superantigens for T cells (stimulating over 50% of the T cell pool) that bind to the T-cell receptor β -chain (TCR-V β) region or major histocompatibility complex (MHC) class II molecules.⁵⁸ Superantigens are inducers of proinflammatory cytokines, which promote and exacerbate skin inflammation in AD patients.⁵⁹ The production of enterotoxins by *S. aureus* is correlated with a more severe course of AD.²⁹ However, animal model studies, such as in vivo mouse model studies, should be conducted to verify whether aPDI might impact the biological function of SEs.

We hypothesized that singlet oxygen could cause oxidative damage at the toxin-binding site, possibly diminishing superantigenicity. A previous report showed that ROS production led to the modification of prosthetic groups, modification of amino acid residues, fragmentation, cross-linking, and protein aggregation.⁶⁰ Oxidation may also alter the structure of the cysteine SE loop, which is thought to be responsible for its emetic activity, and the dodecapeptide region, which is responsible for epithelial penetration of TSST-1 in menstrual toxic shock syndrome (TSS).

Another important aspect of aPDI action in the cell is the change in the level of gene expression. Published data show that aPDI downregulates the expression of genes related to biofilm production and virulence factors in several microbial species.^{61,62} Staphylococcal enterotoxin *seb* gene expression was significantly downregulated after RB- or new methylene blue-mediated aPDI.²⁷ Our experiments indicated a decrease in *sec* expression levels under the influence of aPDI, which is pronounced in the case of Ga³⁺CHP, while in the case of Ga³⁺MPIX, the action of the compound itself cannot be distinguished from aPDI. In contrast, the analysis of *tst* expression levels unexpectedly showed a significant increase under the influence of aPDI with Ga³⁺CHP but not with Ga³⁺MPIX. This result is difficult to interpret and most likely depends on the differences in the properties of both compared PSs as well as aPDI protocols (optimal for each PS but different in terms of concentration 1 μ M Ga³⁺CHP vs 10 μ M Ga³⁺MPIX and light dose—1.59 vs 12.7 J/cm²). The differential expression of both genes may have also resulted from the different regulatory pathways of the individual toxins.⁶³ For instance, the alternative sigma factor σ B is involved in the upregulation of the *tst* gene and the downregulation of the *seb* gene.⁶⁴ The activity of σ B can be altered by several environmental factors, one of which is aPDI.⁶⁵ Likewise, the two-component SrrAB system senses the transition from respiratory to nonrespiratory growth conditions and regulates the expression of virulence factors such as TSST-1.³³ In aerobic growth, SrrAB upregulates the transcription of the *tst* gene, while in anaerobic growth, there is a significant downregulation of the *tst* gene.⁶⁶ SrrAB expression may be altered by the production of singlet oxygen during aPDI (Figure 12). Such an alteration in this regulatory system has thus far been documented only after exposure to H₂O₂ and hypoxia. The Δ srrAB mutant was shown to be sensitive to H₂O₂ exposure and to decrease the expression levels of genes involved in H₂O₂ resistance. The SrrAB system regulates the

transcription of both virulence factor genes and genes involved in aerobic respiration and H₂O₂ resistance.^{33,66} Depending on the state of the respiratory system, *S. aureus* can modify its virulence. Therefore, studying the regulation of gene expression, especially from the point of view of microorganism pathogenicity, in response to photooxidative stress is extremely important for evaluating the safety of the aPDI method.

5. CONCLUSIONS

This study showed the success of aPDI treatment with Ga³⁺MPs in the decolonization of clinical *S. aureus* isolates in planktonic cultures and in an ex vivo porcine skin model. The novel Ga³⁺MP, Ga³⁺CHP, activated with green light effectively reduced the survival of clinical *S. aureus* isolates derived from AD patients and in aPDI treatment of HaCaT keratinocytes with both normal and suppressed filaggrin expression. In addition, the test compound did not show mutagenic activity. Ga³⁺CHP is an efficient generator of singlet oxygen and can be recognized by cellular heme transport systems, mainly Isd, which underlies the efficient accumulation of this compound in bacterial cells. The Ga³⁺CHP photodynamic method eliminates the biological activity of the SEC or TSST-1 superantigens, which are clinically relevant *S. aureus* virulence factors. Green light-activated Ga³⁺MPs (Ga³⁺CHP-mediated aPDI) may be a potential therapeutic strategy in the decolonization of *S. aureus* on atopic skin.

■ ASSOCIATED CONTENT

Supporting Information

The Supporting Information is available free of charge at <https://pubs.acs.org/doi/10.1021/acs.molpharmaceut.3c00399>.

Heat generation during irradiation; accumulation of Ga³⁺MPIX and Ga³⁺CHP; effect of Ga³⁺CHP and Ga³⁺MPIX aPDI on the *S. aureus* biofilm; evaluation of bacterial viability of *S. aureus* XEN40 on an ex vivo porcine skin model; cyto- and phototoxicity of gallium compounds on Ames assay indicator strains; and qRT-PCR conditions used in this study (PDF)

■ AUTHOR INFORMATION

Corresponding Author

Joanna Nakonieczna — Laboratory of Photobiology and Molecular Diagnostics, Intercollegiate Faculty of Biotechnology, University of Gdansk and Medical University of Gdansk, Gdansk 80-307, Poland; orcid.org/0000-0002-2420-664X; Email: joanna.nakonieczna@biotech.ug.edu.pl

Authors

Klaudia Szymczak — Laboratory of Photobiology and Molecular Diagnostics, Intercollegiate Faculty of Biotechnology, University of Gdansk and Medical University of Gdansk, Gdansk 80-307, Poland

Grzegorz Szewczyk — Department of Biophysics, Faculty of Biochemistry, Biophysics and Biotechnology, Jagiellonian University, Krakow 30-387, Poland

Michał Rychłowski — Laboratory of Virus Molecular Biology, Intercollegiate Faculty of Biotechnology, University of Gdansk and Medical University of Gdansk, Gdansk 80-307, Poland

Tadeusz Sarna – Department of Biophysics, Faculty of Biochemistry, Biophysics and Biotechnology, Jagiellonian University, Krakow 30-387, Poland

Lei Zhang – Department of Biochemical Engineering, School of Chemical Engineering and Technology, Frontier Science Center for Synthetic Biology and Key Laboratory of Systems Bioengineering (MOE), Tianjin University, Tianjin 300350, China; orcid.org/0000-0003-3638-6219

Mariusz Grinholc – Laboratory of Photobiology and Molecular Diagnostics, Intercollegiate Faculty of Biotechnology, University of Gdansk and Medical University of Gdansk, Gdansk 80-307, Poland

Complete contact information is available at:

<https://pubs.acs.org/10.1021/acs.molpharmaceut.3c00399>

Notes

The authors declare no competing financial interest.

ACKNOWLEDGMENTS

The excellent technical assistance of Martyna Krupińska and Agnieszka Gawrońska is appreciated (Laboratory of Photobiology and Molecular Diagnostics). The authors would like to thank Adrian Kobiela and Danuta Gutowska-Owsiak for sourcing the isolated PBMC fractions. The eukaryotic cell lines with suppression of filaggrin expression were kindly provided by Danuta Gutowska-Owsiak (Experimental and Translational Immunology Group). This work was supported by SHENG (No. 2018/30/Q/NZ7/00181) and funded by the National Science Centre, Poland, and the National Natural Science Foundation of China (21961132005).

REFERENCES

- (1) Nakonieczna, J.; et al. Photoinactivation of ESKAPE pathogens: Overview of novel therapeutic strategy. *Future Med. Chem.* **2019**, *11*, 443–461.
- (2) Ogonowska, P.; Gilaberte, Y.; Barańska-Rybak, W.; Nakonieczna, J. Colonization With *Staphylococcus aureus* in Atopic Dermatitis Patients: Attempts to Reveal the Unknown. *Front. Microbiol.* **2021**, *11*, No. 567090.
- (3) Mandlik, D. S.; Mandlik, S. K. Atopic dermatitis: new insight into the etiology, pathogenesis, diagnosis and novel treatment strategies. *Immunopharmacol. Immunotoxicol.* **2021**, *43*, 105–125.
- (4) Spaulding, A. R.; et al. Staphylococcal and streptococcal superantigen exotoxins. *Clin. Microbiol. Rev.* **2013**, *26*, 422–447.
- (5) Kobayashi, T.; et al. Dysbiosis and *Staphylococcus aureus* Colonization Drives Inflammation in Atopic Dermatitis. *Immunity* **2015**, *42*, 756–766.
- (6) Geoghegan, J. A.; Irvine, A. D.; Foster, T. J. *Staphylococcus aureus* and Atopic Dermatitis: A Complex and Evolving Relationship. *Trends Microbiol.* **2018**, *26*, 484–497.
- (7) Nakatsuji, T.; et al. *Staphylococcus aureus* Exploits Epidermal Barrier Defects in Atopic Dermatitis to Trigger Cytokine Expression. *J. Invest. Dermatol.* **2016**, *136*, 2192–2200.
- (8) Leung, D. Y. M.; Bieber, T. Atopic dermatitis. *Lancet* **2003**, *361*, 151–160.
- (9) Sroka-Tomaszewska, J.; Trzeciak, M. Molecular Sciences Molecular Mechanisms of Atopic Dermatitis Pathogenesis. *Int. J. Mol. Sci.* **2021**, *22*, 4130.
- (10) Alsterholm, M.; et al. Variation in *Staphylococcus aureus* Colonization in Relation to Disease Severity in Adults with Atopic Dermatitis during a Five-month Follow-up. *Acta Derm. Venereol.* **2017**, *97*, 802–807.
- (11) Clausen, M. L.; et al. *Staphylococcus aureus* colonization in atopic eczema and its association with filaggrin gene mutations. *Br. J. Dermatol.* **2017**, *177*, 1394–1400.
- (12) Osawa, R.; Akiyama, M.; Shimizu, H. Filaggrin Gene Defects and the Risk of Developing Allergic Disorders. *Allergol. Int.* **2011**, *60*, 1–9.
- (13) O'Regan, G. M.; Irvine, A. D. The role of filaggrin loss-of-function mutations in atopic dermatitis. *Curr. Opin. Allergy Clin. Immunol.* **2008**, *8*, 406–410.
- (14) Kim, J.; Kim, B. E.; Leung, D. Y. M. Pathophysiology of atopic dermatitis: Clinical implications. *Allergy Asthma Proc.* **2019**, *40*, 84–92.
- (15) Kashef, N.; Hamblin, M. R. Can microbial cells develop resistance to oxidative stress in antimicrobial photodynamic inactivation? *Drug Resist. Updates* **2017**, *31*, 31–42.
- (16) Rapacka-Zdonczyk, A.; et al. Development of *Staphylococcus aureus* tolerance to antimicrobial photodynamic inactivation and antimicrobial blue light upon sub-lethal treatment. *Sci. Rep.* **2019**, *9*, 9423.
- (17) Morales-de-echegaray, A. V.; et al. Rapid Uptake and Photodynamic Inactivation of *Staphylococci* by Ga(III)-Protoporphyrin IX. *ACS Infect. Dis.* **2018**, *4*, 1564–1573.
- (18) Stojiljkovic, I.; Kumar, V.; Srinivasan, N. Non-iron metalloporphyrins: Potent antibacterial compounds that exploit haem/Hb uptake systems of pathogenic bacteria. *Mol. Microbiol.* **1999**, *31*, 429–442.
- (19) Mazmanian, S. K.; et al. Passage of heme-iron across the envelope of *Staphylococcus aureus*. *Science* **2003**, *299*, 906–909.
- (20) Michalska, K.; et al. Gallium Mesoporphyrin IX-Mediated Photodestruction: A Pharmacological Trojan Horse Strategy To Eliminate Multidrug-Resistant *Staphylococcus aureus*. *Mol. Pharmaceutics* **2022**, *19*, 1434–1448.
- (21) Zhang, H.; et al. Iron-blocking antibacterial therapy with cationic heme-mimetic gallium porphyrin photosensitizer for combating antibiotic resistance and enhancing photodynamic antibacterial activity. *Chem. Eng. J.* **2023**, *451*, No. 138261.
- (22) Osiecka, B. J.; Nockowski, P.; Szeptowski, J. C. Treatment of Actinic Keratosis with Photodynamic Therapy Using Red or Green Light: A Comparative Study. *Acta Derm. Venereol.* **2018**, *98*, 689–693.
- (23) Torres, V. J.; et al. A *Staphylococcus aureus* Regulatory System that Responds to Host Heme and Modulates Virulence. *Cell Host Microbe* **2007**, *1*, 109–119.
- (24) Stauff, D. L.; et al. *Staphylococcus aureus* HrtA Is an ATPase required for protection against heme toxicity and prevention of a transcriptional heme stress response. *J. Bacteriol.* **2008**, *190*, 3588–3596.
- (25) Wang, X. W.; et al. Deficiency of filaggrin regulates endogenous cysteine protease activity, leading to impaired skin barrier function. *Clin. Exp. Dermatol.* **2017**, *42*, 622–631.
- (26) Nakonieczna, J.; et al. Photoinactivation of *Staphylococcus aureus* using protoporphyrin IX: the role of haem-regulated transporter HrtA. *Appl. Microbiol. Biotechnol.* **2016**, *100*, 1393–1405.
- (27) Ogonowska, P.; Nakonieczna, J. Validation of stable reference genes in *Staphylococcus aureus* to study gene expression under photodynamic treatment: a case study of SEB virulence factor analysis. *Sci. Rep.* **2020**, *10*, 1.
- (28) Choby, J. E.; Skaar, E. P. Heme Synthesis and Acquisition in Bacterial Pathogens. *J. Mol. Biol.* **2016**, 3408.
- (29) Bunikowski, R.; et al. Evidence for a disease-promoting effect of *Staphylococcus aureus*-derived exotoxins in atopic dermatitis. *J. Allergy Clin. Immunol.* **2000**, *105*, 814–819.
- (30) Taskapan, M. O.; Kumar, P. Role of staphylococcal superantigens in atopic dermatitis: from colonization to inflammation. *Ann. Allergy, Asthma Immunol.* **2000**, *84*, 3–12.
- (31) Ai, W.; Li, H.; Song, N.; Li, L.; Chen, H. Optimal method to stimulate cytokine production and its use in immunotoxicity assessment. *Int. J. Environ. Res. Public Health* **2013**, *10*, 3834–3842.
- (32) Yokomizo, Y.; et al. Proliferative Response and Cytokine Production of Bovine Peripheral Blood Mononuclear Cells Induced by the Superantigens *Staphylococcal* Enterotoxins and Toxic Shock Syndrome Toxin-1. *J. Vet. Med. Sci.* **1995**, *57*, 299–305.

- (33) Tiwari, N.; et al. The SrrAB two-component system regulates *Staphylococcus aureus* pathogenicity through redox sensitive cysteines. *Biol. Sci.* **2020**, *20*, 10989–10999.
- (34) Fyhrquist, N.; et al. Microbe-host interplay in atopic dermatitis and psoriasis. *Nat. Commun.* **2019**, *10*, 4703.
- (35) Garritsen, F. M.; Brouwer, M. W. D.; Limpens, J.; Spuls, P. I. Photo(chemo)therapy in the management of atopic dermatitis: an updated systematic review with implications for practice and research. *Br. J. Dermatol.* **2014**, *170*, S01–S13.
- (36) Dotterud, L. K.; Wilsgaard, T.; Vorland, L. H.; Falk, E. S. The effect of UVB radiation on skin microbiota in patients with atopic dermatitis and healthy controls. *Int. J. Circumpolar Health* **2008**, *67*, 254–260.
- (37) Lossius, A. H.; et al. Shifts in the Skin Microbiota after UVB Treatment in Adult Atopic Dermatitis. *Dermatology* **2022**, *238*, 109–120.
- (38) Kurosaki, Y.; et al. Effects of 308 nm excimer light treatment on the skin microbiome of atopic dermatitis patients. *Photodermatol. Photoimmunol. Photomed.* **2020**, *36*, 185–191.
- (39) Patrizi, A.; Raone, B.; Ravaoli, G. M. Management of atopic dermatitis: safety and efficacy of phototherapy. *Clin. Cosmet. Investig. Dermatol.* **2015**, *8*, 511.
- (40) Pozzi, G.; Asero, R. Skin photodynamic therapy in severe localized atopic dermatitis: a case report. *Br. J. Dermatol.* **2010**, *163*, 430–431.
- (41) Osiecka, B. J.; Nockowski, P.; Szepietowski, J. C. Treatment of Actinic Keratosis with Photodynamic Therapy Using Red or Green Light: A Comparative Study. *Acta Derm. Venereol.* **2018**, *98*, 689–693.
- (42) Hwang, J. H.; et al. Ex Vivo Live Full-Thickness Porcine Skin Model as a Versatile In Vitro Testing Method for Skin Barrier Research. *Int. J. Mol. Sci.* **2021**, *22*, 657.
- (43) Yang, Q.; et al. Development of a novel ex vivo porcine skin explant model for the assessment of mature bacterial biofilms. *Wound Repair Regen.* **2013**, *21*, 704–714.
- (44) Kelson, A. B.; Carnevali, M.; Truong-le, V. Gallium-based anti-infectives: targeting microbial iron-uptake mechanisms. *Curr. Opin. Pharmacol.* **2013**, *13*, 707–716.
- (45) Hijazi, S.; et al. Antimicrobial activity of gallium compounds on ESKAPE pathogens. *Front. Cell Infect. Microbiol.* **2018**, *8*, 316.
- (46) Chang, D.; et al. Activity of gallium meso-and protoporphyrin ix against biofilms of multidrug-resistant acinetobacter baumannii isolates. *Pharmaceuticals* **2016**, *9*, 16.
- (47) Almeida, A.; Cunha, A.; Faustino, M. A. F.; Neves, M. G. P. M. S.; Tome, A. C. *Porphyryns as Antimicrobial Photosensitizing Agents*; 2011.
- (48) Matsumoto, J.; Shiragami, T.; Hirakawa, K.; Yasuda, M. Water-Solubilization of P(V) and Sb(V) Porphyrins and Their Photobiological Application. *Int. J. Photoenergy* **2015**, *2015*, No. 148964.
- (49) Monsù Scolaro, L.; et al. Aggregation Behavior of Protoporphyrin IX in Aqueous Solutions: Clear Evidence of Vesicle Formation. *J. Phys. Chem. B* **2002**, *106*, 2453–2459.
- (50) Moriwaki, Y.; et al. Molecular basis of recognition of antibacterial porphyrins by heme-transporter IsdH-NEAT3 of *Staphylococcus aureus*. *Biochemistry* **2011**, *50*, 7311–7320.
- (51) Wakeman, C. A.; Stauff, D. L.; Zhang, Y.; Skaar, E. P. Differential activation of *Staphylococcus aureus* heme detoxification machinery by heme analogues. *J. Bacteriol.* **2014**, *196*, 1335–1342.
- (52) Cieplik, F.; Tabenski, L.; Buchalla, W.; Maisch, T. Antimicrobial photodynamic therapy for inactivation of biofilms formed by oral key pathogens. *Front. Microbiol.* **2014**, *5*, 405.
- (53) Fernandez, J. M.; Bilgin, M. D.; Grossweiner, L. I. Singlet oxygen generation by photodynamic agents. *J. Photochem. Photobiol., B* **1997**, *37*, 131–140.
- (54) Dai, T.; et al. Blue light for infectious diseases: Propionibacterium acnes, Helicobacter pylori, and beyond? *Drug Resist. Updat.* **2012**, *15*, 223–236.
- (55) Kossakowska, M.; et al. Discovering the mechanisms of strain-dependent response of *Staphylococcus aureus* to photoinactivation: Oxidative stress toleration, endogenous porphyrin level and strain's virulence. *Photodiagn. Photodyn. Ther.* **2013**, *10*, 348–355.
- (56) Tubby, S.; Wilson, M.; Nair, S. P. Inactivation of staphylococcal virulence factors using a light-activated antimicrobial agent. *BMC Microbiol.* **2009**, *9*, 211.
- (57) Bartolomeu, M.; et al. Effect of photodynamic therapy on the virulence factors of *Staphylococcus aureus*. *Front. Microbiol.* **2016**, *7*, 267.
- (58) Fraser, J. D.; Proft, T. The bacterial superantigen and superantigen-like proteins. *Immunol. Rev.* **2008**, *225*, 226–243.
- (59) Harris, T. O.; et al. Lack of complete correlation between emetic and T-cell-stimulatory activities of staphylococcal enterotoxins. *Infect. Immun.* **1993**, *61*, 3175–3183.
- (60) Alves, E.; et al. An insight on bacterial cellular targets of photodynamic inactivation. *Future Med. Chem.* **2014**, *6*, 141–164.
- (61) Hendiani, S.; Pornour, M.; Kashef, N. Sub-lethal antimicrobial photodynamic inactivation: an in vitro study on quorum sensing-controlled gene expression of *Pseudomonas aeruginosa* biofilm formation. *Lasers Med. Sci.* **2019**, *34*, 1159–1165.
- (62) Fekrirad, Z.; Kashef, N.; Arefian, E. Photodynamic inactivation diminishes quorum sensing-mediated virulence factor production and biofilm formation of *Serratia marcescens*. *World J. Microbiol. Biotechnol.* **2019**, *35*, 191.
- (63) Joo, H.-S.; et al. Mechanism of Gene Regulation by a *Staphylococcus aureus* Toxin. *mBio* **2017**, *4*, 1579–1595.
- (64) Kusch, K.; et al. The influence of SaeRS and σ B on the expression of superantigens in different *Staphylococcus aureus* isolates. *Int. J. Med. Microbiol.* **2011**, *301*, 488–499.
- (65) Kossakowska-Zwierucho, M.; Kaźmierkiewicz, R.; Bielawski, K. P.; Nakonieczna, J. Factors Determining *Staphylococcus aureus* Susceptibility to Photoantimicrobial Chemotherapy: RsbU Activity, Staphyloxanthin Level, and Membrane Fluidity. *Front. Microbiol.* **2016**, *7*, 1141.
- (66) Pragman, A. A.; Ji, Y.; Schlievert, P. M. Repression of *Staphylococcus aureus* SrrAB using inducible antisense srrA alters growth and virulence factor transcript levels. *Biochemistry* **2007**, *46*, 314–321.

5. Manuscript no. 3

Harnessing light-activated gallium porphyrins to combat intracellular *Staphylococcus aureus* in dermatitis: Insights from a simplified model

5.1 Summary of the Manuscript

Intracellular persistence of *S. aureus* in human keratinocytes is a complex process dependent on multiple factors such as *S. aureus* strain, multiplicity of infection (MOI), or host cell type^{40,135}. To avoid being killed by antibiotics, *S. aureus* internalizes into the host cell^{42,44}. The intracellular persistence of *S. aureus* is strongly associated with recurrent infections. Therefore, it is important to develop anti-intracellular methods to control the spread of the bacteria and improve its intracellular eradication.

To address this problem, I hypothesized that aPDI could be an effective antimicrobial method for targeting and eliminating the intracellular reservoir of *S. aureus*. For that purpose, I proposed the three strategies for implementing aPDI in a keratinocyte infection model. Strategy 1 was to test the effect of aPDI on *S. aureus* released from the initially infected cell, thereby lowering transmission to downstream host cells. Strategy 2 investigated whether the aPDI affects the adhesion and internalization of *S. aureus*, while Strategy 3 involved the examination of the efficacy of aPDI against intracellular bacteria. (see **Fig 6 in Introduction** for more information)

In strategy 1, aPDI using Ga³⁺CHP or Ga³⁺MPIX showed efficacy (~4 log₁₀ reduction in CFU/mL) in eliminating bacteria released from cells that were still sensitive likewise suspension cultures of *S. aureus*. This indicates that the metabolic changes that intracellular bacteria undergo during infection do not alter their sensitivity to aPDI. **Combining green light and gallium metalloporphyrins might be a practical approach to combat recurrent staphylococcal infections.**

In the Strategy 2, Ga³⁺CHP-aPDI pretreatment was applied to assess its effect on the adherence, internalization, and infection progression. aPDI pretreatment significantly reduced the number of extracellular bacteria and **decreased the adherence of *S. aureus* to the host cells. However, the number of intracellular bacteria remained unchanged.** The number of bacteria aPDI-treated and untreated remain unchanged, indicating that the reduced adherence was the result of quality of bacterial cells rather than their quantity.

Strategy 3 was based on testing the activity of aPDI against intracellular *S. aureus*. This strategy was found to be the most challenging and at a high risk of failure, since Ga³⁺MPs must first cross the cytoplasmic membrane barrier of keratinocytes and then reach the intracellular bacteria. I first examined Ga³⁺MPs accumulation in host cells to analyze their cellular localization pattern. Ga³⁺MPIX diffused throughout cytoplasm, whereas cationic Ga³⁺CHP was distributed mainly

in a localized manner, partly in lysosomes. Based on colocalization analyses studied by fluorescence microscopy, I confirmed that both intracellular *S. aureus* and Ga³⁺CHP colocalized inside host cells in lysosomal structures. In light-independent action, Ga³⁺CHP decreased the GFP signal by ~30%. After green light excitation of accumulated Ga³⁺CHP in cells, the GFP signal of intracellular *S. aureus* decreased by approximately 70%, as determined by flow cytometry measurements. It should be emphasized that only simultaneous colocalization of Ga³⁺CHP and bacteria in the intracellular clusters resulted as effective elimination of intracellular *S. aureus*. Combination of Ga³⁺CHP and green light is a promising anti-intracellular treatment, with simultaneous moderate phototoxicity on both infected and non-infected keratinocytes. This is the first study to show that the Q-band excitation of gallium(III)-coordinated porphyrins can provide high efficacy in elimination of intracellular *S. aureus* without extensive photodamage to keratinocytes.

5.2 Manuscript

Note: Supplementary material from Manuscript no. 3 can be found in section 9.3. (Attachments).

Harnessing light-activated gallium porphyrins to combat intracellular *Staphylococcus aureus* in dermatitis: Insights from a simplified model.

Klaudia Szymczak¹, Michał Rychłowski², Lei Zhang³, Joanna Nakonieczna^{1*}

¹ Laboratory of Photobiology and Molecular Diagnostics, Intercollegiate Faculty of Biotechnology, University of Gdansk and Medical University of Gdansk, Poland,

² Laboratory of Virus Molecular Biology, Intercollegiate Faculty of Biotechnology, University of Gdansk and Medical University of Gdansk, Poland,

³ Department of Biochemical Engineering, School of Chemical Engineering and Technology, Frontier

Science Center for Synthetic Biology and Key Laboratory of Systems Bioengineering (MOE), Tianjin University, China

* Corresponding author: Joanna Nakonieczna

E-mail: joanna.nakonieczna@biotech.ug.edu.pl

Abstract

The cellular interior of non-professional phagocytes such as keratinocytes is a niche for *Staphylococcus aureus* to survive antibiotic pressure. When antibiotic pressure is off, reinfection with staphylococci begins from the intracellular inoculum. This phenomenon is responsible for recurrent infections. There is a need to develop new antibacterial methods that will be able to eliminate intracellular bacteria, including those with a multi-drug resistant phenotype. In this study, we characterized and used a model of keratinocytes (both wild type and mutants with reduced filaggrin expression) infected with methicillin-resistant *S. aureus* (MRSA), to verify the possibility of using light-activated compounds, here exemplified by heme-mimetic gallium (III) porphyrin (Ga^{3+}CHP) and visible light (the approach known as antimicrobial photodynamic inactivation, aPDI) to eliminate intracellular MRSA. We observed that Ga^{3+}CHP accumulated in infected cells with greater efficiency than in uninfected cells and exhibited accumulation in those cells that harbor intracellular *S. aureus*. Using flow cytometry and fluorescence microscopy, we demonstrated colocalization of intracellular MRSA and accumulated Ga^{3+}CHP mainly in lysosomal structures, and we showed that under the influence of aPDI, MRSA exhibited reduced adhesion to host cells and significantly reduced (by 70%) GFP signal originating from intracellular bacteria. Moreover, the use of light-activated Ga^{3+}CHP resulted in a significant reduction in the number of extracellular bacteria in the infection system, lowering the potential for further infection of host cells. For the first time, we used the infectious model to analyze the toxicity of aPDI in real time, showing that the approach used does not show significant cyto- and phototoxicity.

Author Summary

Staphylococcus aureus is a highly virulent pathogen that is responsible for about 80% of all skin infections. During antibiotic treatment, one of the defense mechanisms of *Staphylococcus aureus* is the invasion of skin cells – keratinocytes. Intracellular bacteria are not accessible to antibiotics, which poorly penetrate the interior of host cells. Consequently, such bacteria contribute to recurrent infections. In our study, we proposed using a combination of a light-activated porphyrin compound loaded with gallium ions, Ga^{3+}CHP , and visible light as a strategy to eliminate intracellular staphylococci. We demonstrated that the tested compound localized in the infected cells along with pathogen, which was an essential condition for effective elimination of intracellular bacteria. We showed that the proposed approach effectively reduced the infection of keratinocytes with methicillin-resistant *S. aureus*, as well as its adhesion to host cells, while remaining safe for host cells. The results presented here provide a basis for developing an effective therapy against staphylococci.

Introduction

Staphylococcus aureus colonizes the skin in about 20% of the world's population and is responsible for 80% of all detected skin infections worldwide (1,2). Moreover, *S. aureus* plays a key role in the pathogenesis of atopic dermatitis (AD) because it is overexpressed in the skin microbiota and enhances inflammatory responses (3). Staphylococcal infections are difficult to treat due to multiple virulence factor production and a high antibiotic resistance profile (4). Despite antibiotics, 30% of patients are reported to develop recurrent staphylococcal infections after initial treatment (5). Recent scientific reports have shown that one of the defense mechanisms of *S. aureus* towards antibiotic action is the invasion of non-professional phagocytes such as keratinocytes or fibroblasts (6–8). *S. aureus* internalization occurs through a complex zipper-like mechanism between fibronectin-binding proteins A and B and fibronectin, which is recognized by $\alpha 5\beta 1$ integrin on host cells (9). The internalization process differs depending on the bacterial strain and host cell type (6). Under antibiotic pressure, *S. aureus* can persist inside the host cells for several days as an intracellular phenotype, known as small colony variant (SCV) (10). This phenotype exhibits changes in the global regulatory networks that can lead to the alteration in the production of virulence factors or modify the response to antibiotics (11,12). When antibiotic pressure is abolished, the intracellular bacterium can escape the endosome and multiply in the cytoplasm. The increased number of bacteria inside the cell leads to cell death, release of bacterium, and recurrence of the bacterial infection extracellularly (13). Despite the increasing scientific data, the mechanism and factors contributing to the entry, survival, and exit of *S. aureus* from the host interior are still not fully understood.

The intracellular phenotype of *S. aureus* is caused and maintained by antibiotic action due to poor penetration of antimicrobials through the cell membrane to achieve efficient intracellular killing (14). There are many proposed new therapies against intracellular *S. aureus* (15). Anti-intracellular strategies are based on modifications of antibiotics to improve their delivery or stimulating cells to enhance bacterial killing by the host (16–19). Our study investigated antimicrobial photodynamic inactivation (aPDI) as a potential therapy against intracellular *S. aureus*. Its mechanism is based on three components: an oxygen environment, the light at the appropriate wavelength, and a small molecular weight compound with photodynamic properties – a photosensitizer (PS) (20,21). An ideal photosensitizer should exhibit a high reactive oxygen species (ROS) quantum yield with high phototoxicity against pathogens and low toxicity against eukaryotic cells. The penetration of PS into the microbial cells should be rapid, with prolonged uptake in the host cells (22,23). Gallium metalloporphyrins (Ga^{3+}MPs) are potent PSs in aPDI that can absorb visible light, e.g., green light used in this work (24–26). Ga^{3+}MPs , due to their structural similarity to heme, can be recognized by bacterial heme-acquisition receptors of the Isd family and efficiently accumulated inside the bacterial cell (27,28). The idea is that the porphyrin

ring of Ga³⁺MPs is cleaved inside bacteria, and gallium ions are released to disrupt iron-dependent metabolism (24). We have previously shown that the Ga³⁺MPs representative, namely cationic modified gallium porphyrin (Ga³⁺CHP), is water-soluble and exhibits photodynamic potential at Q-band excitation (at lower absorption peaks) with high antimicrobial activity and low toxicity to human keratinocytes (29,30).

In this study, a model for infection of human keratinocytes with *S. aureus* was created and characterized to achieve a stable bacterial presence inside the host cells. We used this model to investigate whether light-activated Ga³⁺MPs could be applied to effectively inactivate extracellular and intracellular *S. aureus*. In our experimental approach, we used three research strategies based on photodynamic action (aPDI) (**Fig. 1**). Briefly, Strategy 1 refers to the aPDI treatment of *S. aureus* cells that had escaped from an infected cell (**Fig. 1** Strategy 1). Strategy 2 is the photodynamic treatment of *S. aureus* cells before they invade keratinocytes before contact with host cells (**Fig. 1** Strategy 2). Strategy 3 is aPDI treatment of intracellular *S. aureus* persisting inside host cells (**Fig. 1** Strategy 3). In the current study, we used two Ga³⁺MPs derivatives that we previously characterized for their antimicrobial efficacy on suspension cells: gallium mesoporphyrin IX (Ga³⁺MPIX) (26) and cationic gallium porphyrin (Ga³⁺CHP) (30). We demonstrated the compounds we studied, in particular Ga³⁺CHP are able to effectively penetrate host cells, localizing mainly in lysosomal structures, where we also detected the presence of infecting *S. aureus*. Using excitation of Ga³⁺CHP with green light, we achieved a significant reduction in the GFP signal originated from intracellular *S. aureus* by photodynamic action (aPDI).

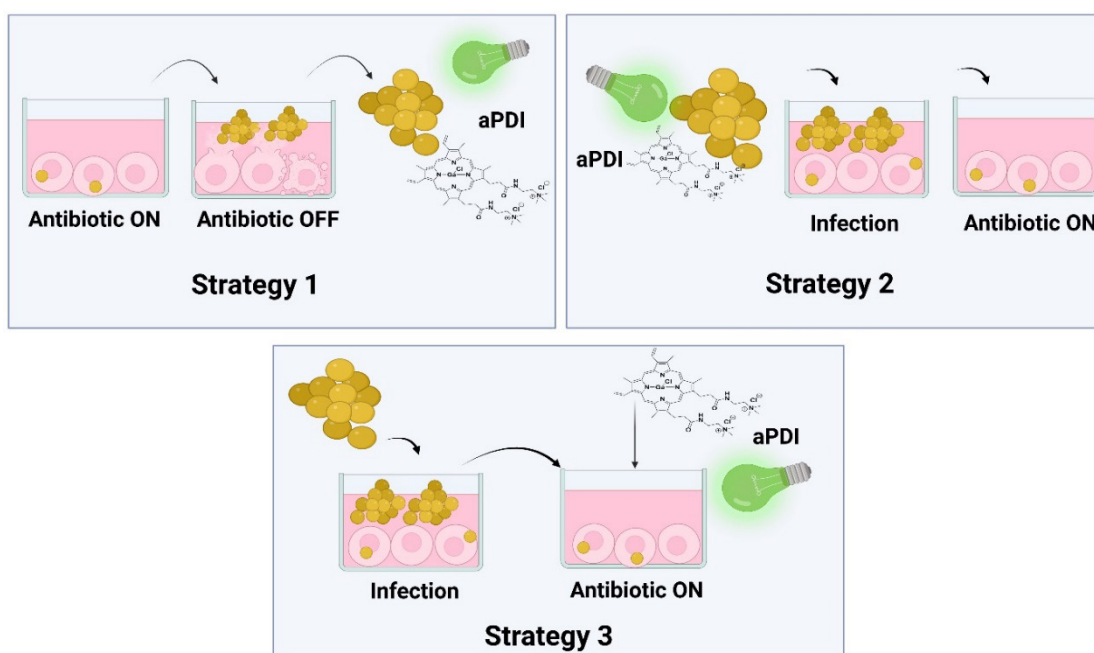


Fig 1. Strategies to implement light-activated gallium metalloporphyrins to overcome *S. aureus* infecting human keratinocytes.

Strategy 1 is to reduce the potential for recurrent infection. Strategy 2 investigates how pre-treatment of bacterial inoculum before infection will affect *S. aureus* adhesion and internalization in the host cells. In Strategy 3, photosensitizers are incubated in the dark to efficiently penetrate and localize inside the host cells to reach intracellular *S. aureus*. After incubation, cells would be treated with light.

Results

Different MOIs affect the infection and internalization of *S. aureus* into human keratinocytes.

First, we developed a model of keratinocyte infection (see Materials and Methods, **Fig 11**) and characterized the process of *S. aureus* internalization to keratinocytes. To confirm the presence of intracellular *S. aureus* after infection, fluorescence microscopy images were taken on the first day after infection. The green fluorescent protein (GFP) signal from the *S. aureus* USA300 bacteria (white arrow) was observed in the presence of host cell nuclei stained with HOEST dye (blue signal, black arrow) (**Fig 2A**). To confirm the intracellular presence of the pathogen, three-dimensional images were taken using a scanning fluorescent microscopy (**Fig 2B**), confirming that bacteria were localized intracellularly. Then, we examined various multiplicities of infection (MOI) (0-100) for the viability of *S. aureus* in medium and inside keratinocytes by studying three fractions after infection. The fractions were as follows: (i) extracellular, (ii) intracellular, and (iii) intracellular + adherent *S. aureus* (**Fig 2C**). The number of extracellular *S. aureus* collected from

the culture medium increased with the higher MOI used for infection. For intracellular *S. aureus*, the viability was estimated as 5.6 log₁₀ CFU/mL for MOI 100, 4.8 log₁₀ for MOI 10, and 4.7 log₁₀ for MOI 1 (**Fig. 2D**). By measuring the GFP signal derived from *S. aureus* strain, the higher number of infected cells was observed for both MOI 10 and 100 as compared with MOI 1. However, there was no significant difference in the rate of intracellular invasion between MOI 10 and 100 inoculum according to the flow cytometry studies (**Fig 2E**). The addition of the pathogen and infection delayed the growth rate of HaCaT cells. However, host cells could grow and proliferate, harboring the intracellular *S. aureus*. The use of different MOIs was also reflected in the host growth. The larger the inoculum used for infection, the greater the effect on HaCaT (**Fig 2F**). The number of viable intracellular pathogens decreased over time, by the mechanism of induced death of infected cells (**Movie S1**). Under antibiotic exposure, *S. aureus* USA300 invades human keratinocytes. The level of *S. aureus* USA300 internalization during this process and the effect of infection on the host cell proliferation strongly depend on the initial MOI used for infection.

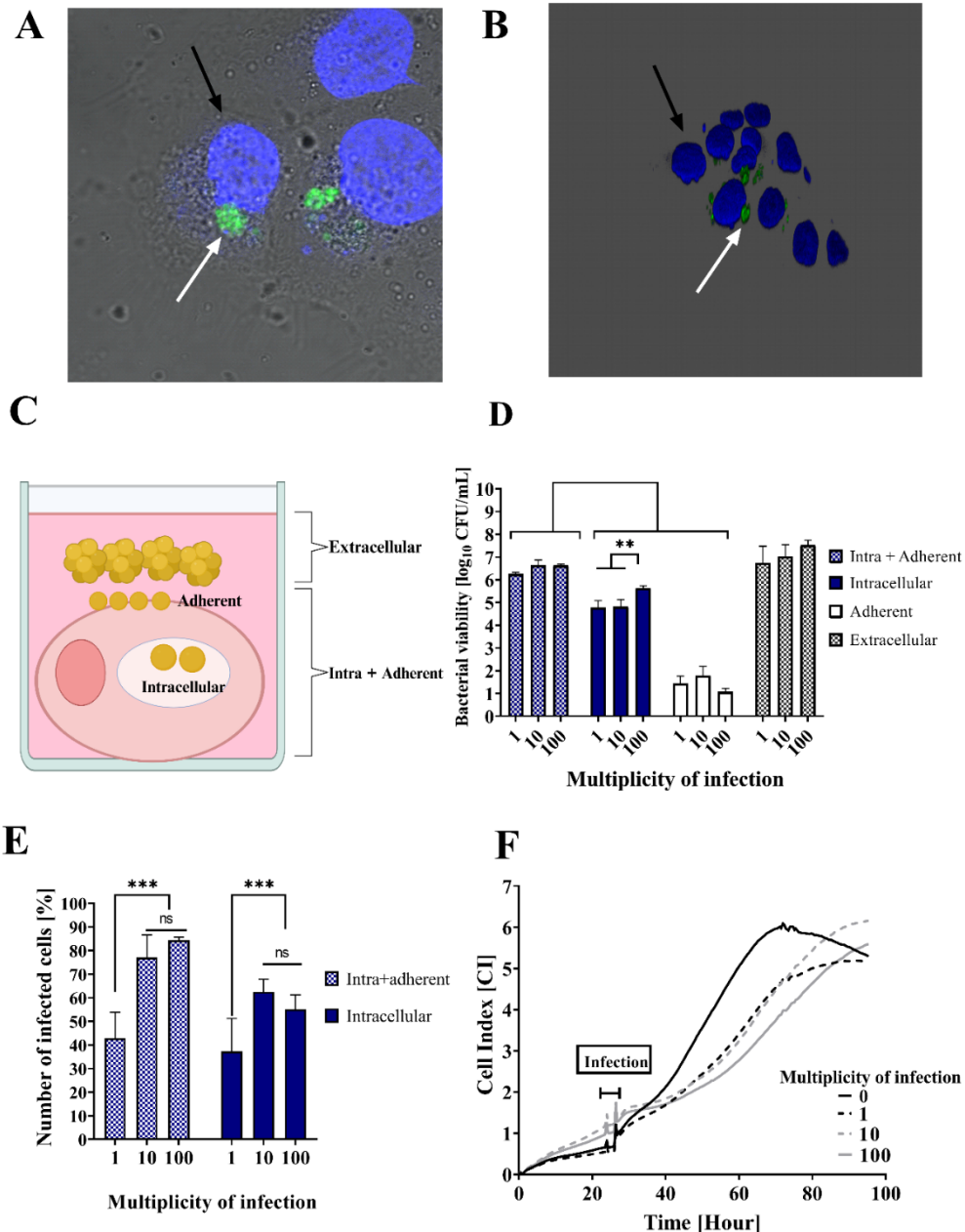


Fig 2. Effect of *S. aureus* multiplicity of infection (MOI) on internalization, infection, and keratinocytes growth.

A) Keratinocytes (HaCaT cell line) infected with *S. aureus* USA300 (green signal, white arrow). The host cell nucleus was stained (blue signal, black arrow). **(B)** 3D-dimension image of the co-culture of HaCaT and *S. aureus* USA300. **(C)** Schematic representation of bacterial fractions collected after each step of co-culture preparation. ‘Extracellular’ refers to free-floating *S. aureus* collected from the growth medium after a 2-hour staphylococcal infection; ‘Adherent’ - *S. aureus* attached to host cell; ‘Intracellular’ - *S. aureus* accumulated inside host cell; ‘Intra+Adherent’ – the combined number of *S. aureus* in adherent and intracellular fraction. **(D)** Bacterial viability was determined by seeding bacteria onto agar plates and counting colony-forming units

(CFU/mL) in each collected fraction. Different ratios of the number of bacteria to the number of host cells were used (multiplicity of infection (MOI) 1-100) for infection model preparation. The significance of infected cell viabilities at the respective p-values is marked with asterisks [$**p < 0.01$] (E) Percentage of infected, GFP-expressing cells collected immediately after infection (MOI 0-100) ('Intra+Adherent' fraction) or after 1-hour antibiotic exposure ('Intracellular' fraction). GFP signal was measured by flow cytometry. The significance of differences among tested samples of infected cell viabilities at the respective p-values was marked with asterisks [$***p < 0.001$] and calculated with respect to uninfected cells at each time point (F) Real-time host growth analysis after infection with *S. aureus* USA300 at MOI 0-100. After 2 hours, the medium was removed, cells were washed, and the antibiotic was implemented to ensure intracellular maintenance of *S. aureus*.

The behavior of intracellular *S. aureus* is strain dependent.

To examine whether there is strain-dependency in staphylococcal invasion into keratinocytes, we compared keratinocytes infections with two *S. aureus* strains: the hypervirulent USA300 strain and the non-virulent strain RN4220. First, we examined the intracellular viability of two bacterial strains during infection and their persistence under antibiotic pressure for several days after infection. The non-virulent RN4220 strain exhibited higher intracellular viability, as shown in a several-day culture model, than the hypervirulent USA300 ($5.8 \log_{10}$ vs. $4.2 \log_{10}$ CFU/mL at 1st day post-infection) (**Fig. 3A**). RN4220 remained intracellularly longer than USA300, which was completely titrated out of the cells (reaching the detection limit of $2 \log_{10}$) at day 5 post-infection. The difference in infection between the two strains was also evident in the host growth rate (**Fig 3B**). RN4220 reduced host cell growth after infection significantly more than USA300. Nevertheless, host cells harboring bacteria intracellularly could grow and proliferate (**Fig 3C and D**). Interestingly, when antibiotic pressure was removed, and the medium was changed to non-antibiotic (Antibiotic OFF) after the 1st day post-infection (dashed gray line), *S. aureus* RN4220 continued to persist intracellularly without escaping the host as part of sustained cell growth, while USA300 was released from the host, causing cell death, restoring extracellular infection, and causing significant toxicity. A similar effect was observed when the antibiotic pressure was maintained longer (up to the 3rd day post-infection) for USA300 (**Fig S1**) showing that even the low-viable intracellular inoculum was able to escape and resume the infection. We observed the strain-dependent behavior of *S. aureus* in the infection process, intracellular persistence, and the ability to escape from the host for reinfection.

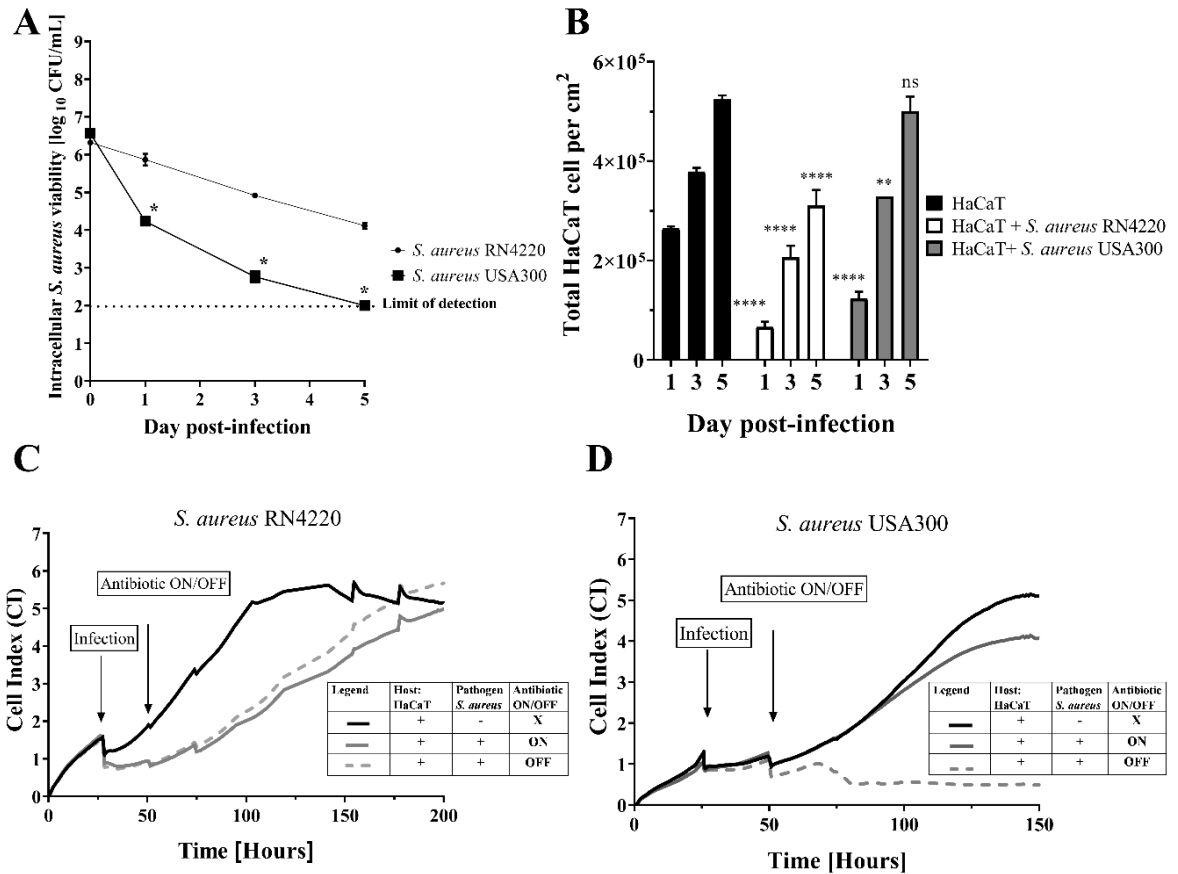


Fig 3. Characterization of intracellular invasion of hypervirulent (USA300) and non-virulent (RN4220) *S. aureus* strains in an infection model over time.

(A) Intracellular viability of two *S. aureus* strains over time after infection (1-5 days). Significant differences in USA300 viability at the tested time points were calculated relative to the reference strain RN4220 with corresponding p-values marked with asterisks [$*p < 0.05$] (B) HaCaT cell viability over time (1-5 days) after infection with two tested *S. aureus* strains. The significance of differences in infected cell viabilities at the respective p-values is marked with asterisks [$*p < 0.05$; $**p < 0.01$; $***p < 0.001$] and was calculated for uninfected cells at each studied time point. Infection of HaCaT cells (A, B) in a medium without antibiotics was performed at an MOI of 10 for 2 hours; then the cells were cultured under antibiotic pressure until the end of the experiment. (C, D) Real-time analysis of HaCaT cells growth after infection with *S. aureus* RN4220 (C) or USA300 (D). HaCaT cells infection was performed at an MOI of 10 for 2 hours; no antibiotic (X), culture under antibiotic pressure (Antibiotic ON) or antibiotic removal (Antibiotic OFF) which was determined at day 1 post-infection.

Filaggrin deficiency results in higher internalization and longer persistence of *S. aureus* inside keratinocytes

In atopic dermatitis patients, there is a high frequency of mutation occurrence in the filaggrin gene (*FLG*), which is linked to increased *S. aureus* skin colonization (31). Filaggrin is a crucial component of the integrity of the epidermal barrier and stabilizes pH and hydration of the skin to control, for instance, microbial penetration (32). We hypothesized that filaggrin presence might be involved in the *S. aureus* internalization and persistence in host cells post-infection. To test that, two HaCaT cell lines: with normal (*FLG* ctrl) and silenced (*FLG* sh) filaggrin status were infected with *S. aureus* USA300. The percentage of infected cells (high expression of GFP) was measured by flow cytometry through days post-infection under constant antibiotic pressure. HaCaT without normal expression of filaggrin (*FLG* sh) showed a significantly higher number of infected cells after infection compared with cells with normal expression ($83\% \pm 3.8$ vs. $71\% \pm 4.3$) (**Fig 4A**). This tendency continued until the 5th day post-infection under the antibiotic pressure. Intracellular *S. aureus* persists longer inside keratinocytes with filaggrin dysfunction (up to 7 days). Moreover, we observed a delayed growth of the filaggrin-silenced cell line relative to the wild-type line due to *S. aureus* infection (**Fig 4B**). However, both cell lines are still able to proliferate with continuous clearance of intracellular infection. Intracellular *S. aureus* is gradually titrated out of cells which are eventually able to reach the plateau phase (*FLG* ctrl cell line at 55 hours of experiment and *FLG* sh cell line at 85h). Impairment of functional filaggrin in the host cell may be beneficial for greater internalization of *S. aureus* and its intracellular persistence.

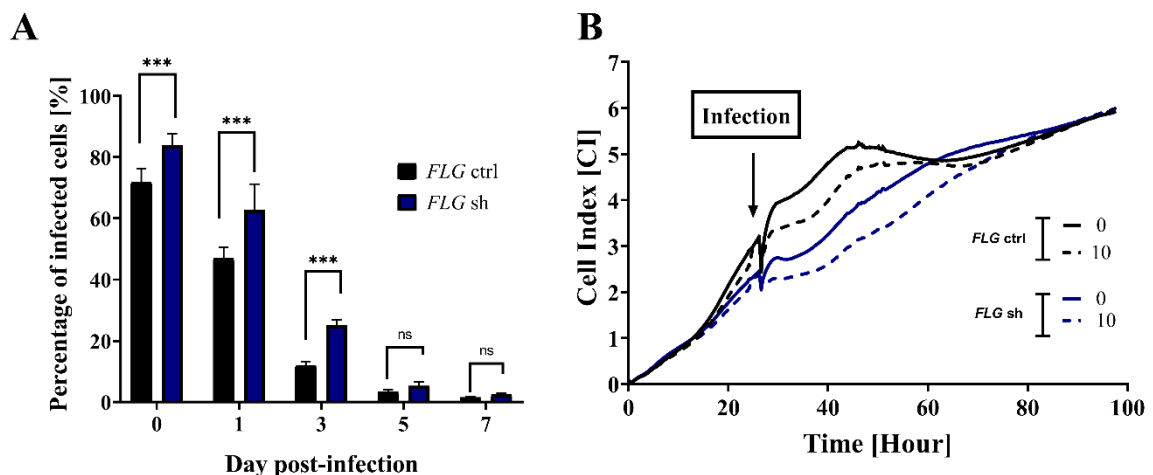


Fig 4. Staphylococcal invasion to human keratinocytes in the context of filaggrin status.

A) Percentage of GFP-expressing infected cells in the culture with divergent filaggrin (*FLG*) expression. HaCaT cells with normal expression of filaggrin (*FLG* ctrl) and knockdown of filaggrin (*FLG* sh) were infected with *S. aureus* USA300 at an MOI of 10 for 2 hours. Antibiotic

pressure was then maintained for up to 7 days. Cells were harvested at each time point after infection, and the number of GFP-expressing cells was determined by flow cytometry. The significance of the respective p-values is marked with asterisks [***p < 0.001] and was calculated with respect to *FLG* ctrl cells at each time point. **B)** Real-time growth analysis of both cell lines infected and non-infected with staphylococcal cells with an MOI of 10 for 2 hours. After the initial infection, the antibiotic pressure was maintained throughout the whole analysis.

Green light-activated Ga³⁺MPs efficiently eliminate staphylococcal recurrent infection

Our previous study showed that light-activated Ga³⁺MPs are able to reduce the viability of clinical *S. aureus* isolates in suspension cultures *in vitro* (29). In the current study, we wanted to verify whether and at what stage of the infection cycle it is possible to use light-activated Ga³⁺MPs (i.e., aPDI) to reduce the number of bacteria that infect host cells. Based on the first proposed aPDI strategy (**Fig 1, Strategy 1**), we evaluated the antimicrobial efficacy of Ga³⁺MPs activated with 522 nm light against *S. aureus* USA300 in the staphylococcal reinfections (**Fig 3D**, dashed line). Briefly, cells were seeded on Day 0, *S. aureus* infection was performed on Day 1, and then cells were cultivated in a medium with an antibiotic (Antibiotic ON) (**Fig 5A**). On Day 2, the culture medium was changed to antibiotic-free (Antibiotic OFF), and cells were cultivated for up to 16 hours. Extracellular bacteria that were released from keratinocytes were isolated, washed, and subjected to aPDI using two Ga³⁺MPs: Ga³⁺MPIX or Ga³⁺CHP to assess their efficacy in reducing *S. aureus* survival rates (**Fig 5B and 5C**). Both gallium compounds effectively eliminated bacteria released from cells with a maximum reduction in cell count of 4 log₁₀ CFU/mL. Ga³⁺CHP was more effective than Ga³⁺MPIX in reducing bacterial survival at lower light doses, corresponding to shorter irradiation times. We found that *S. aureus*, which escaped the host and restarted the infection, responded to aPDI similarly to bacteria in the logarithmic growth phase rather than the stationary phase (**Fig S2**). Despite some adaptive changes of intracellular bacteria that might promote their overall tolerance, the released *S. aureus* shows a similar response to aPDI as sensitive free suspension cultures in the logarithmic growth phase. This demonstrates that aPDI with Ga³⁺MPs can be an effective strategy to combat staphylococcal reinfections.

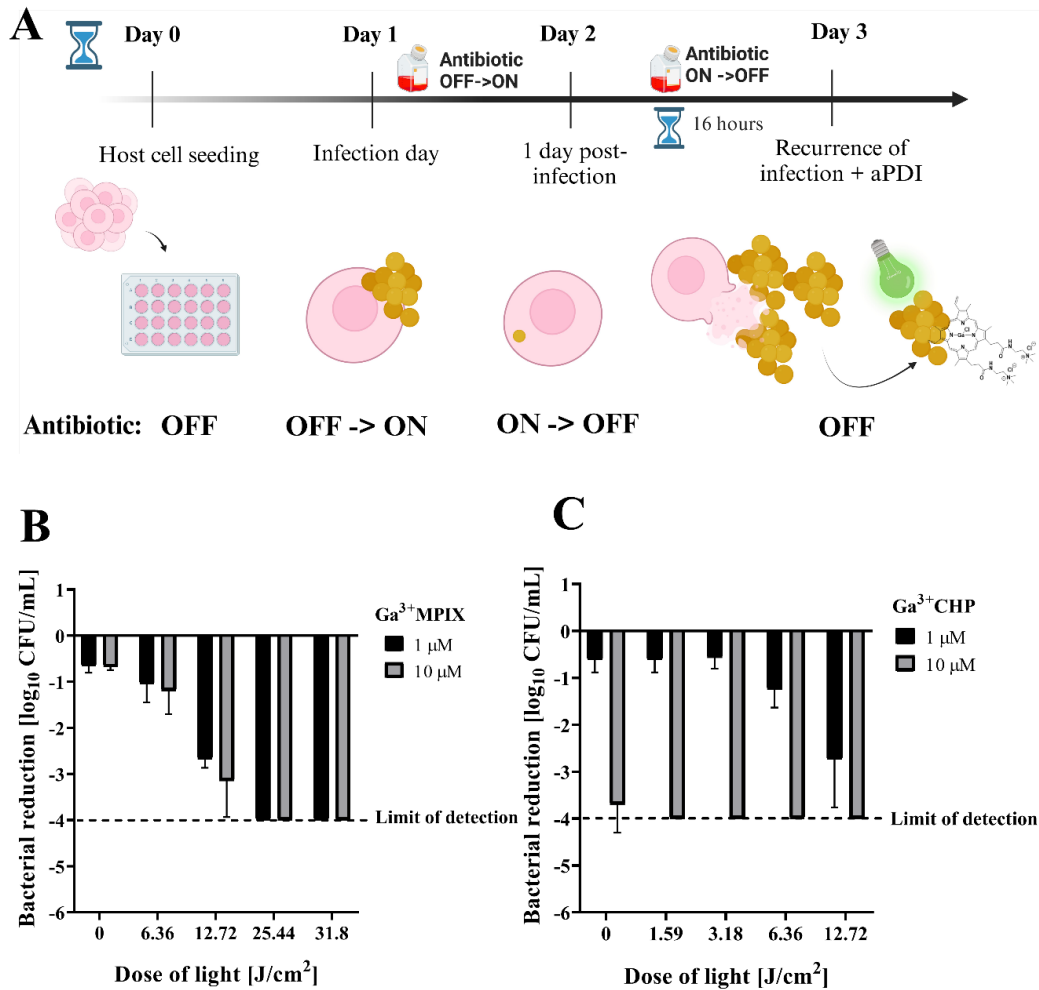


Figure 5. Light-activated Ga³⁺MPs effectively reduce the number of released *S. aureus* USA300 from keratinocytes – Strategy 1.

(A) On Day 1, HaCaT cells were infected with *S. aureus* USA300 (MOI = 10, 2 hours), in a medium without antibiotics (Antibiotic OFF). Antibiotic was added to remove extracellular *S. aureus*, and the cells were cultured under antibiotic pressure until the next day (Antibiotic OFF->ON). The antibiotic was then removed (Antibiotic ON->OFF), and HaCaT cells containing only intracellular *S. aureus* were left in an incubator for 16 hours. During this time, intracellular *S. aureus* was gradually lysed cells and released into the medium. *S. aureus* cells were harvested and washed from DMEM medium, then resuspended in TSB. Bacterial suspensions were transferred to the 24-well plate, proper photosensitizers were then added and, after incubation, illuminated with green light. Bacterial cells were then diluted and, plated, counted (B and C). Reduction of light activation of Ga³⁺CHP (B) or Ga³⁺MPIX (C) in the number of *S. aureus* USA300 bacteria was calculated in relevance to the untreated cells.

aPDI reduces the acuity of *S. aureus* infection and its adherence to the host cell.

We hypothesized that aPDI pre-treatment of the infectious inoculum could affect its further invasion, adherence to host, and growth of the extracellular bacteria (**Fig 1, Strategy 2**). To assess the effect of aPDI pre-treatment on the initial stages of *S. aureus* invasion, we studied the number of bacteria in each fraction collected after infection. As a control, we used non-treated infectious inoculum (**Fig 6**). Notably, we used the same number of bacteria regardless of the treatment. Furthermore, we were interested in the course of infection, so higher and lower amounts of bacteria were used as two MOI values - 10 or 1. For aPDI-treated bacteria, two doses were used: a Low and a High to reduce bacterial viability to an appropriate number of bacteria. The Low dose was used to obtain a higher number of bacteria for MOI 10 (**Fig 6B, Low**), while the High dose was served to have a lower number of bacteria for MOI 1 value (**Fig 6B, High**). After infection, CFU/mL were counted from each fraction collected of: (i) the extracellular fraction from the growth medium after infection (ii) the intracellular+adherent fraction, obtained from a cell lysate containing both intracellular and adherent bacteria, or (iii) the intracellular fraction from a cell lysate where HaCaT cells were washed and cultured under antibiotic pressure for 1 h before lysis to eliminate adherent bacteria (see **Fig. 6A**). The aPDI-treated bacteria used as inoculum for infection behaved differently from the untreated bacteria. Light-activated Ga³⁺CHP treatment of *S. aureus* resulted in a significantly reduced number of extracellular bacteria, the observed decrease was by 2 log₁₀ for low dose treatment or 2.8 log₁₀ for high dose treatment as compared to untreated controls (**Fig 6B**). Moreover, the high dose aPDI resulted in a significant reduction in bacterial adherence to HaCaT cells, with a 1.2 log₁₀ reduction in CFU/mL count compared with adherence of untreated bacteria. It is noteworthy that both types of infections, with aPDI-treated bacteria and non-treated bacteria were applied at the same MOI 1, indicating that the quality of bacteria but not their quantity influenced the adherence. Interestingly, pre-treatment of bacteria with aPDI did not affect the number of intracellular bacteria, suggesting that there is a maximum yield of bacterial burden that can invade host cells, and it is not affected by aPDI. Both aPDI-treated and untreated bacteria penetrated keratinocytes with similar efficiency. However, aPDI treatment itself significantly affects on the growth of extracellular fraction and bacterial adhesion to host cells.

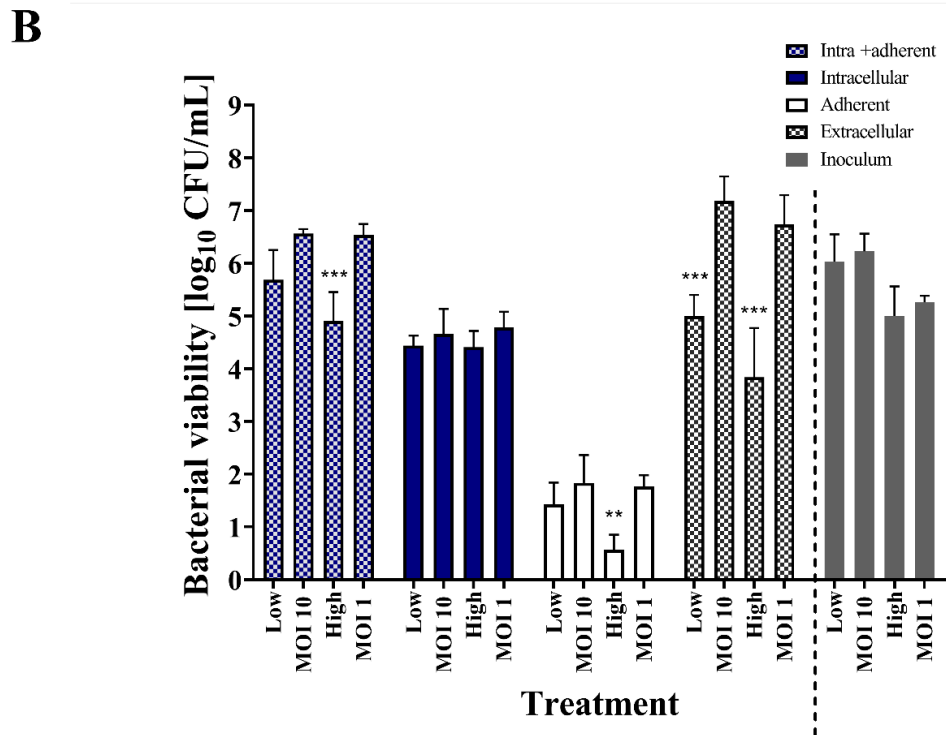
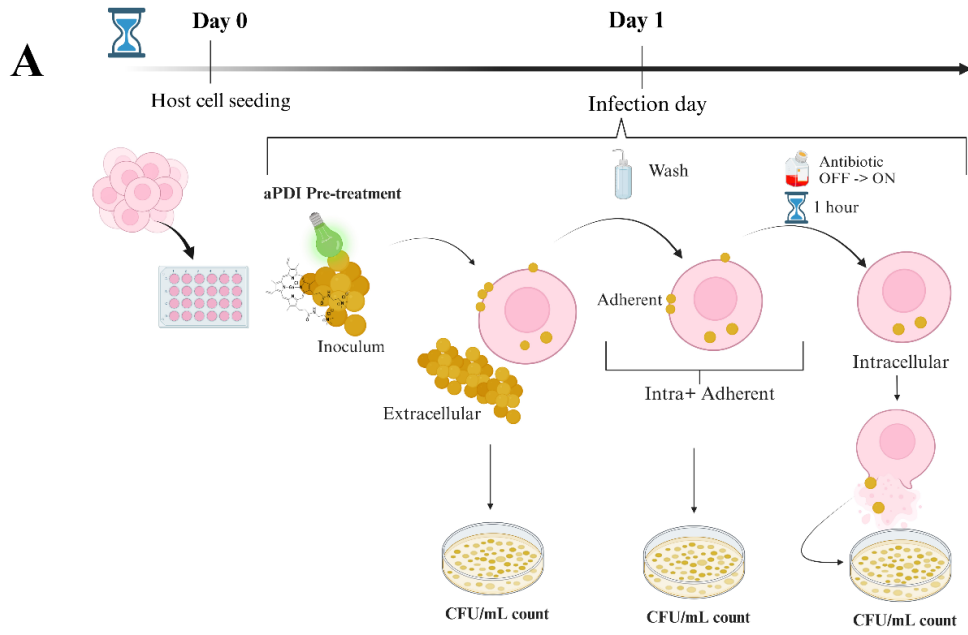


Figure 6. Effect of aPDI (light-activated Ga^{3+}CHP) pre-treatment on *S. aureus* USA300 infection – Strategy 2.

(A) At day 0, HaCaT cells were seeded in a 24-well plate. Then, on Day 1, *S. aureus* USA300 infection was conducted either with non-treated bacteria or bacteria treated with aPDI. After 2 h, the growth medium was collected for plating and counting the extracellular fraction. Host cells were collected for subsequent lysis (intra+adherent fraction) or incubated for 1 hour with antibiotics to eliminate adherent bacteria to obtain the intracellular fraction. All fractions were

diluted serially and plated for CFU/mL enumeration. **(B)** The number of bacteria counted from each fraction collected after infection with untreated or aPDI-treated *S. aureus* inoculum. Before infection, the number of viable *S. aureus* (10^7 CFU/mL) was reduced by aPDI with two dosages: Low with 1 \log_{10} reduction of CFU/mL (to obtain the ratio between *S. aureus* and HaCat cells as MOI 10), and High with 2 \log_{10} reduction of CFU/mL (for MOI 1). Untreated bacteria with an appropriate MOI of 10 or 1 were used as a control. The number of bacteria used for infection was the same whether the bacteria were pre-treated with aPDI or were untreated (please see Inoculum). After infection, several fractions were collected such as Extracellular – referred to as a free-floating *S. aureus* collected from the medium after infection; Adherent - *S. aureus* attached to the host cell; Intracellular - *S. aureus* accumulated inside the host cell in the presence of antibiotic pressure; Intra+Adherent – combined number of intracellular and adherent *S. aureus*; Inoculum – initial number of treated (Low or High) or untreated (MOI 10 or MOI 1) *S. aureus* used for infection. The data are presented as the mean \pm SD of six separate experiments. The significance of infected cell viabilities at the respective p-values is indicated with asterisks [$**p < 0.01$; $***p < 0.001$] and it was calculated relative to the respective control to each pre-treatment.

Divergent pattern of Ga³⁺MPs accumulation inside human keratinocytes

In the next stage of our work, it was important to carefully examine the accumulation of the tested compounds in host cells before applying Strategy 3 (**Fig. 1** Strategy 3), which involves applying aPDI to intracellular bacteria. First, we investigated the accumulation profile of gallium compounds, Ga³⁺CHP and Ga³⁺MPIX inside human keratinocytes to check for possible differences and efficiency of the process. Accumulation of Ga³⁺MPs is the first step indispensable to reach the bacteria inside keratinocytes. The rate of accumulation of both compounds was time dependent. After 1 hour of accumulation, both Ga³⁺CHP and Ga³⁺MPIX were primarily localized at the cell membrane (**Fig 7A**). However, over time, we observed differences in the localization patterns of the gallium derivatives tested. Ga³⁺MPIX was distributed throughout the cell in the cytoplasm, while cationic Ga³⁺CHP was mainly localized as intracellular clusters (**Fig 7A**). Flow cytometry measurements revealed that after 2 hours of accumulation, 60% of keratinocytes accumulated Ga³⁺MPIX, while the corresponding value for Ga³⁺CHP was 7% (**Fig 7B**). After 6 hours, 75% of the cells accumulated Ga³⁺MPIX and 59% Ga³⁺CHP, reducing the differences observed at the 1st and 2nd hours. Interestingly, after 24 hours, nearly every cell accumulated both compounds at the same level (94%). When measuring the number of molecules of Ga³⁺CHP or Ga³⁺MPIX accumulated per cell, we also observed the time-dependent uptake (**Fig 7C**). Remarkably, despite the accumulation in the cells, none of the tested compounds exhibited a significant cytotoxic effect against keratinocytes (**Fig 7D, E**). Even after a 24-hour incubation with the tested compounds, cells continued to grow, further dividing, and finally reaching the plateau phase of growth at a similar time, regardless of the incubation time with the compound.

Based on these results, both compounds accumulate in host cells in a time-dependent manner without significantly affecting host proliferation and viability. However, the accumulation pattern of Ga³⁺MPIX and Ga³⁺CHP inside the cell is highly divergent. It is more likely for Ga³⁺CHP, than Ga³⁺MPIX, to reach intracellular *S. aureus* due to its more localized accumulation inside intracellular clusters.

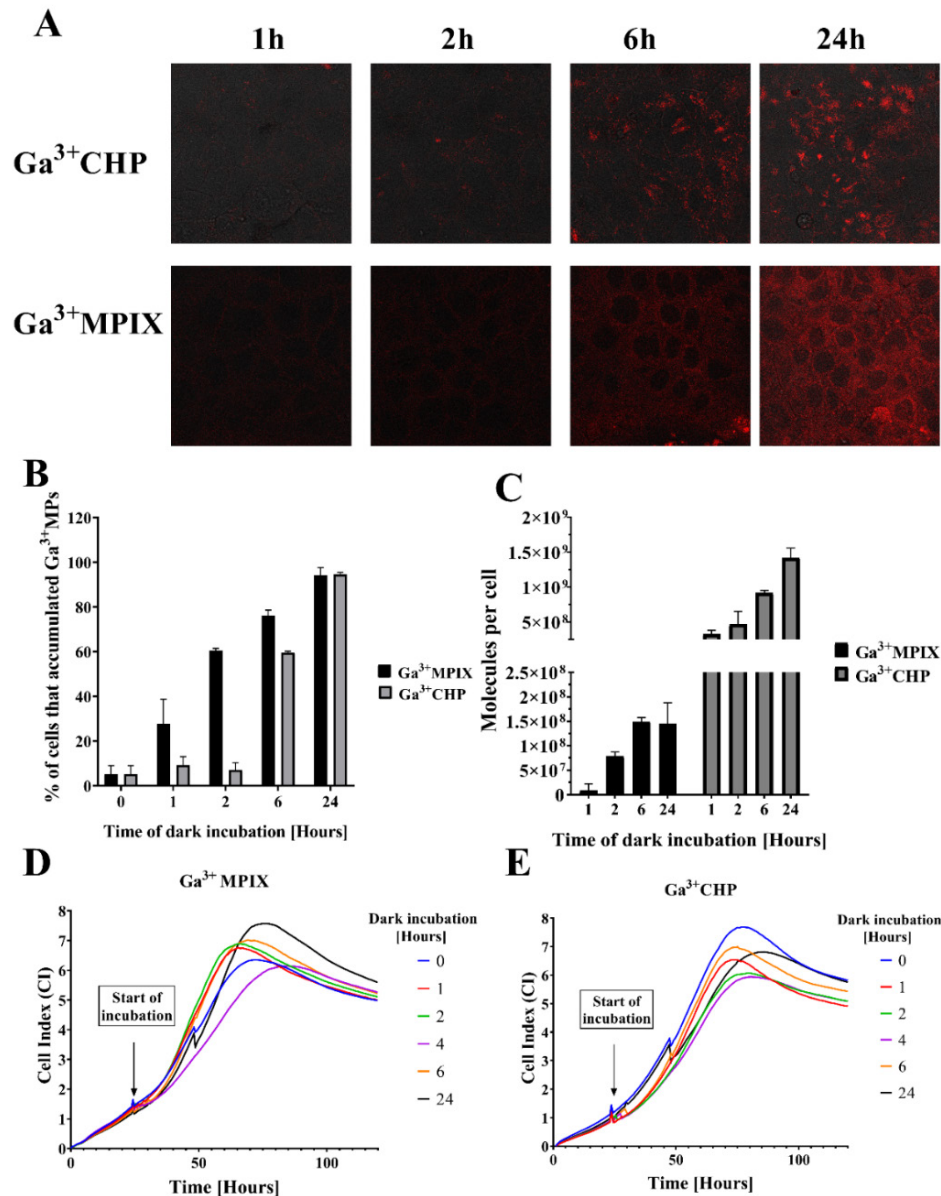


Figure 7. Divergent pattern of accumulation between two gallium metalloporphyrins in human keratinocytes.

(A) Images from a confocal fluorescence microscope presenting accumulation of two gallium compounds - Ga³⁺MPIX and Ga³⁺CHP in HaCaT cells after dark incubation (1-24 hours) at 10 μ M concentration. (B) Percentage of cells that accumulated Ga³⁺MPs among total number of cells measured by flow cytometry. Cells were incubated with 10 μ M Ga³⁺MPIX or Ga³⁺CHP and fixed

at each time point (1-24 hrs) in the absence of light, and then the fluorescence signal in the cells was measured by flow cytometry. (C) The number of accumulated Ga^{3+} MPIX or Ga^{3+} CHP molecules (10 μM) in keratinocytes after incubation for the time indicated on X axis, as measured by the fluorescence intensity of cell lysate. After dark incubation for a particular time, cells were harvested, counted, and lysed with 0.1M NaOH/1% SDS, to measure the fluorescence of each accumulated compound. (D, E) Real-time growth analysis of HaCaT cells after dark incubation (1-24 hours) with 10 μM of Ga^{3+} MPIX (D) or Ga^{3+} CHP (E).

Ga^{3+} CHP accumulates to a greater extent in infected cells.

We next investigated the accumulation of Ga^{3+} CHP in *S. aureus*-infected cells. First, keratinocytes were infected with *S. aureus* for 2 hours (MOI 10) in a medium without antibiotics, then antibiotic was introduced to remove extracellular bacteria and maintain intracellular invasion. For comparison, uninfected cells were cultured separately. The next day, the Ga^{3+} CHP was added to the infected cell culture, and cells were incubated in the dark. After 2, 4, and 6 hours of incubation, cells were collected to detect a red fluorescence signal from the compound accumulated in both infected and uninfected cells (**Fig 8A**). We observed an increase in the accumulation level over time, measured as the percentage of keratinocytes (infected or non-infected) showing fluorescence produced by Ga^{3+} CHP. We observed a very interesting correlation in that infected keratinocytes accumulated more Ga^{3+} CHP compared with uninfected cells. This was most evident after a longer incubation (**Fig. 8A**, 6 hour). Then, we analyzed the compound's accumulation only in the fraction of infected cells containing both signals: red fluorescence from the cationic Ga^{3+} CHP compound (Ga^{3+} CHP+) and green signal from the *S. aureus* strain USA300 (GFP+) (**Fig. 8B**). Over time, the accumulation of a gallium compound in the infected cell fraction (Ga^{3+} CHP+/GFP+) increased. After 6 hours of incubation, the number of infected cells simultaneously possessing both signals increased up to 25%, indicating that the cationic gallium compound accumulates in infected cells. This indicates that the cationic Ga^{3+} CHP may colocalize with intracellular bacteria.

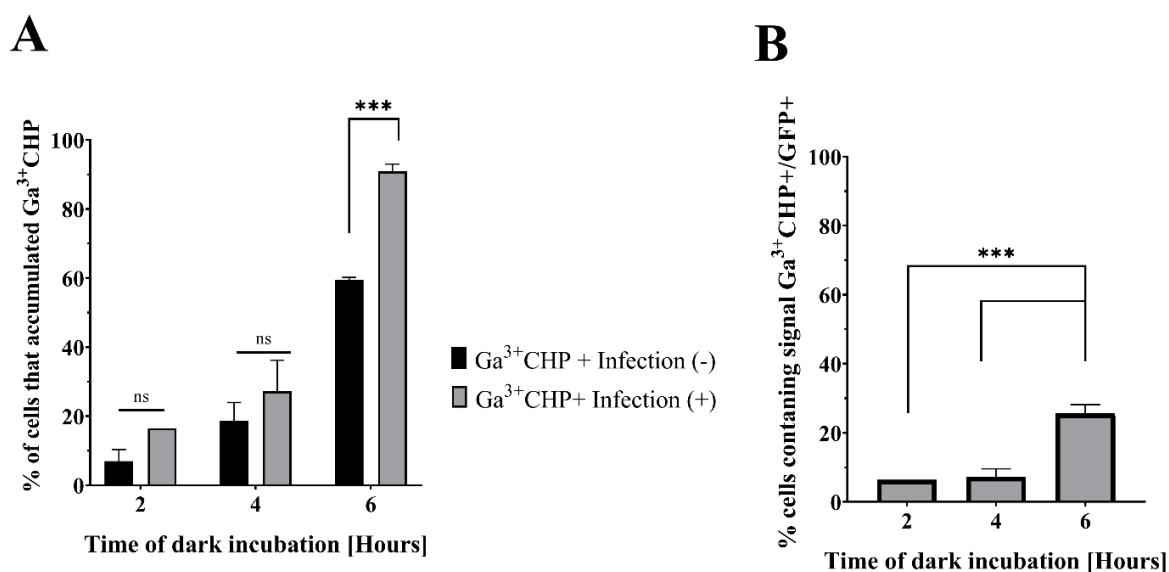


Figure 8. The accumulation rate of Ga³⁺CHP in infected cells.

(A) Accumulation of Ga³⁺CHP in infected and uninfected cells. The cells were infected with *S. aureus* USA300 (MOI 10) for 2 hours in medium without antibiotic, then the cells were washed and covered with medium with antibiotic. In parallel, uninfected cells were cultured. The next day, incubations was started in the dark with a concentration of 10 μ M of Ga³⁺CHP. After the incubation time, cells were washed and collected, then the percentage of cells having a fluorescence signal derived from Ga³⁺CHP was measured by flow cytometry. The accumulation results were compared with uninfected cells. (B) The number of cells harboring both signals: GFP+ and Ga³⁺CHP+ after dark incubation with Ga³⁺CHP in infected cells. The significance was calculated between two compounds, and respective p-values are marked with asterisks [***p < 0.001].

Intracellular *S. aureus* colocalizes with Ga³⁺CHP in keratinocyte lysosomes

Ga³⁺CHP accumulated inside the cells in distinct clusters, thus in the next step, we wanted to identify the organelles in which the studied compound localizes. Fluorescence dyes specific for the Golgi apparatus, mitochondria, or lysosomes, respectively, were used to determine the localization of the compound (Fig S3, Table S1). To assess the colocalization, images were analyzed for two colocalization coefficients: the Pearson correlation (significant colocalization > 0.5) and overlap coefficient (> 0.6). High localization of the compound in lysosomes was observed, but this was not the only site of accumulation. The overlap coefficient between Ga³⁺CHP and LysoTracker™ Deep Red in lysosomes was 0.65 with a Pearson's correlation of 0.46 (Fig 9), indicating partial localization in those eukaryotic clusters. We also observed some Ga³⁺CHP accumulation in the mitochondria (although to a far lesser extent compared with

lysosomes), and no confirmed localization in the Golgi apparatus (**Table S1**). Then, we examined the localization of *S. aureus* inside keratinocytes. However, we did not confirm the lysosomal localization of the bacteria, measured by both - the overlap coefficient and the Pearson's correlation (**Table S2**). Interestingly, when Ga³⁺CHP was incubated with *S. aureus*-infected keratinocytes, colocalization between *S. aureus* and Ga³⁺CHP occurred. Moreover, simultaneous staining of lysosomes and detection of signals from *S. aureus* (GFP) and Ga³⁺CHP indicated the colocalization of these signals in the lysosomes. We thus hypothesized that certain metabolic changes caused by two factors (infection and presence of Ga³⁺CHP) can promote the colocalization of *S. aureus* inside the lysosomes.

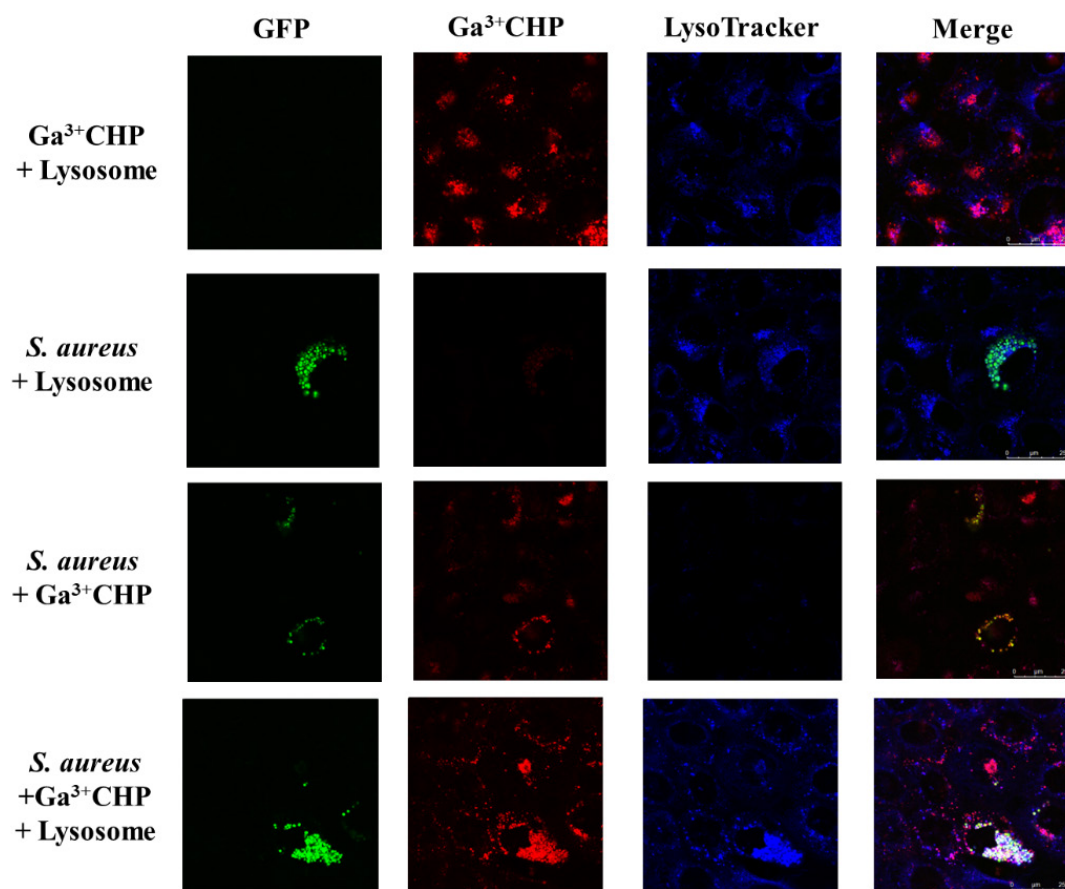


Figure 9. Colocalization of intracellular *S. aureus* and Ga³⁺CHP in lysosomes.

Confocal images of *S. aureus*-infected keratinocytes (HaCaT) at 1st day post-infection, incubated in the dark for 6 hours with cationic Ga³⁺CHP (10 μM). The green signal represents intracellular *S. aureus* USA300-GFP, the red signal is Ga³⁺CHP, while the blue signal is from lysosomes. All colocalization parameters are detailed in **Table S2** in Supporting Information Captions.

Light-activated Ga³⁺CHP reduces the number of infected keratinocytes.

After establishing the colocalization of intracellular bacteria and Ga³⁺CHP we proceeded to analyze the effect of aPDI on intracellular and intra-lysosomal *S. aureus* according to Strategy 3 (Fig. 1 Strategy 3). To this end we applied excitation with green light of Ga³⁺CHP accumulated in cells and checked how it would affect the total number of infected cells. For this purpose, on the first day, we infected keratinocytes, removed extracellular bacteria, and left only intracellular bacteria due to the use of antibiotics in the culture. The next day, we added Ga³⁺CHP to the cells, incubating for 2 or 6 hours in the dark. After incubation, we irradiated the infection model with the green light at doses of 6.36 or 12.72 J/cm² (Fig 10A). Using flow cytometry, we measured the number of infected cells by tracing the GFP signal originating from intracellular *S. aureus*. As a control (100%), the GFP signal was analyzed for infected cells that were not subjected to aPDI (without Ga³⁺CHP addition and irradiation). Incubation of cells with Ga³⁺CHP in the dark reduced the number of cells expressing GFP to ~70%, regardless of incubation time. However, when green light irradiation was added, a significant decrease in the number of GFP-expressing cells to 37-27% was observed which was not dependent on incubation time and the light dose applied (Fig 10B). Treatment with light alone did not reduce the number of infected cells. For Ga³⁺MPIX, which did not accumulate in intracellular clusters, we did not observe any decrease in the number of infected cells after green light illumination (Fig S4). Colocalization of both the photosensitizer and the bacteria is crucial for effective reduction of the intracellular *S. aureus* during the aPDI process.

To verify how aPDI treatment affects the survival and growth of host cells, we analyzed the real-time growth of infected and non-infected cells after illumination with green light (6.36 J/cm²) following a 2-hour incubation with Ga³⁺CHP in the dark (Fig 10 C-E). We observed that incubation of cells with Ga³⁺CHP followed by light application delayed the proliferation rate of both infected and uninfected cells. Interestingly, after aPDI, infected cells exhibited a higher overall growth rate (0.03 CI/h) than uninfected cells (0.019 CI/h) until reaching the plateau phase. However, uninfected cells restored growth much faster immediately after aPDI compared to infected cells (as reflected by the Δ CI parameter: 2.78 vs. 1.8, for non-infected vs. infected cells, respectively). The plateau phase for uninfected cells was reached faster (131 h, CI_{max} = 5.9) than for infected cells (140 h, CI_{max} = 6.9). After aPDI treatment, both - infected and uninfected cells show significant slowdown in growth and a delay in entering the plateau phase compared to untreated cells. Despite some phototoxicity of aPDI, which reduces the rate of cell proliferation after treatment, both infected and uninfected cells can overcome photodamage and begin to proliferate until the plateau phase is reached. This indicates a lack of significant photo- and cytotoxicity against host cells.

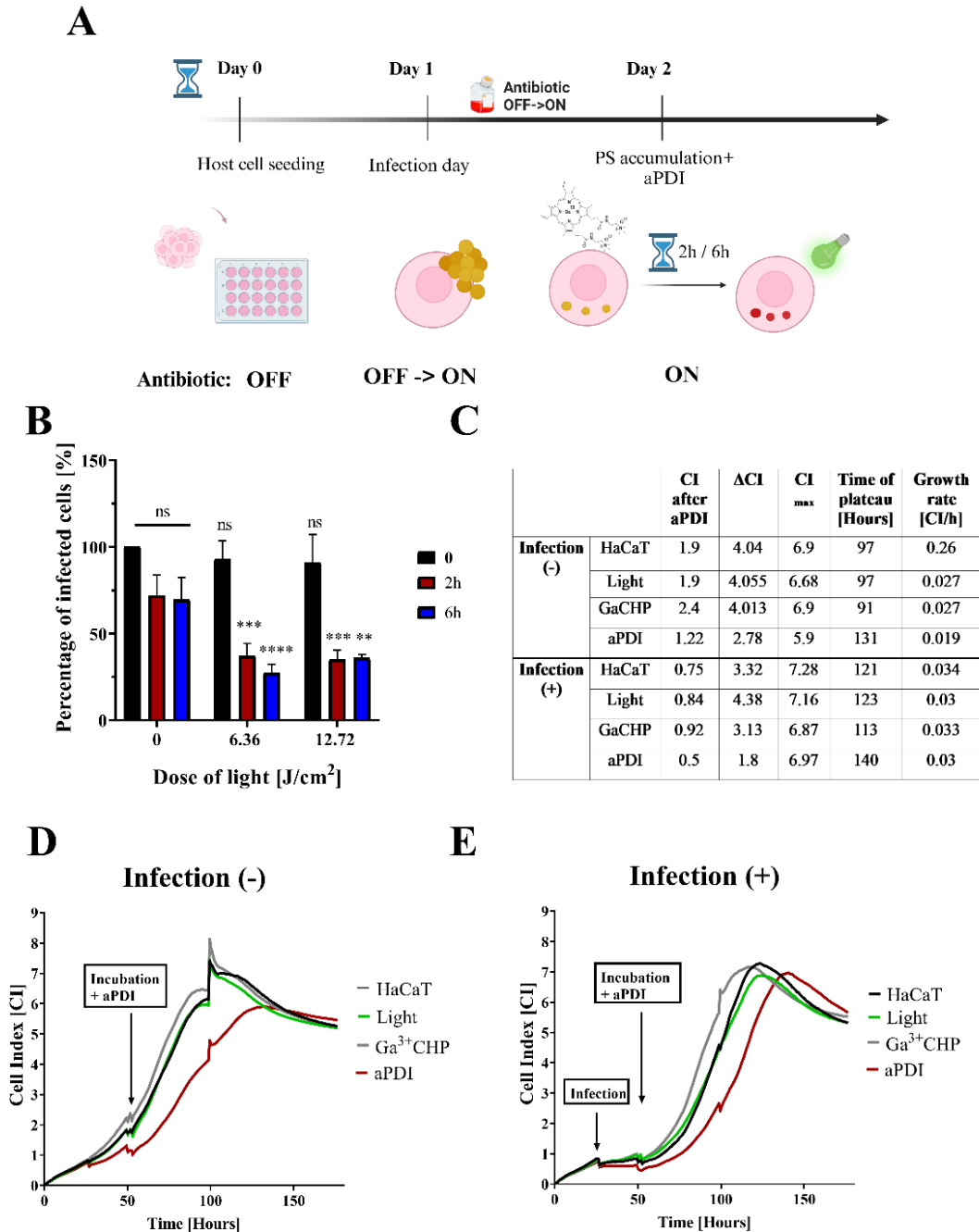


Figure 10. Light-activated Ga³⁺CHP impacts the number of GFP-expressed cells with no severe host damage.

(A) Scheme of the experiment. On day 0., HaCaT cells were seeded in a 24-well plate. On day 1., *S. aureus* USA300 (MOI 10) was added to start a 2-hour infection. Next, the medium was replaced with antibiotic-medium (Antibiotic OFF->ON) to eliminate extracellular bacteria and maintain intracellular invasion. On day 2., Ga³⁺CHP was added to the medium for 2 or 6 hours for dark incubation, then cells were washed, and the green light was applied at the proper dose. (B) Percentage of infected cells after aPDI. The number of GFP-expressing cells after 2- or 6-hour

dark incubation followed with either dark treatment or green light illumination. Cells were collected, fixed and GFP signal was measured by flow cytometry. All results were calculated in reference to the untreated control (cells with no compound and no light exposure). (C) Table containing growth characteristics of individual treatments of infected or uninfected cells. The following parameters were taken into account in the analysis: CI after aPDI – CI measured immediately after aPDI treatment (at 55th hour of the experiment); Δ CI with the characteristics of the growth rate immediately after aPDI treatment, calculated as the difference in the growth of cells after aPDI treatment (from 55 h of the experiment) and cells in the middle of logarithmic growth (~100 h of the experiment); CI_{max}- Maximum CI achieved at the beginning of the plateau phase; Time to plateau phase - time at which cells enter stationary growth phase; Growth rate calculated as the total rate of increase in the logarithmic phase of growth after treatment to time of reaching the plateau phase of the analysis curve. (D, E) Real-time growth analysis of HaCaT cells uninfected (D) or infected (E) after dark incubation at 2 hours with 10 μ M of Ga³⁺CHP and with or without light illumination of 6.36 J/cm². The Cell Index (CI) was measured by the RTCA device every 10 minutes. Experiments were conducted until the cells reached the plateau phase of growth.

Discussion

In patients with chronic and recurrent skin infections, such as patients with AD, the problem of staphylococcal infections is extremely important. The interaction of *S. aureus* with the skin is the subject of intensive research. On the one hand, answers are being sought to the question of whether there are specific characteristics that allow the bacteria to adapt to living on the skin. On the other hand, the subject of interest is host cells, which are not just passive players in the game defined as 'host-pathogen interaction. Methods are constantly being developed to control the spread of staphylococci on skin that is primarily affected by the disease, such as atopic dermatitis. Antibiotics can and are used to combat staphylococci infecting the skin, but the frequent use of antibiotics leads to the selection of strains resistant to the drug used. In this case, other methods are needed, preferably ones that can combat infections caused by drug-resistant bacteria. Such a method is the photodynamic method described in this article as aPDI. It is a method with proven efficacy against *S. aureus*, but also against other microorganisms, including drug-resistant ones (21). To date, however, it has not been shown whether the use of aPDI is effective against intracellular bacteria.

Staphylococcus aureus was initially described as an extracellular pathogen, but recent scientific reports indicate its ability to invade intracellularly non-professional phagocytes, including keratinocytes. In this way, the bacteria avoid the effect of antibiotics whose penetration into host cells is hindered (6,33). In our study, we established and described keratinocyte infection model

with multidrug resistant *S. aureus* for implementing aPDI on the different stages of *S. aureus* infection: adherence, internalization, intracellular persistence, or release of bacteria from the host cell (**Fig 1**). In this study, we used the keratinocyte model of the HaCaT cell line and keratinocytes with reduced filaggrin function as a simplified model of AD. The results of our study presented in this work remain in agreement with previously published data showing that in patients with AD, the impairment in the *FLG* gene is correlated with increased *S. aureus* colonization (32,34). We observed a higher internalization and longer intracellular persistence of *S. aureus* in keratinocytes without functional filaggrin (**Fig. 4**). Higher intracellular *S. aureus* persistence might be responsible for chronic staphylococcal infections in atopic dermatitis and an increased risk of reinfection after initial antibiotic treatment (35).

Once internalized, *S. aureus* is exposed to two selective pressures: antibiotic and intracellular environment of the host. The pathogen undergoes drastic changes in the transcriptome for induced persistence (36,37). Nevertheless, intracellular persisters exhibit metabolic activity despite adaptive changes. Moreover, it has been shown that intracellular phenotype could manifest greater tolerance to antibiotics (38). The reservoir of intracellular *S. aureus* is strongly linked to the recurrence of infection (39–41). Under favorable conditions (i.e., the absence of antibiotic), *S. aureus* USA300 could escape, and restart the infection, even with a lower intracellular load (**Fig 3D, Fig S1**). The same observation was made by Rollin et al., where *S. aureus* resumed extracellular infection after maintaining intracellular inoculum for up to 10 days under selective antibiotic pressure (42). Bacteria that are released from the host might contribute to therapeutic failures. In our study, we evaluated the efficacy of aPDI action (Strategy 1) in eliminating *S. aureus* released from the host cells, that regrown from the intracellular inoculum. Based on our results bacteria released from cells were still sensitive to aPDI likewise suspension cultures of *S. aureus* grown *in vitro* (**Fig. 5**). The adaptive changes that occur during infection did not alter the bacterial sensitivity to aPDI. This indicates that the combination of green light and Ga³⁺MPs might be an efficient strategy to combat recurrent staphylococcal infections.

In Strategy 2, we assessed the effect of aPDI pretreatment on *S. aureus* adherence and internalization. Treatment with Ga³⁺CHP of initial inoculum before infection significantly decreased the adherence of bacteria to keratinocytes. In our previous study, the light-activated Ga³⁺CHP was shown as an efficient singlet oxygen producer (29). The singlet oxygen, generated during aPDI pre-treatment, might affect the structure of bacterial surface proteins responsible for their attachment to the host (43). It was shown that aPDI reduces biofilm adherence to abiotic surfaces (44). Our results show for the first time that aPDI using green light induced Ga³⁺CHP reduces the adhesion of *S. aureus* to a biotic surface, namely keratinocyte (**Fig. 6**). Interestingly, pre-treatment with aPDI did not significantly change the level of internalization of *S. aureus*, regardless of inoculum size (MOI 10 vs. MOI 1) and aPDI strength (High vs. Low), the number

of intracellular *S. aureus* did not change (**Fig. 6**). This indicates a particular priority of *S. aureus* action during infection, which is dominated by internalization. This happens until a certain capacity of host internalization is achieved. Finally, the bacterial inoculum also showed a weaker proliferation rate after aPDI treatment, which we observed as a significant reduction in the growth of extracellular fraction.

In a study by Akilov et al., some limitations have been presented that need to be overcome for aPDI to be an anti-intracellular therapy (45). The ideal situation would be to kill infected keratinocytes while non-infected one would be spared. To achieve this, a major challenge must be faced: the accumulation of PS inside host cells and perhaps inside intracellular vesicles where the pathogen may reside. For this reason, investigating the intracellular localization of both the pathogen and the PS is key to verifying the potential of aPDI as a method that works on intracellular pathogens. The second important issue is the effective concentration of PS in cells, which depends not only on the accumulation process, but also on the potential efflux of PS or the unwanted interaction of PS with host cell biomolecules. Ga³⁺MPs studied by us revealed the divergent cellular localization pattern in keratinocytes. In general, the accumulation of porphyrins into eukaryotic cells occurs through a slow passive-diffusion process with partial accumulation within mitochondria (45,46). In our study, cationic Ga³⁺CHP is colocalized in cellular organelles, mostly in lysosomal structures (**Fig 9**), and partially in mitochondria (**Fig S3B**). The presence of cationic quaternary ammonium moieties in the structure of Ga³⁺CHP might promote increased uptake and tracking to lysosomes through electrostatic attraction (47,48). At this stage of research, it is difficult to determine whether Ga³⁺CHP first accumulates in lysosomes, attracting bacteria to these structures, or whether bacteria capture Ga³⁺CHP via highly specialized heme import systems and consequently end up in lysosomes. On the one hand, the environment of the lysosome is nutrient-poor, which favors the bacterial cell in changing its phenotype to a dormant one, and thus more resistant to antimicrobials. On the other hand, in a poor environment, a pathogen such as *S. aureus* produces highly specialized proteins that efficiently capture nutrients such as heme or its structural analogs, as demonstrated in this work and our previous studies (**Fig. 8**) (26,29). Interestingly, we did not confirm the lysosomal localization of intracellular *S. aureus* itself (**Fig. 9; S. aureus + Lysosome**). However, simultaneous colocalization of intracellular bacteria with Ga³⁺CHP in the lysosomal structures of the host was confirmed (**Fig. 9; S. aureus + Ga³⁺CHP + Lysosome**). The presence of both: *S. aureus* and Ga³⁺CHP may influence metabolic changes that favor the colocalization of *S. aureus* inside lysosomes. Therefore, there is a high probability that Ga³⁺CHP will reach intracellular bacteria or even be intracellularly accumulated by them through heme receptor acquisition systems as a part of the light-independent action of Ga³⁺MPs.

According to Strategy 3 presented in this study, we tested the effectiveness of aPDI on the intracellular load of *S. aureus* in the non-professional phagocytes as keratinocytes. So far, there

are a few studies on the aPDI effectiveness in the anti-intracellular approach. For instance, efficient aPDI killing of intracellular *S. aureus* in HeLa cells was achieved with red light and a conjugate of the cell-binding domain of phage endolysin (CBD3) and silicon phthalocyanine (700DX) (49). Furthermore, blue light-activated gallium-substituted hemoglobin on silver nanoparticles was used against intracellular *S. aureus*, which persisted inside professional phagocytes (50). Both examples use high-molecular-weight bioconjugates, which may have more difficulty accumulating inside eukaryotic cells than low-molecular-weight compounds. Previous studies on aPDI efficacy in this field have mainly focused on the infection model involving either cancer cell line or professional phagocytes as macrophages (49,50). Our study is the first evaluation of the aPDI efficacy on the infection model of *S. aureus* inside non-professional phagocytes such as human keratinocytes. Accumulation of bioconjugates may be difficult for non-professional phagocytes, due to the lower accumulation capacity of these cells (51). We used small molecular weight compounds - gallium metalloporphyrins rather than bioconjugation with bulky molecules. The addition of a positive charge gained by quaternary ammonium moieties increases the compound's hydrophilicity, which might be important for the lysosomal localization of photosensitizer inside eukaryotic cells (52). This was observed in the case of intracellular localization of hydrophilic sulphonated tetraphenyl porphyrins (53). Moreover, it has been reported that adding a cationic charge was necessary for effective photokilling and higher accumulation of benzophenoxazine in the intracellular pathogen *Leishmania* (54). Ga³⁺CHP was previously reported by us as a biocompatible and safe agent both *in vitro* and *in vivo* studies (30). Green light excitation of Ga³⁺CHP did not exhibit pronounced phototoxicity in studies on HaCaT cell cultures alone (29), nor in our infectious model (**Fig. 10**) as discussed below.

Previous studies on aPDI in an anti-intracellular approach have mainly focused on intracellular photokilling efficacy without testing eukaryotic safety as a part of the infection model (49,50). Monitoring aPDI phototoxicity was focused on uninfected cell cultures separately rather than on infected cells, harboring the intracellular *S. aureus* (49,50). This approach does not reflect the actual impact of aPDI on infected cells, especially since the infection itself contributes to a significant reduction in host growth. In our approach, we monitored growth in real-time during ongoing infection, subsequent dark accumulation with Ga³⁺CHP, and green light irradiation until the plateau phase. After aPDI with Ga³⁺CHP both infected and uninfected cells exhibited some phototoxicity reflected as growth delay (**Fig. 10 D vs. E**). Surprisingly, uninfected cells' growth rate was relatively slower than that of the infected cells, despite higher survival immediately after aPDI. Nevertheless, both infected and uninfected cells eventually reached a plateau phase, indicating that the photodamage could be overcome by cell line. aPDI combined with Ga³⁺CHP is a promising anti-intracellular treatment, which exhibited a low phototoxicity impact on keratinocytes despite the infection status. One limitation of this study is the inability to distinguish

whether aPDI causes elimination of only intracellular bacteria without damaging keratinocytes, or the bacteria together with keratinocytes that incorporate them.

Overall, this research presents the application potential of light-activated compounds for: i) elimination of staphylococcal recurrent infections, ii) decrease of the infection process and bacterial attachment to the host cells, iii) reduction of the intracellular *S. aureus*. We highlighted the great importance of the simultaneous colocalization of a photosensitizer and intracellular bacteria within the host's intracellular clusters for efficient reduction the number of infected cells in the aPDI process. This study reveals the broad spectrum of aPDI application to overcome staphylococcal intracellular infections.

Material and Methods

Bacterial strains and growth conditions

In this study, we used two GFP-expressing *S. aureus* strains: hypervirulent USA300 (AH3369) derived from A. Horswill (55) and non-hypervirulent, *agr*-deficient RN4220 from BEI Resources, USA. Both strains were grown in trypticase soy broth (TSB, bioMérieux, France) at 37 °C with 10 µg/mL of either chloramphenicol for USA300 or trimethoprim for RN4220 to sustain the GFP plasmid. To obtain bacteria in the stationary phase of growth, overnight cultures were grown for 16-20 hours and diluted to 0.5 McFarland (~10⁷ CFU/mL). For infection, stationary overnight cultures were diluted to 1:100 in flask and grown with shaking (150 rpm/37°C) to obtain logarithmic phase up to 2 hours then diluted to 0.5 McFarland for further investigations.

Cell line and culture media (Antibiotic ON/OFF)

The human immortalized keratinocyte HaCaT cell line was used in this study. As the cell line for the filaggrin deficient cell line (*FLG* sh), we used knockdown cells after lentiviral particles *FLG* shRNA (sc-43364-V) infection, characterized previously (56). Control cells were treated with an empty vector (*FLG* ctrl). Culture medium with antibiotic (Antibiotic ON) consisted of Dulbecco's modified Eagle's medium (DMEM) with 10% fetal bovine serum (FBS), 4.5 g/L glucose, 1 mM sodium pyruvate, 100 U/mL penicillin, 100 µg/mL streptomycin, 2 mM l-glutamine, and 1 mM nonessential amino acids. The medium without antibiotic (Antibiotic OFF) was based on the previously given composition of DMEM HaCaT growth medium but without the addition of streptomycin and penicillin. All media components were derived from Gibco, Thermo Fisher Scientific, USA. Cells were grown in a standard humidified incubator at 37 °C in a 5% CO₂ atmosphere.

Co-culture methodology

To obtain intracellular *S. aureus*, we proposed the infection model protocol, provided in detail on **Fig 11**. Briefly, HaCaT cells were seeded in the antibiotic-free medium (Antibiotic OFF) prior to infection day, referred to as Day 0, at a density of 10^5 cells/per well in a 24-well plate (Corning, USA). The next day (Day 1), overnight *S. aureus* cultures were diluted 1:100 in the 10 mL of TSB with proper antibiotic to sustain the plasmid in the flask. Cells were grown for 2 hours with 150 rpm shaking at 37°C to achieve logarithmic growth. Bacterial suspensions were diluted in TSB to 0.5 McFarland ($\sim 2 \times 10^7$ CFU/mL), and depending on the MOI for infection, the appropriate concentration of bacteria was added to the growth medium of HaCaT cells. After 2 hours of infection incubator at 37 °C in a 5% CO₂ atmosphere, cells were washed with PBS, and the medium was changed to contain the standard cultures antibiotics (Antibiotic ON). During the following days (Day 2-7), either the antibiotic pressure was maintained, or the medium was changed for non-antibiotic (OFF) to release bacteria from the host.

To investigate the *S. aureus* fraction to count CFU/mL, we collected each fraction at the proper time point of the infection model preparation. For extracellular *S. aureus*, the fraction was collected from the growth medium after 2 hours of infection. For the intra+adherent fraction, after infection, cells were washed three times with PBS, and trypsinized with TrypLE™ Express (Thermofisher Scientific, USA). Cells were collected, washed, centrifuged, then resuspended in the 0.1% TritonX-100 in MiliQ for 30 minutes for cell lysis. For intracellular *S. aureus*, 2 hours after the addition of *S. aureus* infectious inoculum, cells were washed, and the growth medium was change to fresh medium with antibiotic (Antibiotic ON) for kill the adherent and extracellular bacteria. After 1 hour incubation with antibiotics, the cells were washed and harvested. After that, samples were washed and lysed with lysis buffer. Each fraction was serially diluted and placed on TSA agar plate for CFU/mL counting.

To prepare the fraction of *S. aureus* from different stages of infection for analysis on the flow cytometer. After infection, cells were washed with PBS, then trypsinized and harvested. Culture medium was used to neutralize the trypsin, and the cells were washed with PBS and resuspended in BD Cytofix/CytoPrem™ kit (BD Biosciences, USA). After a 20-minute incubation in the dark with pre-fix buffer, the cells were centrifuged, washed twice, and resuspended in PBS for further analysis on flow cytometer.

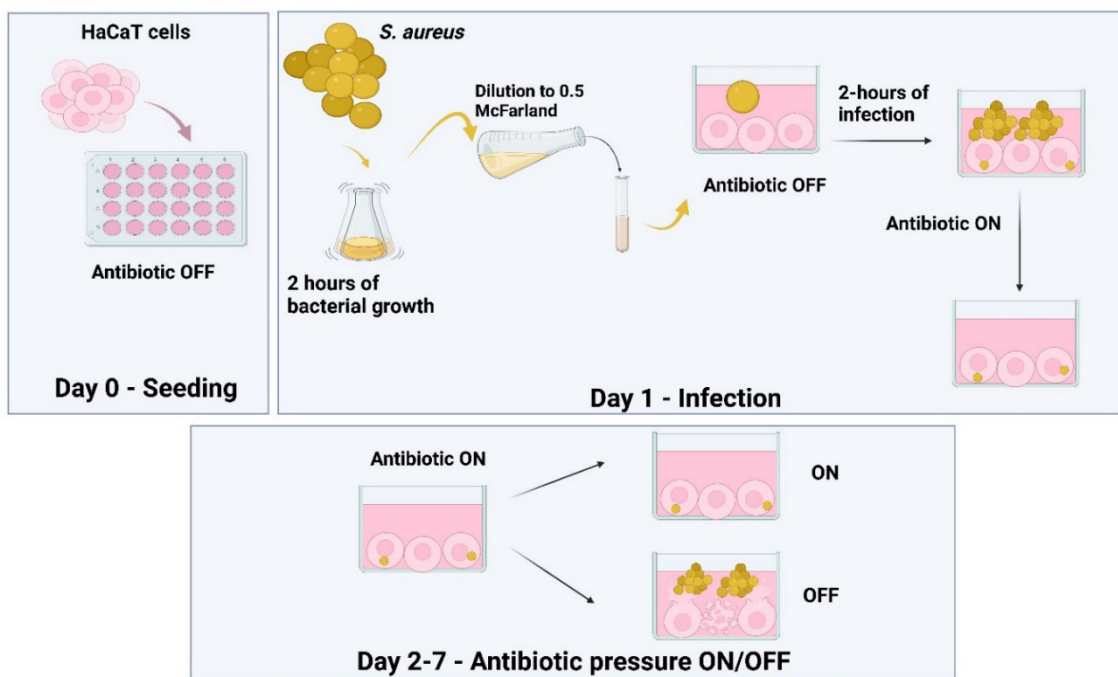


Figure 11. Methodology of the infection model preparation.

On the Day 0, HaCaT cells were seeded at the 24-well plate in a non-antibiotic medium (Antibiotic OFF). On day 1, *S. aureus* overnight cultures were diluted and grown by 2 hours to achieve a logarithmic growth phase. Afterward, cultures were diluted and transferred to the cells at a proper multiplicity of infection. Then, after 2 hours of infection, the growth medium was changed to antibiotic (Antibiotic ON) to put antibiotic pressure on intracellular invasion. On days 2-7, the antibiotic pressure was maintained or lifted by changing the medium to non-antibiotic (Antibiotic OFF) to release extracellularly intracellular *S. aureus*.

Gallium compounds

The synthesis and structure characterization of cationic gallium porphyrin (Ga^{3+}CHP) and Ga^{3+} mesoporphyrin IX chloride ($\text{Ga}^{3+}\text{MPIX}$) was previously described in detail (29,30). The initial stock of Ga^{3+}CHP was prepared in Milli-Q water, while $\text{Ga}^{3+}\text{MPIX}$ in the 0.1 M NaOH solution.

Compound accumulation

The intracellular accumulation of each photosensitizer inside human keratinocytes was analyzed by two methods: flow cytometer analysis and measurements of fluorescence intensity of cell lysates. $\text{Ga}^{3+}\text{MPIX}$ or Ga^{3+}CHP at 10 μM were added to the medium of HaCaT cells either infected or uninfected. After dark incubation at the desired time, the external photosensitizer was removed, then cells were trypsinized and collected. Cells were either fixed with BD Cytotfix/CytoPrem™ kit for flow cytometry analysis or counted and then lysed with 0.1M NaOH/1%SDS buffer for fluorescence lysate measurements. The fluorescence intensity of each sample was measured with an EnVision Multilabel Plate Reader (PerkinElmer, USA) at the

following emission/excitation wavelengths: Ga³⁺MPIX at 406/573 nm and Ga³⁺CHP at 406/582 nm. Accumulation calculations for each PS were made from a compound calibration curve prepared in the lysis solution. The uptake values are presented as PS molecules accumulated per HaCaT cell number in the well. The molecular weight of Ga³⁺CHP was calculated to be 907.08 g/mol, and that of Ga³⁺MPIX was estimated to be 669.85 g/mol.

Flow cytometry

Prepared fixed cells were analyzed by GFP signal originating from *S. aureus* that was detected with the green detector channel (exc 488 nm, ems 525/30 nm). For the accumulation of photosensitizer - the PS signal detected the Red Detector channel (exc 642 nm, ems 664/20 nm). Cells were analyzed using Guava easyCyte™ flow cytometer and guavaSoft 3.1.1. software with an analysis of 10,000 events.

Light activation of Ga³⁺MPs (Strategy 1, 2 and 3)

For the light-activation of gallium compounds, we used a light-emitting diode (LED) light emitting green 522 nm light (irradiance= 10.6 mW/cm², FWHM= 34 nm) to excitement either Ga³⁺MPIX or Ga³⁺CHP. The excitement of gallium compounds within Q-bands at the emission spectra of lamp with the excitement of gallium compound was previously characterized in our previous research (57).

We applied light-activation of gallium metalloporphyrins on the infection model at different stages of the preparation, based on our proposed strategies (**Fig 2**). In strategy 1, HaCaT cells were infected with *S. aureus* at MOI 10 for 2 hours in an antibiotic-free medium (Antibiotic OFF). Then, cells were washed with PBS, and the medium was changed to antibiotic (Antibiotic ON). The next day, the medium was removed, adherent cells were washed with PBS, then the antibiotic-free medium was again applied (Antibiotic OFF) and cultivated for 16-20 hours to release the intracellular *S. aureus* from the host. Then, the medium was collected and centrifuged (10 000 rpm, 5 min), and bacterial sediment was resuspended in 1 mL of fresh TSB. The 10 µL of the bacterial sample was taken to count the number of bacteria released from the co-culture. The bacterial aliquot of 450 µL was mixed with 50 µL of 10x concentrated PS, then incubated in the dark with shaking at 37°C. The light illumination was applied, and surviving bacteria were serially diluted and placed on the TSA agar plates for CFU/mL counting.

For bacteria pre-treatment with aPDI at Strategy 2, the overnight *S. aureus* was diluted to 0.5 McFarland (10⁷ CFU/mL), then 900 µL of bacterial aliquots were placed on the 24-well plates with 100 µL of 10x concentrated photosensitizer, followed by 10 min dark incubation with shaking at 37°C. Then, samples were illuminated. For a low dose of aPDI, 1 µM of Ga³⁺CHP was used with 2 J/cm² dose of green light (1 log₁₀ of reduction in bacterial survival, final bacterial

concentration of $\sim 10^6$ CFU/mL), while for a high dose, we used 1 μ M of Ga³⁺CHP and 5 J/cm² (2 log₁₀ of reduction, final bacterial concentration: $\sim 10^5$ CFU/mL). Samples were centrifuged (10 000 rpm/5 min), then resuspended in 100 μ L of fresh TSB before addition to the 10⁵ HaCaT cells to start the infection. Untreated cells were added at the proper MOI (10 or 1) as a corresponding control.

In strategy 3, either Ga³⁺MPIX or Ga³⁺CHP at 10 μ M concentration was added to infected cells at the 1st day post-infection. Then samples were left for dark incubation in the CO₂ incubator for 2 or 6 hours. The PS-containing medium was replaced with PS-free medium for green light illumination at dose of either 6.36 J/cm² or 12.72 J/cm². Afterwards, cells were prepared for flow cytometry analysis. The same protocol was conducted for real-time growth analysis of the cells on the xCELLigence device, however, after illumination, cells were left for measurements of the Cell Index parameter.

Real-time growth analysis

For real-time analysis of cell growth dynamics, HaCaT cells were seeded the day before at a density of 10⁴ per well on an E-plate (ACEA Biosciences Inc., USA) on the xCELLigence real-time cell analysis (RTCA) device (ACEA Biosciences Inc., USA). The next day, cells were treated as appropriate to the experimental purpose; either infection with proper MOI was conducted, or photosensitizer was added to the dark incubation studies. The Cell Index (X-axis) monitored the change in the flow of electrons between electrodes on the E-plate. The flow of impedance depends on the cell type, the density, its shape, and the degree of adhesion to the well (58). The CI parameter was monitored every 10 minutes until the plateau phase of the cell growth was reached.

Confocal imaging

Specimens were imaged using a confocal laser scanning microscope (Leica SP8X equipped with an incubation chamber for the live analysis) with a 63 \times oil immersion lens (Leica, Germany). Cell nucleus for intracellular persistence studies and 3D-dimension images was stained with HOEST 33342 dye (Thermofisher Scientific, USA). For lysosomal staining the LysoTracker™ Deep Red (Sigma-Aldrich, USA) was used; for mitochondria – Mito RED (Sigma-Aldrich, USA); for the Golgi apparatus – GOLGI tracker NBD c6 ceramide (Thermofisher Scientific, USA). Pixel intensities were quantified and evaluated using the Pearson's correlation or the overlap coefficient to derive the colocalization rate (%). Quantitative analyses of colocalizations were performed using Leica Application Suite X, version 3.5.2.18963.

Statistics

Statistical analysis was performed using GraphPad Prism 8 (GraphPad Software, Inc., CA, USA). Quantitative variables were characterized by the arithmetic mean and the standard deviation of the mean. Data were analyzed using one-way or two-way ANOVA with Dunnett's multiple comparison test.

Acknowledgments

This work was supported by UGrants–start no. 533-0C30-GS28-23 (KS) funded by the University of Gdańsk. We express our sincere thanks to Dr. Andrea Lipińska for her valuable assistance with the flow cytometric analyses. We thank Dr. Agnieszka Bernat-Wójtowska for a constructive discussion on the infection model used.

References

1. Tong SYC, Davis JS, Eichenberger E, Holland TL, Fowler VG. Staphylococcus aureus infections: Epidemiology, pathophysiology, clinical manifestations, and management. *Clin Microbiol Rev* [Internet]. 2015 [cited 2023 Oct 2];28(3):603–61. Available from: <https://journals.asm.org/doi/10.1128/cmr.00134-14>
2. Peterson LR, Schora DM. Methicillin-Resistant Staphylococcus aureus Control in the 21st Century: Laboratory Involvement Affecting Disease Impact and Economic Benefit from Large Population Studies. *J Clin Microbiol* [Internet]. 2016 Nov 1 [cited 2023 Oct 2];54(11):2647–54. Available from: <https://journals.asm.org/doi/10.1128/jcm.00698-16>
3. Kobayashi T, Glatz M, Horiuchi K, Kawasaki H, Akiyama H, Kaplan DH, et al. Dysbiosis and Staphylococcus aureus Colonization Drives Inflammation in Atopic Dermatitis. *Immunity* [Internet]. 2015 Apr 21 [cited 2023 Oct 2];42(4):756–66. Available from: <http://www.cell.com/article/S1074761315001284/fulltext>
4. Ogonowska P, Szymczak K, Empel J, Urbaś M, Woźniak-Pawlikowska A, Barańska-Rybak W, et al. Staphylococcus aureus from Atopic Dermatitis Patients: Its Genetic Structure and Susceptibility to Phototreatment. *Microbiol Spectr* [Internet]. 2023 Jun 15 [cited 2023 Oct 2];11(3). Available from: <https://pubmed.ncbi.nlm.nih.gov/37140374/>
5. Horn J, Stelzner K, Rudel T, Fraunholz M. Inside job: Staphylococcus aureus host-pathogen interactions. *International Journal of Medical Microbiology* [Internet]. 2018;308(6):607–24. Available from: <https://doi.org/10.1016/j.ijmm.2017.11.009>
6. Strobel M, Pfortner H, Tuchscher L, Völker U, Schmidt F, Kramko N, et al. Post-invasion events after infection with Staphylococcus aureus are strongly dependent on both the host cell type and the infecting S. aureus strain. *Clinical Microbiology and Infection* [Internet]. 2016 Sep 1 [cited 2022 May 6];22(9):799–809. Available from: <https://linkinghub.elsevier.com/retrieve/pii/S1198743X16302233>
7. Kintarak S, Whawell SA, Speight PM, Packer S, Nair SP. Internalization of Staphylococcus aureus by human keratinocytes. *Infect Immun* [Internet]. 2004 Oct [cited 2023 Oct 2];72(10):5668–75. Available from: <https://journals.asm.org/doi/10.1128/iai.72.10.5668-5675.2004>
8. Löffler B, Tuchscher L, Niemann S, Peters G. Staphylococcus aureus persistence in non-professional phagocytes. *Int J Med Microbiol* [Internet]. 2014 Mar [cited 2023 Oct 2];304(2):170–6. Available from: <https://pubmed.ncbi.nlm.nih.gov/24365645/>
9. Foster TJ, Geoghegan JA, Ganesh VK, Höök M. Adhesion, invasion and evasion: the many functions of the surface proteins of Staphylococcus aureus. *Nat Rev Microbiol* [Internet]. 2014 Jan [cited 2023 Oct 2];12(1):49–62. Available from: <https://pubmed.ncbi.nlm.nih.gov/24336184/>
10. Tuchscher L, Heitmann V, Hussain M, Viemann D, Roth J, von Eiff C, et al. Staphylococcus aureus Small-Colony Variants Are Adapted Phenotypes for Intracellular Persistence. *J Infect Dis* [Internet]. 2010 Oct 1;202(7):1031–40. Available from: <https://doi.org/10.1086/656047>
11. Garzoni C, Francois P, Huyghe A, Couzinet S, Tapparel C, Charbonnier Y, et al. A global view of Staphylococcus aureus whole genome expression upon internalization in human epithelial cells. *BMC Genomics* [Internet]. 2007 Jun 14 [cited 2023 Oct 2];8(1):1–14. Available from: <https://bmcbgenomics.biomedcentral.com/articles/10.1186/1471-2164-8-171>
12. Al Kindi A, Alkahtani AM, Nalubega M, El-Chami C, O'neill C, Arkwright PD, et al. Staphylococcus aureus internalized by skin keratinocytes evade antibiotic killing. *Front Microbiol*. 2019 Sep 1;10(SEP):481150.
13. Moldovan A, Fraunholz MJ. In or out: Phagosomal escape of Staphylococcus aureus. *Cell Microbiol* [Internet]. 2019 Mar 1 [cited 2023 Oct 2];21(3):e12997. Available from: <https://onlinelibrary.wiley.com/doi/full/10.1111/cmi.12997>
14. Holmes B, Quie PG, Windhorst DB, Pollara B, Good RA. Protection of phagocytized bacteria from the killing action of antibiotics. *Nature* [Internet]. 1966 [cited 2023 Oct 3];210(5041):1131–2. Available from: <https://pubmed.ncbi.nlm.nih.gov/5964315/>

15. Surewaard BGJ, Deniset JF, Zemp FJ, Amrein M, Otto M, Conly J, et al. Identification and treatment of the *Staphylococcus aureus* reservoir in vivo. *J Exp Med* [Internet]. 2016 Jun 27 [cited 2023 Oct 3];213(7):1141–51. Available from: <https://pubmed.ncbi.nlm.nih.gov/27325887/>
16. Li Y, Liu Y, Ren Y, Su L, Li A, An Y, et al. Coating of a Novel Antimicrobial Nanoparticle with a Macrophage Membrane for the Selective Entry into Infected Macrophages and Killing of Intracellular *Staphylococci*. *Adv Funct Mater* [Internet]. 2020 Nov 1 [cited 2023 Oct 3];30(48):2004942. Available from: <https://onlinelibrary.wiley.com/doi/full/10.1002/adfm.202004942>
17. Zhou K, Li C, Chen D, Pan Y, Tao Y, Qu W, et al. A review on nanosystems as an effective approach against infections of *Staphylococcus aureus*. *Int J Nanomedicine* [Internet]. 2018 [cited 2023 Oct 3];13:7333–47. Available from: <https://www.tandfonline.com/action/journalInformation?journalCode=dijn20>
18. Zhang X, de Boer L, Heiligers L, Man-Bovenkerk S, Selbo PK, Drijfhout JW, et al. Photochemical internalization enhances cytosolic release of antibiotic and increases its efficacy against staphylococcal infection. *Journal of Controlled Release*. 2018 Aug 10;283:214–22.
19. Noore J, Noore A, Li B. Cationic antimicrobial peptide LL-37 is effective against both extra- and intracellular *Staphylococcus aureus*. *Antimicrob Agents Chemother* [Internet]. 2013 Mar [cited 2023 Oct 3];57(3):1283–90. Available from: <https://pubmed.ncbi.nlm.nih.gov/23274662/>
20. Hamblin MR, Hasan T. Photodynamic therapy: A new antimicrobial approach to infectious disease? *Photochemical and Photobiological Sciences*. 2004;3(5):436–50.
21. Nakonieczna J, Wozniak A, Pieranski M, Rapacka-Zdonczyk A, Ogonowska P, Grinholc M. Photoinactivation of ESKAPE pathogens: Overview of novel therapeutic strategy. *Future Med Chem*. 2019;11(5):443–61.
22. Kashef N, Huang YY, Hamblin MR. Advances in antimicrobial photodynamic inactivation at the nanoscale. *Nanophotonics* [Internet]. 2017 Aug 28 [cited 2023 Oct 3];6(5):853–79. Available from: <https://www.degruyter.com/document/doi/10.1515/nanoph-2016-0189/html>
23. Tim M. *Journal of Photochemistry and Photobiology B : Biology Strategies to optimize photosensitizers for photodynamic inactivation of bacteria*. *J Photochem Photobiol B* [Internet]. 2015; Available from: <http://dx.doi.org/10.1016/j.jphotobiol.2015.05.010>
24. Stojiljkovic I, Kumar V, Srinivasan N. Non-iron metalloporphyrins: Potent antibacterial compounds that exploit haem/Hb uptake systems of pathogenic bacteria. *Mol Microbiol*. 1999;31(2):429–42.
25. Kelson AB, Carnevali M, Truong-le V. Gallium-based anti-infectives : targeting microbial iron-uptake mechanisms. *Curr Opin Pharmacol* [Internet]. 2013;13(5):707–16. Available from: <http://dx.doi.org/10.1016/j.coph.2013.07.001>
26. Michalska K, Rychłowski M, Krupińska M, Szewczyk G, Sarna T, Nakonieczna J. Gallium Mesoporphyrin IX-Mediated Photodestruction: A Pharmacological Trojan Horse Strategy To Eliminate Multidrug-Resistant *Staphylococcus aureus*. *Mol Pharm* [Internet]. 2022 May 2;19(5):1434–48. Available from: <https://pubs.acs.org/doi/10.1021/acs.molpharmaceut.1c00993>
27. Reniere ML, Torres VJ, Skaar EP. Intracellular metalloporphyrin metabolism in *Staphylococcus aureus*. *BioMetals*. 2007;20(3–4):333–45.
28. Wakeman CA, Stauff DL, Zhang Y, Skaar EP. Differential activation of *Staphylococcus aureus* heme detoxification machinery by heme analogues. *J Bacteriol*. 2014;196(7):1335–42.
29. Szyczak K, Szewczyk G, Rychłowski M, Sarna T, Zhang L, Grinholc M, et al. Photoactivated Gallium Porphyrin Reduces *Staphylococcus aureus* Colonization on the Skin and Suppresses Its Ability to Produce Enterotoxin C and TSST-1. *Mol Pharm* [Internet]. 2023 Aug 31 [cited 2023 Oct 3];20(10). Available from: <https://pubmed.ncbi.nlm.nih.gov/37653709/>
30. Zhang H, Li Q, Qi X, Li Y, Ma H, Grinholc M, et al. Iron-blocking antibacterial therapy with cationic heme-mimetic gallium porphyrin photosensitizer for combating antibiotic resistance and enhancing photodynamic antibacterial activity. *Chemical Engineering Journal*. 2023 Jan 1;451:138261.
31. Alsterholm M, Strömbeck L, Ljung A, Karami N, Widjestam J, Gillstedt M, et al. Variation in *Staphylococcus aureus* Colonization in Relation to Disease Severity in Adults with Atopic Dermatitis during a Five-month Follow-up. *Acta Derm Venereol* [Internet]. 2017 [cited 2022 Dec 29];97(7):802–7. Available from: <https://pubmed.ncbi.nlm.nih.gov/28374043/>
32. O'Regan GM, Irvine AD. The role of filaggrin loss-of-function mutations in atopic dermatitis. *Curr Opin Allergy Clin Immunol* [Internet]. 2008 Oct [cited 2022 Dec 29];8(5):406–10. Available from: <https://pubmed.ncbi.nlm.nih.gov/18769192/>
33. Balasubramanian D, Harper L, Shopsin B, Torres VJ. *Staphylococcus aureus* pathogenesis in diverse host environments. *Pathog Dis* [Internet]. 2017 [cited 2023 Oct 4];75(1):5. Available from: <https://pmc/articles/PMC5353994/>
34. Geoghegan JA, Irvine AD, Foster TJ. *Staphylococcus aureus* and Atopic Dermatitis: A Complex and Evolving Relationship. *Trends Microbiol* [Internet]. 2018 Jun 1 [cited 2022 Dec 29];26(6):484–97. Available from: <https://pubmed.ncbi.nlm.nih.gov/29233606/>
35. Alexander H, Paller AS, Traidl-Hoffmann C, Beck LA, De Benedetto A, Dhar S, et al. The role of bacterial skin infections in atopic dermatitis: expert statement and review from the International Eczema Council Skin Infection Group. *British Journal of Dermatology* [Internet]. 2020 Jun 1 [cited 2023 Oct 4];182(6):1331–42. Available from: <https://onlinelibrary.wiley.com/doi/full/10.1111/bjd.18643>
36. Peyrusson F, Varet H, Nguyen TK, Legendre R, Sismeiro O, Coppée JY, et al. Intracellular *Staphylococcus aureus* persists upon antibiotic exposure. *Nat Commun* [Internet]. 2020;11(1). Available from: <http://dx.doi.org/10.1038/s41467-020-15966-7>

37. Jubrail J, Morris P, Bewley MA, Stoneham S, Johnston SA, Foster SJ, et al. Inability to sustain intraphagolysosomal killing of *Staphylococcus aureus* predisposes to bacterial persistence in macrophages. *Cell Microbiol* [Internet]. 2016 Jan 1 [cited 2023 Oct 6];18(1):80–96. Available from: <https://pubmed.ncbi.nlm.nih.gov/26248337/>
38. Rodrigues Lopes I, Alcantara LM, Silva RJ, Josse J, Vega EP, Cabrerizo AM, et al. Microscopy-based phenotypic profiling of infection by *Staphylococcus aureus* clinical isolates reveals intracellular lifestyle as a prevalent feature. *Nature Communications* 2022 13:1 [Internet]. 2022 Nov 22 [cited 2023 Oct 4];13(1):1–18. Available from: <https://www.nature.com/articles/s41467-022-34790-9>
39. Garzoni C, Kelley WL. *Staphylococcus aureus*: new evidence for intracellular persistence. *Trends Microbiol* [Internet]. 2009 Feb [cited 2023 Oct 13];17(2):59–65. Available from: <https://pubmed.ncbi.nlm.nih.gov/19208480/>
40. Miller LG, Diep BA. Colonization, fomites, and virulence: Rethinking the pathogenesis of community-associated methicillin-resistant *Staphylococcus aureus* infection. *Clinical Infectious Diseases* [Internet]. 2008 Mar 1 [cited 2023 Oct 13];46(5):752–60. Available from: <https://dx.doi.org/10.1086/526773>
41. Proctor RA, von Eiff C, Kahl BC, Becker K, McNamara P, Herrmann M, et al. Small colony variants: A pathogenic form of bacteria that facilitates persistent and recurrent infections. Vol. 4, *Nature Reviews Microbiology*. 2006. p. 295–305.
42. Rollin G, Tan X, Tros F, Dupuis M, Nassif X, Charbit A, et al. Intracellular survival of *Staphylococcus aureus* in endothelial cells: A matter of growth or persistence. *Front Microbiol*. 2017 Jul 19;8(JUL):281354.
43. Jensen RL, Arnbjerg J, Birkedal H, Ogilby PR. Singlet oxygen's response to protein dynamics. *J Am Chem Soc*. 2011 May 11;133(18):7166–73.
44. Li X, Liu Z, Liu H, Chen X, Liu Y, Tan H. Photodynamic inactivation of fibroblasts and inhibition of *Staphylococcus epidermidis* adhesion and biofilm formation by toluidine blue O. *Mol Med Rep* [Internet]. 2017 Apr 1 [cited 2023 Nov 10];15(4):1816–22. Available from: <http://www.spandidos-publications.com/10.3892/mmr.2017.6184/abstract>
45. Akilov OE, O'Riordan K, Kosaka S, Hasan T. Photodynamic therapy against intracellular pathogens: Problems and potentials. *Medical Laser Application*. 2006 Nov 15;21(4):251–60.
46. Van Graft M, Boot JH. Photodynamic effects of protoporphyrin on the cellular level—an in vitro approach. *In Vitro Cell Dev Biol Anim* [Internet]. 1996 [cited 2023 Oct 27];32(7):394–8. Available from: <https://pubmed.ncbi.nlm.nih.gov/8856338/>
47. Mohapatra S, Yutao L, Goh SG, Ng C, Luhua Y, Tran NH, et al. Quaternary ammonium compounds of emerging concern: Classification, occurrence, fate, toxicity and antimicrobial resistance. *J Hazard Mater* [Internet]. 2023 Mar 3 [cited 2023 Oct 6];445:130393. Available from: <https://pubmed.ncbi.nlm.nih.gov/39663149/>
48. Salajkova S, Sramek M, Malinak D, Havel F, Musilek K, Benkova M, et al. Highly hydrophilic cationic gold nanorods stabilized by novel quaternary ammonium surfactant with negligible cytotoxicity. *J Biophotonics* [Internet]. 2019 Dec 1 [cited 2023 Oct 6];12(12):e201900024. Available from: <https://onlinelibrary.wiley.com/doi/full/10.1002/jbio.201900024>
49. Bispo M, Santos SB, Melo LDR, Azeredo J, Diji JM van. Targeted Antimicrobial Photodynamic Therapy of Biofilm-Embedded and Intracellular *Staphylococci* with a Phage Endolysin's Cell Binding Domain. *Microbiol Spectr* [Internet]. 2022 Feb 23 [cited 2023 Oct 6];10(1). Available from: <https://pubmed.ncbi.nlm.nih.gov/38865409/>
50. Morales-de-Echegaray A V, Lin L, Sivasubramaniam B, Yermembetova A, Wang Q, Abutaleb NS, et al. Antimicrobial Photodynamic Activity of Gallium-Substituted Haemoglobin on Silver Nanoparticles. *Nanoscale*. 2016;176(1):100–106.
51. Rabinovitch M. Professional and non-professional phagocytes: an introduction. *Trends Cell Biol*. 1995 Mar 1;5(3):85–7.
52. Maisch T, Bosl C, Szeimies RM, Lehn N, Abels C. Photodynamic Effects of Novel XF Porphyrin Derivatives on Prokaryotic and Eukaryotic Cells. *Antimicrob Agents Chemother* [Internet]. 2005 Apr [cited 2023 Nov 13];49(4):1542. Available from: <https://pubmed.ncbi.nlm.nih.gov/1068608/>
53. Berg K, Prydz K, Moan J. Photochemical treatment with the lysosomally localized dye tetra(4-sulfonatophenyl)porphine results in lysosomal release of the dye but not of beta-N-acetyl-D-glucosaminidase activity. *Biochim Biophys Acta* [Internet]. 1993 Nov 28 [cited 2023 Nov 13];1158(3):300–6. Available from: <https://pubmed.ncbi.nlm.nih.gov/8251531/>
54. Akilov OE, Kosaka S, O'Riordan K, Song X, Sherwood M, Flotte TJ, et al. The Role of Photosensitizer Molecular Charge and Structure on the Efficacy of Photodynamic Therapy against *Leishmania* Parasites. *Chem Biol*. 2006 Aug 1;13(8):839–47.
55. Pang YY, Schwartz J, Thoendel M, Ackermann LW, Horswill AR, Nauseef WM. agr-Dependent interactions of *Staphylococcus aureus* USA300 with human polymorphonuclear neutrophils. *J Innate Immun* [Internet]. 2010 Oct [cited 2023 Oct 3];2(6):546–59. Available from: <https://pubmed.ncbi.nlm.nih.gov/20829608/>
56. Wang XW, Wang JJ, Gutowska-Owsiak D, Salimi M, Selvakumar TA, Gwela A, et al. Deficiency of filaggrin regulates endogenous cysteine protease activity, leading to impaired skin barrier function. *Clin Exp Dermatol*. 2017 Aug 1;42(6):622–31.
57. Ogonowska P, Woźniak A, Pierański MK, Wasylew T, Kwiec P, Brasel M, et al. Application and characterization of light-emitting diodes for photodynamic inactivation of bacteria. *Lighting Research and Technology*. 2019;51(4):612–24.
58. Scrace S, O'Neill E, Hammond EM, Pires IM. Use of the xCELLigence system for real-time analysis of changes in cellular motility and adhesion in physiological conditions. *Methods in Molecular Biology* [Internet]. 2013 [cited 2023 Oct 3];1046:295–306. Available from: https://link.springer.com/protocol/10.1007/978-1-62703-538-5_1

6. Summary

Upon illumination with green light in the Q-band, gallium(III)-coordinated porphyrins photogenerated the singlet oxygen with low but detectable levels of superoxide anion production. Acting as a Type II photosensitizer, gallium(III)-coordinated porphyrins continued to exhibit photodynamic properties despite structural modifications. In light-dependent pathway, Ga³⁺MPs exhibited the antimicrobial action reflected in the reduction of *S. aureus* viability, tested in suspension cultures, or staphylococcal biofilms models: *in vitro* and *ex vivo*. By using green light as a light source, gallium(III)-coordinated porphyrins did not cause extensive phototoxicity to human cells, while still maintaining a strong antimicrobial effect. When looking for suitable aPDI conditions for clinical applications, a balance between antimicrobial efficacy and toxicity to human cells should be sought. The combination of green light and Ga³⁺MPs can provide an equilibrium between those two factors.

Despite the minor modification implemented in the structure of Ga³⁺MPIX (vinyl groups) or Ga³⁺CHP (cationic moieties), both gallium compounds were still strongly accumulated through an iron- and heme-dependent acquisition mechanism with recognition by receptors from the Isd system. Interestingly, by blocking the heme efflux pump, we observed the increased toxicity of gallium(III)-coordinated porphyrins in both pathways: light-dependent and light-independent.

In the light-dependent pathway, Ga³⁺CHP effectively reduced virulence factors (SEC, or TSST-1) at the level of gene expression or protein production pool, but most importantly in terms of biological activity. Ga³⁺CHP-mediated aPDI reduced the biological functionality of both SEC and TSST-1 as superantigens. ROS produced in the photodynamic process can cause modifications and oxidations of sensitive amino acid residues of toxins to promote their inactivation.

In this thesis, the efficacy of light-dependent action of Ga³⁺CHP was examined on the infection model of human keratinocytes with *S. aureus*. This was the first study to demonstrate such potential of aPDI in eliminating recurrent staphylococcal infection released from host cells. The aPDI response of the released bacteria did not change and remained as sensitive as the standard suspension culture after treatment. Moreover, bacterial adherence, but not internalization, was significantly reduced after aPDI pretreatment. This indicates that aPDI affected the quality of bacterial adherence to the host. Furthermore, combination of Ga³⁺CHP and green light significantly reduced the GPF signal derived from intracellular *S. aureus*, which may indicate that the number of bacteria was reduced. It should be emphasized that due to the simultaneous colocalization of Ga³⁺CHP and intracellular *S. aureus* in host lysosomes, such aPDI efficiency was achieved. It may be possible that Ga³⁺CHP, which is a heme analog, may be accumulated by intracellular *S. aureus* as part of a Trojan Horse strategy. However, further accumulation studies on intracellular *S. aureus* should be encouraged to confirm this thesis.

Besides, the applied aPDI anti-intracellular conditions was examined against infected and uninfected human keratinocytes. The aPDI treatment showed moderate phototoxicity to both types of keratinocytes. Nevertheless, cells were still able to proliferate until they reached the plateau phase, despite their infection status. To date, this is the first study that consider the additive effects of infection and aPDI on host viability and proliferation rate, measured in real time. Those findings create a broad new field of aPDI applications as a method with anti-intracellular potential. Further research should be conducted with other photosensitizers commonly used in aPDI to find the best therapeutic option with the highest effectiveness against intracellular *S. aureus* with low phototoxicity to human cells.

The findings presented in this thesis lead to the following conclusions:

1. Gallium(III)-coordinated porphyrins, specifically cationic-modified Ga³⁺CHP, are efficient photosensitizers in aPDI against *S. aureus*,
2. Upon green light illumination, Ga³⁺CHP is less phototoxic than Ga³⁺MPIX to keratinocytes,
3. Both, Ga³⁺CHP and Ga³⁺MPIX can be naturally recognized by the existing heme recognition and detoxification system in *S. aureus*
4. Ga³⁺CHP-based aPDI is an effective strategy for reduction the biological activity of virulence factors such as staphylococcal enterotoxin C and toxic shock syndrome toxin-1,
5. Application of aPDI with either Ga³⁺MPIX or Ga³⁺CHP is highly effective against *S. aureus* released from keratinocytes,
6. Application of aPDI with Ga³⁺CHP before infection changes the process of the infection and reduces bacterial adhesion to keratinocytes,
7. Cationic Ga³⁺CHP and *S. aureus* colocalize in the lysosomal structures of keratinocytes, ensuring the accumulation of the compound by the bacterium,
8. The combination of light and accumulated Ga³⁺CHP reduces the number of intracellular *S. aureus* in keratinocytes indicating the potential of Ga³⁺CHP-based aPDI in the eliminating intracellular *S. aureus*,
9. The combination of Ga³⁺CHP and green light did not promote the extensive photo-toxicity towards keratinocytes.

7. Other PhD accomplishment

7.1 Publications not included in the thesis.

- Rapacka-Zdończyk A, Woźniak A, **Michalska K**, Pierański M, Ogonowska P, Grinholc M, Nakonieczna J. Factors Determining the Susceptibility of Bacteria to Antibacterial Photodynamic Inactivation. *Front Med (Lausanne)*. 2021 May 12;8:642609. doi: 10.3389/fmed.2021.642609. PMID: 34055830; PMCID: PMC8149737. IF= 3.9, Q1
- Ogonowska P, **Szymczak K**, Empel J, Urbaś M, Woźniak-Pawlikowska A, Barańska-Rybak W, Świetlik D, Nakonieczna J. Staphylococcus aureus from Atopic Dermatitis Patients: Its Genetic Structure and Susceptibility to Phototreatment. *Microbiol Spectr*. 2023 Jun 15;11(3):e0459822. doi: 10.1128/spectrum.04598-22. Epub 2023 May 4. PMID: 37140374; PMCID: PMC10269521. IF=3.7, Q2
- Pierański MK, Kosiński JG, **Szymczak K**, Sadowski P, Grinholc M. Antimicrobial Photodynamic Inactivation: An Alternative for Group B Streptococcus Vaginal Colonization in a Murine Experimental Model. *Antioxidants (Basel)*. 2023 Apr 1;12(4):847. doi: 10.3390/antiox12040847. PMID: 37107222; PMCID: PMC10135335. IF= 7.0, Q1
- **Szymczak K**#, Woźniak-Pawlikowska A#, Burzyńska N, Król M, Zhang L, Nakonieczna J, Grinholc M, Decrease of ESKAPE virulence with a cationic heme-mimetic gallium porphyrin photosensitizer: the Trojan horse strategy that could help address antimicrobial resistance” (manuscript submitted) # Authors declare equal contribution.

7.2 Conferences

Oral presentations:

- **Szymczak K**, Woźniak-Pawlikowska A, Król M, Zhang L, Nakonieczna J, Grinholc M, Photodynamic inactivation with novel gallium metalloporphyrin – the non-antibiotic method to overcome S. aureus and P. aeruginosa biofilms, The 20th Congress of the European Society of Photobiology (Lyon, Francja, 2023)
- **Szymczak K**, Zhang L, Grinholc M, Nakonieczna J, Green light-activated gallium porphyrin as a tool to decolonize Staphylococcus aureus from atopic skin, 18th International Photodynamic Association World Congress (Tampere, Finland, 2023)

Poster presentations:

- **Michalska K**, Nakonieczna J, Grinholc M, Phototreatment with water-soluble Ga-CHP impacts *Staphylococcus aureus* viability and staphyloxanthin level, PDT Update 2022 (Nancy, France, 2022)
- **Michalska K**, Woźniak A, Grinholc M, Nakonieczna J Antimicrobial potential of water-soluble cationic gallium porphyrin and blue light towards ESKAPE pathogens, 6th ESP PHOTOBIOLOGY SCHOOL (Brixen/Bressanone, Italy, 2022)
- **Michalska K**, Sarna T, Rychłowski M, Krupińska M, Nakonieczna J, Gallium mesoporphyrin IX-mediated photodestruction: a pharmacological Trojan horse strategy to eliminate multidrug-resistant *Staphylococcus aureus*, ASM Microbe 2022 (Washington, USA, 2022)
- **Michalska K**, Nakonieczna J, Targeted photodynamic approach: the case study of Ga³⁺ meso-PPIX and heme transporters, The 19th Congress of the European Society of Photobiology (on-line, Salzburg, Austria, 2020)
- **Michalska K**, Woźniak A, Krupińska M, Moszyńska A, Nakonieczna J, Grinholc M, The impact of photoinactivation with Ga³⁺ meso-PPIX on virulence factors of *Staphylococcus aureus* and *Pseudomonas aeruginosa* (online, Salzburg, Austria, 2020)

7.3 Grants

- Principal investigator, Small Grants UGrants-start No 3.
- Principal investigator, Small Grants UGrants-start No. 1
- PhD student position at NCN Sheng 1 project, no. 2018/30/Q/NZ7/00281

7.4 Trainings

- Analysis of Prokaryotic RNA-Seq data, Gdańsk, Poland,
- Course of Photobiology at a Ph.D. level at the 6th ESP PHOTOBIOLOGY SCHOOL (Brixen/Bressanone, Italy, 2022)
- "Requirements of the new standard PN-EN ISO/IEC 17025:2018-02" Gdańsk, Poland
- Operating autoclaves and sterilizers - Gdańsk, Poland

7.5 Awards

- Award of the Polish Academy of Sciences in Gdańsk for young scientists for work published in 2022 in the field of medicine (2022)

8. Literature

1. O'Neill, Tracking Drug-Resistant Infections Globally: Final Report and Recommendation. The review on Antimicrobial Resistance. (2016)
2. Mulani, M. S., Kamble, E. E., Kumkar, S. N., Tawre, M. S. & Pardesi, K. R. Emerging Strategies to Combat ESKAPE Pathogens in the Era of Antimicrobial Resistance: A Review. *Front Microbiol* 10, 539 (2019).
3. De Oliveira, D. M. P. et al. Antimicrobial Resistance in ESKAPE Pathogens. *Clin Microbiol Rev* 33, (2020).
4. Nakonieczna, J. et al. Photoinactivation of ESKAPE pathogens: Overview of novel therapeutic strategy. *Future Med Chem* 11, 443–461 (2019).
5. Sakoulas, G. & Moellering, R. C. Increasing Antibiotic Resistance among Methicillin-Resistant *Staphylococcus aureus* Strains. *Clinical Infectious Diseases* 46, S360–S367 (2008).
6. Miller, L. G. & Diep, B. A. Colonization, fomites, and virulence: Rethinking the pathogenesis of community-associated methicillin-resistant *Staphylococcus aureus* infection. *Clinical Infectious Diseases* 46, 752–760 (2008).
7. Noskin, G. A. et al. National trends in *Staphylococcus aureus* infection rates: Impact on economic burden and mortality over a 6-year period (1998-2003). *Clinical Infectious Diseases* 45, 1132–1140 (2007).
8. Macía-Rodríguez, C., Alende-Castro, V., Vazquez-Ledo, L., Novo-Veleiro, I. & González-Quintela, A. Skin and soft-tissue infections: Factors associated with mortality and re-admissions. *Enferm Infecc Microbiol Clin* 35, 76–81 (2017).
9. Tong, S. Y. C., Davis, J. S., Eichenberger, E., Holland, T. L. & Fowler, V. G. *Staphylococcus aureus* infections: Epidemiology, pathophysiology, clinical manifestations, and management. *Clin Microbiol Rev* 28, 603–661 (2015).
10. Kobayashi, T. et al. Dysbiosis and *Staphylococcus aureus* Colonization Drives Inflammation in Atopic Dermatitis. *Immunity* 42, 756–766 (2015).
11. Hassoun, A., Linden, P. K. & Friedman, B. Incidence, prevalence, and management of MRSA bacteremia across patient populations—a review of recent developments in MRSA management and treatment. *Crit Care* 21, 211 (2017).
12. Cheung, G. Y. C., Bae, J. S. & Otto, M. Pathogenicity and virulence of *Staphylococcus aureus*. *Virulence* 12, 547 (2021).
13. Dinges, M. M., Orwin, P. M., Schlievert, P. M., Biology, S. & The, O. F. Exotoxins of *Staphylococcus aureus*. *Clin Microbiol Rev* 13, 16–34 (2000).
14. Spaulding, A. R. et al. Staphylococcal and streptococcal superantigen exotoxins. *Clin Microbiol Rev* 26, 422–447 (2013).
15. Harris, T. O. et al. Lack of complete correlation between emetic and T-cell-stimulatory activities of staphylococcal enterotoxins. *Infect Immun* 61, 3175–3183 (1993).
16. Salgado-Pabón, W., Case-Cook, L. C. & Schlievert, P. M. Molecular analysis of staphylococcal superantigens. *Methods in Molecular Biology* 1085, 169–185 (2014).
17. Hall, C. W. & Mah, T. F. Molecular mechanisms of biofilm-based antibiotic resistance and tolerance in pathogenic bacteria. *FEMS Microbiol Rev* 41, 276–301 (2017).
18. Brady, R. A., Leid, J. G., Calhoun, J. H., Costerton, J. W. & Shirtliff, M. E. Osteomyelitis and the role of biofilms in chronic infection. *FEMS Immunol Med Microbiol* 52, 13–22 (2008).
19. Rapacka-zdonczyk, A., Wozniak, A., Nakonieczna, J. & Grinholc, M. Development of Antimicrobial Phototreatment Tolerance: Why the Methodology Matters. *Int J Mol Sci* 22, 1–27 (2021).
20. Ceri, H. et al. The Calgary Biofilm Device: new technology for rapid determination of antibiotic susceptibilities of bacterial biofilms. *J Clin Microbiol* 37, 1771–1776 (1999).
21. Gulías, Ò., McKenzie, G., Bayó, M., Agut, M. & Nonell, S. Effective Photodynamic Inactivation of 26 *Escherichia coli* Strains with Different Antibiotic Susceptibility Profiles: a Planktonic and Biofilm Study. *Antibiotics (Basel)* 9, (2020).

22. Gonzalez, T., Biagini Myers, J. M., Herr, A. B. & Khurana Hershey, G. K. Staphylococcal Biofilms in Atopic Dermatitis. *Curr Allergy Asthma Rep* 17, 81 (2017).
23. Paharik, A. E. & Horswill, A. R. The Staphylococcal Biofilm: Adhesins, Regulation, and Host Response. *Microbiol Spectr* 4, (2016).
24. Scherr, T. D., Heim, C. E., Morrison, J. M. & Kielian, T. Hiding in Plain Sight: Interplay between Staphylococcal Biofilms and Host Immunity. *Front Immunol* 5, (2014).
25. Den Reijer, P. M. et al. Detection of Alpha-Toxin and Other Virulence Factors in Biofilms of *Staphylococcus aureus* on Polystyrene and a Human Epidermal Model. *PLoS One* 11, (2016).
26. Son, E. D. et al. *Staphylococcus aureus* inhibits terminal differentiation of normal human keratinocytes by stimulating interleukin-6 secretion. *J Dermatol Sci* 74, 64–71 (2014).
27. Miller, L. G. et al. *Staphylococcus aureus* skin infection recurrences among household members: an examination of host, behavioral, and pathogen-level predictors. *Clin Infect Dis* 60, 753–763 (2015).
28. Atalla, H., Gyles, C. & Mallard, B. *Staphylococcus aureus* small colony variants (SCVs) and their role in disease. *Anim Health Res Rev* 12, 33–45 (2011).
29. Proctor, R. A., Van Langevelde, P., Kristjansson, M., Maslow, J. N. & Arbeit, R. D. Persistent and relapsing infections associated with small-colony variants of *staphylococcus aureus*. *Clinical Infectious Diseases* 20, 95–102 (1995).
30. Conlon, B. P. *Staphylococcus aureus* chronic and relapsing infections: Evidence of a role for persister cells. *BioEssays* 36, 991–996 (2014).
31. von Eiff, C., Peters, G. & Becker, K. The small colony variant (SCV) concept—the role of staphylococcal SCVs in persistent infections. *Injury* 37, S26–S33 (2006).
32. Proctor, R. A. et al. Small colony variants: A pathogenic form of bacteria that facilitates persistent and recurrent infections. *Nature Reviews Microbiology* vol. 4 295–305 Preprint at <https://doi.org/10.1038/nrmicro1384> (2006).
33. Sendi, P. & Proctor, R. A. *Staphylococcus aureus* as an intracellular pathogen: the role of small colony variants. *Trends Microbiol* 17, 54–58 (2009).
34. Vulin, C., Leimer, N., Huemer, M., Ackermann, M. & Zinkernagel, A. S. Prolonged bacterial lag time results in small colony variants that represent a sub-population of persisters. *Nature Communications* 2018 9:1 9, 1–8 (2018).
35. Garzoni, C. & Kelley, W. L. *Staphylococcus aureus*: new evidence for intracellular persistence. *Trends Microbiol* 17, 59–65 (2009).
36. Fraunholz, M. & Sinha, B. Intracellular *staphylococcus aureus*: Live-in and let die. *Front Cell Infect Microbiol* 2, (2012).
37. Hudson, M. C., Ramp, W. K., Nicholson, N. C., Williams, A. S. & Nousiainen, M. T. Internalization of *Staphylococcus aureus* by cultured osteoblasts. *Microb Pathog* 19, 409–19 (1995).
38. Hinman, K. D. et al. Bi-fluorescent *Staphylococcus aureus* infection enables single-cell analysis of intracellular killing in vivo. *Front Immunol* 14, (2023).
39. Reilly, S. S., Hudson, M. C., Kellam, J. F. & Ramp, W. K. In vivo internalization of *Staphylococcus aureus* by embryonic chick osteoblasts. *Bone* 26, 63–70 (2000).
40. Strobel, M. et al. Post-invasion events after infection with *Staphylococcus aureus* are strongly dependent on both the host cell type and the infecting *S. aureus* strain. *Clinical Microbiology and Infection* 22, 799–809 (2016).
41. Jang, K. O., Lee, Y. W., Kim, H. & Chung, D. K. Complement Inactivation Strategy of *Staphylococcus aureus* Using Decay-Accelerating Factor and the Response of Infected HaCaT Cells. *Int J Mol Sci* 22, (2021).
42. Al Kindi, A. et al. *Staphylococcus aureus* internalized by skin keratinocytes evade antibiotic killing. *Front Microbiol* 10, 481150 (2019).
43. Tuscherr, L., Löffler, B. & Proctor, R. A. Persistence of *Staphylococcus aureus*: Multiple Metabolic Pathways Impact the Expression of Virulence Factors in Small-Colony Variants (SCVs). *Frontiers in Microbiology* vol. 11 Preprint at <https://doi.org/10.3389/fmicb.2020.01028> (2020).

44. Peyrusson, F. et al. Intracellular *Staphylococcus aureus* persists upon antibiotic exposure. *Nat Commun* 11, (2020).
45. Rollin, G. et al. Intracellular survival of *Staphylococcus aureus* in endothelial cells: A matter of growth or persistence. *Front Microbiol* 8, 281354 (2017).
46. Fraunholz, M. & Sinha, B. Intracellular *Staphylococcus aureus*: live-in and let die. *Frontiers in cellular and infection microbiology* vol. 2 43 Preprint at <https://doi.org/10.3389/fcimb.2012.00043> (2012).
47. Schröder, A., Kland, R., Peschel, A., Von Eiff, C. & Aepfelbacher, M. Live cell imaging of phagosome maturation in *Staphylococcus aureus* infected human endothelial cells: Small colony variants are able to survive in lysosomes. *Med Microbiol Immunol* 195, 185–194 (2006).
48. Foster, T. J., Geoghegan, J. A., Ganesh, V. K. & Höök, M. Adhesion, invasion and evasion: the many functions of the surface proteins of *Staphylococcus aureus*. *Nature Reviews Microbiology* 2013 12:1 12, 49–62 (2013).
49. Sayedyahosseini, S. et al. *Staphylococcus aureus* keratinocyte invasion is mediated by integrin-linked kinase and Rac1. *FASEB Journal* 29, 711–723 (2015).
50. Garzoni, C. et al. A global view of *Staphylococcus aureus* whole genome expression upon internalization in human epithelial cells. *BMC Genomics* 8, 1–14 (2007).
51. Löffler, B., Tuchscher, L., Niemann, S. & Peters, G. *Staphylococcus aureus* persistence in non-professional phagocytes. *Int J Med Microbiol* 304, 170–176 (2014).
52. Hachani, A. et al. A high-throughput cytotoxicity screening platform reveals agr-independent mutations in bacteraemia-associated *Staphylococcus aureus* that promote intracellular persistence. *Elife* 12, (2023).
53. Rodrigues Lopes, I. et al. Microscopy-based phenotypic profiling of infection by *Staphylococcus aureus* clinical isolates reveals intracellular lifestyle as a prevalent feature. *Nature Communications* 2022 13:1 13, 1–18 (2022).
54. Lee, S. O. et al. Dysfunctional accessory gene regulator (*agr*) as a prognostic factor in invasive *Staphylococcus aureus* infection: a systematic review and meta-analysis. *Scientific Reports* 2020 10:1 10, 1–14 (2020).
55. Jarry, T. M., Memmi, G. & Cheung, A. L. The expression of alpha-haemolysin is required for *Staphylococcus aureus* phagosomal escape after internalization in CFT-1 cells. *Cell Microbiol* 10, 1801–1814 (2008).
56. Grosz, M. et al. Cytoplasmic replication of *Staphylococcus aureus* upon phagosomal escape triggered by phenol-soluble modulins. *Cell Microbiol* 16, 451–465 (2014).
57. Chi, C. Y. et al. Pantone-Valentine Leukocidin Facilitates the Escape of *Staphylococcus aureus* From Human Keratinocyte Endosomes and Induces Apoptosis. *J Infect Dis* 209, 224–235 (2014).
58. Howden, B. P. et al. *Staphylococcus aureus* host interactions and adaptation. *Nature Reviews Microbiology* 2023 21:6 21, 380–395 (2023).
59. Zelmer, A. R., Nelson, R., Richter, K. & Atkins, G. J. Can intracellular *Staphylococcus aureus* in osteomyelitis be treated using current antibiotics? A systematic review and narrative synthesis. *Bone Res* 10, (2022).
60. Broekgaarden, M., Weijer, R., van Gulik, T. M., Hamblin, M. R. & Heger, M. Tumor cell survival pathways activated by photodynamic therapy: a molecular basis for pharmacological inhibition strategies. *Cancer Metastasis Rev* 34, 643–690 (2015).
61. Hamblin, M. R. Antimicrobial photodynamic inactivation: a bright new technique to kill resistant microbes. *Curr Opin Microbiol* 33, 67–73 (2017).
62. Zhang, Y. et al. Potentiation of antimicrobial photodynamic inactivation mediated by a cationic fullerene by added iodide: in vitro and in vivo studies. <https://doi.org/10.2217/nmm.14.131> 10, 603–614 (2015).
63. Grinholc, M., Rapacka-Zdonczyk, A., Rybak, B., Szabados, F. & Bielawski, K. P. Multiresistant strains are as susceptible to photodynamic inactivation as their naïve counterparts: Protoporphyrin IX-mediated photoinactivation reveals differences between methicillin-resistant and methicillin-sensitive *Staphylococcus aureus* strains. *Photomed Laser Surg* 32, 121–129 (2014).
64. Tubby, S., Wilson, M. & Nair, S. P. Inactivation of staphylococcal virulence factors using a light-activated antimicrobial agent. *BMC Microbiol* 9, 1–10 (2009).

65. Bartolomeu, M. et al. Effect of photodynamic therapy on the virulence factors of *Staphylococcus aureus*. *Front Microbiol* 7, (2016).
66. Fila, G., Kawiak, A. & Grinholc, M. S. Blue light treatment of *Pseudomonas aeruginosa*: Strong bactericidal activity, synergism with antibiotics and inactivation of virulence factors. *Virulence* 8, 938–958 (2017).
67. Wozniak, A. & Grinholc, M. Combined antimicrobial activity of photodynamic inactivation and antimicrobials-state of the art. *Frontiers in Microbiology* vol. 9 Preprint at <https://doi.org/10.3389/fmicb.2018.00930> (2018).
68. Wozniak, A., Rapacka-Zdonczyk, A., Mutters, N. T. & Grinholc, M. Antimicrobials are a photodynamic inactivation adjuvant for the eradication of extensively drug-resistant *Acinetobacter baumannii*. *Front Microbiol* 10, (2019).
69. Hamblin, M. R., Abrahamse, H., Hospital, M. G. & Africa, S. Can light-based approaches overcome antimicrobial resistance? *Drug Dev Res.* 80, 48–67 (2019).
70. Rapacka-Zdonczyk, A. et al. Development of *Staphylococcus aureus* tolerance to antimicrobial photodynamic inactivation and antimicrobial blue light upon sub-lethal treatment. *Sci Rep* 9, 1–18 (2019).
71. Pieranski, M., Sitkiewicz, I. & Grinholc, M. Increased photoinactivation stress tolerance of *Streptococcus agalactiae* upon consecutive sublethal phototreatments. *Free Radic Biol Med* 160, 657–669 (2020).
72. Cieplik, F. et al. Antimicrobial photodynamic therapy—what we know and what we don't. *Crit Rev Microbiol* 44, 571–589 (2018).
73. Cieplik, F., Tabenski, L., Buchalla, W. & Maisch, T. Antimicrobial photodynamic therapy for inactivation of biofilms formed by oral key pathogens. *Front Microbiol* 5, (2014).
74. Ash, C., Dubec, M., Donne, K. & Bashford, T. Effect of wavelength and beam width on penetration in light-tissue interaction using computational methods. *Lasers Med Sci* 32, 1909–1918 (2017).
75. Ash, C., Dubec, M., Donne, K. & Bashford, T. Effect of wavelength and beam width on penetration in light-tissue interaction using computational methods. *Lasers Med Sci* 32, 1909–1918 (2017).
76. Lawrence, K. P. et al. The UV/Visible Radiation Boundary Region (385–405 nm) Damages Skin Cells and Induces “dark” Cyclobutane Pyrimidine Dimers in Human Skin in vivo. *Scientific Reports* 2018 8:1 8, 1–12 (2018).
77. Osiecka, B. J., Nockowski, P. & Szepietowski, J. C. Treatment of Actinic Keratosis with Photodynamic Therapy Using Red or Green Light: A Comparative Study. *Acta Derm Venereol* 98, 689–693 (2018).
78. Fritsch, C. et al. Green light is effective and less painful than red light in photodynamic therapy of facial solar keratoses. *Photodermatol Photoimmunol Photomed* 13, 181–185 (1997).
79. Ibrahim, M. M. et al. Long-lasting antinociceptive effects of green light in acute and chronic pain in rats. *Pain* 158, 347–360 (2017).
80. Martin, L. F. et al. Green Light Exposure Elicits Anti-inflammation, Endogenous Opioid Release and Dampens Synaptic Potentiation to Relieve Post-surgical Pain. *J Pain* 24, 509–529 (2023).
81. Tim, M. *Journal of Photochemistry and Photobiology B: Biology Strategies to optimize photosensitizers for photodynamic inactivation of bacteria.* *J Photochem Photobiol B* (2015) doi:10.1016/j.jphotobiol.2015.05.010.
82. Maisch, T. A New Strategy to Destroy Antibiotic Resistant Microorganisms: Antimicrobial Photodynamic Treatment. *Mini-Reviews in Medicinal Chemistry* 9, 974–983 (2012).
83. Minnock, A. et al. Mechanism of Uptake of a Cationic Water-Soluble Pyridinium Zinc Phthalocyanine across the Outer Membrane of *Escherichia coli*. *Antimicrob Agents Chemother.* 44, 522–527 (2000).
84. Gsponer, N. S., Spesia, M. B. & Durantini, E. N. Effects of divalent cations, EDTA and chitosan on the uptake and photoinactivation of *Escherichia coli* mediated by cationic and anionic porphyrins. *Photodiagnosis Photodyn Ther* 12, 67–75 (2015).

85. George, S., Hamblin, R. & Kishen, A. Uptake pathways of anionic and cationic photosensitizers into bacteria. *Photochemical & Photobiological Sciences* 8, 788–795 (2009).
86. Magadla, A., Openda, Y. I. & Nyokong, T. The implications of ortho-, meta- and para-directors on the in-vitro photodynamic antimicrobial chemotherapy activity of cationic pyridyl-dihydrothiazole phthalocyanines. *Photodiagnosis Photodyn Ther* 39, 103029 (2022).
87. Almeida, A., Cunha, A., Faustino, M. A. F., Neves, M. G. P. M. S. & Tome, A. C. Porphyrins as Antimicrobial Photosensitizing Agents. (2011).
88. Akilov, O. E., O’Riordan, K., Kosaka, S. & Hasan, T. Photodynamic therapy against intracellular pathogens: Problems and potentials. *Medical Laser Application* 21, 251–260 (2006).
89. Van Graft, M. & Boot, J. H. Photodynamic effects of protoporphyrin on the cellular level-an in vitro approach. *In Vitro Cell Dev Biol Anim* 32, 394–398 (1996).
90. Akilov, O. E. et al. The Role of Photosensitizer Molecular Charge and Structure on the Efficacy of Photodynamic Therapy against Leishmania Parasites. *Chem Biol* 13, 839–847 (2006).
91. Choby, J. E. & Skaar, E. P. Heme Synthesis and Acquisition in Bacterial Pathogens. *J Mol Biol* (2016) doi:10.1016/j.jmb.2016.03.01.
92. Donegan, R. K., Moore, C. M., Hanna, D. A. & Reddi, A. R. Handling heme: The mechanisms underlying the movement of heme within and between cells. *Free Radic Biol Med* 133, 88 (2019).
93. Shirasu, N., Nam, S. O. & Kuroki, M. Tumor-targeted photodynamic therapy. *Anticancer Res* 33, 2823–2832 (2013).
94. Drury, S. L. et al. Simultaneous Exposure to Intracellular and Extracellular Photosensitizers for the Treatment of Staphylococcus aureus Infections. *Antimicrob Agents Chemother* 65, e00919-21 (2022).
95. Shirasu, N., Nam, S. O. & Kuroki, M. Tumor-targeted photodynamic therapy. *Anticancer Res* 33, 2823–2832 (2013).
96. Stojiljkovic, I., Kumar, V. & Srinivasan, N. Non-iron metalloporphyrins: Potent antibacterial compounds that exploit haem/Hb uptake systems of pathogenic bacteria. *Mol Microbiol* 31, 429–442 (1999).
97. Morales-de-echegaray, A. V. et al. Rapid Uptake and Photodynamic Inactivation of Staphylococci by Ga(III)-Protoporphyrin IX. *ACS Infect Dis* 4, 1564–1573 (2018).
98. Zhang, H. et al. Iron-blocking antibacterial therapy with cationic heme-mimetic gallium porphyrin photosensitizer for combating antibiotic resistance and enhancing photodynamic antibacterial activity. *Chemical Engineering Journal* 451, 138261 (2023).
99. Crichton, R. Inorganic Biochemistry of Iron Metabolism. *Inorganic Biochemistry of Iron Metabolism* (2001) doi:10.1002/0470845791.
100. Holt, E., Bullen, by J., Griffith New York, E. & Wiley, J. Iron and Infection. *Molecular, Physiological and Clinical Aspects. Yale J Biol Med* 61, 560 (1988).
101. Haley, K. P. & Skaar, E. P. A battle for iron: host sequestration and Staphylococcus aureus acquisition. *Microbes Infect.* 14, 217–227 (2012).
102. Mazmanian, S. K. et al. Passage of heme-iron across the envelope of Staphylococcus aureus. *Science* (1979) 299, 906–909 (2003).
103. Moriwaki, Y. et al. Molecular basis of recognition of antibacterial porphyrins by heme-transporter IsdH-NEAT3 of Staphylococcus aureus. *Biochemistry* 50, 7311–7320 (2011).
104. Hammer, N. D. et al. Two heme-dependent terminal oxidases power Staphylococcus aureus organ-specific colonization of the vertebrate host. *mBio* 4, 1–9 (2013).
105. Bériault, R. et al. The overexpression of NADPH-producing enzymes counters the oxidative stress evoked by gallium, an iron mimetic. *BioMetals* 20, 165–176 (2007).
106. Kelson, A. B., Carnevali, M. & Truong-le, V. Gallium-based anti-infectives : targeting microbial iron-uptake mechanisms. *Curr Opin Pharmacol* 13, 707–716 (2013).
107. Hijazi, S., Visca, P. & Frangipani, E. Gallium-Protoporphyrin IX Inhibits Pseudomonas aeruginosa Growth by Targeting Cytochromes. *Front Cell Infect Microbiol* 7, 1–15 (2017).

108. Richter, K. et al. Mind “De GaPP”: in vitro efficacy of deferiprone and gallium-protoporphyrin against. *Int Forum Allergy Rhinol* 1–7 (2016) doi:10.1002/alr.21735.
109. Arivett, B. A. et al. Antimicrobial Activity of Gallium Protoporphyrin IX against *Acinetobacter baumannii* Strains Displaying Different Antibiotic Resistance Phenotypes. *59*, 7657–7665 (2015).
110. Kaneko, Y., Thoendel, M., Olakanmi, O., Britigan, B. E. & Singh, P. K. The transition metal gallium disrupts *Pseudomonas aeruginosa* iron metabolism and has antimicrobial and antibiofilm activity. *Journal of Clinical Investigation* 117, 877–888 (2007).
111. Goss, C. H. et al. Gallium disrupts bacterial iron metabolism and has therapeutic effects in mice and humans with lung infections. *Sci Transl Med.* 10, (2019).
112. Hijazi, S. et al. Antimicrobial activity of gallium compounds on ESKAPE pathogens. *Front Cell Infect Microbiol* 8, 1–11 (2018).
113. Bozja, J., Yi, K., Shafer, W. M. & Stojiljkovic, I. Porphyrin-based compounds exert antibacterial action against the sexually transmitted pathogens *Neisseria gonorrhoeae* and *Haemophilus ducreyi*. *Int J Antimicrob Agents* 24, 578–584 (2004).
114. Anzaldi, L. L. & Skaar, E. P. Overcoming the heme paradox: Heme toxicity and tolerance in bacterial pathogens. *Infect Immun* 78, 4977–4989 (2010).
115. Stauff, D. L. et al. *Staphylococcus aureus* HrtA Is an ATPase required for protection against heme toxicity and prevention of a transcriptional heme stress response. *J Bacteriol* 190, 3588–3596 (2008).
116. Stauff, D. L., Torres, V. J. & Skaar, E. P. Signaling and DNA-binding activities of the *Staphylococcus aureus* HssR-HssS two-component system required for heme sensing. *Journal of Biological Chemistry* 282, 26111–26121 (2007).
117. Wakeman, C. A., Stauff, D. L., Zhang, Y. & Skaar, E. P. Differential activation of *Staphylococcus aureus* heme detoxification machinery by heme analogues. *J Bacteriol* 196, 1335–1342 (2014).
118. Hommes, J. W. & Surewaard, B. G. J. Intracellular Habitation of *Staphylococcus aureus*: Molecular Mechanisms and Prospects for Antimicrobial Therapy. *Biomedicines* 10, (2022).
119. Omolo, C. A. et al. Liposomes with pH responsive ‘on and off’ switches for targeted and intracellular delivery of antibiotics. *J Liposome Res* 31, 45–63 (2021).
120. Maji, R. et al. PH-Responsive Lipid-Dendrimer Hybrid Nanoparticles: An Approach to Target and Eliminate Intracellular Pathogens. *Mol Pharm* 16, 4594–4609 (2019).
121. Lehar, S. M. et al. Novel antibody–antibiotic conjugate eliminates intracellular *S. aureus*. *Nature* 2015 527:7578 527, 323–328 (2015).
122. Röhrig, C. et al. Targeting Hidden Pathogens: Cell-Penetrating Eradicate Intracellular Drug-Resistant *Staphylococcus aureus*. *mBio* 11, (2020).
123. Kim, Y. J. et al. Prospective, comparative clinical pilot study of cold atmospheric plasma device in the treatment of atopic dermatitis. *Scientific Reports* 2021 11:1 11, 1–8 (2021).
124. Guryanova, S. V. & Khaitov, R. M. Strategies for Using Muramyl Peptides - Modulators of Innate Immunity of Bacterial Origin - in Medicine. *Front Immunol* 12, 607178 (2021).
125. Bispo, M., Santos, S. B., Melo, L. D. R., Azeredo, J. & Dijn, J. M. van. Targeted Antimicrobial Photodynamic Therapy of Biofilm-Embedded and Intracellular *Staphylococci* with a Phage Endolysin’s Cell Binding Domain. *Microbiol Spectr* 10, (2022).
126. Morales-de-Echegaray, Ana V. Lina, L., Sivasubramaniama, B., Yermembetovaa, A., Wanga, O. & Wei, A. Antimicrobial Photodynamic Activity of Gallium-Substituted Haemoglobin on Silver Nanoparticles. *Nanoscale* 176, 100–106 (2016).
127. Nakonieczna, J. et al. Photoinactivation of *Staphylococcus aureus* using protoporphyrin IX: the role of haem-regulated transporter HrtA. *Appl Microbiol Biotechnol* 100, 1393–1405 (2016).
128. Piksa, M. et al. The role of the light source in antimicrobial photodynamic therapy. *Chem. Soc. Rev* 52, 1697 (2023).
129. Kim, J., Eui Kim, B., M Leung, D. Y. & Leung, D. Y. Pathophysiology of atopic dermatitis: Clinical implications. *Allergy Asthma Proc* 40, 84–92 (2019).

130. O'Regan, G. M. & Irvine, A. D. The role of filaggrin loss-of-function mutations in atopic dermatitis. *Curr Opin Allergy Clin Immunol* 8, 406–410 (2008).
131. Fyhrquist, N. et al. Microbe-host interplay in atopic dermatitis and psoriasis. *Nature Communications* 2019 10:1 10, 1–15 (2019).
132. Geoghegan, J. A., Irvine, A. D. & Foster, T. J. *Staphylococcus aureus* and Atopic Dermatitis: A Complex and Evolving Relationship. *Trends Microbiol* 26, 484–497 (2018).
133. Ogonowska, P. et al. *Staphylococcus aureus* from Atopic Dermatitis Patients: Its Genetic Structure and Susceptibility to Phototreatment. *Microbiol Spectr* 11, (2023).
134. Fleischer, B. & Schrezenmeier, H. T cell stimulation by staphylococcal enterotoxins: Clonally variable response and requirement for major histocompatibility complex class II molecules on accessory or target cells. *Journal of Experimental Medicine* 167, 1697–1707 (1988).
135. Tuchscher, L. et al. Clinical *S. aureus* isolates vary in their virulence to promote adaptation to the host. *Toxins (Basel)* 11, (2019).

9. Attachments

9.1 Supplementary Materials from Publication no. 1

Supplementary Materials to Gallium mesoporphyrin IX mediated photodestruction: a pharmacological Trojan horse strategy to eliminate multidrug-resistant *Staphylococcus aureus*

Klaudia Michalska K, Michał Rychłowski², Martyna Krupińska¹, Grzegorz Szewczyk³, Tadeusz Sarna³, Joanna Nakoneczna¹

| | |
|--|-----------|
| Bacterial strains characterization | 2 |
| Chemicals used in the study..... | 3 |
| Gallium MPs delayed staphylococcal growth light-independently..... | 4 |
| ROS detection and Quenchers in Ga³⁺MPIX phototreatment | 5 |
| Phototreatment of <i>S. aureus</i> with Ga³⁺MPIX or Ga³⁺PPIX reduced bacterial viability after additional wash-step | 6 |
| Ga³⁺MPIX-mediated photoinactivation of SCVs | 7 |
| Impairment in the HrtA detoxification efflux pump promotes dark toxicity of Ga³⁺MPIX..... | 8 |
| Ga³⁺MPIX accumulation under confocal microscopic image..... | 9 |
| Ga³⁺MPIX does not promote extensive and prolonged cytotoxicity or phototoxicity against human keratinocytes..... | 12 |

Bacterial strains characterization

Table S1. Drug resistance of *S. aureus* 1814/06 and 4046/13 MDR strains used in this study.

| Antibiotic | <i>S. aureus</i> 1814/06 | <i>S. aureus</i> 4046/13 |
|------------|--------------------------|--------------------------|
| <i>FOX</i> | R | R |
| <i>ERY</i> | R | R |
| <i>CLI</i> | R | S |
| <i>QDA</i> | S | S |
| <i>MUP</i> | S | S |
| <i>SXT</i> | S | R |
| <i>VAN</i> | S | S |
| <i>TEI</i> | S | S |
| <i>TET</i> | R | R |
| <i>DK</i> | R | R |
| <i>TGC</i> | S | S |
| <i>MIN</i> | R | R |
| <i>CIP</i> | S | R |
| <i>GEN</i> | R | R |
| <i>FA</i> | S | S |
| <i>RIF</i> | S | S |
| <i>TLV</i> | S | S |
| <i>DAP</i> | S | S |

Legend: *R*- Resistance *S*- Susceptible; *FOX*- fosfomycin, *ERY*-erythromycin, *CLI*- clindamycin , *QDA*- quinupristin-dalfopristin, *MUP*-mupirocin , *SXT*- trimethoprim-sulfamethoxazole, *VAN*- vancomycin, *TEI*- teicoplanin; *TET*- tetracycline; *DK*-Dicloxacillin ;*TGC*- tigecycline; *MIN*- minocycline; *CIP*- ciprofloxacin; *GEN*- gentamycin; *FA*- fusidic acid; *RIF*- rifampicin; *TLV*- telavancin , *DAP*- daptomycin

Chemicals used in the study

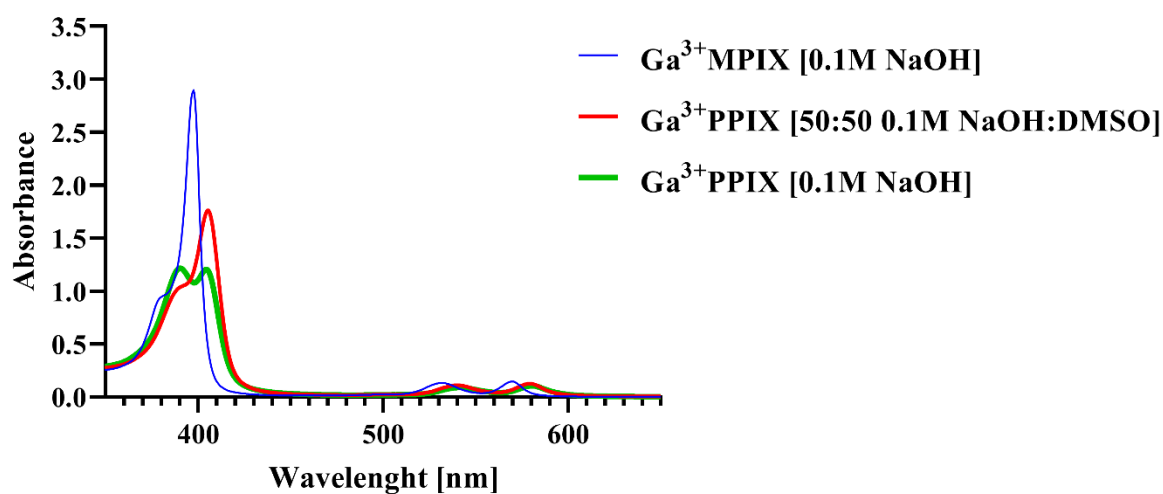
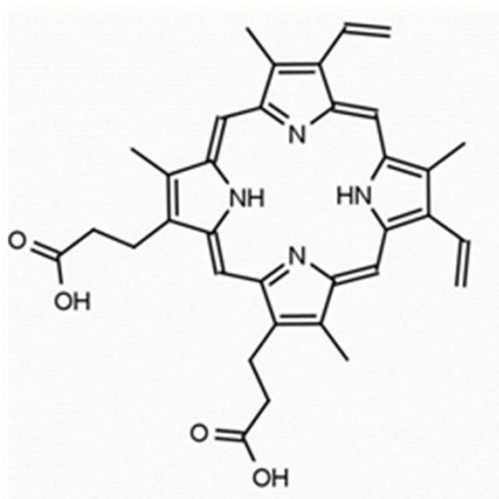


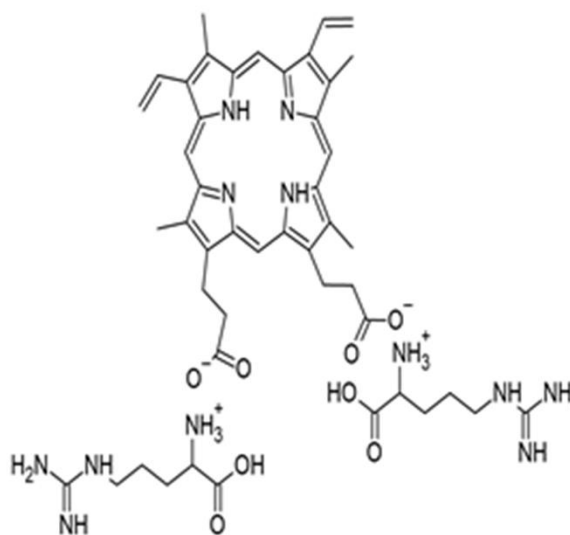
Figure S1. Absorbance spectra of Ga³⁺MPIX or Ga³⁺PPIX in different solvents. Absorbance spectra of 10 μ M stock of Ga³⁺MPIX or Ga³⁺PPIX initially diluted in different type of solvents (0.1 M NaOH or 0.1 M NaOH:DMSO) were dissolved in PBS buffer. Stock solution (1 mM) Ga³⁺MPIX in 0.1 M NaOH (blue line) was dissolved in PBS to a working concentration of 10 μ M. stock solution (1mM) Ga³⁺PPIX in an organic solution 50:50 (v: v) 0.1M NaOH: DMSO (red line) or in an aqueous solvent of 0.1M NaOH (green line) were dissolved in PBS to a working solution of 10 μ M. Each spectrum recorded is the mean of three independent replicates.

A)



PPIX
Formula: C₃₄H₃₄N₄O₄
Mass: 562.658 g/mol

B)



PPIXArg₂
Formula: C₄₆H₆₂N₁₄O₈
Mass: 911.061 g/mol

Figure S2. Molecular characteristic of compounds used in this study. A) Protoporphyrin IX (PPIX) B) Protoporphyrin IX diarginate (PPArg₂).

Gallium MPs delayed staphylococcal growth light-independently

Table S2. Staphylococcal growth under exposure to porphyrin compounds, calculated in the reference to the Fig 3.

| Treatment | Parameters of <i>S. aureus</i> growth | | | | |
|----------------------------|---------------------------------------|---------------|---|--|--|
| | μ_{max} [OD ₆₀₀ /h] | Td [hours] | A _{max} [OD _{600max}] | Time of obtained stationary phase [min] | <i>S. aureus</i> growth at the end of exponential phase [%] |
| Ga³⁺MPIX | 0.15 | 4.65 | 0.621 | 480 | <u>77.43 ± 0.67 ***</u> |
| Ga³⁺PPIX | 0.126 | 5.5 | 0.52 | 450 | <u>67.6 ± 0.8 ***</u> |
| PPIX | 0.282 | 2.45 | 0.75 | 390 | 101.9 ± 1.08 |
| PPIXArg₂ | 0.282 | 2.45 | 0.76 | 390 | 104.5 ± 1.2 |
| Untreated | 0.354 | 1.95 | 0.77 | 390 | 100 |

Legend: μ_{max} - maximum specific growth rate during exponential phase of bacterial growth; Td- Time of duplication, also known as generation time; A_{max}- maximal absorbance value with maximal bacterial density; Time of the obtained stationary phase - defined as the point of curve flattening; *S. aureus* growth at the end of exponential phase [%] at 240 min as the inflection point of the exponential growth curve calculated in the reference to control- untreated cells (100%). Significance at the respective p-values is marked with asterisks [***p < 0.001] with respect to untreated *S. aureus* 25923 cells.

ROS detection and Quenchers in Ga³⁺MPIX phototreatment

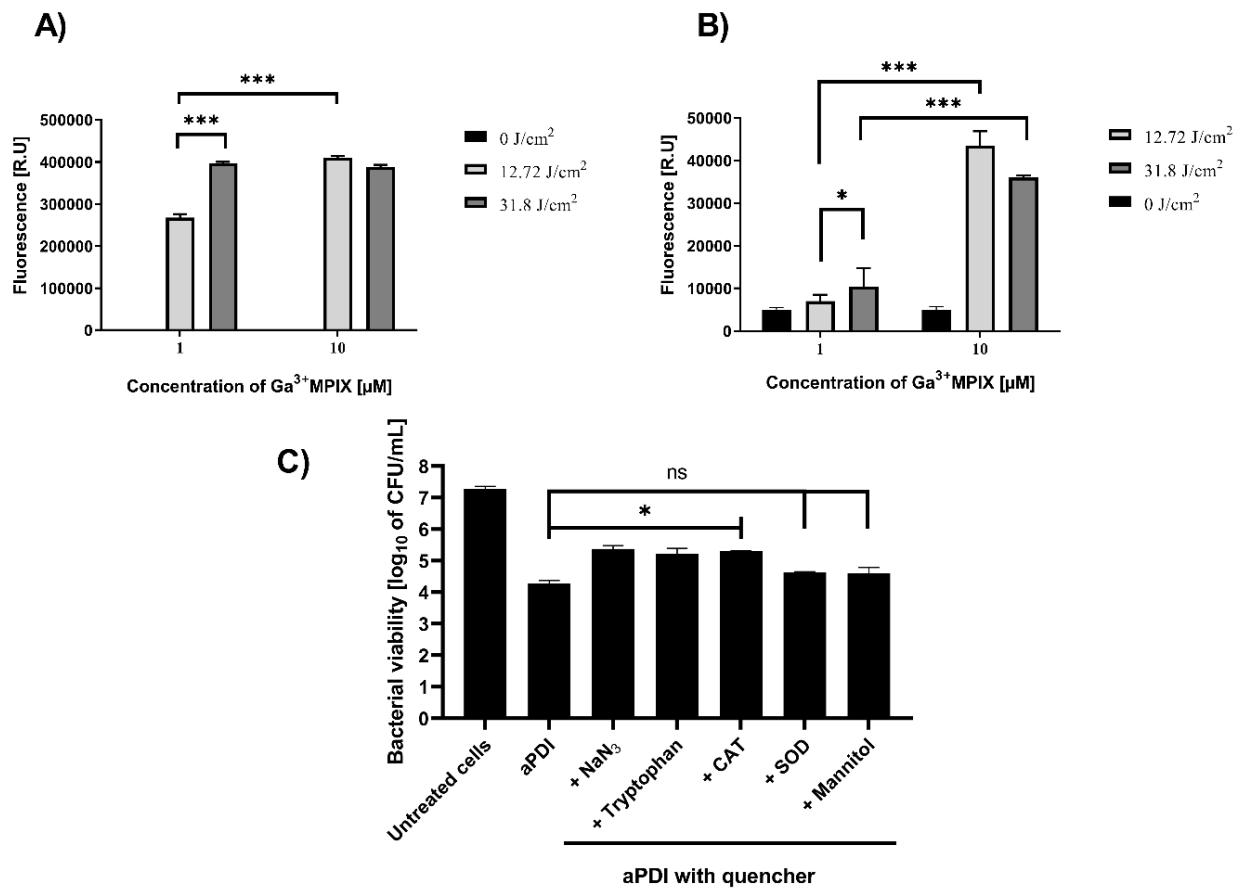


Figure S3. ROS detection and quenching in Ga³⁺MPIX-mediated phototreatment. Cell-free suspensions of Ga³⁺MPIX were incubated with ROS-detecting fluorescent probes: hydroxyl radical – HPF (3'-(p-hydroxyphenyl) Sigma–Aldrich, USA) (A) or singlet oxygen – Singlet Oxygen Sensor Green reagent (SOSG, Thermo Fisher Scientific, USA) (B) upon irradiation with LED light as indicated in the legend. Ga³⁺MPIX was dissolved in PBS buffer, and then each fluorescent probe was added in darkness to a desired concentration of 5 μ M. The fluorescence signal for both probes was detected immediately after green light irradiation at 12.72 J/cm² and 31.8 J/cm² doses, measured on an EnVision Multilabel Plate Reader at excitation/emission of 488/525 nm for SOSG and 490/515 nm for HPF. The values are the means of three separate experiments. (C) *S. aureus* 25923 (~10⁷ CFU ml⁻¹) was incubated with 10 μ M of Ga³⁺MPIX exposed to LED-light at a dose of 25.44 J cm⁻² (referred to as aPDI). A type II quencher (0.1 mM sodium azide, NaN₃), type I quencher (10 mM Mannitol, 1.35 units of superoxide dismutase - SOD, and 10 units of catalase - CAT), and a mixed type I/II quencher (0.1 mM tryptophan) were, respectively, pre-incubated with the mixture of PS and bacterial suspensions for 10 min prior to illumination. The experiment was conducted in three independent biological repetitions. Significance at the respective p values is marked with asterisks [* p < 0.05; *** p < 0.001].

Phototreatment of *S. aureus* with Ga³⁺MPIX or Ga³⁺PPIX reduced bacterial viability after additional wash-step

Table S3. Phototreatment of *S. aureus* strains with Ga³⁺PPIX or Ga³⁺MPIX with green LED light with wash-step.

| Strain | Mean reduction of survival (log ₁₀ CFU/mL) ¹ ± SD | | | | |
|----------------|---|-------------|------------------------|--------------|-------------|
| | Ga ³⁺ MPIX | | Ga ³⁺ PPIX | | Light only |
| | Light (+) | Light (-) | Light (+) | Light (-) | |
| 25923 | <u>5.26 ± 0.83****</u> | 0.38 ± 0.54 | 2.25 ± 0.16** | 0.615 ± 0.6 | 0.24 ± 0.26 |
| 4046/13 | <u>3.00 ± 0.13****</u> | 0.26 ± 0.19 | 1.26 ± 0.2**** | 0.25 ± 0.2 | 0.08 ± 0.01 |
| 1814/06 | <u>5.22 ± 0.39****</u> | 0.93 ± 0.13 | <u>3.54 ± 0.52****</u> | 0.28 ± 0.048 | 0.8 ± 0.09 |
| 5N | 2.18 ± 0.68** | 0.1 ± 0.39 | 0.84 ± 0.69 | -0.11 ± 0.05 | 0.14 ± 0.28 |

¹ phototreatment conditions: 10 μM Ga³⁺PPIX or Ga³⁺MPIX; green LED light 31.8 J/cm²; log₁₀ CFU/mL reduction was assessed with respect to non-treated cells, initial number of cell ~10⁷ CFU/mL, cells were incubated with proper PS for 10 min, then washed once with PBS buffer and resuspended into fresh TSB medium. Light (+)- light dependent; Light (-)- light independent; light only- bacterial cells irradiated without any PS applied. Significance at the respective p-values is marked with asterisks [^{*}p < 0.05; ^{**}p < 0.01; ^{***}p < 0.001, ^{****}p < 0.0001] with respect to Light only treated cells.

Ga³⁺MPIX-mediated photoinactivation of SCVs

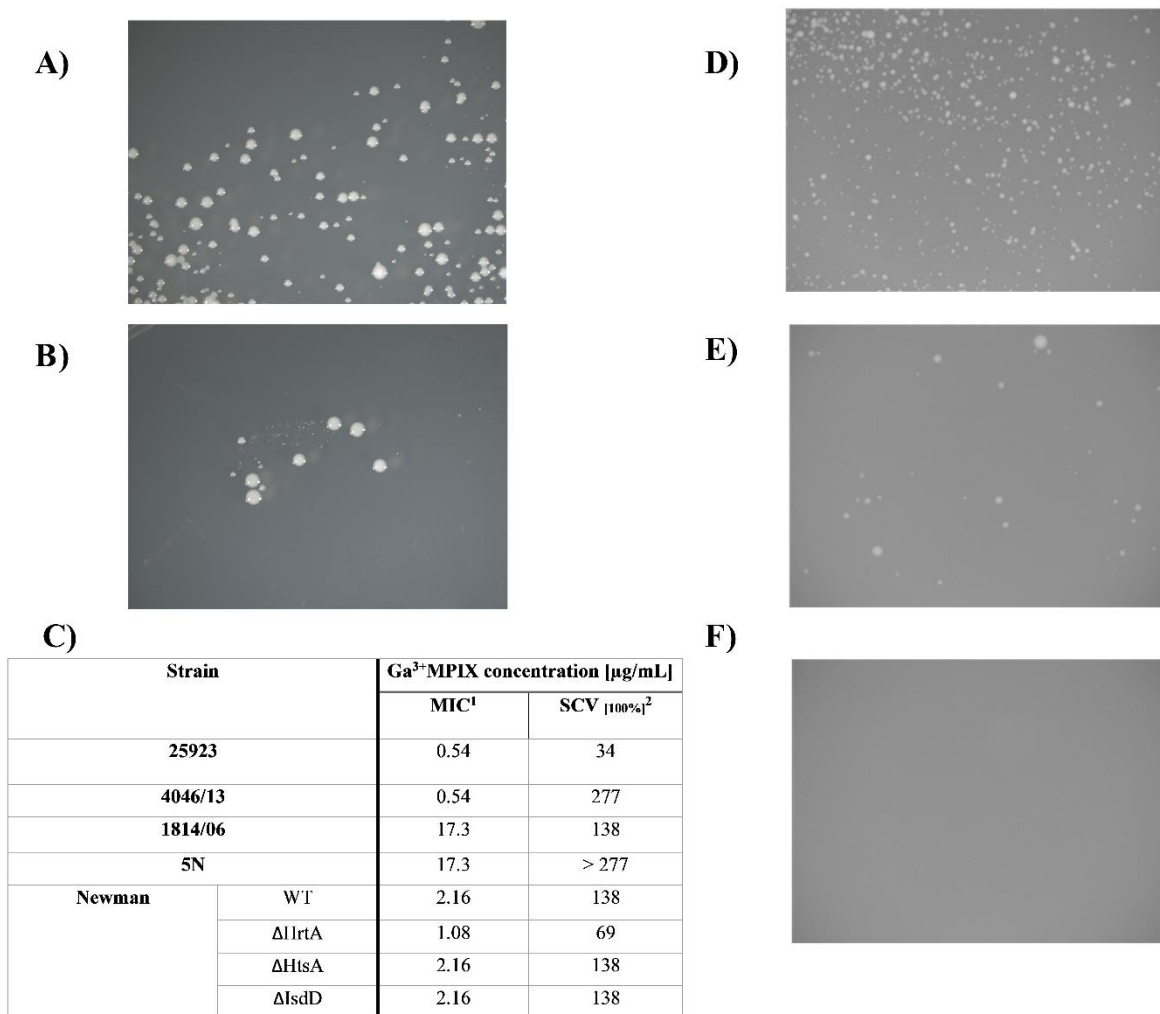


Figure S4. A, B) SCVs generated after Ga³⁺MPIX-mediated aPDI treatment. *S. aureus* 25923 bacteria plated on TSA plates (100 μl aliquots) survived after treatment (1 μM Ga³⁺MPIX, 25.4 J/cm²) with (A) or without (B) iron in the culture medium. The microscopic photographs of plates were taken under a Leica MZ10 stereoscopic microscopy (Leica, Germany). **C) Effect of light-independent action of Ga³⁺MPIX on several staphylococcal strains used in this study.** Overnight bacterial cultures were adjusted in fresh MHB medium to 0.5 McFarland, 100-fold diluted and finally transferred with or without PS to a 96-well plate. After 20 hours of incubation in 37°C, cells were plated to TSA agar plates and morphology of colonies were tested. ¹ MIC referred as compound concentration when the inhibition of bacterial growth was significantly delayed; ² SCV_[100%] - Concentration of Ga³⁺MPIX in which only SCV morphology was detected (100%). **D, E, F) Efficiency of green light irradiation in SCVs photokilling after 20 hours exposure to Ga³⁺MPIX [138 $\mu\text{g/mL}$].** *S. aureus* Newman WT was exposed to SCV_[100%] concentration of Ga³⁺MPIX, then cells were illuminated with green light dosage of 12.72 J/cm² (E) or 25.44 J/cm² (F). Untreated cells were left for dark control (D). After that, cells were plated to TSA agar plates and microscopic photographs were taken under Leica MZ10 stereoscopic microscopy (Leica, Germany).

Impairment in the HrtA detoxification efflux pump promotes dark toxicity of Ga³⁺MPIX

Table S4. *S. aureus* Newman and its isogenic mutants growth under exposure to gallium- MPs, calculated in the reference to the Figure 8.

| <i>S. aureus</i> isogenic mutant | Treatment | Parameters of <i>Staphylococcus aureus</i> growth curve | | | | |
|----------------------------------|-----------------------|---|---------------|---|---|--|
| | | μ_{max} [OD ₆₀₀ /h] | Td [hours] | A _{max} [OD _{600max}] | Time to reach stationary phase [min] | Growth at the end of exponential phase [%] |
| WT | Untreated | 0.498 | 1.39 | 0.645 | 330 | 100 |
| | Ga ³⁺ MPIX | 0.414 | 1.67 | 0.568 | 330 | 93 ± 1.44 |
| | Ga ³⁺ PPIX | 0.39 | 1.7 | 0.45 | 390 | 74 ± 0.66 |
| Δ HrtA | Untreated | 0.52 | 1.32 | 0.654 | 360 | 100 |
| | Ga ³⁺ MPIX | 0.36 | 1.9 | 0.586 | 480 | 82 ± 2.3 |
| | Ga ³⁺ PPIX | 0.35 | 1.95 | 0.54 | 480 | 77 ± 1.5 |
| Δ IsdD | Untreated | 0.474 | 1.46 | 0.75 | 330 | 100 |
| | Ga ³⁺ MPIX | 0.336 | 2.06 | 0.57 | 360 | 90 ± 2.93 |
| | Ga ³⁺ PPIX | 0.37 | 1.86 | 0.49 | 360 | 73 ± 4.4 |
| Δ HtsA | Untreated | 0.47 | 1.48 | 0.7 | 330 | 100 |
| | Ga ³⁺ MPIX | 0.43 | 1.62 | 0.63 | 390 | 90 ± 1.6 |
| | Ga ³⁺ PPIX | 0.39 | 1.77 | 0.5 | 390 | 72 ± 1.5 |

Legend: μ_{max} - maximum specific growth rate during exponential phase of bacterial growth; Td- Time of duplication, also known as generation time; A_{max}- maximal absorbance value with maximal bacterial density; Time to reach stationary phase - defined as the point of curve flattening; *S. aureus* growth at the end of exponential phase [%] at 270 min as the inflection point of the exponential growth curve calculated in the reference to control- untreated cells (100%).

Ga³⁺MPIX accumulation under confocal microscopic image

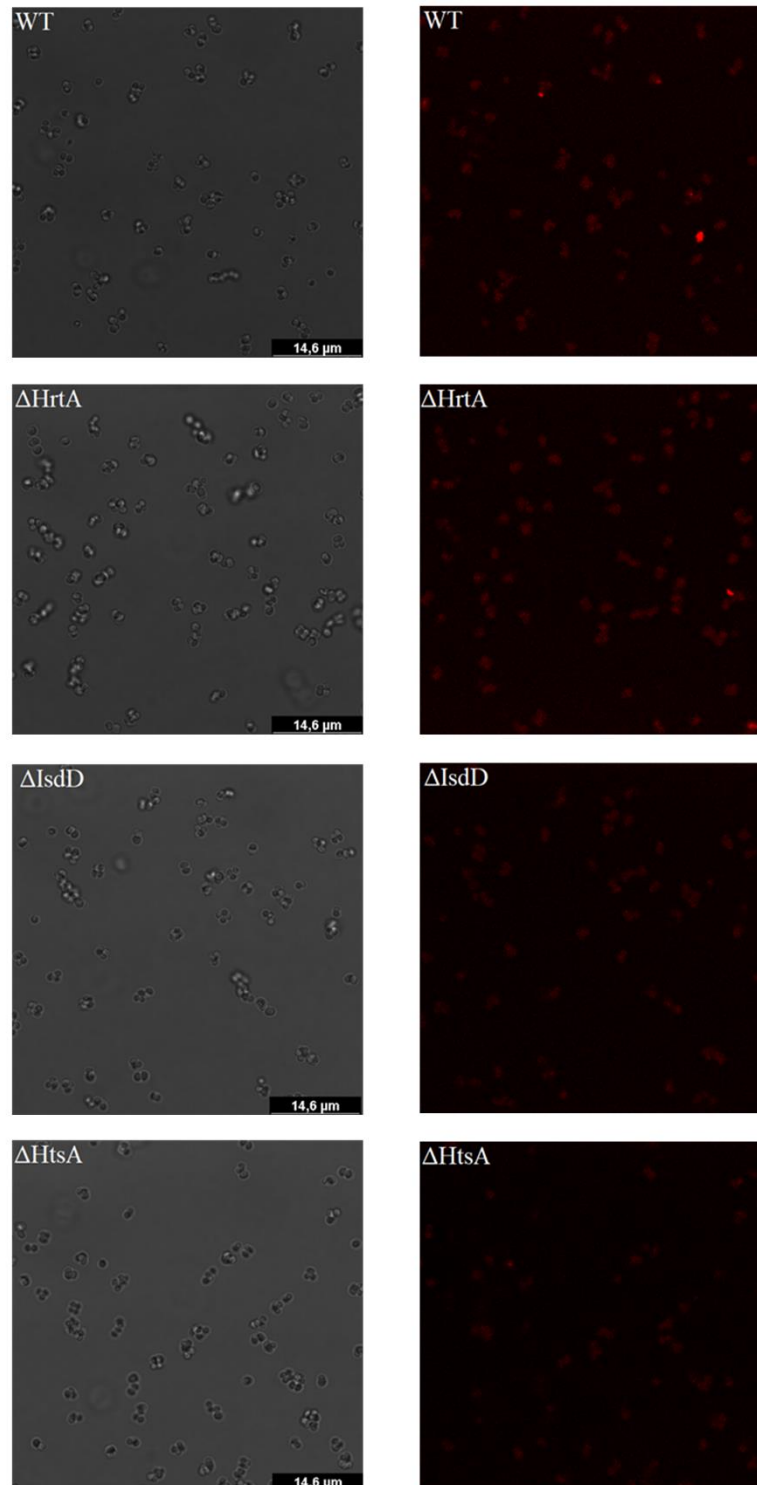


Figure S5. Ga³⁺MPIX uptake in *S. aureus* Newman and its isogenic mutant (Δ HrtA, Δ IsdD and Δ HtsA) in the presence of iron. Overnight bacterial cultures were diluted and incubated with photosensitizer for 2 hours at 37°C with shaking. Then, washed once with PBS buffer. Specimens were imaged using a confocal laser scanning microscope Leica SP8X with a 63 \times oil immersion lens with excitation of 405 nm and fluorescence emission in 551-701 nm (Leica, Germany)

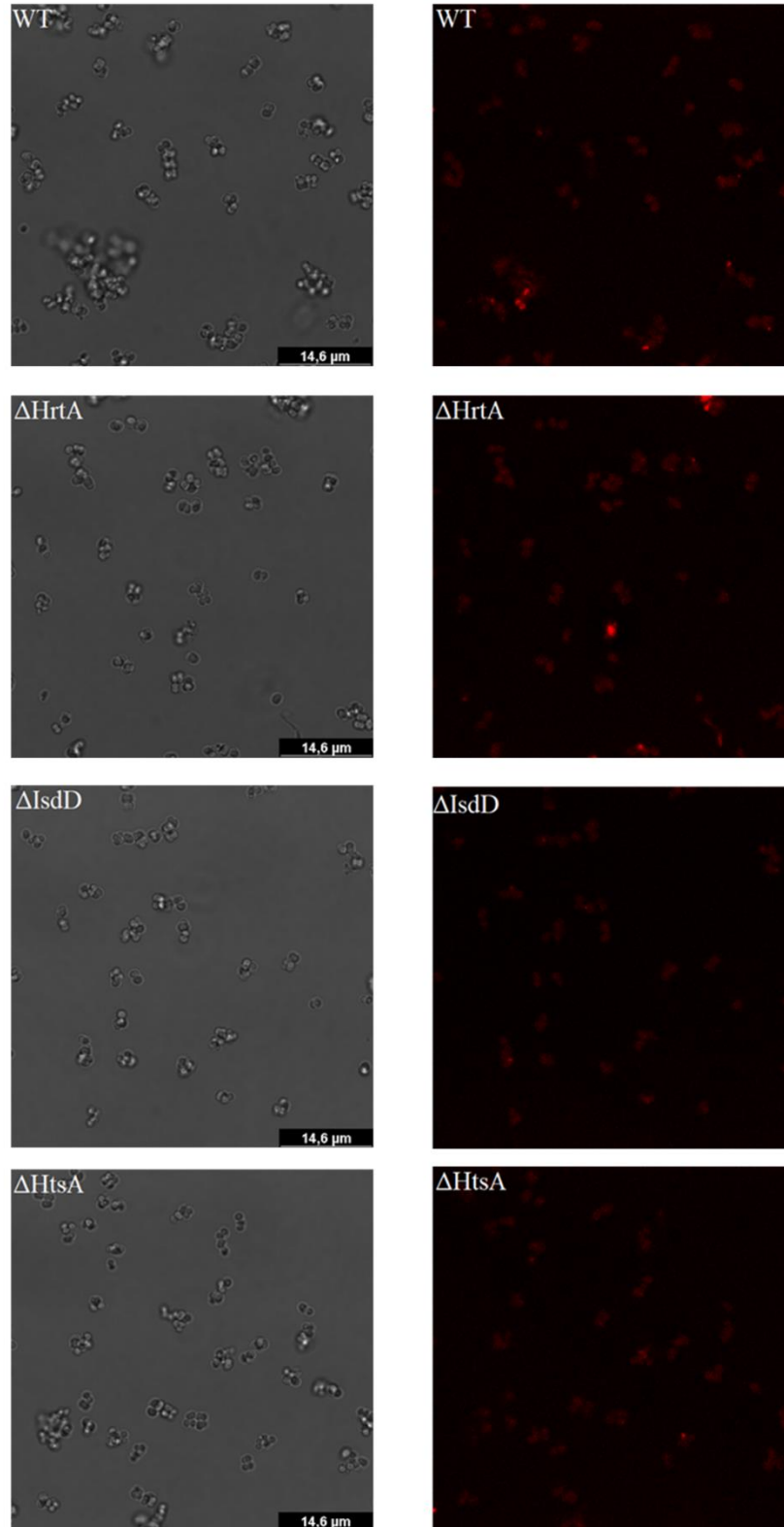


Figure S6. Ga^{3+} MPIX uptake in *S. aureus* Newman and its isogenic mutant (ΔHrtA , ΔIsdD and ΔHtsA) in the absence of iron. Overnight bacterial cultures were diluted and incubated with photosensitizer for 2 hours at 37°C with shaking. Then, washed once with PBS buffer. Specimens were imaged using a confocal laser scanning microscope Leica SP8X with a 63× oil immersion lens with excitation of 405 nm and fluorescence emission in 551-701 nm (Leica, Germany)

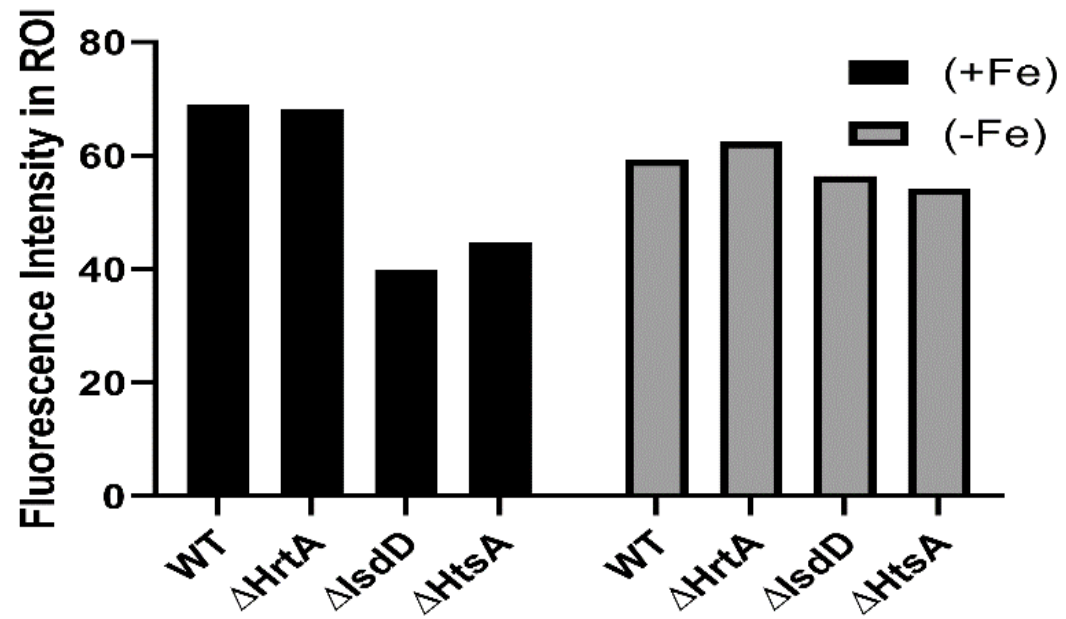


Figure S7. Maximal Fluorescence Intensity Amplitude in ROI measured on confocal microscopic images of uptake in *S. aureus* Newman and its isogenic mutant (Δ HrtA, Δ IsdD and Δ HtsA). Overnight bacterial cultures were diluted and incubated with Ga³⁺MPIX for 2 hours at 37°C with shaking. Then, washed once with PBS buffer. The values represented on graph are the highest amplitudes of fluorescence measured in ROI length of 12.59 μ m.

Ga³⁺MPIX does not promote extensive and prolonged cytotoxicity or phototoxicity against human keratinocytes

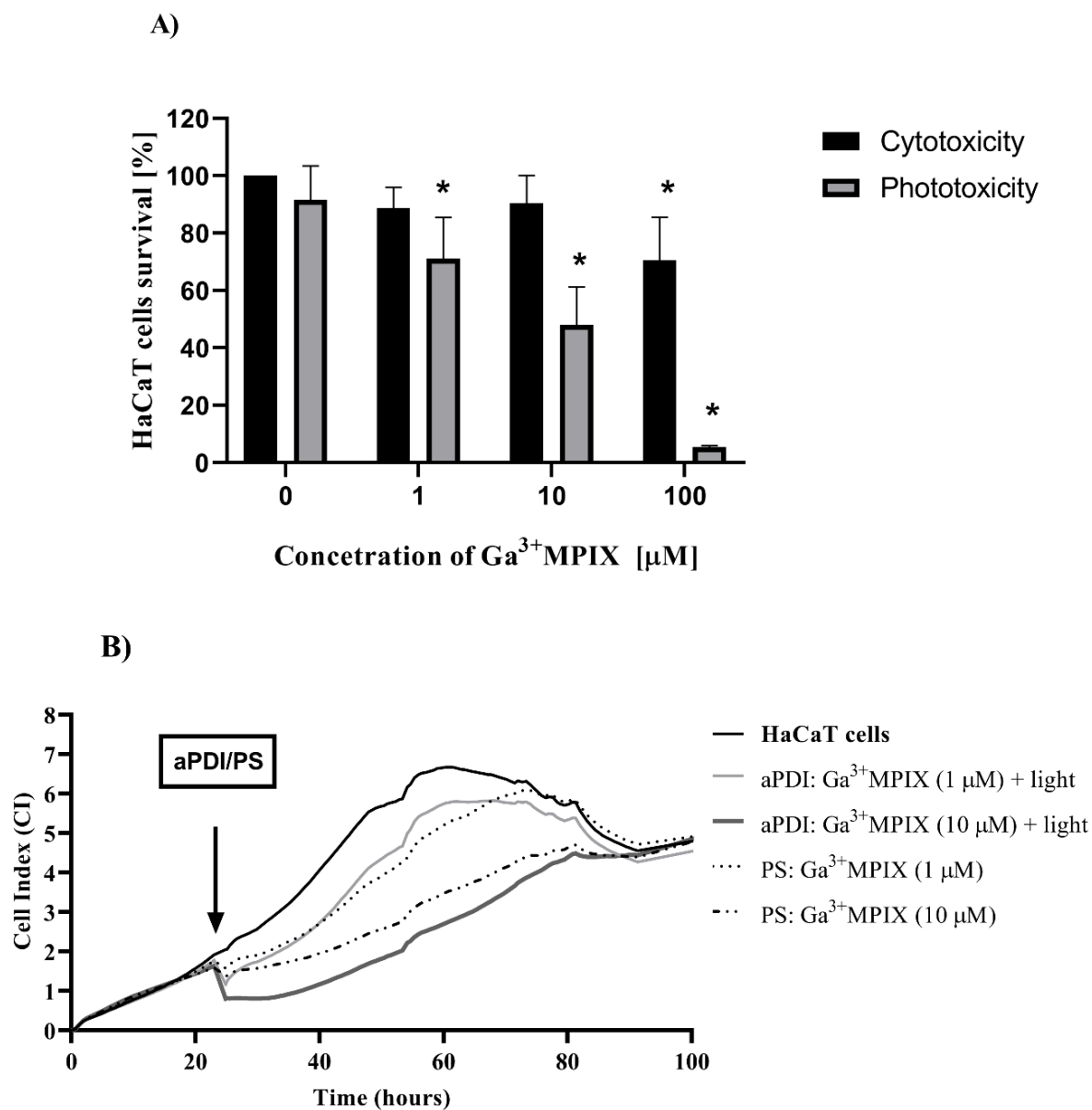


Figure S8. Effect of aPDI with Ga³⁺MPIX on the HaCaT cell line model with one-wash step. A) MTT cell viability assay. HaCaT cells were exposed to various concentrations of Ga³⁺MPIX. Control cells (0 µM) to which no test compound was added. After incubation with Ga³⁺MPIX, cells were washed with PBS and either irradiated with green light (31.8 J/cm²) represented by gray bars (Phototoxicity) or kept simultaneously in the dark (black bars for Cytotoxicity). Each result is the mean ± SD of the mean. Significance at the respective p values is marked with asterisks (* p < 0.05) for untreated cells (0 µM, Cytotoxicity). B) Cell growth dynamics. Cells were seeded at 10⁴ cells/well and after obtaining a cell index (CI) 2, cells were treated with Ga³⁺MPIX in the dark, incubated at 37 °C for 10 minutes. The samples were washed once then illuminated with a green light dose of 31.8 J/cm², while the HaCaT cells or PS-only treatment was allowed to incubate in the dark at room temperature. The CI (represented at the Y axis) was measured for each condition every 10 min. The x-axis shows the experiment duration in hours. The values presented are the average of the seven technical repetitions

9.2 Supplementary Materials from Publication no. 2

Photoactivated gallium porphyrin reduces *Staphylococcus aureus* colonization on the skin and suppresses its ability to produce enterotoxin C and TSST-1

Klaudia Szymczak, Grzegorz Szewczyk, Michał Rychłowski, Tadeusz Sarna, Lei Zhang, Mariusz Grinholc, Joanna Nakonieczna (#)

- Supplementary Materials

| | |
|--|---|
| 1. Heat generation during irradiation..... | 2 |
| 2. Accumulation of Ga ³⁺ MPIX and Ga ³⁺ CHP | 3 |
| 3. Effect of Ga ³⁺ CHP and Ga ³⁺ MPIX aPDI on <i>S. aureus</i> biofilm | 4 |
| 4. Evaluation of bacterial viability of <i>S. aureus</i> XEN40 on ex vivo porcine skin model | 5 |
| 5. The cyto- and phototoxicity of gallium compounds on Ames assay indicator strains | 6 |
| 6. Supplementary information on qRT-PCR | 7 |

1. Heat generation during irradiation

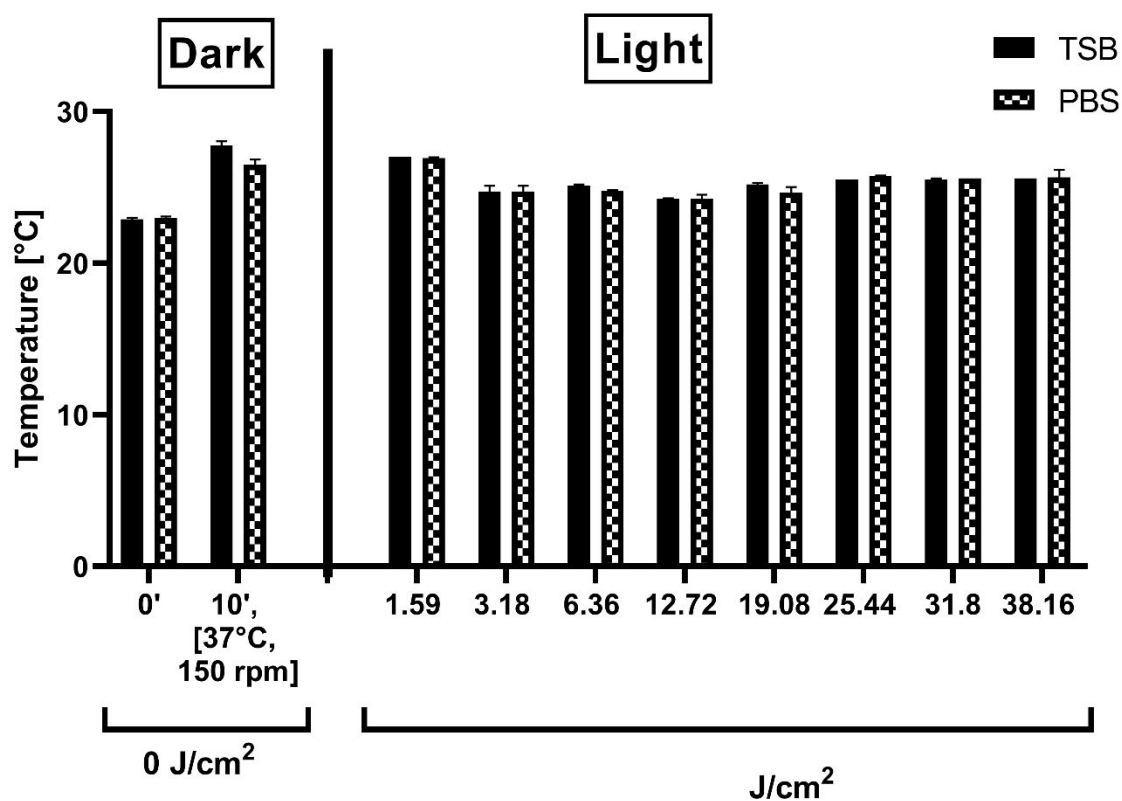


Figure S1. Temperature measurement over time. Bacterial cells were incubated in Tryptic soy broth (TSB) medium or phosphate buffer saline (PBS) for 10 minutes in the dark at 37 °C (Dark). The cells were then exposed to light (LED, 10.6 mW/cm²) at 522 nm for up to 60 min. Temperature was measured at successive time points corresponding to specific light doses (indicated on the X axis).

2. Accumulation of Ga³⁺MPIX and Ga³⁺CHP

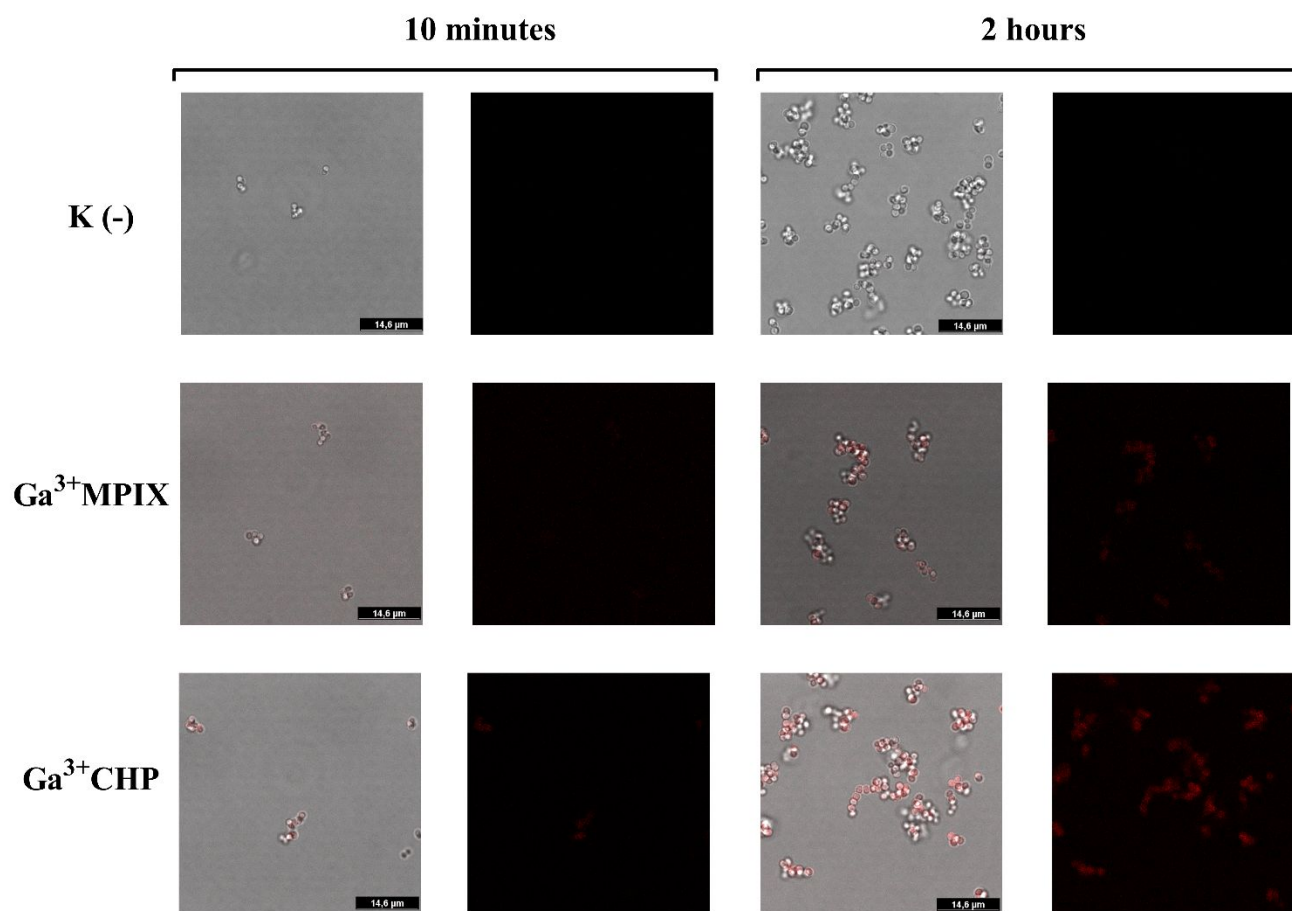


Figure S2. Ga³⁺MPIX and Ga³⁺CHP uptake in *S. aureus* 25923. Overnight bacterial cultures were diluted and incubated with 10 μM of each photosensitizer for 10 minutes or 2 hours at 37°C with shaking. Then, washed once with PBS buffer. Specimens were imaged with a Leica SP8X confocal laser scanning microscope with a 100× immersion lens with excitation at 405 nm and fluorescence emission at 551-701 nm (Leica, Germany).

3. Effect of Ga³⁺CHP and Ga³⁺MPIX aPDI on *S. aureus* biofilm

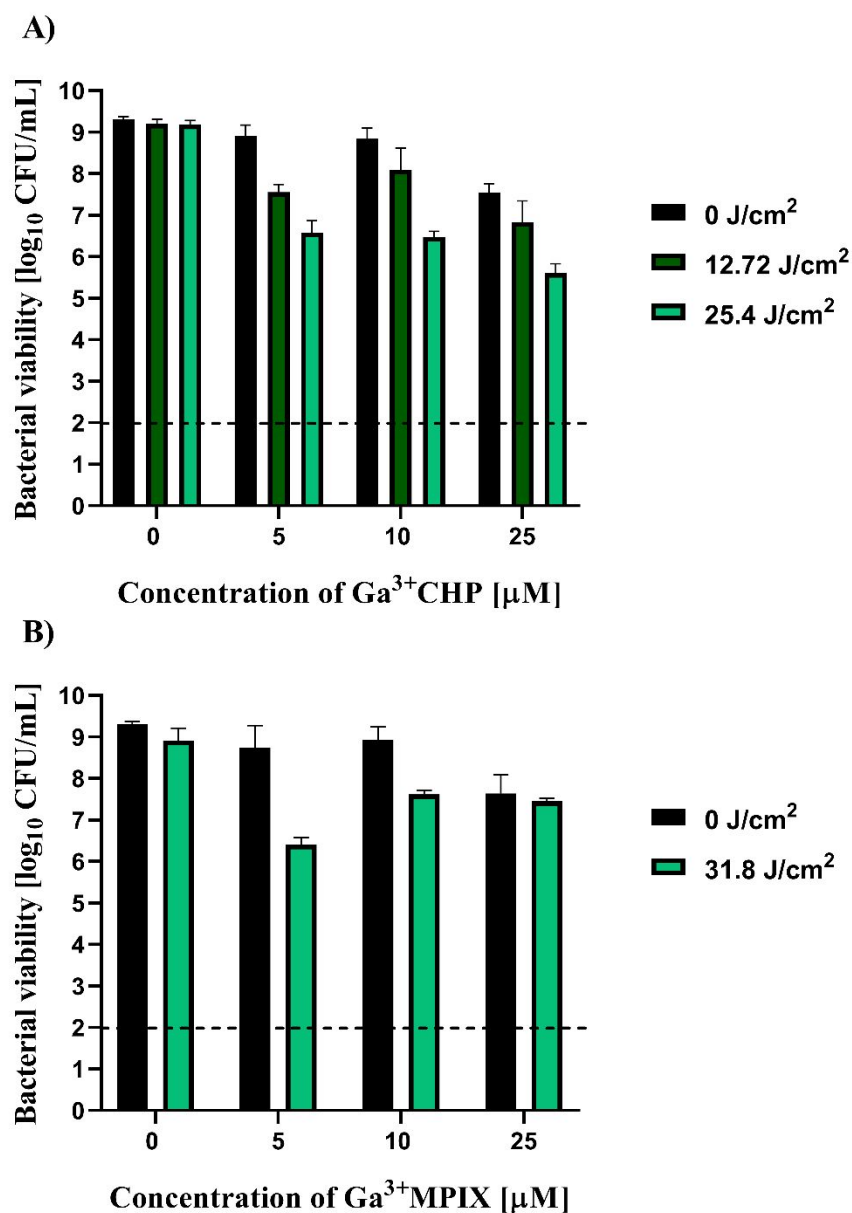


Figure S3. Effect of Ga³⁺CHP and Ga³⁺MPIX aPDI on *S. aureus* 5N biofilm viability. Overnight bacterial cultures were diluted to 10⁷ CFU/mL and placed into 96-well microtiter plate. Then, after 4h incubation at 37°C the medium was removed, replaced with 200 μL of fresh medium, and incubated at 37 °C for 20 h. Afterward, the biofilm was washed, and then 30 minutes of incubation with photosensitizer (Ga³⁺CHP or Ga³⁺MPIX; 0-25 μM) started, then washed once and illuminated with 522 nm light at the doses indicated in the legend. After dispersing and serial dilutions, samples were plated on TSA plates to evaluate the impact on the biofilm viability.

4. Evaluation of bacterial viability of *S. aureus* XEN40 on ex vivo porcine skin model

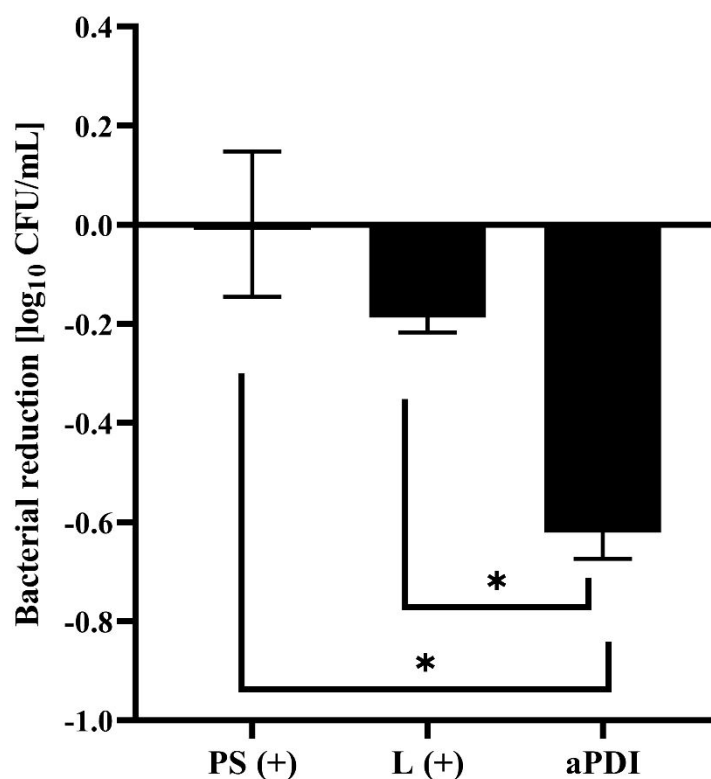


Figure S4. Evaluation of bacterial viability of *S. aureus* XEN40 on ex vivo porcine skin model after Ga³⁺CHP-mediated aPDI treatment. *S. aureus* XEN40 strain was applied to clean porcine skin grafts 24 hours before treatment. A 200 μ L of MiliQ or 10 μ M of Ga³⁺CHP was applied on the graft and incubated at 37 °C for 10 min prior to irradiation (12.72 J/cm²). Then, bacteria were collected with a sterile swab into 300 μ L PBS. Samples were centrifuged (5min x 14 000 rcf) and resuspended in 100 μ L. Bacterial suspensions were serially diluted and placed into TSA agar plates for CFU counting. Results are the mean of the *S. aureus* reduction in bacterial viability after either photosensitizer-, light- or aPDI- treatment in respect to untreated cells. Significance at the respective p-values is marked with an asterisk (* p < 0.05) with respect to the “aPDI” group by Dunnett's multiple comparisons test.

5. The cyto- and phototoxicity of gallium compounds against indicator strains used in the Ames test

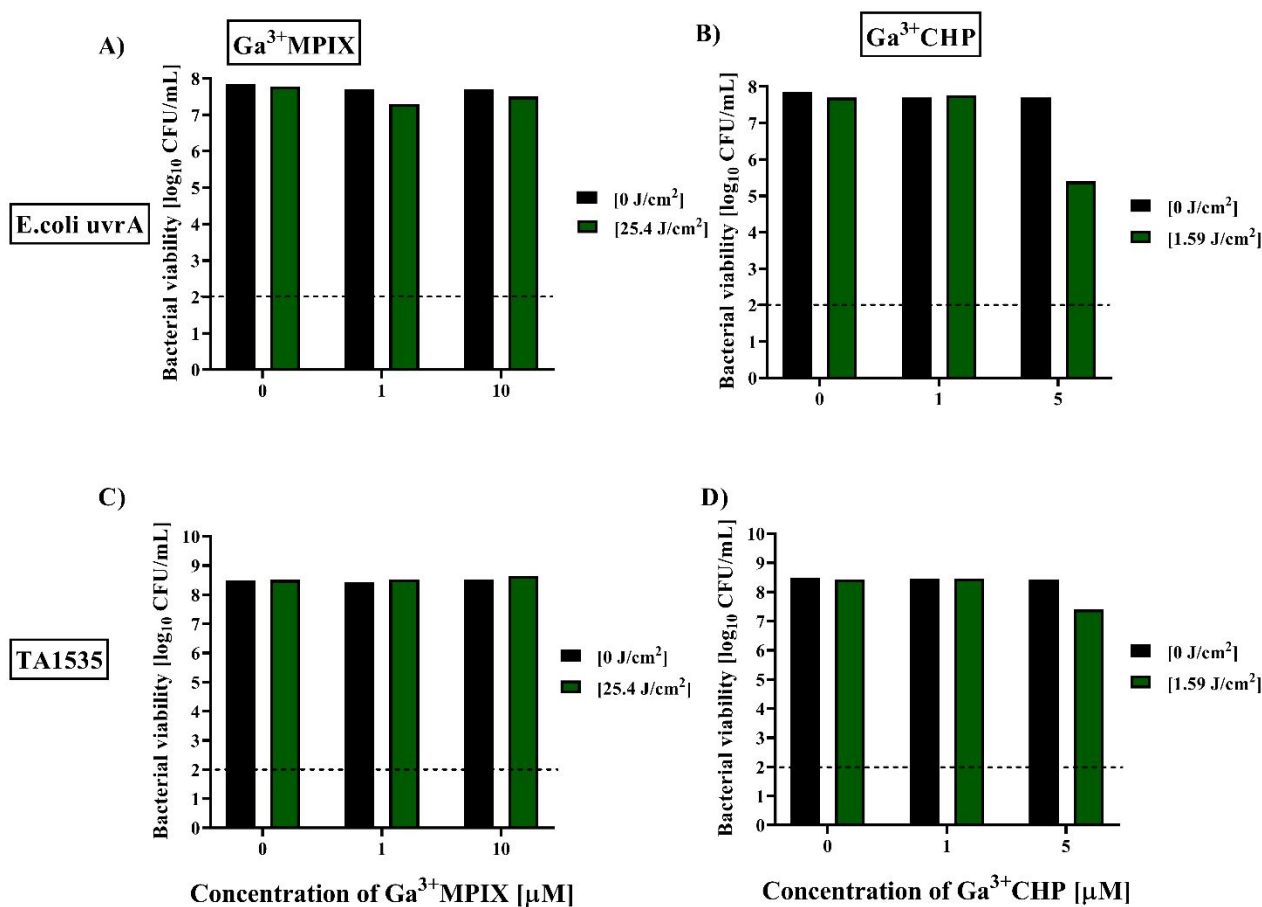


Figure S5. The cyto- and phototoxicity of gallium compounds against indicator strains (*E. coli uvrA* and TA1535). *E. coli uvrA* (A, B) and TA1535 (C, D) strains were exposed to both gallium compounds: Ga³⁺MPIX (A, C) or Ga³⁺CHP (B, D) either in the dark or under green light conditions. For the light-activated treatment groups, after 10 minutes of incubation with compounds, cells were exposed to the green light at the proper dosage (25.4 J/cm² for Ga³⁺MPIX or 1.59 J/cm² for Ga³⁺CHP). Then, cells were serially diluted and placed on the TSA agar plates to examine the bacterial viability.

6. Supplementary information on qRT-PCR

Table S1. Primers used into qRT-PCR analysis (“F-forward; “R”-Reverse)

| Gene | Primer sequence (5’-3’) |
|-------------|---|
| <i>gmk</i> | F: AATCGTTTTATCAGG ACC R: CTTCACCTTCACGCATT |
| <i>sec</i> | F: AATAAAACGGTTGATTCTAAAAGTGTGAA R: ATCAAAATCGGATTAACATTATCCATTC |
| <i>tst</i> | F: TCATCAGCTAACTCAAATACATGGATT R: TGTGGATCCGTCATTCATTGTT |
| <i>srrA</i> | F: AGCATGTGTGGGAGGTATGA R: CCTCTTGGCCATTACTIONTGCTT |
| <i>srrB</i> | F: AGCCGGCTAAATAGTGTCGT R: ATGGCATTTCGGTTTCTTG |

Table S2. qRT-PCR conditions used in this study.

| Step | Temperature | Time | Cycles |
|----------------|--------------------|-------------|---------------|
| Pre-incubation | 95 °C | 5 min | 1 |
| Amplification | 95 °C | 15 s | 45 |
| | 60 °C | 15 s | |
| | 72 °C | 15 s | |
| Melting curves | 95 °C | 5 s | 1 |
| | 65 °C -> 97 °C | 1 min | |
| Cool down | 40 °C | 30 s | 1 |

9.3 Supplementary Materials from Manuscript no. 3

Supporting information captions

Harnessing light-activated gallium porphyrins to combat intracellular *Staphylococcus aureus* in dermatitis: Insights from a simplified model.

Klaudia Szymczak¹, Michał Rychłowski², Lei Zhang³, Joanna Nakonieczna^{1*}



<https://drive.google.com/file/d/1gyq29vGoXZ3APQPzTSjIdkl8XyerziOS/view?usp=sharing>

Movie S1. Cell death of infected HaCaT cell under antibiotic pressure (Antibiotic ON)
Fluorescence *S. aureus* USA300 bacteria (green signal), HaCaT cells Transmitted Light (gray signal). 17-hour time lapse microscopy analyze, 15-min interval.

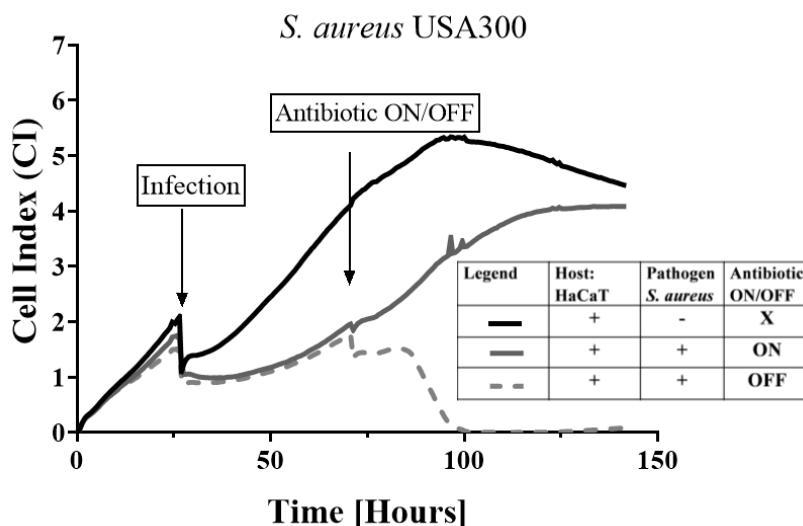


Fig S1. Recurrent infection of *S. aureus* USA300 at 3d day post-infection

Infection of HaCaT cells in a medium without antibiotics was carried out at an MOI of 10 for 2 hours, then the cells were cultured under antibiotic pressure (Antibiotic ON) until the medium was changed to with or without antibiotic (Antibiotic OFF) at 3^d day post-infection.

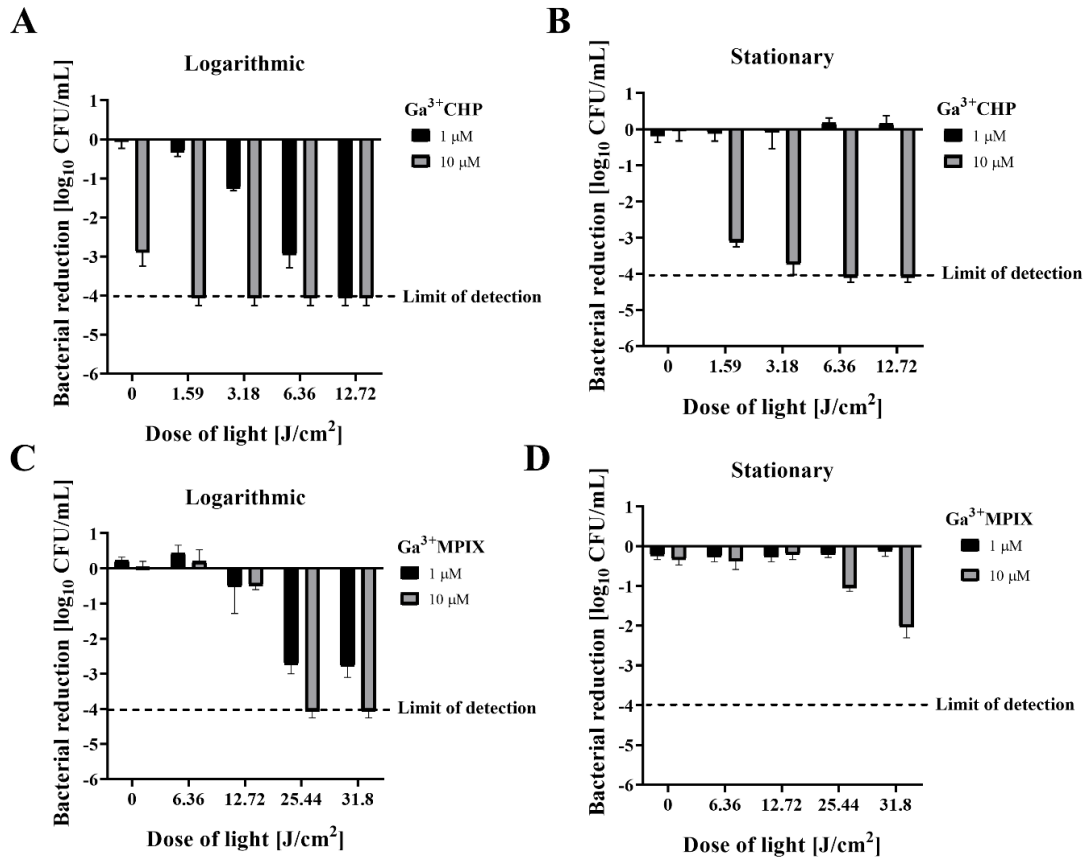


Fig S2. Photoinactivation of *S. aureus* USA300 with gallium metalloporphyrins at bacterial logarithmic or stationary growth phase.

Two photosensitizers, Ga³⁺CHP (A, B) and Ga³⁺MPIX (C, D), activated with green (522 nm) light were used to evaluate the *S. aureus* USA300 susceptibility to aPDI during logarithmic (A, C) or stationary phase (B, D) of growth. The bacterial reduction was calculated with respect to the untreated cells. Each experiment was performed in three independent biological replicates. The data are presented as the mean ± SD of three separate experiments.

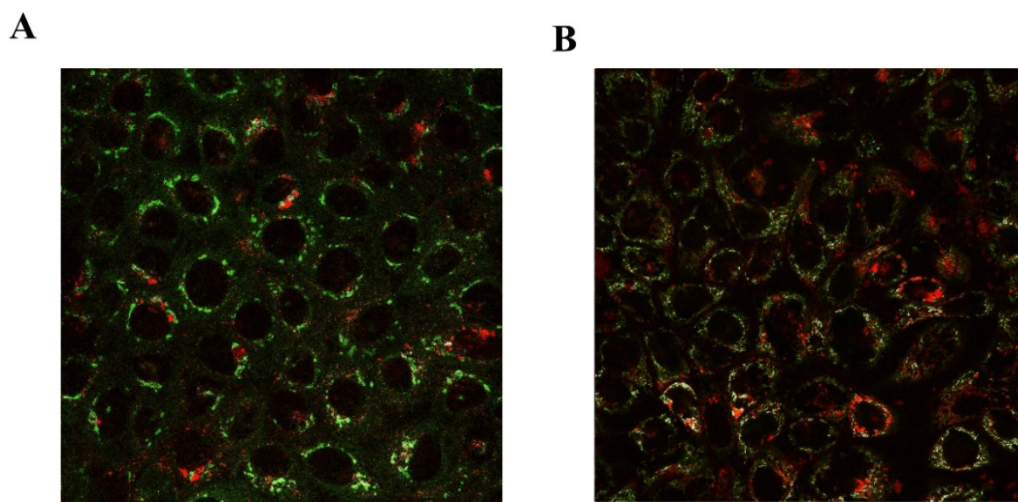


Fig S3. Colocalization of intracellular Ga³⁺CHP in Golgi apparatus and mitochondria.

Intracellular localization of Ga³⁺CHP in human keratinocytes after 6 hours of incubation. Analysis was performed with compounds' colocalization in the Golgi apparatus (A) and mitochondria (B). The red signal represents Ga³⁺CHP, while the green signal is from either Golgi (A) or mitochondria (B). Areas of colocalization are marked in white. All colocalization parameters are detailed in the **Table S1**.

Table S1. Coefficients of Ga³⁺CHP accumulation in the specific cellular compartments.

| Type accumulation | The Pearson's coefficient | Overlap coefficient |
|--|---------------------------|---------------------|
| Ga ³⁺ CHP + Lysosome | 0.4695 | 0.65 |
| Ga ³⁺ CHP + Golgi apparatus | 0.18 | 0.44 |
| Ga ³⁺ CHP + Mitochondria | 0.39 | 0.61 |

The results are reported as Pearson correlation coefficients and colocalization rates (%). The Pearson's coefficient ranges from -1 to +1 with a statistically significant score colocalization value above 0.5. The overlap factor ranges from 0 to 1 with co-localization values above 0.6. The quantitative analysis of colocalization was performed with Leica Application Suite X version 3.5.2.18963.

Table S2. Coefficients of Ga³⁺CHP and *S. aureus* colocalization within lysosomal structures of human keratinocytes.

| Type of image | | The Pearson's coefficient | Overlap coefficient |
|--|---|----------------------------------|----------------------------|
| Ga³⁺CHP + Lysosome | | 0.4695 | 0.65 |
| <i>S. aureus</i> + Lysosome | | 0.19 | 0.3064 |
| <i>S. aureus</i> + Ga³⁺CHP | | 0.5085 | 0.6 |
| <i>S. aureus</i> +Ga³⁺CHP + Lysosome | <i>S. aureus</i> +Ga³⁺CHP | 0.67 | 0.7 |
| | <i>S. aureus</i> + Lysosome | 0.6145 | 0.6352 |
| | Ga³⁺CHP + Lysosome | 0.6759 | 0.7563 |

The results are reported as Pearson correlation coefficients and colocalization rates (%). The Pearson's coefficient ranges from -1 to +1 with a statistically significant score colocalization value above 0.5. The overlap factor ranges from 0 to 1 with co-localization values above 0.6. The quantitative analysis of colocalization was performed with Leica Application Suite X version 3.5.2.18963

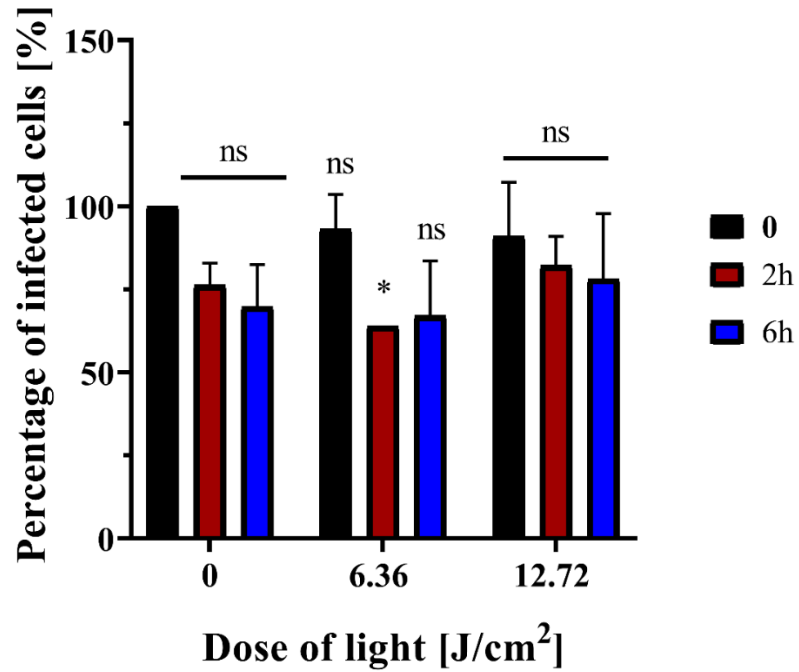


Figure S4. Light-activated Ga³⁺MPIX has no impact on the number of GFP-expressed cells.

Percentage of infected cells after aPDI with Ga³⁺MPIX. The number of GFP-expressing cells after 2- or 6-hour dark incubation followed with either dark treatment or green light illumination. Cells were collected, fixed and GFP signal was measured by flow cytometry. All results were calculated in reference to the untreated control (cells with no compound and no light exposure).

Gdańsk, 11.10.2023 r.

MSc Klaudia Szymczak (panieńskie: Michalska)
Laboratory of Photobiology and Molecular Diagnostics
Intercollegiate Faculty of Biotechnology
University of Gdansk and Medical University of Gdansk
Abrahama 58
80-307 Gdańsk

Co-authorship statement

I hereby declare my contribution to the publication:

Klaudia Michalska, Michał Rychłowski, Martyna Krupińska, Grzegorz Szewczyk, Tadeusz Sarna, and Joanna Nakonieczna,

"*Gallium Mesoporphyrin IX-Mediated Photodestruction: A Pharmacological Trojan Horse Strategy To Eliminate Multidrug-Resistant Staphylococcus aureus*". *Mol. Pharmaceutics* 2022, 19, 5, 1434–1448, <https://doi.org/10.1021/acs.molpharmaceut.1c00993>

As follows:

| Co-author | Ideas | Work | Writing | Stewardship | Adjusted Authorship contribution |
|-------------------------|-------|------|---------|-------------|----------------------------------|
| | 20% | 30% | 30% | 20% | % |
| K. Szymczak (Michalska) | 20 | 55 | 50 | 30 | 40 |
| M. Rychłowski | 15 | 15 | 0 | 0 | 10 |
| M. Krupińska | 0 | 15 | 0 | 0 | 5 |
| G. Szewczyk | 5 | 15 | 10 | 0 | 10 |
| T. Sarna | 5 | 0 | 10 | 10 | 5 |
| J. Nakonieczna | 55 | 0 | 30 | 60 | 30 |



Signature

Gdańsk, 11.10.2023 r.

Dr Michał Rychłowski
Laboratory of Virus Molecular Biology
Intercollegiate Faculty of Biotechnology
University of Gdansk and Medical University of Gdansk
Abrahama 58
80-307 Gdańsk

Co-authorship statement

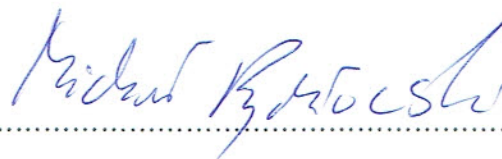
I hereby declare my contribution to the publication:

Klaudia Michalska, Michał Rychłowski, Martyna Krupińska, Grzegorz Szewczyk, Tadeusz Sarna, and Joanna Nakonieczna,

"*Gallium Mesoporphyrin IX-Mediated Photodestruction: A Pharmacological Trojan Horse Strategy To Eliminate Multidrug-Resistant Staphylococcus aureus*". *Mol. Pharmaceutics* 2022, 19, 5, 1434–1448, <https://doi.org/10.1021/acs.molpharmaceut.1c00993>

As follows:

| Co-author | Ideas | Work | Writing | Stewardship | Adjusted Authorship contribution |
|--------------------------------|-------|------|---------|-------------|----------------------------------|
| | 20% | 30% | 30% | 20% | % |
| K. Szymczak (Michalska) | 20 | 55 | 50 | 30 | 40 |
| M. Rychłowski | 15 | 15 | 0 | 0 | 10 |
| M. Krupińska | 0 | 15 | 0 | 0 | 5 |
| G. Szewczyk | 5 | 15 | 10 | 0 | 10 |
| T. Sarna | 5 | 0 | 10 | 10 | 5 |
| J. Nakonieczna | 55 | 0 | 30 | 60 | 30 |



.....
Signature

Gdańsk, 11.10.2023 r.

MSc Martyna Krupińska
Laboratory of Photobiology and Molecular Diagnostics
Intercollegiate Faculty of Biotechnology
University of Gdansk and Medical University of Gdansk
Abrahama 58
80-307 Gdańsk

Co-authorship statement

I hereby declare my contribution to the publication:

Klaudia Michalska, Michał Rychłowski, Martyna Krupińska, Grzegorz Szewczyk, Tadeusz Sarna, and Joanna Nakonieczna,

"*Gallium Mesoporphyrin IX-Mediated Photodestruction: A Pharmacological Trojan Horse Strategy To Eliminate Multidrug-Resistant Staphylococcus aureus*". *Mol. Pharmaceutics* 2022, 19, 5, 1434–1448, <https://doi.org/10.1021/acs.molpharmaceut.1c00993>

As follows:

| | Ideas | Work | Writing | Stewardship | Adjusted Authorship contribution |
|--------------------------------|--------------|-------------|----------------|--------------------|---|
| Co-author | 20% | 30% | 30% | 20% | % |
| K. Szymczak (Michalska) | 20 | 55 | 50 | 30 | 40 |
| M. Rychłowski | 15 | 15 | 0 | 0 | 10 |
| M. Krupińska | 0 | 15 | 0 | 0 | 5 |
| G. Szewczyk | 5 | 15 | 10 | 0 | 10 |
| T. Sarna | 5 | 0 | 10 | 10 | 5 |
| J. Nakonieczna | 55 | 0 | 30 | 60 | 30 |

.....


Signature

Kraków, 11.10.2023 r.

Dr Grzegorz Szewczyk
Department of Biophysics,
Faculty of Biochemistry, Biophysics and Biotechnology,
Jagiellonian University, Gronostajowa 7,
Krakow
30-387, Poland

Co-authorship statement

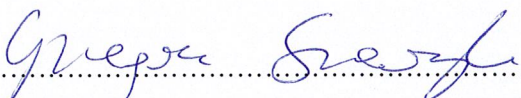
I hereby declare my contribution to the publication:

Klaudia Michalska, Michał Rychłowski, Martyna Krupińska, Grzegorz Szewczyk, Tadeusz Sarna, and Joanna Nakonieczna,

"Gallium Mesoporphyrin IX-Mediated Photodestruction: A Pharmacological Trojan Horse Strategy To Eliminate Multidrug-Resistant Staphylococcus aureus". Mol. Pharmaceutics 2022, 19, 5, 1434–1448, <https://doi.org/10.1021/acs.molpharmaceut.1c00993>

As follows:

| Co-author | Ideas | Work | Writing | Stewardship | Adjusted Authorship contribution |
|--------------------------------|-------|------|---------|-------------|----------------------------------|
| | 20% | 30% | 30% | 20% | % |
| K. Szymczak (Michalska) | 20 | 55 | 50 | 30 | 40 |
| M. Rychłowski | 15 | 15 | 0 | 0 | 10 |
| M. Krupińska | 0 | 15 | 0 | 0 | 5 |
| G. Szewczyk | 5 | 15 | 10 | 0 | 10 |
| T. Sarna | 5 | 0 | 10 | 10 | 5 |
| J. Nakonieczna | 55 | 0 | 30 | 60 | 30 |



Signature

Kraków, 11.10.2023 r.

prof. dr hab. Tadeusz Sarna
Department of Biophysics,
Faculty of Biochemistry, Biophysics and Biotechnology,
Jagiellonian University
Gronostajowa 7, Krakow 30-387, Poland

Co-authorship statement

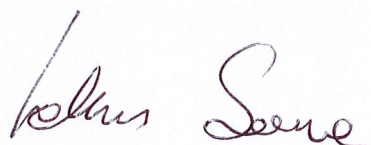
I hereby declare my contribution to the publication:

Klaudia Michalska, Michał Rychłowski, Martyna Krupińska, Grzegorz Szewczyk, Tadeusz Sarna, and Joanna Nakonieczna,

"*Gallium Mesoporphyrin IX-Mediated Photodestruction: A Pharmacological Trojan Horse Strategy To Eliminate Multidrug-Resistant Staphylococcus aureus*". *Mol. Pharmaceutics* 2022, 19, 5, 1434–1448, <https://doi.org/10.1021/acs.molpharmaceut.1c00993>

As follows:

| Co-author | Ideas | Work | Writing | Stewardship | Adjusted Authorship contribution |
|--------------------------------|-------|------|---------|-------------|----------------------------------|
| | 20% | 30% | 30% | 20% | % |
| K. Szymczak (Michalska) | 20 | 55 | 50 | 30 | 40 |
| M. Rychłowski | 15 | 15 | 0 | 0 | 10 |
| M. Krupińska | 0 | 15 | 0 | 0 | 5 |
| G. Szewczyk | 5 | 15 | 10 | 0 | 10 |
| T. Sarna | 5 | 0 | 10 | 10 | 5 |
| J. Nakonieczna | 55 | 0 | 30 | 60 | 30 |



.....
Signature

Gdańsk, 11.10.2023 r.

Dr hab. Joanna Nakonieczna, prof. UG
Laboratory of Photobiology and Molecular Diagnostics
Intercollegiate Faculty of Biotechnology
University of Gdansk and Medical University of Gdansk
Abrahama 58
80-307 Gdańsk

Co-authorship statement

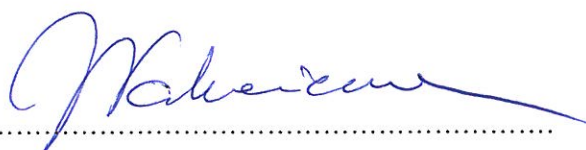
I hereby declare my contribution to the publication:

Klaudia Michalska, Michał Rychłowski, Martyna Krupińska, Grzegorz Szewczyk, Tadeusz Sarna, and Joanna Nakonieczna,

"*Gallium Mesoporphyrin IX-Mediated Photodestruction: A Pharmacological Trojan Horse Strategy To Eliminate Multidrug-Resistant Staphylococcus aureus*". *Mol. Pharmaceutics* 2022, 19, 5, 1434–1448, <https://doi.org/10.1021/acs.molpharmaceut.1c00993>

As follows:

| Co-author | Ideas | Work | Writing | Stewardship | Adjusted Authorship contribution |
|-------------------------|-------|------|---------|-------------|----------------------------------|
| | 20% | 30% | 30% | 20% | % |
| K. Szymczak (Michalska) | 20 | 55 | 50 | 30 | 40 |
| M. Rychłowski | 15 | 15 | 0 | 0 | 10 |
| M. Krupińska | 0 | 15 | 0 | 0 | 5 |
| G. Szewczyk | 5 | 15 | 10 | 0 | 10 |
| T. Sarna | 5 | 0 | 10 | 10 | 5 |
| J. Nakonieczna | 55 | 0 | 30 | 60 | 30 |



Signature

Gdańsk, 11.10.2023 r.

MSc Klaudia Szymczak
Laboratory of Photobiology and Molecular Diagnostics
Intercollegiate Faculty of Biotechnology
University of Gdansk and Medical University of Gdansk
Abrahama 58
80-307 Gdańsk

Co-authorship statement

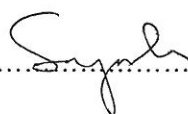
I hereby declare my contribution to the publication:

Klaudia Szymczak, Grzegorz Szewczyk, Michał Rychłowski, Tadeusz Sarna, Lei Zhang, Mariusz Grinholc, and Joanna Nakonieczna

"Photoactivated Gallium Porphyrin Reduces Staphylococcus aureus Colonization on the Skin and Suppresses Its Ability to Produce Enterotoxin C and TSST-1". Mol. Pharmaceutics 2023, 20, 10, 5108–5124, <https://doi.org/10.1021/acs.molpharmaceut.3c00399>

As follows:

| Co-author | Ideas | Work | Writing | Stewardship | Adjusted Authorship contribution |
|----------------|-------|------|---------|-------------|----------------------------------|
| | 20% | 30% | 30% | 20% | % |
| K. Szymczak | 10 | 70 | 40 | 10 | 40 |
| G. Szewczyk | 0 | 20 | 0 | 0 | 10 |
| M. Rychłowski | 0 | 10 | 0 | 0 | 5 |
| T. Sarna | 0 | 0 | 10 | 0 | 5 |
| L. Zhang | 10 | 0 | 10 | 0 | 5 |
| M. Grinholc | 10 | 0 | 10 | 50 | 10 |
| J. Nakonieczna | 50 | 0 | 30 | 40 | 25 |



.....
Signature

Kraków, 11.10.2023 r.

Dr Grzegorz Szewczyk
Department of Biophysics,
Faculty of Biochemistry, Biophysics and Biotechnology,
Jagiellonian University, Gronostajowa 7,
Krakow
30-387, Poland

Co-authorship statement

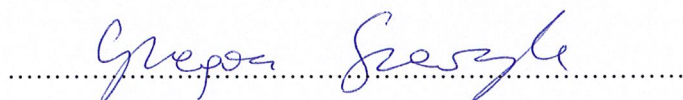
I hereby declare my contribution to the publication:

Klaudia Szymczak, Grzegorz Szewczyk, Michał Rychłowski, Tadeusz Sarna, Lei Zhang, Mariusz Grinholc, and Joanna Nakonieczna

"Photoactivated Gallium Porphyrin Reduces *Staphylococcus aureus* Colonization on the Skin and Suppresses Its Ability to Produce Enterotoxin C and TSST-1". *Mol. Pharmaceutics* 2023, 20, 10, 5108–5124, <https://doi.org/10.1021/acs.molpharmaceut.3c00399>

As follows:

| Co-author | Ideas | Work | Writing | Stewardship | Adjusted Authorship contribution |
|----------------|-------|------|---------|-------------|----------------------------------|
| | 20% | 30% | 30% | 20% | % |
| K. Szymczak | 10 | 70 | 40 | 10 | 40 |
| G. Szewczyk | 0 | 20 | 0 | 0 | 10 |
| M. Rychłowski | 0 | 10 | 0 | 0 | 5 |
| T. Sarna | 0 | 0 | 10 | 0 | 5 |
| L. Zhang | 10 | 0 | 10 | 0 | 5 |
| M. Grinholc | 10 | 0 | 10 | 50 | 10 |
| J. Nakonieczna | 50 | 0 | 30 | 40 | 25 |



Signature

Gdańsk, 11.10.2023 r.

Dr Michał Rychłowski
Laboratory of Virus Molecular Biology
Intercollegiate Faculty of Biotechnology
University of Gdansk and Medical University of Gdansk
Abrahama 58
80-307 Gdańsk

Co-authorship statement

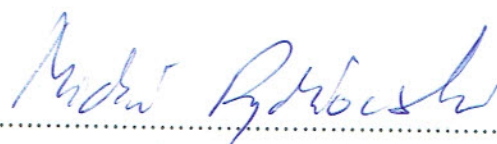
I hereby declare my contribution to the publication:

Klaudia Szymczak, Grzegorz Szewczyk, Michał Rychłowski, Tadeusz Sarna, Lei Zhang, Mariusz Grinholc, and Joanna Nakonieczna

"Photoactivated Gallium Porphyrin Reduces Staphylococcus aureus Colonization on the Skin and Suppresses Its Ability to Produce Enterotoxin C and TSST-1". Mol. Pharmaceutics 2023, 20, 10, 5108–5124, <https://doi.org/10.1021/acs.molpharmaceut.3c00399>

As follows:

| Co-author | Ideas | Work | Writing | Stewardship | Adjusted Authorship contribution |
|-----------------------|-------|------|---------|-------------|----------------------------------|
| | 20% | 30% | 30% | 20% | % |
| K. Szymczak | 10 | 70 | 40 | 10 | 40 |
| G. Szewczyk | 0 | 20 | 0 | 0 | 10 |
| M. Rychłowski | 0 | 10 | 0 | 0 | 5 |
| T. Sarna | 0 | 0 | 10 | 0 | 5 |
| L. Zhang | 10 | 0 | 10 | 0 | 5 |
| M. Grinholc | 10 | 0 | 10 | 50 | 10 |
| J. Nakonieczna | 50 | 0 | 30 | 40 | 25 |



Signature

Kraków, 11.10.2023 r.

prof. dr hab. Tadeusz Sarna
Department of Biophysics,
Faculty of Biochemistry, Biophysics and Biotechnology,
Jagiellonian University
Gronostajowa 7, Krakow 30-387, Poland

Co-authorship statement

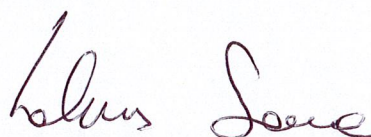
I hereby declare my contribution to the publication:

Klaudia Szymczak, Grzegorz Szewczyk, Michał Rychłowski, Tadeusz Sarna, Lei Zhang, Mariusz Grinholc, and Joanna Nakonieczna

"Photoactivated Gallium Porphyrin Reduces Staphylococcus aureus Colonization on the Skin and Suppresses Its Ability to Produce Enterotoxin C and TSST-1". Mol. Pharmaceutics 2023, 20, 10, 5108–5124, <https://doi.org/10.1021/acs.molpharmaceut.3c00399>

As follows:

| Co-author | Ideas | Work | Writing | Stewardship | Adjusted Authorship contribution |
|----------------|-------|------|---------|-------------|----------------------------------|
| | 20% | 30% | 30% | 20% | % |
| K. Szymczak | 10 | 70 | 40 | 10 | 40 |
| G. Szewczyk | 0 | 20 | 0 | 0 | 10 |
| M. Rychłowski | 0 | 10 | 0 | 0 | 5 |
| T. Sarna | 0 | 0 | 10 | 0 | 5 |
| L. Zhang | 10 | 0 | 10 | 0 | 5 |
| M. Grinholc | 10 | 0 | 10 | 50 | 10 |
| J. Nakonieczna | 50 | 0 | 30 | 40 | 25 |



.....
Signature

Tianjin, 11.10.2023 r.

Prof. Lei Zhang
Department of Biochemical Engineering,
School of Chemical Engineering and Technology,
Frontier Science Center for Synthetic Biology and Key Laboratory of Systems
Bioengineering (MOE),
Tianjin University, Tianjin 300350, China

Co-authorship statement

I hereby declare my contribution to the publication:

Klaudia Szymczak, Grzegorz Szewczyk, Michał Rychłowski, Tadeusz Sarna, Lei Zhang, Mariusz Grinholc, and Joanna Nakonieczna
"Photoactivated Gallium Porphyrin Reduces Staphylococcus aureus Colonization on the Skin and Suppresses Its Ability to Produce Enterotoxin C and TSST-1". Mol. Pharmaceutics 2023, 20, 10, 5108–5124, <https://doi.org/10.1021/acs.molpharmaceut.3c00399>

As follows:

| | Ideas | Work | Writing | Stewardship | Adjusted Authorship contribution |
|-----------------------|-------|------|---------|-------------|----------------------------------|
| Co-author | 20% | 30% | 30% | 20% | % |
| K. Szymczak | 10 | 70 | 40 | 10 | 40 |
| G. Szewczyk | 0 | 20 | 0 | 0 | 10 |
| M. Rychłowski | 0 | 10 | 0 | 0 | 5 |
| T. Sarna | 0 | 0 | 10 | 0 | 5 |
| L. Zhang | 10 | 0 | 10 | 0 | 5 |
| M. Grinholc | 10 | 0 | 10 | 50 | 10 |
| J. Nakonieczna | 50 | 0 | 30 | 40 | 25 |



.....
Signature

Gdańsk, 11.10.2023 r.

Dr hab. Mariusz Grinholc, prof. UG
Laboratory of Photobiology and Molecular Diagnostics
Intercollegiate Faculty of Biotechnology
University of Gdansk and Medical University of Gdansk
Abrahama 58
80-307 Gdańsk

Co-authorship statement

I hereby declare my contribution to the publication:

Klaudia Szymczak, Grzegorz Szewczyk, Michał Rychłowski, Tadeusz Sarna, Lei Zhang, Mariusz Grinholc, and Joanna Nakonieczna

"Photoactivated Gallium Porphyrin Reduces Staphylococcus aureus Colonization on the Skin and Suppresses Its Ability to Produce Enterotoxin C and TSST-1". Mol. Pharmaceutics 2023, 20, 10, 5108–5124, <https://doi.org/10.1021/acs.molpharmaceut.3c00399>

As follows:

| Co-author | Ideas | Work | Writing | Stewardship | Adjusted Authorship contribution |
|----------------|-------|------|---------|-------------|----------------------------------|
| | 20% | 30% | 30% | 20% | % |
| K. Szymczak | 10 | 70 | 40 | 10 | 40 |
| G. Szewczyk | 0 | 20 | 0 | 0 | 10 |
| M. Rychłowski | 0 | 10 | 0 | 0 | 5 |
| T. Sarna | 0 | 0 | 10 | 0 | 5 |
| L. Zhang | 10 | 0 | 10 | 0 | 5 |
| M. Grinholc | 10 | 0 | 10 | 50 | 10 |
| J. Nakonieczna | 50 | 0 | 30 | 40 | 25 |



.....
Signature

Gdańsk, 11.10.2023 r.

Dr hab. Joanna Nakonieczna, prof. UG
Laboratory of Photobiology and Molecular Diagnostics
Intercollegiate Faculty of Biotechnology
University of Gdansk and Medical University of Gdansk
Abrahama 58
80-307 Gdańsk

Co-authorship statement

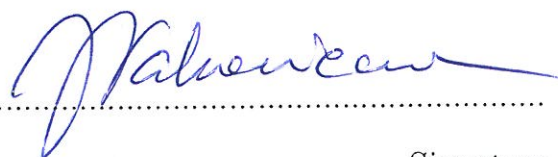
I hereby declare my contribution to the publication:

Klaudia Szymczak, Grzegorz Szewczyk, Michał Rychłowski, Tadeusz Sarna, Lei Zhang, Mariusz Grinholc, and Joanna Nakonieczna

"Photoactivated Gallium Porphyrin Reduces Staphylococcus aureus Colonization on the Skin and Suppresses Its Ability to Produce Enterotoxin C and TSST-1". Mol. Pharmaceutics 2023, 20, 10, 5108–5124, <https://doi.org/10.1021/acs.molpharmaceut.3c00399>

As follows:

| Co-author | Ideas | Work | Writing | Stewardship | Adjusted Authorship contribution |
|----------------|-------|------|---------|-------------|----------------------------------|
| | 20% | 30% | 30% | 20% | % |
| K. Szymczak | 10 | 70 | 40 | 10 | 40 |
| G. Szewczyk | 0 | 20 | 0 | 0 | 10 |
| M. Rychłowski | 0 | 10 | 0 | 0 | 5 |
| T. Sarna | 0 | 0 | 10 | 0 | 5 |
| L. Zhang | 10 | 0 | 10 | 0 | 5 |
| M. Grinholc | 10 | 0 | 10 | 50 | 10 |
| J. Nakonieczna | 50 | 0 | 30 | 40 | 25 |



Signature

Gdańsk, 16.11.2023 r.

MSc Klaudia Szymczak
Laboratory of Photobiology and Molecular Diagnostics
Intercollegiate Faculty of Biotechnology
University of Gdansk and Medical University of Gdansk
Abrahama 58
80-307 Gdańsk

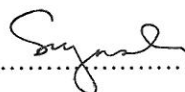
Co-authorship statement

I hereby declare my contribution to the manuscript:

Klaudia Szymczak, Michał Rychłowski, Lei Zhang, Joanna Nakonieczna
Harnessing light-activated gallium porphyrins to combat intracellular Staphylococcus aureus in dermatitis: Insights from a simplified model

As follows:

| Co-author | Ideas | Work | Writing | Stewardship | Adjusted Authorship contribution |
|-----------------------|-------|------|---------|-------------|----------------------------------|
| | 20% | 30% | 30% | 20% | % |
| K. Szymczak | 30 | 60 | 40 | 35 | 40 |
| M. Rychłowski | 15 | 30 | 0 | 5 | 15 |
| L. Zhang | 0 | 10 | 0 | 10 | 5 |
| J. Nakonieczna | 55 | 0 | 60 | 50 | 40 |



.....
Signature

Gdańsk, 16.11.2023 r.

Dr hab. Joanna Nakonieczna, prof. UG
Laboratory of Photobiology and Molecular Diagnostics
Intercollegiate Faculty of Biotechnology
University of Gdansk and Medical University of Gdansk
Abrahama 58
80-307 Gdańsk


Co-authorship statement

I hereby declare my contribution to the manuscript:

Klaudia Szymczak, Michał Rychłowski, Lei Zhang, Joanna Nakonieczna
Harnessing light-activated gallium porphyrins to combat intracellular Staphylococcus aureus in dermatitis: Insights from a simplified model

As follows:

| | Ideas | Work | Writing | Stewardship | Adjusted Authorship contribution |
|-----------------------|-------|------|---------|-------------|----------------------------------|
| Co-author | 20% | 30% | 30% | 20% | % |
| K. Szymczak | 30 | 60 | 40 | 35 | 40 |
| M. Rychłowski | 15 | 30 | 0 | 5 | 15 |
| L. Zhang | 0 | 10 | 0 | 10 | 5 |
| J. Nakonieczna | 55 | 0 | 60 | 50 | 40 |



Signature

Gdańsk, 16.11.2023 r.

Dr Michał Rychłowski
Laboratory of Virus Molecular Biology
Intercollegiate Faculty of Biotechnology
University of Gdansk and Medical University of Gdansk
Abrahama 58
80-307 Gdańsk

Co-authorship statement

I hereby declare my contribution to the manuscript:

Klaudia Szymczak, Michał Rychłowski, Lei Zhang, Joanna Nakonieczna
Harnessing light-activated gallium porphyrins to combat intracellular Staphylococcus aureus in dermatitis: Insights from a simplified model

As follows:

| Co-author | Ideas | Work | Writing | Stewardship | Adjusted Authorship contribution |
|-----------------------|-------|------|---------|-------------|----------------------------------|
| | 20% | 30% | 30% | 20% | % |
| K. Szymczak | 30 | 60 | 40 | 35 | 40 |
| M. Rychłowski | 15 | 30 | 0 | 5 | 15 |
| L. Zhang | 0 | 10 | 0 | 10 | 5 |
| J. Nakonieczna | 55 | 0 | 60 | 50 | 40 |



.....
Signature

Tianjin, 16.11.2023 r.

Prof. Lei Zhang
Department of Biochemical Engineering,
School of Chemical Engineering and Technology,
Frontier Science Center for Synthetic Biology and Key Laboratory of Systems
Bioengineering (MOE),
Tianjin University, Tianjin 300350, China

Co-authorship statement

I hereby declare my contribution to the manuscript:

Klaudia Szymczak, Michał Rychłowski, Lei Zhang, Joanna Nakonieczna
Harnessing light-activated gallium porphyrins to combat intracellular Staphylococcus aureus in dermatitis: Insights from a simplified model

As follows:

| | Ideas | Work | Writing | Stewardship | Adjusted Authorship contribution |
|-----------------------|-------|------|---------|-------------|----------------------------------|
| Co-author | 20% | 30% | 30% | 20% | % |
| K. Szymczak | 30 | 60 | 40 | 35 | 40 |
| M. Rychłowski | 15 | 30 | 0 | 5 | 15 |
| L. Zhang | 0 | 10 | 0 | 10 | 5 |
| J. Nakonieczna | 55 | 0 | 60 | 50 | 40 |



.....

Signature